Table of Contents

Acknowledgements

When I was 16, after the results of an aptitude test my career guidance teacher told me that I would never make it through a science degree. Therefore I would like to acknowledge David Oates and say that you can achieve anything when you put your mind to it.

I would first like to thank my supervisor Prof. Paul Moynagh, for the opportunity to do my PhD in his lab and also for all the help and supervision over the last 3 years and for always allowing me to follow up any ideas I may have had. It is without doubt one of the best labs in the country and I count myself lucky for the opportunity I have had to work in it. I would also like to thank all past and present members of the Molecular Immunology Lab who have all helped me inside and outside the lab on numerous occasions. In particular Mark, Bingwei and RJ for technical help and advice on animal work, Eric for proof-reading abstracts and CVs, Yang for useful conversations and ideas about experiments and Jakub for always giving me a positive outlook on life when experiments weren't going so well. I would also like to give a special thanks to my friend and former mentor Nezira from whom I inherited a challenging exciting project, who taught me a lot and always looked out for me in my early days in the lab. I would also like to thank the people pre-Moynagh lab who has helped me throughout my degree and PhD. My former teachers Dr Stephen Carberry, Dr Bernadette Moore, and supervisors Dr Sean Doyle and Dr Shirley O'Dea.

I would not have got here today without the support from my family and friends. My sister Ger for always asking me how things were going in the lab, my brother Colm 'Chiller' for always making me laugh with his stories when I came home from work feeling like a piece of garbage and my Mam and Dad. Ligi and all the 'Hund' and blanch lads. I would also like to give a special thanks to Tony Davy and Isabel Murray who bought me a laptop when I was in 3rd year of college. My good friend Ciaran Skerry for all his help throughout my degree, all the good advice and all them hilarious days we spent studying in the library and the many a Saturday afternoon burger king in blanch shopping centre. A special mention to my little dog Tara who

passed away earlier this year, you were probably the only living thing who was always happy to see me and you always cheered me up after a rough day in the lab.

Finally I would like to say thank you to the woman in my life. Edel, the love and kindness you show me every day is what gets me up in the morning. Thank you for everything you have done for me and continue to do for me, it’s more than you will ever know.

Abstract

Toll-like receptor (TLR) signalling represents the first line of defence against infection. TLRs respond to recognition of pathogens by activating transcription factors such as NFκB and the interferon regulatory factors (IRF)s to induce pro-inflammatory cytokines and IFNs. Whilst many of the components of the TLR signal transduction pathways have been identified, a full understanding of these complex regulatory systems remains to be delineated. This thesis probes the molecular, cellular and physiological roles of a protein termed evolutionary conserved signalling intermediate in toll (ECSIT) in innate immune signalling pathways. ECSIT was initially described as a TRAF6 interacting protein that bridged the TLR signalling intermediate TRAF6 to MEKK1 and downstream activation of NFκB. Subsequent data revealed an important developmental role for ECSIT in the BMP signalling pathway based on the embryonic lethal phenotype in the ECSIT knockout mouse. Other studies have indicated an important role for ECSIT in bacterial killing during infection via the production of mitochondrial reactive oxygen species (mROS). To date no information on the human orthologue of ECSIT (hECSIT) has been available. In this study we describe novel functional roles for hECSIT in TLR signalling. Through use of knockdown studies and a humanised animal model we demonstrate that hECSIT negatively regulates innate immune signalling pathways despite its 80% sequence homology to mECSIT. We show that phosphorylation, ubiquitination and processing of hECSIT leads to an inhibitory C-terminal form that contains both E3 ligase and DUB activity. We also demonstrate that hECSIT can independently target and regulate the ubiquitination of TRAF6, TRAF3 and RIP1 in TLR4/IL-1R, TLR3 and TNF-α signalling, respectively. These findings identify hECSIT as a novel regulator of innate immune signalling and highlight a sophisticated evolutionary difference between two highly conserved proteins.

Abbreviations

ABIN-1:	A20 binding and inhibitor of NFκB
AP-1:	activator protein-1
Apaf1:	apoptosis-inducing factor1
APS:	ammonium persulfate
Bcl:	B cell lymphoma
BID:	BH3 interacting domain death agonist
BLAST:	blast local alignment search tool
ATP:	adenosine triphosphate
bp:	base pair
BSA:	bovine serum albumin
C:	carboxy;
cAMP:	cyclic adenosine 3’ 5’ -monophosphate
CARD:	caspase-recruiting domain
CD14:	cluster of differentiation antigen 14
cDNA:	complementary DNA
cFLIP:	cellular FADD-Like IL-1-beta converting enzyme inhibitor protein
CHX:	cycloheximide
cIAP1:	cellular Inhibitor of apoptosis protein1
CpG:	2′-deoxyribo cytidine-phosphate-guanosine
CREB:	cAMP-responsive element binding protein
CYLD:	cylindromatosis
DAMPs:	danger-associated molecular patterns
DAPI:	4′ 6-diamidino-2-phenylindole
DC:	dendritic cell
DD:	death domain
DED:	death effector domain
DEPC:	diethylpyrocarbonate
D-Gal:	D-galactosamine
DISC:	death inducing signalling complex
DMEM:	Dulbecco’s Modified Eagle’s medium
DMSO:	dimethylsulfoxide
DNA:	deoxyribonucleic acid
dNTPs :	deoxyribonucleic triphosphates
dsRNA:	double-stranded RNA
dToll:	*Drosophila* Toll
DTT:	dithiothreitol
E.coli:	*Escherichia coli*
EDTA:	ethylenediaminetetraacetic acid
EGFP:	enhanced-green fluorescent protein
ELISA:	enzyme-linked immunosorbant assay
EMSA:	electrophoresis mobility shift assay
ER:	endoplasmic reticulum
ERK:	extracellular signal regulated kinase
EST:	expressed sequence tag
FACS:	*fluorescence activated cell* sorting

FADD:	Fas-associated death domain
FBS:	foetal bovine serum
FHA:	forkhead-associated
FITC:	fluorescein isothiocyanate
Fn:	fibronectin III domain
g:	gravity
GAPDH:	glyceraldehyde-3-phosphate dehydrogenase
GFP:	green fluorescent protein
GLUD:	glutamate dehydrogenase
GLUL:	glutamate-ammonia ligase
GPI:	glycosylphosphatidylinositol
hr:	hour
H&E:	haematoxylin and eosin
H_2O_2:	hydrogen peroxide solution
H_2SO_4:	sulphuric acid
HBSS:	Hank's balanced salt solution
HEK:	human embryonic kidney
HEPE:	hydroxyeicosapentaenoic acid
HRP:	horseradish-peroxidase
HSP:	heat shock protein
HCl:	hydrochloric acid
ID:	intermediary domain
IFN:	interferon
Ig:	immunoglobulin
IKK:	IκB Kinase
IL:	interleukin
IL-1R:	IL1 receptor
IL-1Ra:	IL-1 receptor antagonist
IL-1RacP:	IL-1 receptor accessory protein
IPTG:	isopropyl β-D-1 thiogalactopyranoside
IRAK:	IL-1 receptor associated kinase
IRF:	interferon-regulatory factor
IPTG:	isopropyl β-D-1 thiogalactopyranoside
ISRE:	interferon-stimulated response element
IκB:	inhibitor of κB
JNK:	c-Jun N-terminal kinase
Kb:	kilobase
kD:	kilodalton
LB:	lysogeny broth
LPS:	lipopolysaccharide
LRR:	leucine-rich repeat
MAPK:	mitogen activated protein kinase
MAPKK:	MAPK kinase
MAPKKK:	MAPKK kinase
MD2:	myeloid differentiation protein2
MEF:	mouse embryonic fibroblast
min:	minute
MKK:	mitogen activated protein kinase kinase

mM:	milli molar
M-MLV:	moloney murine leukemia virus
mRNA:	messenger RNA
MSCV:	murine stem cell virus
MTT:	3- 4 5-dimethylthiazol-2-yl -2 5-diphenyltetrazolium bromide
MyD88:	myeloid differentiation protein 88
Na_3VO_4:	sodium orthovanadate
NaCl:	sodium chloride
NADPH:	nicotinamide adenine dinucleotide phosphate
Nec-1:	necrostatin-1
NEMO:	NF-κB essential modulator
NF-κB:	nuclear factor kappa B
ng:	nanogrammes
NIK:	NF-κB Inducing Kinase
Ni-NTA:	nickel-nitrilotriacetic acid
NK:	natural killer
NLS:	nuclear localization sequence
nM:	nanomolar
NOX1:	NADPH oxidase1
NOXA1:	NOX activator 1
NOXO1:	NOX organizer 1
nt:	nucleotide
NTP:	nucleotide triphospahte
OD:	optical density
PAGE:	polyacrylamide gel electrophoresis
PAMP:	pathogen-associated molecular pattern
PARP:	poly-ADP-ribose- polymerase
PBMC:	peripheral blood mononuclear cell
PBS:	phosphate buffered saline
PCR:	polymerase chain reaction
pDC:	plasmacytoid dendritic cell
PGN:	peptidoglycan
PGRP:	peptidoglycan recognition protein
PMSF:	phenylmethylsulfonyl fluoride
Poly I:C:	polyinosinic-polycytidylic acid
PRR:	pattern-recognition receptor
PYGL:	glycogen phosphorylase
RANTES:	regulated upon activation normal T cell expressed and secreted
RHIM:	RIP homotypic interaction motif
RING:	really interesting new gene
RIP:	receptor interacting protein
RNA:	ribonucleic acid
ROS:	reactive oxygen species
RPMI:	roswell park memorial institute
RT:	room temperature; reverse transcriptase
SAPK:	stress-activated protein kinase
SARM:	sterile α and heat-armadillo motifs

SDS:	sodium dodecyl sulphate
SIMRA:	stabilized immune-modulatory RNA
siRNA:	small interfering RNA
SOC:	super optimal broth with catabolic repressor
SOCS:	suppressor of cytokine signalling
SODD:	silencer of death domain
ssRNA:	single-stranded RNA
SUMO:	small-ubiquitin-related-modifier
TAB:	TAK1-binding protein
TACE:	TNFα-converting enzyme
TAE:	Tris-acetate-EDTA
TAK1:	TGF-β-activated protein kinase 1
TANK:	TRAF-family-member-associated NF-κB activator
Taq:	*Thermophilus aquaticus*
TBE:	Tris-Borate-EDTA
TBK1:	TANK binding kinase
TBS:	Tris-buffered saline
TBST:	Tris-buffered saline containing Tween 20
Ct:	threshold cycle
TD:	transactivation domain
TE:	Tris-EDTA
TEMED:	N N N' N' - Tetramethylethylene-diamine
TGF-β:	transforming growth factor-β
TIR:	Toll-IL-1 receptor domain
TIRAP:	TIR domain-containing protein
TLR:	Toll-like receptor
TMB:	3 3' 5 5'-Tetramethylbenzidine
TNF α:	tumour necrosis factor alpha
TNFR:	TNF receptor
Tollip:	Toll-interacting protein
TRADD:	TNF receptor –associated death domain
TRAF:	TNF receptor associated factor
TRAILR:	TNF-related apoptosis-inducing ligand receptor
TRAM:	TRIF-related adaptor molecule
TRIF:	TIR domain-containing adaptor inducing IFN-β
TUNEL:	terminal deoxynucleotidyl transferase mediated dutp nick end labeling
Ubc:	ubiquitin conjugating enzyme
USP21:	ubiquitin specific peptidase 21
UV:	ultraviolet light
UXT-V1	ubiquitously expressed transcript-v1
WT:	wild-type
XIAP:	X chromosome-linked IAP
Z-VAD-fmk:	benzyloxycarbonyl-valine-alanine-aspartate-fluoromethyl ketone
µg:	micro grammes
µl:	micro liter
µM:	micromolar

Chapter 1 General Introduction

1.1 The Mammalian Immune System

The mammalian immune system systematically eradicates infection through the cooperation of two components of immunity, innate and adaptive. The innate immune system consists of evolutionary conserved pattern recognition receptors (PRRs) that detect infection of micro-organisms and activate adaptive immunity. The adaptive immune system uses randomly generated, clonally expressed receptors with limitless specificity to clear infections (Medzhitov and Janeway, 1997). It is the combination of these two systems that make mammalian immunity extremely efficacious.

PRRs detect the presence of microbial infection to activate the appropriate innate immune response (Akira et al, 2006). The elements of the innate immune system comprise of anatomical, humoral and cellular barriers to infection. Anatomical barriers include the skin, internal epithelial layers acting as physical barriers to infection and mucosal layers which provide protection against inhaled or ingested micro-organisms. Secretery fluids such as saliva, tears and sweat all act as deterrents for microbial infection. If these barriers are compromised in any way infection may occur which leads to acute inflammation. Humoral factors play important roles in the inflammatory process and they are constitutively present at the site of infection. The complement system is an important component of the innate immune system and can lead to enhanced vascular permeability, recruitment of phagocytes and lysis of bacteria (Morgan et al, 2005).

The initiation of the inflammatory response results in the recruitment of many immune cells via the secretion of various chemo attractants. Neutrophils, macrophages, dendritic cells (DCs) and natural killer cells are recruited to the site of infection during inflammation. These immune cells serve as a link between adaptive and innate immunity by phagocytosing and presenting antigens to T and B cells of the adaptive immune system via the antigen presenting molecules MHC class I and II. Activation of the adaptive immune system relies on signals from the innate immune system in order to initiate the clonal expansion of antigen specific B and T cell lymphocytes which direct antibody and cellular immune responses.

The innate and adaptive immune systems are ideal partners because of the differing strategies they employ to recognize infection which provides complementary advantages and disadvantages to the host (Palm and Medzhitov, 2009). Adaptive

immunity uses random, diverse, clonally expressed receptors produced via somatic recombination of genes and therefore is highly effective in specifically targeting immune responses towards the infection which spares the surrounding uninfected host tissues. The innate immune system uses germ line encoded receptors to recognize invariant features of typical classes of microbes and is extremely efficient at distinguishing self from non-self (Janeway CA Jnr, 1989). However the non-clonal activation of the innate immune system has the potential to cause significant damage to self-tissues resulting in immunopathology, which is seen in autoimmune diseases such as arthritis, colitis and Lupus. As a result cells of the innate immune system are not able to detect every possible antigen; instead they have evolved to recognize highly conserved structural components of microbes that are not found in mammalian cells. These highly conserved structures are referred to as Pathogen Associated Molecular Patterns (PAMPs). It is the receptors of the innate immune system that recognize these PAMPs and trigger the first immune response to infection (Palm and Medzhitov, 2009).

1.2 Pattern Recognition Receptors

1.2.1Toll like Receptors

Toll like receptors were the first PRRs to be identified and as a result have become the best characterized PPRs (Akira et al, 2006). TLRs are type 1 transmembrane proteins that contain leucine rich repeats that mediate recognition of PAMPs, a transmembrane region and a cytosolic Toll-IL1/R (TIR) domain that activates downstream signaling pathways. TLRs are expressed on the cell surface or associated with intracellular vesicles such as the endoplasmic reticulum, endosomes, lysosomes and endolysosomes (Blasius and Beutler, 2010). To date 10 and 12 functional TLRs have been identified in human and mouse, respectively. Each TLR detects specific PAMPs derived from micro-organisms such as bacteria, viruses, mycobacteria, fungi and parasites. The different ranges of PAMPs recognized by TLRs are summarized in Table 1.1. TLR1, 2, 4, 5 and 6 are localized on the cell surface and largely recognize microbial membrane components whereas TLR3, 7, 8 and 9 are expressed within intracellular vesicles and recognize viral nucleic acids (Blasius and Beutler, 2010).

Upon TLR activation a specific set of adaptor proteins are recruited. These TIR domain containing proteins initiate downstream signaling events that lead to the production of pro-inflammatory cytokines, type 1 IFNs and chemokines (Kawai and Akira, 2010). Currently there are five known TIR adaptor proteins, myeloid differentiation primary response protein 88 (MyD88), MyD88 adaptor like (MAL), TIR domain containing adaptor protein inducing IFN-β (TRIF), TRIF related adaptor molecule (TRAM) and sterile A and HEAT-armadillo motifs (SARM). The specific response elicited by each TLR depends on the recruitment of a single, or a specific combination of TIR domain containing adaptor proteins. MyD88 is utilized by all TLRs, with the exception of TLR3, and the IL-1R to transmit signals culminating in NFκB and MAP kinase activation. TLR3 and TLR4 use the adaptor TRIF to activate a MyD88-independent pathway leading to the activation of NFκB and IRF3 and the induction of type 1 IFNs. It is on this basis that signaling through TLRs can be separated as MyD88-dependent or MyD88-independent.

Receptor	Ligands	Origin of ligands
TLR1	Tri-acyl lipopeptides	Bacteria, mycobacteria
	Soluble factors	Neisseria meningitides
TLR2	Lipoprotein/lipopeptides	A variety of pathogens
	Peptidoglycan	Gram-positive bacteria
	Lipoteichoic acid	Gram-positive bacteria
	Lipoarabinomannan	Mycobacteria
	A phenol-soluble modulin	*Staphylococcus epidermidis*
	Glycoinositolphospholipids	*Trypanosoma cruzi*
	Glycolipids	*Treponema maltophilum*
	Porins	Neisseria
	Zymosan	Fungi
	Atypical LPS	*Leptospira interrogans*
	Atypical LPS	*Porphyromonas gingivalis*
	LPS	*Porphyromonas gingivalis*
	HSP70	Host
TLR3	Double-stranded RNA	Virus
TLR4	LPS	Gram-negative bacteria
	Taxol	Plant
	Fusion protein	RSV
	Envelope proteins	MMTV
	HSP60	*Chlamydia pneumoniae*
	HSP60	Host
	HSP70	Host
	Type III repeat extra domain A of fibronectin	Host
		Host
	Oligosaccharides of hyaluronic acid	Host
	Polysaccharide fragments of heparan sulfate	Host
	Fibrinogen	
TLR5	Flagellin	Bacteria
TLR6	Di-acyl lipopeptides	Mycoplasma
TLR7	Imidazoquinoline	Synthetic compounds
	Loxoribine	Synthetic compounds
	Bropirimine	Synthetic compounds
	Sigle-stranded RNA	Virus
TLR8	Imidazoquinoline	Synthetic compounds
	Sigle-stranded RNA	Virus
TLR9	CpG DNA	Bacteria
TLR10	N.D.	N.D.
TLR11	Uropathogenic *E.coli* strains	Uropathogenic bacteria
	Profilin-like molecule	

Table 1.1 Toll-like receptors and their ligands

N.D.: not determined (Adapted from Akira and Takeda, 2004)

1.2.2.1 MyD88 dependent signalling

MyD88 contains a C-terminal TIR domain which enables it to bind to TLRs and an N-terminal death domain (DD) which allows MyD88 to bind other DD-containing proteins such as the IL-1 receptor associated kinases (IRAKs) (Dunne et al, 2009). TLR2 and TLR4 use MAL as an additional adaptor protein to recruit MyD88. Activated MyD88 interacts with IRAK4 which recruits and activates IRAK1 through phosphorylation. IRAK1 then phosphorylates itself and leads to the activation of TRAF6 (Moynagh, 2009) IRAK1 and 4 are also regulated by the Pellino protein family. The stimulation of IL-1R/TLR results in the interaction between Pellinos and IRAK1. This results in the phosphorylation of the Pellinos by IRAK which activates their E3 ligase activity and the subsequent ubiquitination of IRAK1 (Butler et al, 2007). TRAF6 is oligomerized and ubiquitinated following activation by IRAK1. Ubiquitinated TRAF6 then recruits the transforming growth factor-β (TGF-β) activated kinase (TAK1) complex which is made up of TAK1 and its associated adaptor proteins TGF-β binding proteins TAB1,2,3 (Mendoza et al, 2008) and the recently described TAB4 (Prickett et al, 2008). Activated TAK1 can then activate the inhibitor of Iκb kinase (IKK) complex, p38, c-jun N-Terminal kinase (JNK) and the Mitogen Activated Protein Kinase (MAPK) (Wang et al, 2001). The IKK complex consists of IKK-α and IKK-β, the two catalytic subunits and the regulatory subunit, Nuclear Factor Kappa B Essential Modifier (NEMO). NEMO is associated with TRAF6 and is capable of binding ubiquitin chains for stability of the IKK complex (Crosetto et al, 2006). The IKKs directly phosphorylate members of the inhibitory IκB family which normally sequester NFκB in an inactive form in the cytoplasm (Vi et al, 1998). The phosphorylation of the IκB proteins represents a signal for polyubiquitination followed by their degradation by the 26S proteasome which enables the release of NFκB and its subsequent translocation to the nucleus (Medzhitov et al, 1997). While most TLRs use the MyD88 signaling pathway, TLR3 exclusively uses the MyD88-independent pathway. Interestingly TLR4 utilizes the MyD88-dependent and independent pathways to induce type 1 IFNs.

1.2.2.2 MyD88 Independent signalling

TLR4 is the only TLR that can activate both the MyD88 dependent pathway and MyD88 independent pathway (Kawai et al, 1999). TLR4 activates both pathways by using four different adaptor proteins. Upon activation of TLR4 by its ligand LPS, it initially recruits Mal and MyD88, Mal localizes to the plasma membrane where it interacts with phosphatidylinositol 4,5-bisphosphate (PIP2) and serves as a bridge between MyD88 and TLR4 (Barton and Kagan, 2009). MyD88 then recruits IRAKs and TRAF6 to activate the TAK1 complex that results in the early phase activation of NFκB and MAP kinases (Kawai and Akira, 2010). TLR4 is then endocytosed and delivered to intracellular vesicles to form a complex with its other two adaptors TRIF and TRAM. TRAM, like MAL, acts as a bridge between TLR4 and TRIF. TRIF then recruits the protein kinases TBK1 and IKKε which catalyze the phosphorylation of IRF3 leading to the induction of type 1 IFNs (Barton and Kagan, 2009).

TLR3 is the only TLR that is completely MyD88 independent and activation of TLR3 results in the recruitment of TRIF and subsequent activation of the kinases TBK1 and IKKε (Fitzgerald et al, 2003). TRAF3 also functions in the TLR3 pathway to link TRIF and TBK1 (Saha et al, 2006). Receptor interacting protein 1 (RIP1) is also an important adaptor protein in TLR3 signaling and has been shown to be critical in the activation of NFκB by TLR3 via its interaction with TRIF (Meylan et al, 2003). Pellino 1 has also been implicated in TLR3 signalling via RIP1. Pellino1 E3 ligase activity is required for the ubiquitination of RIP1 to facilitate the downstream activation of NFκB. Pellino 1 deficient mice were shown to have impaired NFκB activation in response to TLR3 stimulation (Chang et al, 2009). MyD88 dependent and independent signalling is summarized in Figure 1.1.

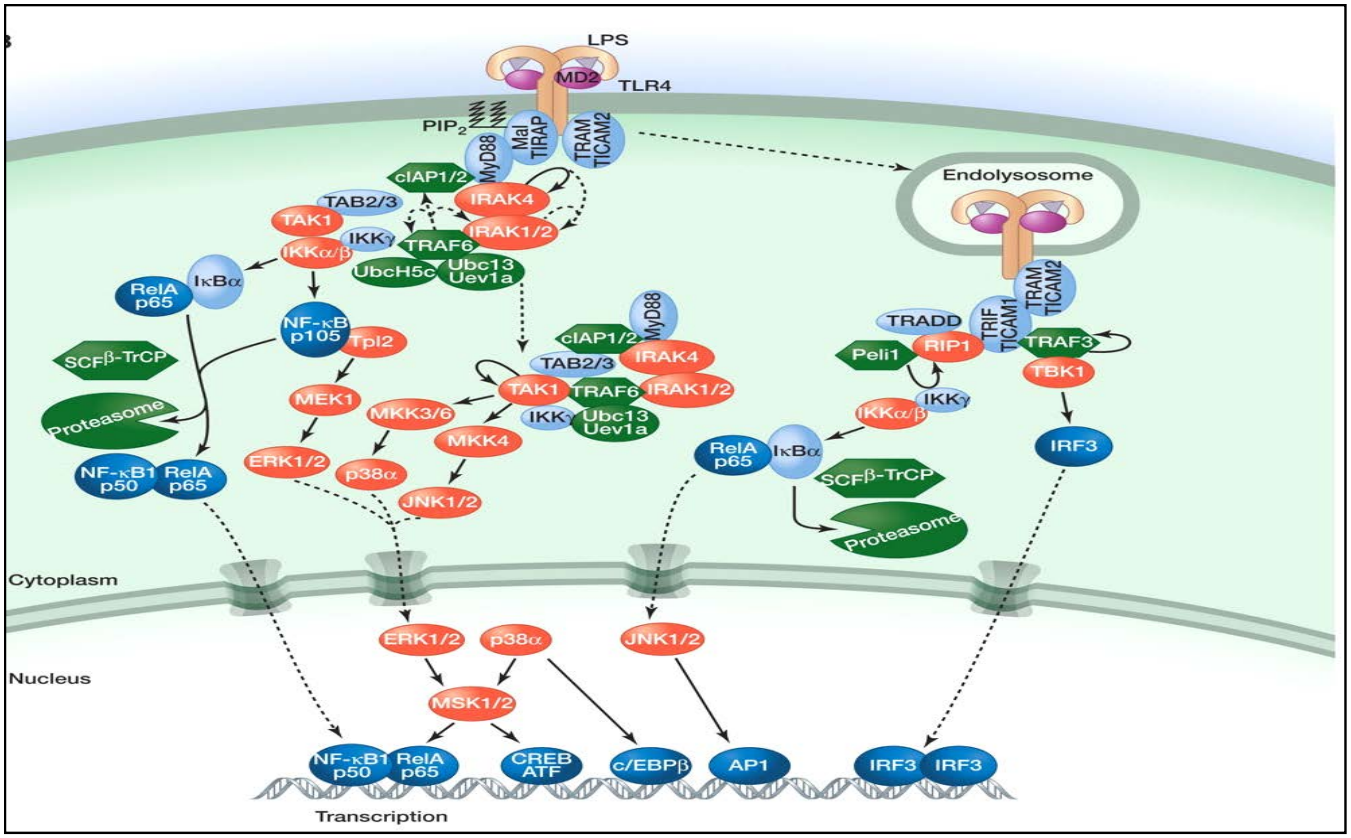

Figure 1.1 MyD88 dependent and Independent signalling

TLR4 engagement by LPS results in the recruitment of MYD88 and the rapid assembly of a large multiprotein complex at the cytoplasmic face of the plasma membrane. Complex formation results in TRAF6 activation and K63 ubiquitination of cIAP proteins, which enhances their K48-specific ubiquitin ligase activity towards TRAF3. Proteasomal degradation of TRAF3 results in cytoplasmic translocation of the MYD88-associated multiprotein complex, thereby allowing activation of TAK1, its downstream MAPKs and the eventual induction of pro-inflammatory cytokines and chemokines. Activated TLR4 also translocates to an endosomal compartment, and this is accompanied by the recruitment of TIR domain-containing adaptor protein inducing IFN-β (TRIF), TRAF3 and other proteins. Unlike the MYD88 complex, the TRIF-assembled complex does not contain cIAP and its formation results in the activation and K63 ubiquitination of TRAF3. This causes the activation of TBK1 and IKKε, which phosphorylate interferon regulatory factor 3 (IRF3) to induce the type I IFN response. TRIF-dependent signalling also leads to the activation of NFκB, JNK and p38, albeit with slower kinetics than MyD88 signalling (Adapted from Newton and Dixit, 2011).

1.2.2NOD like Receptors

Nucleotide-binding oligomerization domains like receptor (NLR) proteins are a family of proteins with a wide range of functions in innate immune signaling. The NLR receptors are grouped based on their shared Nucleotide binding domain (NBD) and a leucine rich repeat (LRR) domain (Flavell et al, 2011). Two well-studied receptors in the NLR family that function in the antimicrobial response are NOD1 and NOD2. NOD1 and NOD2 are cytosolic receptors that recognize distinct building blocks of peptidoglycan, a polymer that consists of glycan chains cross linked via short peptides (Fritz et al, 2006). Both NOD1 and NOD2 are highly expressed in epithelial cells and antigen presenting cells such as Neutrophils, macrophages and dendritic cells (Kanneganti et al, 2007). NOD2 expression is induced in response to TLR ligands such as LPS and by inflammatory cytokines such as TNF-α, IL-17 and IFN-γ (Flavell et al, 2011). NOD1 and NOD2 have been implicated in the recognition of different bacterial species such as *Helicobacter Pylori* (Viala et al, 2004), *Clostridium difficile* (Hasegawa et al, 2011), *Legionella Pneumophilia* (Berrington et al, 2010), *Listeria monocytogenes* (Boreca et al, 2007) and *Staphylococcus. Aureus* (Travassos et al 2005).

In contrast to the NOD proteins other members of the NLR group form signaling complexes which are known as 'Inflammasomes'. The formation of an inflammasome results in the activation of Pro-Caspase 1 and the subsequent processing of Pro-IL1β and Pro-IL18 for secretion of their mature forms (Flavell et al, 2011). The activation of the inflammasome is a two-step process. The first signal is required to activate the transcription of the genes encoding the precursor forms of IL1β and IL18 and is usually provided by TLR and NFκB signaling. The second signal is required for inflammasome assembly. However much debate still exists on the second signal. Danger signals such as mitochondrial DNA and mitochondrial ROS from defective mitochondria have been proposed as signals for IL-1 processing (Nakahira et al, 2011; Zhou et al, 2011) The inflammasome NLRs that function as sensors of exogenous and endogenous PAMPs and DAMPs include NLRP1, NLRP3, NLRC4 and AIM2 (Sutterwala et al, 2007).

1.2.3 RLRs (RIG-I like receptors)

The RIG-I like receptors are a family of DExD/H box RNA helicases that function as intracellular sensors of PAMPs within viral RNA. The RLRs signal to downstream IRF transcription factors to drive type 1 IFN production (Gale et al 2001). To date 3 RLRs have been discovered, RIG-I (Retinoic acid inducible gene 1), Mda-5 (Melanoma differentiation associated factor 5) and LGP2 (Laboratory of genetics and physiology 2). RLR expression is normally maintained at low levels in the cell. However upon IFN exposure and after viral infection the level of RLR expression is greatly increased (Kang et al, 2001). RIG-I and Mda5 recognize dsRNA viruses and their activation leads to the production of type 1 IFN. LGP2 is a helicase that can detect dsRNA but is unable to transmit a downstream signal and has been shown to function as a negative regulator of RIG-I and Mda5 (Thompson and Locarnini, 2007).

RIG-I and Mda5 induce type 1 IFN production in response to viral infection via a common adaptor protein known as mitochondrial anti-viral signaling protein (MAVS). The interaction of RIG-I and Mda5 with MAVS facilitates the recruitment of the RLRs to Mitochondria associated membranes where they initiate the downstream signaling events to form the MAVS signalosome to drive IFN production (Hiscott et al, 2006). TRAF3 binds to the TRAF interacting motif (TIM) which is found in the Proline rich region of MAVS and recruits the IRF3 activating kinases TBK1 and IKKε (Hacker et al, 2006). More recently it has become evident that RLR signaling can be separated into two signaling pathways that results in IFNβ production and IL-1 and IL-18 maturity. The latter pathway results in the binding of RIG-I to the adaptor ASC to activate Caspase 1 (Poeck et al 2010).

Like TLR signaling, RLR signaling pathways are tightly regulated by a number of different mechanisms to prevent aberrant IFN production that can lead to immune toxicity or immune disorders. Post-translational modifications such as ubiquitination or deubiquitination of RLR pathway components are major regulators of the pathway. RNF135 is an ubiquitin ligase that interacts with RIG-I but not Mda5 (Oshiumi et al, 2009). It is has been shown to mediate the conjugation of K63 linked polyubiquitin chains within its CARD domain at K154, K164 and K172 during viral infection. This modification has also been shown to stabilize the RIG-I and MAVS interaction to induce IFN production (Gack et al, 2008). RNF125 is another ubiquitin ligase that

utilizes the E2 enzyme UbcHSc to ligate K48 linked ubiquitin chains onto RIG-I, Mda5 and MAVS to initiate proteasomal degradation (Arimoto et al, 2007). RIG-I signaling is also negatively regulated by the ubiquitin editing enzyme A20 via its C-terminal domain (Lin et al, 2006). TRAF3 activity is also tightly regulated in RLR signaling. The E3 ligase Triad3a targets TRAF3 for degradation via K48 ubiquitination during viral infection (Wakhaei et al, 2009). TRAF3 is also regulated by OTUB1/OTUB2 (Li et al, 2010), DUBA (Kagayaki et al, 2007) and the IFN inducible gene FLN29 (Mashima et al, 2005) in an ubiquitination dependent manner. More recently the ubiquitin binding protein NEMO has been shown to negatively regulate RIG-I signalling when it is linearly ubiquitinated by the Linear Ubiquitin Assembly Complex (LUBAC) (Belgnaoui et al, 2012).

1.3 TNFR1 Signalling

Inflammation is an essential component of innate immunity and the host response to infection. In response to viral or bacterial infection innate cells produce potent pro-inflammatory cytokines such as TNF-α and IL-1ß which trigger the inflammatory response (Serhan et al, 2008). TNF-α initiates a complex cascade of signaling events that lead to the induction of proinflammatory cytokines, cell proliferation, and differentiation or programmed cell death (Chen and Goeddel, 2002). The binding of TNF to its receptor TNFR1 leads to association of TNF-R1 associated death domain protein (TRADD) (Hsu et al, 1995) with the receptor complex followed by recruitment of FAS associated death domain protein (FADD), TRAF2 and RIP1 (Hsu et al, 1996). Whilst FADD can trigger activation of Caspase 8 leading to cell apoptosis (Wilson et al, 2009), TRAF2 and RIP1 mediate the activation of NFκB and MAP kinase in response to TNF-α (Karin and Gallagher, 2009). The K63 and linear ubiquitination of RIP1 facilitates the recruitment of IKK complexes (Ea et al, 2006) and subsequent activation of NFκB. However this model has been challenged in a recent study that revealed RIP1 is not required for activation of NFκB in response to TNF-α (Wong et al, 2010). The TNF pathway is heavily dependent on ubiquitination and until recently it was thought that K63 and K48 ubiquitination were the two linkages that regulated the pathway. Recent reports now show linear ubiquitination of

TNF components as a critical step in the activation of NFκB by TNF-α (Tokunaga et al, 2009; Tokunaga and Iwai, 2012; Ikeda et al, 2011)

LUBAC is recruited to the TNFR via ubiquitin chains that are attached to components of the TNFR1 signalling complex such as RIP1 and NEMO (Lo et al, 2009). The recruitment of LUBAC results in the stabilization of the TNFR1 signalling complex (Haas et al, 2009) LUBAC consists of three components, the heme oxidized IRP2 ubiquitin ligase-1 (HOIL-1), HOIL-1 interacting protein (HOIP) and the newly characterized SHANK associated RH-domain interacting protein (SHARPIN) (Dixic et al, 2011; Iwai et al, 2011;Walczak et al, 2011). LUBAC is currently the only known E3 ligase that promotes the synthesis of head-to-tail linear linked chains and can use multiple E2 conjugating enzymes, such as UbcH5, E2-25 and UbcH7, to generate head-to-tail ubiquitin conjugates (Kirisako et al, 2006). HOIP has been shown to be the major contributor to LUBAC binding to ubiquitin chains (Haas et al, 2009) whereas SHARPIN and HOIL-1 mediate the ubiquitination of NEMO to activate the IKK complex and NFκB (Dixic et al, 2009). It has been suggested that ubiquitination of cIAPs, following TNF stimulation, leads to recruitment of LUBAC and linear ubiquitination of components of the TNFR complex leading to persistent activation of NFκB and inhibition of TNF induced cell death (Haas et al, 2009). The importance of the LUBAC complex in the TNF pathway has been highlighted through the use of HOIL-IL and SHARPIN knockout mice (Togunaka et al, 2009; Gerlach et al, 2011; Ikeda et al, 2011). However a mouse lacking all 3 LUBAC components has yet to be described and we thus await a full understanding of the function of the LUBAC complex in the TNF pathway. K11 polyubiquitination has also been described in TNF signaling (Dynek et al, 2010), which suggested that K11 linked chains play a role in signal transduction as well as degradative signals in cell cycle regulation (Kirkpatrick et al, 2000). The E3 ligase cIAP1 facilitates the K11 linked ubiquitination of RIP1 in TNFR1 signalling (Dynek et al, 2010).

As mentioned the activation of the TNFR1 can also lead to programmed cell death. Ligand binding to the TNFR triggers the assembly of the death-inducing signaling complex (DISC) (Guicciardi and Gores, 2009). Recruitment of the adaptor FAS-associated DEATH domain protein (FADD) or TNFR1 associated DEATH domain protein and Caspase 8 leads to DISC formation. Caspase 8 is activated and the death domain signal is amplified by the subsequent proteolytic activation of the downstream effector caspases 3 and 7 which culminates in apoptotic death (Wertz et

al, 2011). In the presence of cIAP proteins TNFR1 predominantly activates canonical NFκB and MAPK proinflammatory and cell survival whilst the absence of cIAP proteins transforms TNF-α into a pro-apoptotic ligand (Bertrand et al, 2008). In the absence of cIAPs RIP1 is not ubiquitinated and can associate with FADD and Caspase 8 to form a secondary death promoting signalling complex that dissociates from the receptor (Peterson et al, 2007). Alternatively and independently of Caspase 8 activity, non-ubiquitinated RIP1 can bind to RIP3 to promote programmed necrosis or necroptosis (Vandenabeele et al, 2010). This form of cell death relies on the kinase activity of RIP1 and RIP3 (Cho et al, 2009).

Like TLR signalling the TNFR1 pathway is also heavily regulated in a ubiquitin-dependent manner. A20 participates in a negative feedback loop to attenuate TNF-α induced NFκB activation (Krikos et al, 1992). The A20 signalling complex targets RIP1 for deubiquitination and degradation in a unique system via two different domains. A20 first removes K63 chains from RIP1 via its OUT DUB domain and promotes the addition of K48 chains on RIP1 via its zinc-finger-4 motif (Wertz et al, 2004). A20 carries out its dual ubiquitin editing function via its interaction with the A20 complex proteins, Tax1bp1, RNF11, Itch and the ABIN-1. RNF11 is required for the association between RIP1 and A20 and interacts with Tax1bp1 and A20 in a TNF-α dependent manner (Shembade et al, 2009). An important PPxY motif in RNF11 is required for the formation of the A20 signalling complex and for termination of NFκB signalling. ABIN-1 was initially described in a yeast-2-hyrid screen as an A20 interacting protein (Heyninck et al, 1999). ABIN-1 serves as an adaptor molecule between A20 and NEMO to facilitate its deubiquitination (Mauro et al, 2006). Similarly to the A20 complex the DUB CYLD has been shown to form a complex with the A20 complex protein Itch, through critical PPxY motifs to negatively regulate the TNF pathway via the deubiquitination and K48 ubiquitination of TAK1 (Ahmed et al, 2011). CYLD has also been shown to deubiquitinate RIP1 (Vucic et al, 2011). However the exact role of CYLD in RIP1 deubiquitination remains unclear as CYLD deficient cells have revealed no difference in TNF-α induced RIP1 ubiquitination (Zhang et al, 2006). However CYLD has been shown to be required for programmed necrosis (O'Donnell et al, 2012). Also CYLD deubiquitinates linear ubiquitin chains and may play a role in regulating LUBAC (Haas et al, 2009). A schematic representation of the TNF pathway is summarised in Figure 1.2.

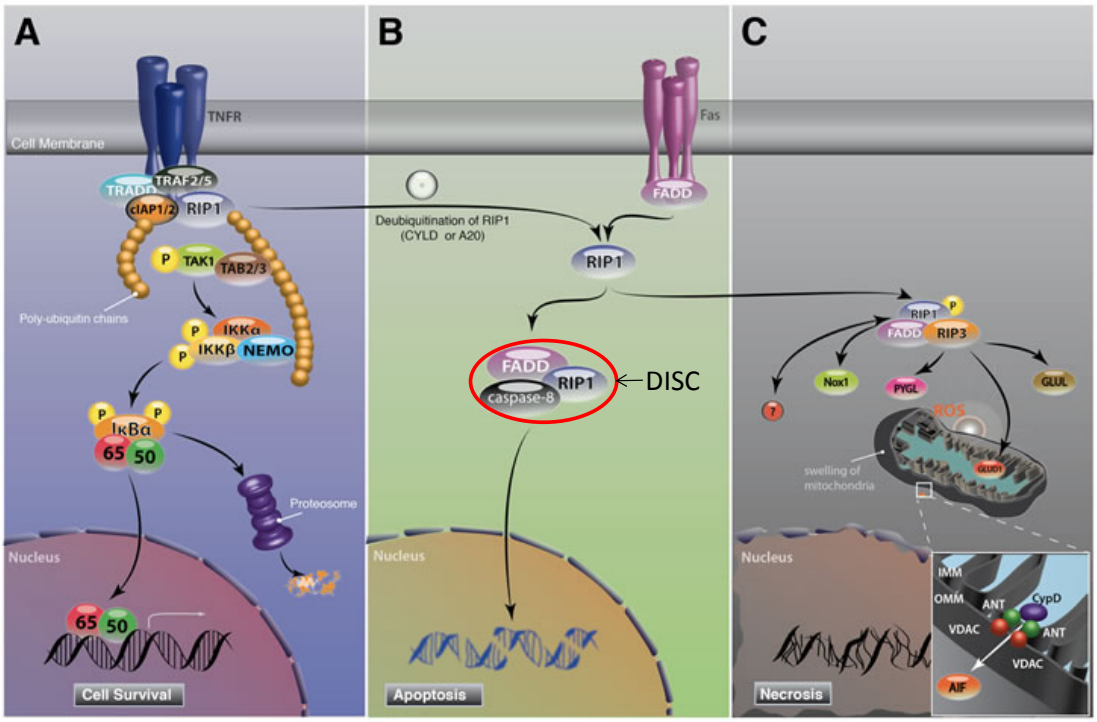

Figure 1.2 TNFR1-elicited signalling pathways.

A. In response to TNF-stimulation, RIP1 is recruited to TNFR and forms a membrane associated complex I with TRADD, TRAF2/5 and cIAP1/2, which in turn leads to polyubiquitination of RIP1 and pro-survival NFκB activation. B. when RIP1 is not ubiquitinated by A20 or CYLD, deubiquitination of RIP1 leads to the formation of cytosolic DISC with FADD and caspase-8. Activation of caspase-8 in DISC leads to apoptosis induction. During apoptosis, RIP1 is cleaved and inactivated by caspase-8. C. In conditions where caspases are blocked or cannot be activated efficiently, RIP1 binds to RIP3 leading to necrosis. (Adapted from Murakami, 2011).

1.4 NFκB

In innate immune signaling NFκB is activated via two distinct pathways termed the Canonical or Classical NFκB pathway or the non-canonical or non-classical pathway. The canonical NFκB pathway is activated by most TRAF dependent signaling pathways whereas the non-canonical pathway relies on activation by a set of TNFRs such as CD40 and BAFFR and the Lymphotoxin-β-receptor (LTβR). The classical NFκB pathway regulates the expression of a number of target genes that function in immune responses, cell survival and inflammation. The non-canonical pathway is mainly involved in the in the regulation of lymphoid organ development, adaptive immune responses and B-cell survival (Bonizyei et al, 2004).

The NFκB family of transcription factors consists of NFκB1 (p50 and its precursor p105), NFκB2 (p52 and its precursor p100), p65, c-Rel and Rel-B, all of which contain an N-terminal Rel homology domain (RHD) which mediates homo and heterodimerization as well as sequence specific DNA binding. p65, c-Rel and Rel-B also contain a C-terminal transcription activation domain (TAD) whereas p52 and p50 subunits do not and rely on other factors to positively regulate transcription (Hayden and Ghosh, 2008). Rel-B preferentially dimerizes with p100 and its processed form p52 (Senfitleben et al 2001). P65 and c-Rel heterodimerize with p50 (Karin et al, 2000).

The inhibitors of NFκB, the IκB proteins sequester IκB dimers in the cytoplasm of resting cells. The IκB proteins consist of IκB-α, IκB-β and IκB-ε (Karin et al, 2009). The IκB proteins are characterized based on the presence of multiple ankyrin repeats that mediate binding to NFκB dimers. A number of post-translational modifications at different sites on the dimers including phosphorylation and acetylating further modulate DNA binding and transcriptional activities (Perkins, 2006). The three major IκBs undergo signal-induced proteasomal degradation (Hoffman, 2002). IκB-α is degraded in response to pro-inflammatory stimuli such as LPS and TNF-α. Following degradation and subsequent translocation of the NFκB dimers a negative feedback loop induces de novo synthesis of IκB-α to enter the nucleus and associate with de-acetylated p-65: p50 dimers and shuttle them back into the cytoplasm (Chen et al, 2001). The degradation of the IκB proteins is an essential step in the activation of NFκB and is facilitated by the IKK complex as described previously.

1.5 MAP Kinases

MAPK pathways exist in all eukaryotic cells, regulating cellular activities from proliferation, differentiation, development and transformation to apoptosis. There are 3 extensively studied groups of mammalian MAPKs including the Extra Cellular Signal-Regulated Kinase (ERK), JNK/SAPK and p38 MAPK. In general, ERK1 and ERK2 are activated in response to growth factors and phorbol esters and function in regulating meiosis, mitosis, and post-mitotic processes in differentiated cells (Jonhson and Lapadat, 2002). The JNK and p38 kinases are more responsive to stress stimuli such as cytokines, ultraviolet irradiation, heat shock, and osmotic shock and are involved in cell differentiation and apoptosis (Chen et al, 2009). Each family of MAPKs is composed of a set of three evolutionarily conserved kinases, which are activated in series: a MAPK, a MAPKK (MAPK kinase) and a MAPKKK (MAPKK kinase). To date, at least 14 MAPKKKs, 7 MAPKKs, and 12 MAPKs have been identified in mammalian cells (Widmann et al, 1999). Stimuli from outside the cell initiate the cascade in which MAPKKK phosphorylates and activates a dual-specificity protein kinase (MAPKK) that, in turn, phosphorylates and activates a MAP kinase. MAPK signalling is summarised in Figure 1.3.

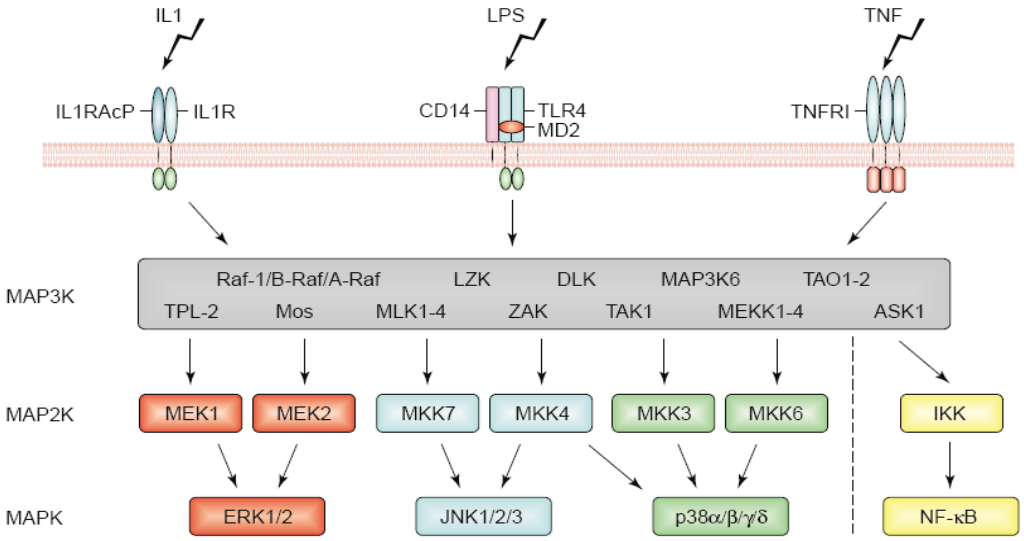

Figure 1.3 MAP Kinase Activation by innate immune receptors

Activation of TLRs, IL-1R and TNFR initiate the MAPK cascade in which MAPKKK phosphorylates and activates a dual specificity protein kinase (MAPKK) that, in turn. Phosphorylates and activates a MAPK. The MAPK cascade is determined by the substrate selection. (Adapted from Symons et al, 2006)

1.6 Interferon Regulatory Factors (IRFs)

The activation of PRR pathways can also lead to the activation of the Interferon regulatory factors (IRFs) family of transcription factors. To date nine IRFs have been identified in humans (Taniguchi et al, 2001). IRFs are involved in the regulation of cell cycle, apoptosis and tumour suppression; however they are best known for their roles as drivers of type 1 IFN expression that is essential in the innate anti-viral response (Honda et al, 2006).

IRF3 and IRF7 to date have been the most intensely studies members of the IRF family and have key roles in initiating the transcription of the type 1 IFNs, IFN-α and IFN-β in response to viral infection. Activation of IRF3 and IRF7 is mediated by the phosphorylation of C-terminal serine residues by the two IKK related kinases TBK1 and IKKε (Fitzgerald et al, 2003). IRF3 primarily activates the IFN promoter in tandem with other transcriptional factors such as NFκB. Once IFN-β is produced it subsequently activates the IFN pathway which results in the formation of IFN-stimulated gene factor 3 (ISGF3). ISGF3 in turn induces the expression of IRF7 which is then subject to phosphorylation in a similar manner to IRF3 (Moynagh, 2005). Plasmacytoid Dendritic cells (pDCs) are specialized at producing extremely high levels of type 1 IFNs in response to viral challenge (Liu et al, 2005). pDCs are unique in expressing high basal levels of IRF7 and this facilitates high induction of type 1 IFNs following stimulation of TLR7, 8 and 9 (Honda, 2005).

1.7 Ubiquitination

Ubiquitination is a post-translational modification that results in the attachment of 8kDa ubiquitin proteins, in a variety of lengths and conformations to regulate cell signaling (Picart and Fushmann, 2004). The process of ubiquitination is now recognized as an important regulator of processes such as cell cycle progression, apoptosis, cell proliferation, signal transduction and DNA damage responses (Taylor and Jobin, 2005). Ubiquitination occurs in a three step process catalyzed by three different enzymes E1, E2 and E3. The E1 enzyme first activates the ubiquitin molecule by covalent attachment to the ubiquitin moiety via a thiol-ester bond. The

activated ubiquitin can then be transferred to an E2 ubiquitin conjugating enzyme. The E2 enzyme-ubiquitin complex can then interact with an E3 ubiquitin ligase that facilitates the transfer of the ubiquitin protein to a lysine residue on the target protein. There are 2 known E1 enzymes that activate ubiquitin molecules for virtually all mammalian ubiquitination events. Approximately 38 E2 enzymes are predicted to exist and over 600 E3 ligases (Ye and Rape, 2009). E3 ubiquitin ligases confer substrate specificity to the ubiquitin reaction by binding to and transferring the ubiquitin molecule to the substrate protein. The ubiquitination process is summarized in Figure 1.4.

Ubiquitination can occur in multiple forms including mono- and polyubiquitination. Mono-ubiquitination occurs when a single ubiquitin protein is attached via its C-terminal glycine residue to a lysine residue of a target protein. Polyubiquitination occurs when ubiquitin chains are formed by the sequential attachment of ubiquitin proteins to other ubiquitin molecules resulting in the formation of ubiquitin chains (Terzic et al, 2007). Ubiquitin contains 7 lysine residues (K6, K11, K27, K29, K33, K48 and K63) that can be targeted for further ubiquitination with the lysine linkage being important for dictating the function of the polyubiquitination process. Furthermore N-terminal amino group of ubiquitin can also be targeted by the C-terminal glycine of another ubiquitin thus forming distinct linear chains (Komande et al, 2009).

K48 polyubiquitin chains facilitate proteasomal degradation to terminate signaling whereas K63-linked chains regulate the activation of pro-inflammatory signaling (Zhou et al, 2003). More recently ubiquitin linkages such as K11 (Vucic et al, 2010) and K27 (Zotti et al, 2011) and linear ubiquitination (Ikeda et al, 2011), (Gerlach et al, 2011) have been highlighted as important linkages in the regulation of innate immune signaling.

The removal of ubiquitin residues from substrate proteins is another important regulatory process and is carried out by a number of de-ubiquitnating (DUBs) enzymes. DUBs are cysteine metalloproteases that hydrolyze the amide bond after the glycine 76 residue of ubiquitin (Glickman, 2002). There are approximately 100 DUBs encoded in the human genome (Skaug and Chen, 2009), subdivided into five families based on specific structural domains: ubiquitin C-terminal hydrolases (UCHs), ubiquitin-specific proteases (USPs), ovarian tumorproteases (OTUs), Josephins, and JAB1/MPN/MOV34 metalloenzymes (JAMMs) (Nijman et al, 2009). The UCH,

USP, OUT, and Josephin. DUBs are cysteine proteases, whereas JAMMs are zinc metalloproteases (Cope et al, 2002).

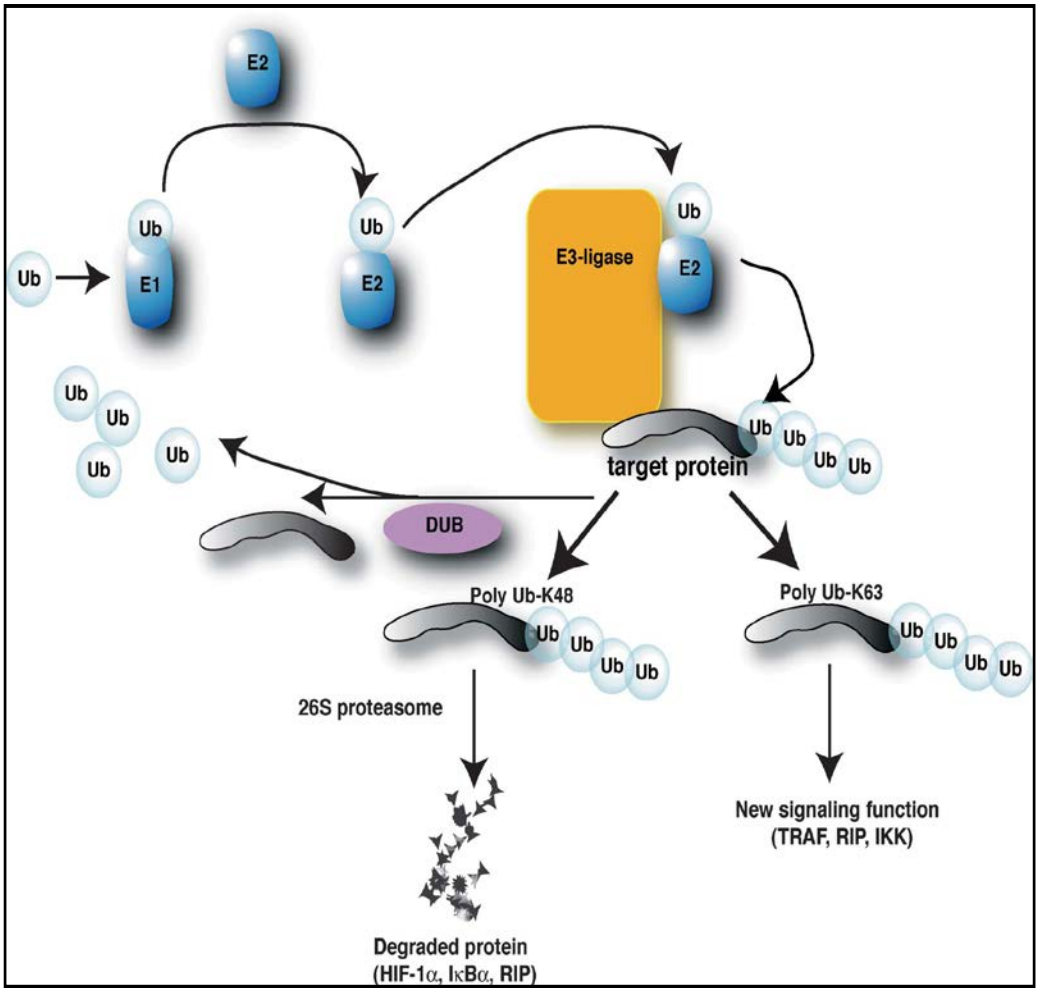

Figure 1.4 Ubiquitination system

Ubiquitination of a target protein is carried out by an enzymatic cascade comprised of E1, E2 and E3. E1 is a ubiquitin activating enzyme, activated ubiquitin is then transferred to a conjugating enzyme, E2, which in conjunction with an E3 ligase conjugates ubiquitin onto a lysine residue of the target protein. Poly-ubiquitin chains can be formed on target proteins by addition of subsequent ubiquitin proteins through one of seven lysine residues on the ubiquitin itself. (Adapted from Taylor and Jobin, 2005)

1.8 TRAF Proteins

TRAF proteins function as adaptors in innate immune signaling pathways and mediate responses to a large range of innate receptors such as TLRs, RLRs and TNFRs. Apart from their role as signaling adaptors TRAF proteins also serve as E3 ligases, a function which is extremely important for downstream signaling events and the activation of NFκB and the IRFs. TRAF1 and TRAF2 were initially identified based on their interaction with TNFR2 and their C-terminal region (TRAF domain) became the hallmark feature of the TRAF family (Rothe et al, 1994). Most TRAFs with the exception of TRAF1 share a N-terminal domain that consists of several zinc finger domains and an N-terminal RING domain. The RING domain is a common domain found in many E3 ubiquitin ligases and RING domain mediated protein ubiquitination has emerged as a key mechanism in TRAF dependent signal transduction (Bhoj and Chen, 2009). TRAF proteins can generate both K48 and K63 linked ubiquitin chains however to date only the direct generation of K63 chains by TRAF proteins in conjunction with the E2 enzyme Ubc13-UeV1a has been demonstrated *in vitro* (Zeng et al, 2009). Currently there are seven known proteins in the TRAF family, TRAF1-7 with TRAF3 and TRAF6 being especially relevant for the present study.

1.8.1 TRAF3

TRAF3 was originally described as a CD40 receptor interacting protein but unlike TRAF2, 5 and 6 it inhibits CD40-mediated activation of NFκB (Chen et al, 1995). Pattern recognition via different receptors such as TLRs and cytoplasmic RLRs results in the production of type 1 IFNs. Both receptor families use TRAF3 in order to induce the production of IFN-α and IFN-β. The TIR adaptors Myd88 and TRIF interact with TRAF3 to activate IRF3 and IRF7 to facilitate the transcription of IFN-α and IFN-β (Kawai and Akira, 2008).

TLR4 activation by LPS leads to the TRIF dependent K63 ubiquitination of TRAF3 in the endosome thus triggering activation of TBK1 and IKKε and resulting in phosphorylation and activation of IRF3 (Hacker and Karin, 2006). Mutational analysis of the TRAF3 RING domain resulted in loss of TRAF3 ubiquitination and its

ability to induce type I IFNIFN (Tseng et al, 2009). TRAF3 is also an important adaptor protein in TLR3 signaling. This was highlighted in a recent study that revealed a loss of function mutation in patients (R118W) which resulted in impaired IFN production to viral infection (Perez de Diego et al, 2010). In addition to TLR signaling TRAF3 also plays a role in RLR induced IFN production. Following ligand stimulation of RIG-I or Mda5 TRAF3 binds directly to MAVS which results in K63 linked ubiquitination of TRAF3 and subsequent recruitment of the IRF3 activating kinase TBK1 (Paz et al 2011).

The activation of TLR4 results in the degradation of TRAF3 which is facilitated by the K48 ubiquitination of TRAF3 by cIAP1. When TRAF3 is degraded it releases TAK1 and the MAP kinase pathway is activated (Tseng et al, 2009).The ability of TRAF3 to positively regulate IFN production and negatively regulate P38 and JNK activation is attributed to the compartmentalisation of the activated TLR complex. TRAF3 dependent activation of the IFN response is initiated by signaling complexes that are assembled by the adaptor TRIF at an endosomal location. Signaling complexes assembled by MyD88 are located at the plasma membrane. In the endosome TRAF3 is able to positively regulate the production of type 1 IFN however at plasma membrane locations TRAF3 negatively regulates MAP kinase signaling by sequestering TAK1 (Barton et al, 2009).

In addition to the negative regulation of the MAP kinases TRAF3 also functions as a negative regulator of non-canonical NFκB activation. TRAF3 is constitutively bound to NIK in resting cells. Following stimulation of the non-canonical pathway TRAF3 is degraded which results in the accumulation of NIK (Xiao et al, 2004). The increase in free NIK results in its autophosphorylation leading to IKK-α activation and the processing of p100 (Cheng et al, 2008). This mechanism has been highlighted in TRAF3 -/- B-cells which contain high levels of NIK and exhibit constitutive p100 processing which can be rescued in a TRAF3 NIK double -/- (Gardam et al, 2008). Further investigation also revealed a role for cIAPs and TRAF2 in the regulation of NIK by TRAF3. These roles were first highlighted in experiments showing that over expression of cIAP leads to NIK degradation and this was dependent on the RING domain and the TRAF2 interacting motif of cIAP (Verfolomeev et al, 2007). This suggested that TRAF2-dependent cIAP activation is required for NIK ubiquitination. It was later shown that TRAF3 acts a molecular bridge between cIAP and NIK (Vallabhapurapu et al, 2008) facilitating persistent K48

ubiquitination and degradation of NIK in unstimulated cells. Following stimulation of the cell with LPS cIAP1 is K63 ubiquitinated by TRAF2, causing cIAP1 to promote K48 ubiquitination and degradation of TRAF3 Newly synthesized NIK is then no longer able to interact with the cIAP-TRAF2 complex and is free to autophosphorylate and activate the IKK complex and trigger non-canonical activation of NFκB (Zarnegar et al, 2008).

1.8.2 TRAF6

TRAF6 is one of the most divergent members of the TRAF family sharing only a 30% sequence homology of its C-terminal TRAF domain with TRAFs 1-5. TRAF6 is an essential activator of the IKK complex and JNK in Toll/IL-1R signaling. It is a well characterized E3 ubiquitin ligase, is activated following oligomerization and promotes activation of TAK1 (Ninomiya-Tsuji et al, 1999). TRAF6 utilizes the E2 ubiquitin conjugating enzyme Ubc13-Uev1a to catalyze the formation of K63 linked polyubiquitin chains on target proteins (Kenny et al, 2007). TRAF6 has also been reported to play a role in TRIF mediated activation of NFκB (Sasai et al, 2010). However other studies have concluded that TRAF6 is dispensable for TLR3 signalling (Jiang et al, 2004). Such a discrepancy in relation to the role of TRAF6 may be due to cell specific roles for TRAF6 and/or functional redundancy of TRAF6 with other members of the TRAF family (Sato et al, 2003). TRAF6 has also been implicated in mitochondrial reactive oxygen species production (mROS) via its E3 ligase activity (West et al, 2011). Like TRAF3, TRAF6 is heavily regulated in a ubiquitin dependent manner. Following pathway activation TRAF6 is subject to regulation by deubiquitinating enzymes such as A20, Cezanne and OTUB1/2 (Dixit and Harhaj, 2012).

As previously discussed A20 can regulate TNF-induced NFκB activation via its interaction with RIP1 however A20 can also regulate TRAF6 through deubiquitination. A20 removes K63 chains from TRAF6 via its N-terminal domain resulting in the inhibition of signal transduction (Boone et al, 2004). This is further highlighted in A20-deficient MEF cells that exhibit persistent LPS induced TRAF6 ubiquitination (Shembade et al, 2010). In a similar manner the deubiquitinating

activity of the A20 like proteins Cezanne (Evans et al, 2001) and OTUB1/2 (Li et al, 2009) also facilitate the removal of K63 chains from TRAF6 to inhibit signaling.

1.9 Evolutionary Conserved Signalling intermediate in Toll (ECSIT)

In 1999 Kopp *et al* used murine TRAF6 as a bait in a yeast two-hybrid screen and reported the identification of a novel interacting protein termed ECSIT. Murine ESCIT was shown to positively regulate NFκB via an interaction with TRAF6 which enhanced the processing of MEKK1. Furthermore, over expression studies showed that mECSIT alone, can induce the activation of NFκB, whilst a dominant negative mutant inhibited NFκB activation by IL-1R and TLR pathways. The authors also demonstrated that *Drosophila* ECSIT (dECSIT) had a role in the insect immune system. dECSIT was found to bind to dTRAF6 and induce the production of antimicrobial peptides, defensin and attacin, therefore demonstrating that ECSIT is evolutionary conserved.

To further characterize the physiological role of mECSIT in innate immune signaling, null mutant mice were generated (Xiao et al, 2003). However *Ecsit* $^{-/-}$ embryos died in utero due to the absence of mesoderm formation, a phenotype that mirrored the Bmpr1$^{-/-}$. The deletion of mECSIT prevented the expression of Bmp target genes and blocked embryonic development at the beginning of gastrulation. The resulting study demonstrated that ECSIT is an important intermediate of Bmp signaling. The embryonic lethality of mECSIT -/- mice prevented further characterization of the *in vivo* role of ECSIT in innate immunity. In an attempt to further understand the role of ECSIT Xiao *et al* used a complementary approach to knock down the expression of ECSIT using short hairpin RNA. From this it was revealed that suppression of endogenous mECSIT resulted in impaired LPS induced NFκB activation.

In addition to these described roles in TLR and BMP signaling pathways a subsequent report described a mitochondrial role for ECSIT. Vogel *et al* showed that a 45kDa splice variant of ECSIT contains an essential N-terminal targeting signal that recruits ECSIT to the mitochondria where it interacts with the chaperone NDUFAF1 to facilitate the assembly and stabilization of the mitochondrial complex I. Complex I is one of five enzymatic complexes that are part of the oxidative phosphorylation

system, important for the generation of ATP from NADH and $FADH_2$ (Janssen et al, 2006). Knock down of ECSIT by siRNA resulted in decreased NDUFAF1 and complex I protein levels (Vogel et al, 2007).

A more recent study further implicated mECSIT as an important mediator of reactive oxygen species (ROS) production from the mitochondria in response to TLR1, 2 and 4 activation (West et al, 2011). Upon stimulation of the surface receptors TLR1, 2 and 4, production of mitochondrial ROS (mROS) was triggered. This was mediated by the interaction of TRAF6 and mECSIT signaling at the surface of the mitochondria. These data was supported by an earlier study that identified a role for ECSIT in oxidative phosphorylation complex I assembly in the mitochondria (Nouws et al, 2010). It was also noted that mECSIT had no role mROS production in response to endosomal TLR ligands and TNF-α. The role of ECSIT has mainly been described in the context of the mitochondria and contains an N-terminal mitochondria localization sequence which is required for its positive role in mitochondrial ROS production. Furthermore constructs lacking this N-terminal localization sequence exhibit a dominant negative effect and inhibit mitochondrial ROS production during TLR signalling (West et al, 2011). However no other information on different functional protein domains has been shown.

To date no characterization of hECSIT has been reported. The hECSIT gene had subsequently been cloned by the Molecular Immunology lab in NUI Maynooth and preliminary characterization of its role in TLR signaling had been undertaken. Human and murine forms of ECSIT share a sequence homology of 80% (Figure 1.5). Interestingly hECSIT was shown to negatively regulate TLR-induced activation of NFκB and this was associated with its ability to decrease the level of ubiquitinated TRAF6 (Nezira Delagic PhD thesis, 2011). This contrasted with the earlier described positive role of mECSIT in the NFκB pathway. Functional differences between evolutionary conserved protein are not without precedent with many observed differences between murine and human immune systems including differential expression of some TLRs (Masters and Hughes, 2004) and specificity for exogenous ligands including the TLR7/8 ligand CpG.

This thesis aims to build on the earlier findings from this lab and further investigate the role of hECSIT in innate immune signalling pathways.

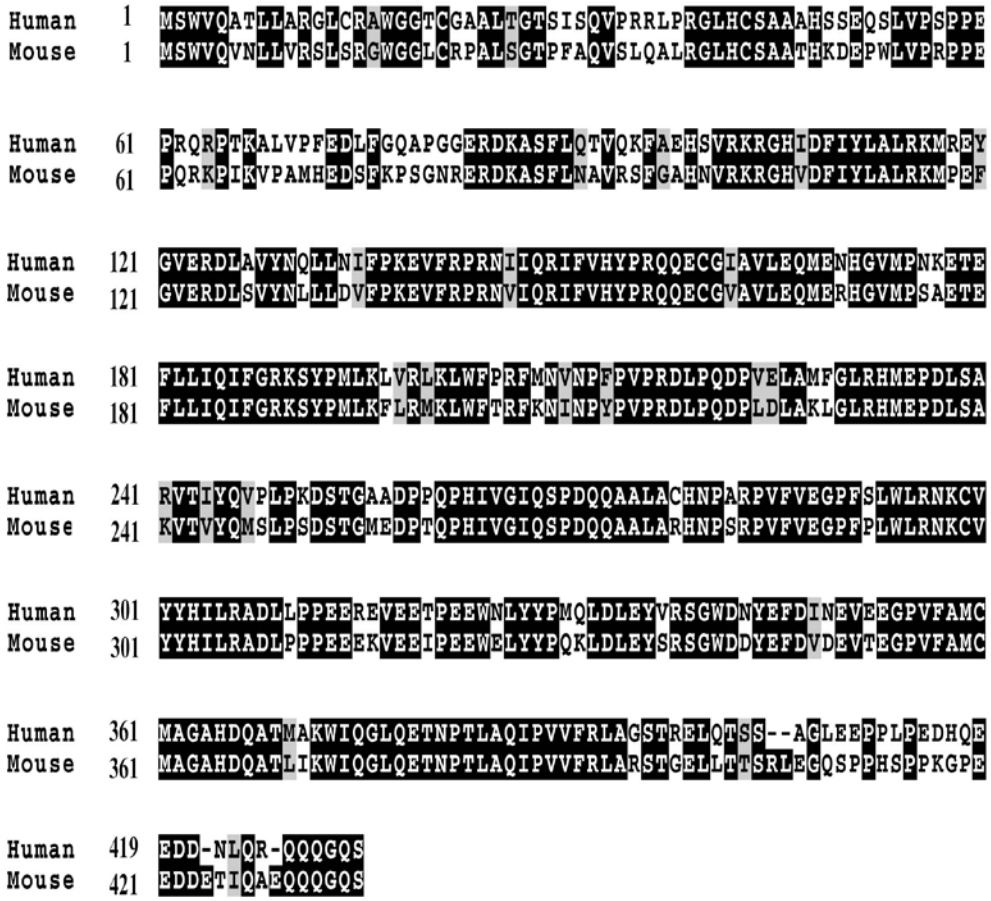

Figure 1.5 An alignment of the amino acid sequences of human and murine ECSIT

Sequence identity is represented by black shading and sequence similarity by grey shading.

1.10 Project Aims

The specific aims of this study were to:

- Explore the molecular basis to the effects of hECSIT in innate immune signalling pathways
- Characterise the regulatory pathways that control hECSIT function
- Characterise the role of hECSIT in TNF- signalling
- Characterise the role of hECSIT in anti-viral signalling
- Generate hECSIT knock-in mouse to characterise the physiological role of hECSIT

Chapter 2 Materials and Methods

2.1 Materials

2.1.1 Reagents

Reagents	Supplier
Agar	Sigma
Agarose	Promega
Agarose, low melting point	Sigma
Ampicillin	Sigma
APS	Sigma
Bovine serum albumin (BSA)	Sigma
Bradford reagent dye	Bio-Rad
Bromophenol blue	Sigma
Chloroform	Sigma
Clonables™ 2X Ligation Premix	Merck
Coomassie Blue (G250)	Sigma
Cycloheximide (CHX)	Sigma
DAB (3,3'-Diaminobenzidine)	Vector Labs
DAPI (4',6-Diamidino-2-Phenylindole)	Sigma
DEPC (diethylpyrocarbonate)-treated water	Ambion
D-galactosamine (D-Gal)	Sigma
DMEM (Dulbecco's Modified Eagle's medium)	Invitrogen
DMSO (dimethyl sulfoxid)	Sigma
DNA ladder & Loading dye	Promega
dNTPs (deoxyribonucleotide triphosphates)	Promega
DTT (dithiothreitol)	Sigma
E.coli - TOP10 competent cells	Invitrogen
EDTA (ethylenedia~nine tetra-acetic acid)	Sigma
Ethanol	Sigma
Ethidium bromide	Sigma
FBS (fetal bovine serum)	Invitrogen
Formalin solution	Sigma

Glacial acetic acid	Merck
Glycerol	Sigma
Glycine	Sigma
GoTaq® Green Master Mix	Promega
HEPE (hydroxyeicosapentaenoic acid)	Sigma
Hoechst 33342	Sigma
hydrochloric acid (HCl)	Merck
Hydrogen peroxide solution (H_2O_2)	Sigma
Igepal	Sigma
Imidazole	Sigma
Isopropanol	Sigma
IPTG (isopropyl β-D-1 thiogalactopyranoside)	Sigma
Kanamycin	Sigma
Lipofectamine 2000	Invitrogen
Lysogeny broth (LB)	Sigma
Magnesium Chloride	Sigma
Methanol	BDH
Microlon 96-well plates	Greiner
MTT (3-(4,5-dimethylthiazol-2-yl)-2,5-diphenyltetrazolium bromide)	Protech
Ni-NTA (nickel-nitrilotriacetic acid) Resin	Qiagen
NF-κB IRDye Labelled Oligonucleotides	Licor Biosciences
OptiMEM	Invitrogen
PBS (Phosphate buffered saline)	Oxoid
Penicillin / Streptomycin / Glutamine	Invitrogen
PMSF (phenylmethylsulfonyl fluoride)	Sigma
Polybrene	Sigma
Prestained molecular weight marker	Invitrogen
Protease inhibitor mixture	Roche
Protease inhibitor mixture (EDTA free)	Roche
Protein A/G-agarose	Santa Cruz
Protogel	National Diagnostics
Puromycin	Sigma
Random primers	Invitrogen
Restriction enzymes	NewEngland

RNase Zap	Ambion
SDS (sodium dodecyl sulphate)	Sigma
siRNA Pellino3 specific	Ambion
siRNA Lamin a/c	Ambion
Skim milk powder	Sigma
Sodium chloride (NaCl)	Sigma
Sodium hydroxide (NaOH)	Sigma
Sodium orthovanadate (Na_3VO_4)	Sigma
Sodium Phosphate (Na_3PO_4)	Sigma
Sulphuric acid (H_2SO_4)	Sigma
Synthetic oligonucleotides	MWG Biotech
Taq polymerase	Invitrogen
TEMED (N, N, N′, N′-tetramethylethylenediamine)	Sigma
TMB (3, 3', 5, 5'-Tetramethylbenzidine liquid substrate)	Sigma
TNFα	R&D Systems
Tris-base	Sigma
Tris-HCl	Sigma
Trypsin/EDTA	Invitrogen
Tween-20	Sigma
Z-VAD-FMK (benzyloxycarbonyl-valine-alanine-aspartate-fluoromethyl ketone)	Promega.

2.1.2 Buffers

Buffer	**Composition**
PBS	2.7mM KCl, 1.5mM KH_2PO_4, 137mM NaCl, 8mM Na_2HPO_4, pH 7.4
TBS (Tris buffered saline)	25mM Tris, pH7.4, containing 0.14M NaCl.
Blocking Buffer	1X TBS, 0.1% (v/v) Tween-20 with 5 % w/v nonfat dry milk or 5% w/v BSA
Cell lysis Buffer	20 mM Tris-HCl, pH 7.4, 150 mM NaCl, 0.2% (v/v) Igepal, 10% (w/v) glycerol, 50 mM NaF,1 mM Na_3VO_4, 1 mM DTT, 1 mM PMSF, complete protease inhibitor cocktail (Roche, mini)
EMSA Buffer-A	10 mM HEPES pH 7.9, 10 mM KCl, 1.5 mM $MgCl_2$; shortly before use add: 0.5 mM DTT and 0.5 mM PMSF
EMSA Buffer-C	20 mM HEPES pH 7.9, 420 mM NaCl, 1.5 mM $MgCl_2$, 0.2 mM EDTA, 25% (w/v) glycerol; shortly before use add: 0.5 mM PMSF
EMSA Buffer-D	10 mM HEPES pH 7.9, 50 mM KCl, 0.2 mM EDTA, 20% (w/v) glycerol; shortly before use add: 0.5 mM PMSF and 0.5 mM DTT
In Vitro Binding Buffer	20 mM Tris-HCl, pH 7.4, 150 mM NaCl, 0.2% (v/v) Igepal, 10% (w/v) glycerol and complete protease inhibitor cocktail
Laemmli sample buffer (1x Concentrations)	62.5 mM Tris-HCl, pH 6.8, 10% (w/v) glycerol, 2% (w/v) SDS, 0.7 M β-mercaptoethanol , 0.001% (w/v) bromophenol blue
Qiagen native lysis buffer	50 mM $NaH_2PO_4.H_2O$, 300 mM NaCl 10 mM Imidazole, 10mM β-mercaptoethanol
Qiagen native wash Buffer	50 mM $NaH_2PO_4.H_2O$, 300 mM NaCl, 20 mM Imidazole
Qiagen native elution Buffer	37.5 mM NaH_2PO_4, 225mM NaCl,

	250 mM Imidazole
SDS running Buffer	25 mM Tris, 192 mM glycine, 0.1% SDS.
SOC medium	2% peptone, 0.5% Yeast extract, 10mM NaCl,
(Super Optimal broth with	2.5mM KCl, 10mM $MgCl_2$, 10mM $MgSO_4$,
Catabolic Repressor medium)	20 mM Glucose
Reagent diluent for ELISA	0.1% (w/v) BSA, 0.05% (v/v) Tween in TBS
Transfer Buffer	25 mM Tris, 192 mM glycine, 20% methanol
TAE (Tris-acetate-EDTA) Buffer	40 mM Tris base, 0.1% (v/v) glacial acetic acid, 1 mM EDTA
TBE	89 mM Tris Base,89 mM Boric Acid,
(Tris-Borate-EDTA) Buffer	2 mM EDTA
TE (Tris-EDTA) buffer	10 M Tris-HCl, 1 mM EDTA pH 8.0,

2.1.3 Antibodies

Antibodies	**Supplier**
β-actin	Sigma
ECSIT	MyBiociences
ERK	Cell Signalling
FLAG M2	Sigma
His-HRP (horseradish peroxidase)	Sigma
HA-Tag (6E2)	Cell Signalling
IκB-α	Santa Cruz
JNK	Cell Signalling
Myc-Tag (9B11)	Cell Signalling
P38	Cell Signalling
Phosho-ERK	Cell Signalling
Phosho-IκB-α	Cell Signalling
Phosho-JNK	Cell Signalling
Phosho- p38	Cell Signalling

RIP1	Transduction Labs
PARP (Poly-ADP-ribose- polymerase)	Cell Signalling
IKK-β	Cell Signalling
TRAF6	Santa Cruz
TRAF3	Santa Cruz
TAK1	Santa Cruz
Phospho-IKK-α/β	Cell Signalling
Secondary Antibodies：	Supplier
Anti-mouse / rabbit-HRP	Cell Signalling
IRDye 800CW Goat Anti-Rabbit	Licor Biosciences
IRDye 680 Goat Anti-Mouse	Licor Biosciences
IRDye 800CW Donkey Anti-goat	Rockland

2.1.4 Cells

Cells	**Description**
HEK293T	Human embryonic kidney cells
HeLa	Human epithelial carcinoma cell line
U373-MG	Human glioblastoma-astrocytoma, epithelial-like cell line
THP1	Human acute monocytic leukemia cell line
MEF	Murine Embryonic Fibroblasts

2.1.5 Animals

Humanised ECSIT mice and their wild-type littermates were bred at the animal facility at the Institute of Immunology, National University of Ireland Maynooth. Genotyping was performed by PCR analysis of genomic DNA from ear punches as described in 2.2.. Mice were housed in standard rodent cages, enriched with cardboard housing and nesting material. The animals were kept at room temperature (22 – 24°C) in a 12hr light/dark cycle (lights on at 8:00 a.m.) with *ad libitum* access to food and water. All mice were used under the guidelines of the Irish Department of Health, and all procedures were approved by the research ethics committee of the National University of Ireland Maynooth.

2.1.6 Gifts

Cell lines:

- HEK293 cells and HEK293 stably expressing TLR4 or TLR3 - Prof. Douglas T. Golenbock (The University of Massachusetts Medical School, Worcestor, Massachusetts 01605, USA).

Constructs:

- pFR-luciferase Gal4 reporter construct – Dr. Andrew Bowie (Trinity College Dublin, Ireland)
- NF-κB-luciferase reporter construct – Prof. Luke O'Neill (Trinity College Dublin, Ireland)
- HA-tagged Ubiquitin wild type – Dr. Jim Johnson (University of Queens, Belfast Northern Ireland)
- FLAG Tagged cIAP1 – Dr Mikihiko Naito (National Institute of Health sciences, Tokyo, Japan)
- FLAG Tagged TAK1-KD – Dr Daniel O'Toole (NUIG, Galway, Ireland)
- FLAG Tagged TAK1-K158a/ TAK1-K209a – Dr Jianhua Yang (Baylor College of Medicine, Texas, USA)
- Myc-tagged C-Terminal truncated hECSIT/ N-terminal truncated hECSIT – Dr Daniel O'Toole (NUIG, Galway, Ireland)

2.2 Methods

2.2.1 Cell culture

2.2.1.1 HEK293, U373, HeLa and THP1 cells

The parental human embryonic kidney HEK293 cells, HEK293 cells that stably express the TLR3 / TLR4 receptors, U373 and HeLa cells were maintained in Dulbecco's Modified Eagle Medium (DMEM), which was supplemented with 10% (v/v) foetal bovine serum (FBS), penicillin (100 µg/ml) and streptomycin 100 µg/ml. G418 (500 µg/ml) was used to select for stably transfected TLR cell lines. Cells were maintained in a 37ºC humidified atmosphere with 5% CO_2. Cells were passaged every 2 to 3 days using 1% (w/v) Trypsin/ethylenediaminetetraacetic acid (EDTA) solution in phosphate-buffered saline (PBS). THP1 cells were grown in RPMI supplemented with 10% (v/v) FBS and penicillin (100 µg/ml) and streptomycin 100 µg/ml and passaged every 3 to 4 days.

2.2.1.5 MEF Cells

For the preparation of primary MEFs *ECSIT*$^{+/-}$ mice were intercrossed to produce *ECSIT* +/+ ,+/- and -/- embryos. Mouse breeder pairs were set up and the following morning female mice were checked for copulatory plugs to indicate day zero. At day 13.5, pregnant mice were euthanized according to standard protocols. The uterus containing the embryos was dissected from the mouse and placed in a sterile Petri dish. Embryos were individually removed from the uterus and placed in a Petri dish containing sterile PBS in a laminar flow hood. The head and all soft tissues from each embryo were removed. Heads were retained for genotyping the embryos. The remaining embryo carcasses were minced using a scalpel and placed in 50ml falcon tube containing 1.5ml of trypsin (1X) and 0.5ml H_20. The suspension was incubated at 37 degrees for 10 min, mixed using a pipette and incubated again at 37 for 10 min. DMEM (12 ml) was then added to each tube. Tissue clumps were removed and the

contents of each tube were transferred to an individual T75 cell culture flask. MEF cells were passaged every 3-4 days.

2.2.2 Site directed mutagenesis

Primers incorporating desired mutations were designed and the following considerations were applied in primer design :

- Both of the primers contained the desired mutation and annealed to the complementary sequences on opposite strands of the plasmid.
- Primers were between 25 and 45 bases in length, with a melting temperature of < 75^{o}C.

The following formula was used for estimating the T_m of the primers:

$$T_m = 81.5 + 0.41(\%GC) - 675/N - \%\ \text{mismatch}$$

Where *N* is the primer length in bases.

- The desired mutation (insertion or deletion) was in the middle of the primer with approximately 10-15 bases of unaltered sequence on both sides.
- The primers usually terminated in one or more C or G bases.

Pfu Turbo, a high fidelity DNA polymerase which amplifies longer targets more efficiently than other enzymes, was used for PCR amplification using the following conditions:

Reagent	**Volume**
Template 50 ng plasmid DNA	1 μl
10X Pfu Buffer	5 μl
Primers (125ng)	1 μl each
dNTP mix (10 mM each)	1 μl

Pfu Turbo	1 μl
PCR-grade water	to 50 μl

Each reaction was initially heated to 94^{o}C for 5 min. This was followed by 22 cycles of 94^{o}C for 30 s, a target-specific annealing temperature (Ta) for 30 s and an elongation phase of 72^{o}C for 7 min,. Samples were then incubated at 72^{o}C for 10 min.

2.2.3 Propagation of DNA

2.2.3.1 Rapid transformation of competent cells

TOP10 chemically competent *E.coli* were used for propagation of plasmids and for the cloning of ligation reaction products. 100-400ng of plasmid or 70 % of a ligation reaction product were added to 5 μl or 50 μl of TOP10 cells, respectively. DNA and the cells were mixed gently with a pipette and incubated on ice for 30 min. The plasmids were allowed to enter the bacterial cells by heat shocking the mixture at 42^{o}C for 60 seconds. The cells become permeable to allow easy entry of the plasmid and cooling on ice for 2 min makes the cells once again impermeable. The transformed cells were then incubated in 1 ml Luria Bertoni (LB) broth (1% (w/v) tryptone, 0.5% (w/v) yeast extract, 85 mM NaCl) at 37^{o}C on a shaker at 220 rpm for 1 h. An aliqout of the mix (50-100 μl for plasmid propagation; 1 ml for cloning of ligation reaction products) was then plated out on LB agar plates (LB broth with 1.5% (w/v) agar) containing 100 μg/ml ampicillin. Plates were inverted and incubated overnight at 37^{o}C. Plates were then stored at 4^{o}C for up to four weeks.

2.2.3.2 Small scale preparation of DNA from E. coli

LB broth (2 ml) containing ampicillin (50 μg/ml) was inoculated with a single transformed *E coli* colony from an agar plate. The culture was incubated overnight at 37^{o}C shaking at 220 rpm. Small plasmid preparations were made using the Qiaprep Spin Miniprep kit from Qiagen Inc. The bacterial cells were centrifuged at 9000 rpm for 3 min and the supernatant was discarded and the plasmid DNA was extracted as

outlined in the manufacturer's handbook. DNA was quantified using a Cary spectrophotometer. After diluting the DNA appropriately in Tris-EDTA (TE) buffer, pH 8.0, (10 mM Tris-HCl, 1 mM EDTA) the absorbance of the solution was measured at 260 nm and 280 nm. All samples used had an optical density OD_{260}/OD_{280} ratio in the range of 1.7 to 1.9. Ratios below 1.7 or above 1.9 indicated RNA or protein contamination, respectively. The concentration was calculated using the formula:

$$\mu g/ml\ DNA = 50\ \mu g/ml/OD_{260} \times (OD_{260}\ measured) \times (dilution\ factor)$$

2.2.3.3 Large scale preparation of DNA from *E. coli*

A starter culture of LB broth (2 ml) containing ampicillin (50 μg/ml) was inoculated with a single transformed *E.coli* colony and incubated at 37°C with shaking at 220 rpm for 6-8 h. This was then added to a larger volume of LB broth (100 ml) containing the relevant antibiotic and incubated at 37°C overnight with shaking at 220 rpm. Large plasmid preparations were made using the Qiagen high speed plasmid midi kit from Qiagen. The bacterial cells were centrifuged at 3000 rpm for 40 min and the supernatant was discarded and the plasmid DNA was extracted as outlined in the manufacturer's handbook. DNA was quantified as outlined in Section 2.2.4.2.

2.2.4 Transient transfection

2.2.4.1 Transfection of cells for luciferase reporter assay

HEK293-TLR3 and -TLR4 cells were seeded in 96-well plates and allowed to adhere for 24 h to approximately 50% confluency. Cells were transfected using Lipofectamine 2000. For each well to be transfected, 25 μl of OptiMEM (Invitrogen) was mixed with the DNA. DNA mixes were made up for the appropriate luciferase construct as outlined in section 2.2.6. Lipofectamine 2000 (0.4 μl) was diluted in OptiMEM (25 μl/sample) and the reaction was mixed gently and left at room temperature for 5 min. After the incubation, the Lipofectamine/OptiMEM solution was added to the DNA/OptiMEM mix (total volume 50 μl/well to be transfected) and the combined reaction was mixed gently and incubated at room temperature for 20

min. The transfection mixture was then added to each well and mixed gently by tapping the side of the plate. Each sample was transfected in triplicate. 24 h after transfection the cells were treated as indicated and supernatants were removed, cell lysates were generated and used to measure luciferase activity.

2.2.4.2 Transfection of cells for Western Blot analysis

HEK293T cells were seeded in 6-well plates. Cells were grown for 24 h to approximately 70% confluency. For each well of a 6-well plate to be transfected, DNA (amount depending on individual assays as outlined in relevant sections) was diluted in OptiMEM (250 μl) (Invitrogen) and mixed gently. Lipofectamine 2000 (4 μl) was then diluted in OptiMEM (250 μl) and incubated at room temperature. After 5 min incubation, the diluted DNA was combined with the diluted Lipofectamine 2000, mixed gently, and incubated at room temperature for 20 min. 1 ml of medium was removed from each well before adding the DNA-Lipofectamine complexes (500 μl). For co-immunoprecipitation studies, constructs encoding potential interacting partners were transfected at a ratio 1:1; for ubiquitin studies 1 μg of each construct was used; for degradation studies a number of different ratios were utilised. After 24 h, cell lysates were generated for co-immunoprecipitation studies (section 2.2.8) or ubiquitination studies (section 2.2.9) To determine protein concentration the Bradford method was used as outlined in section 2.2.16 and lysates were analysed using SDS-polyacrylamide gel electrophoresis (SDS-PAGE) (section 2.2.7).

2.2.5 Luciferase Assays

HEK293-TLR3 or -TLR4 cells were seeded in 96-well plates (200 μl DMEM/well) and grown for 24 h. All transfections were performed using Lipofectamine 2000 transfection reagents (as described in section 2.2.4.1). Details of the constructs transfected are given below. 24 h post-transfection, the medium was removed from the cells and reporter lysis buffer (100 μl, Promega) was added to each well using a multi-channel pipette. The plate was then wrapped in aluminum foil and

placed on a rocking platform for 30 min at room temperature before being placed at -80^{o}C for a minimum of 1 h. After thawing at room temperature, aliquots (40 μl) of each were assayed for firefly luciferase activity using firefly luciferase substrate (40 μl, Promega), while *Renilla* luciferase activity was assayed using coelenterazine (0.1 μg/ml in PBS). Luminescence was monitored with a Glomax microplate luminometer (Promega).

2.2.5.1 NFκB assay

To measure activation of the NFκB pathway, cells were transfected with NFκB -regulated firefly luciferase reporter plasmid (80 ng), constitutively expressed *Renilla*-luciferase reporter construct phRL-TK (20 ng) and varying amounts of expression constructs (detailed in figure legends). The total amount of DNA was maintained at 200-250 ng using pcDNA3.1.

2.2.5.2 IRF3 assay

To measure the activation of IRF3, cells were transfected with pFR-Luc (60 ng), the *trans*-activator plasmid pFA-IRF3 (IRF3 fused downstream of the yeast Gal4 DNA binding domain, 30 ng), phRL-TK (20 ng) and varying amounts of expression constructs (Outlined in figure legends). The total DNA concentration was maintained at 210 ng using pcDNA3.1.

2.2.5.3 IRF7 assay

To measure the activation of IRF7, cells were transfected with pFR-Luc (60 ng), the *trans*-activator plasmid pFA-IRF7 (IRF7 fused downstream of the yeast Gal4 DNA binding domain, 25 ng), phRL-TK (20 ng) and varying amounts of expression constructs (Outlined in figure legends). The total DNA concentration was maintained at 210 ng using the pcDNA3.1.

2.2.6 siRNA Studies

Pre-designed siRNA targeting hECSIT was purchased from Ambion Inc. (target sequence: 5'-GGTTCCTTTGCCCAAAGACTT-3'), while Lamin a/c siRNA was used as a control, also purchased from Ambion.

2.2.6.1 Transfection of siRNA for knockdown studies

HEK293 TLR4, TLR3, HeLa or U373 cells were seeded in 6-well plates. Cells were grown for 24 h to approximately 70% confluency. hECSIT-specific siRNA (30 nM) or Lamin a/c control siRNA, , were diluted in OptiMEM (250 µl) mixed gently and incubated for 5 min, Lipofectamine 2000 (4 µl) was also diluted in 250 µl of OptiMEM per sample, the reaction was mixed gently and left at room temperature for 5 min. After the incubation, the Lipofectamine/OptiMEM solution was added to the OptiMEM-siRNA mix (total volume 500 µl per well to be transfected) and the combined reaction mixed gently and incubated at room temperature for further 20 min. 500 µl sample was then added to each well and mixed gently by rocking the plate back and forth. Cells were incubated for 48 h prior to analysis for the expression of hECSIT by Western Blotting.

2.2.6.2 Transfection of siRNA for luciferase assays

HEK293 TLR3 or TLR4 cells were seeded in 96-well plates. Cells were grown for 24 h to approximately 50% confluency. To determine the effect of hECSIT-specific siRNA on the activation of NFκB, IRF3 and IRF7, DNA mixes were made up for the appropriate luciferase construct as outlined in section 2.2.6. The appropriate amount of hECSIT or Lamin a/c control siRNA (for a final concentration of 10 nM per well) was diluted in OptiMEM (25 µl) and mixed gently with the DNA. Lipofectamine 2000 (0.4 µl) was diluted in OptiMEM (25 µl) per sample, the reaction was mixed gently and left at room temperature for 5 min. After the incubation, the Lipofectamine/OptiMEM solution was added to the DNA-siRNA mix (total volume

50 µl per well to be transfected) and the combined reaction mixed gently and incubated at room temperature for 20 min. Samples (50 µl) were added to each well and mixed gently by tapping the side of the plate. Cells were incubated for 24 h prior to overnight treatment with ligands. 48 h post-transfection supernatants were collected and stored at -20ºC, while cell lysates were generated and assayed for luciferase activity as outlined in section 2.2.5.

2.2.7 Western Blot Analysis

2.2.7.1 Preparation of Samples

Cytosolic extracts were added to 4x sample buffer (0.125 Tris-HCl pH 6.8, 20% (w/v) glycerol, 4% (w/v) SDS, 1.4 M β-mercaptoethanol and 0.0025% (w/v) bromophenol blue) and boiled for 5-10 min prior to loading. For analysis of whole cell extracts, 10% of total lysate was boiled for 5-10 min before loading.

2.2.7.2 SDS-polyacrylamide gel electrophoresis (SDS-PAGE)

SDS-PAGE was conducted according to the method of Laemmli (Laemmli, 1970), as modified by Studier (Studier, 1973). Samples and appropriate prestained (26.6-180 kDa) protein markers were loaded into separate wells. Electrophoresis was performed at 80 V through a 5% SDS polyacrylamide stacking gel and then through a 10% SDS polyacrylamide resolving gel at 80 V for 1.5-3 h, depending on the size of the proteins being electrophoresed.

2.2.7.3 Immunoblotting

Following separation by electrophoresis, the proteins were transferred electrophoretically to nitrocellulose membranes in a Hoefer TE 70 Semiphor semi-dry transfer unit at 90 mA for 1.5 h or a Thermo Fisher Wet transfer unit using Whatmann and nitrocellulose pre-soaked in cold transfer buffer (25 mM Tris Base, 0.2 M glycine

and 20% (v/v) methanol) for 10 min. Following transfer, non-specific binding was blocked by incubating the nitrocellulose membranes at room temperature for 1 h (or overnight) in TBS (20 mM Tris-HCl pH 7.5, containing 0.05% (v/v) Tween 20 and 0.5 M NaCl) containing 5% (w/v) skimmed milk powder. The membranes were then washed 3 times for 10 min each in TBS prior to incubation at 4^{o}C overnight with the primary antibodies diluted in TBS containing 5% (w/v) skimmed milk powder. The membranes were subsequently subjected to 5 x 10 min washes in TBS prior to incubation with secondary antibody (1:5000 dilution) specific for the primary antibody in question (anti-rabbit or anti-mouse) in Odyssey Blocking Buffer (Licor, Bioscience) for 1 h in the dark at room temperature. The membranes were then washed a further 5 times for 10 min each in TBS in the dark. The immunoreactive bands were detected using Odyssey Infrared Imaging System from Licor Biosciences or E.C.L chemiluminescence, according to the instructions of the manufacturer.

1^{o} antibody	**Dilution**	**2^{o} antibody***
β-Actin	1:10000	mouse
c-Myc	1:2000	mouse
ECSIT	1:1000	rabbit
Flag	1:2000	mouse
HA	1:1000	mouse
TRAF3	1:200	mouse
TRAF-6	1:500	mouse
RIP1	1:1000	mouse
Ubiquitin	1.500	mouse
p-IκB-α	1:500	mouse
IκB-α	1:500	rabbit
p-P65	1:500	rabbit
P65	1:1000	rabbit
p-IKK-α/β	1:750	rabbit
IKK-α/β	1:1000	rabbit
PARP	1:1000	rabbit
p-JNK	1:500	rabbit

JNK	1:1000	rabbit
p-P38	1:500	rabbit
P38	1:1000	rabbit
p-TAK1	1:500	rabbit
TAK1	1:1000	rabbit

***** All Licor secondary antibodies were used at a dilution of 1:5000. HRP-linked secondary antibodies were used at a dilution of 1:1000

2.2.8 Co-Immunoprecipitation (Co-IP)

2.2.8.1 Co-immunoprecipitation analysis of over expressed proteins

HEK293T cells were transfected with Lipofectamine 2000 as previously described in section 2.2.5.2 at a 1:1 ratio of expression constructs. Cell extracts were generated on ice or at 4^{o}C according to the following experimental strategy. Cells were first washed with pre-chilled PBS (1 ml) then lysed with pre-chilled 250µl co-immunoprecipitation (Co-IP) lysis buffer (50 mM Tris-HCl, pH 7.5, containing 150 mM NaCl, 0.5% (w/v) igepal and 50 mM NaF, with 1 mM $Na3VO_4$, 1 mM dithiothreitol (DTT), 1 mM phenylmethylsulfonyl fluoride (PMSF) and protease inhibitor mixture (leupeptin (25 µg/ml), aprotinin (25 µg/ml), benzamidine (1 mM), trypsin inhibitor (10 µg/ml)) for 30 min on a rocking platform at 4^{o}C. Lysates were scraped into pre-chilled 1.5 ml microcentrifuge tubes and centrifuged at 12,000 g for 10 min at 4^{o}C. Supernatants were removed to fresh tubes (10% of sample was retained for whole cell lysate analysis) and incubated for 30 min with mouse or rabbit immunoglobulin (Ig) G (1µg) (depending on the host species of the primary antibody) and Protein A/G agarose beads (10 µl) on a rotator at 4 ^{o}C. Samples were centrifuged at 1000 g for 5 min at 4^{o}C to pellet beads with non-specific protein and supernatants were removed to fresh pre-chilled tubes. Samples were incubated overnight with primary antibody (2 µg). The following day Protein A/G agarose beads (20-30 µl) were added to each sample and they were again incubated at 4^{o}C for ~ 6 h / overnight. The subsequent day samples were centrifuged at 8000 g for 1 minute. The beads were washed with CoIP lysis buffer (500 µl) and subject to re-centrifugation. This step was

repeated five times. The supernatant was then removed and 40 µl of 2 x sample buffer (0.125 M Tris-HCl, pH 6.8, containing 20% (w/v) glycerol, 4% (w/v) SDS, 1.4 M β-mercaptoethanol and 0.0025% (w/v) bromophenol blue) was added to the columns for 30 min at RT. Samples were centrifuged at 16000 g for 2 min, to elute immunocomplexes and subsequently boiled at 100^{o}C for 5-10 min and analyzed using SDS polyacrylamide gel electrophoresis and western blotting (section 2.2.7).

2.2.8.2 Co-immunoprecipitation analysis of endogenous proteins

For analysis of endogenous protein interactions, cells were stimulated for various times with TNF-α (50ng) or LPS (100ng/ml) or IL-1 (10ng/ml) or Poly (I:C) (25ug/ml). Cells were then lysed for immunoprecipitation and western blotting analysis as described above.

2.2.9 Analysis of Ubiquitinated proteins

2.2.9.1 Analysis of Ubiquitination of over expressed proteins

HEK293T cells were co-transfected with HA-tagged ubiquitin wild type (1 µg) and 1 µg of various expression constructs encoding different proteins (as outlined in figure legends) using Lipofectamine 2000. The following day cells were harvested in 200µl of RIPA buffer (1M Tris HCl Ph 7.4, containing 5M NaCl, 20% IgePal , 10% (w/v) sodium deoxycholate, 20% (w/v) SDS with , with 1 mM $Na3VO_4$, 1 mM dithiothreitol (DTT), 1 mM phenylmethylsulfonyl fluoride (PMSF) and protease inhibitor mixture (leupeptin (25 µg/ml), aprotinin (25 µg/ml), benzamidine (1 mM), trypsin inhibitor (10 µg/ml)) on ice for 40 mins. Lysates were then centrifuged at 12,000g for 10 mins and transferred to fresh tubes. 20µl of 10% (w/v) SDS was added to each sample followed by incubation at 95ºC for 5 mins to remove any associated proteins from the ubiquitinated protein of interest. 10% of sample was retained for whole cell extract analysis. Samples were then incubated overnight with primary antibody (2µg) in 1.5ml of RIPA buffer. Samples were then co-immunoprecipitated as described in section 2.2.8..

2.2.9.2 Analysis of ubiquitination status of endogenous proteins

HeLa or U373 cells were seeded (density) in cell culture 10cm petri dishes. The following day cells were stimulated with the appropriate ligand for various time points. Cells were then lysed as described in section 2.2.9. Samples were co-immunoprecipitated using the appropriate antibody and analysed by Western immunoblotting using an anti-ubiquitin antibody.

2.2.10 *In vitro* Ubiquitination Assay

Recombinant TRAF3 or TRAF6 was incubated with recombinant hECSIT or C-terminal hECSIT in the following reaction mixture:

E1	50 ng
E2 UbcH13/Uev1a	400 ng
Ubiquitin Recombinant	2 μg
$MgCl_2$	2 mM
ATP	2 mM
Protease Inhibitor (EDTA free) - 1 tablet in 2ml dH_2O	1:10
TRAF3/6 Recombinant	500ng
ECSIT Recombinant	500 ng
dH2O	to 30 μl

Reactions were incubated at 37ºC for 2 h and terminated by addition of 10 μl 4 x SDS-PAGE sample buffer (0.125 M Tris-HCl, pH 6.8, containing 20% (w/v) glycerol,

4% (w/v) SDS, 1.4 M β-mercaptoethanol and 0.0025% (w/v) bromophenol blue). Samples were boiled for 5-10 min, resolved by SDS-PAGE and subsequently analysed by Western immunoblotting (section 2.2.7) using anti-ubiquitin antibody.

2.2.11 Lentiviral shRNA Infection

2.2.11.1 Lentiviral production

HEK293T cells were seeded in a T75 flask (15 ml DMEM/flask) and grown for 24 h to approximately 70% confluency. The cells were transfected as described in section 2.2.4.2. The DNA mixture contained packaging plasmid (5µg), envelop plasmid (5µg) and the hECSIT-shRNA (10 µg) (Sigma). shRNA hECSIT sequences were as follows:

- shRNA hECSIT A7

5’-CCGGGCCCTTTGAGTGTACAGCAAACTCGAGTTTGCTGTACA CTCAAAG GGCTTTTTG -3’

- shRNA hECSIT A8

5’-CCGGCCCTCGATTCATGAACGTCAACTCGAGTTGACGTTCA TGAATCGAGGGTTTTTG -3’

A control shRNA was also used in the transfection. It was a non-targeting shRNA vector that activates the RNA-induced silencing complex (RISC) and the RNAi pathway, but does not target any human or mouse genes. The short-hairpin sequence contains 5 base pair mismatches to any known human or mouse gene. To remove the transfection reagent, the media was changed 24 h post-transfection and replaced with fresh high serum (30%) growth media. The cells were then incubated for 24 h. The media containing lentivirus were harvested ~ 48 h post-transfection and transferred to a polypropylene tube for storage at -20°C. The media was replaced with fresh high serum (30%) growth media and the cells were incubated for further 24 h. The virus was harvested one more time and after the final harvest the packaging cells were discarded.

2.2.11.2 Lentiviral infection

U373 cells were seeded at 2 x 10^5 cells/ml in T75 flasks or culture dishes (10ml/dish DMEM). The following day virus was added to cells (1:1 virus DMEM). Polybrene (8 μg/ml) was added to improve transduction efficiency. The flasks were incubated at 37^{o}C. The media was removed 48 h post-infection and replaced with fresh growth media containing puromycin (5 μg/ml) to select for cells transduced with shRNA. The polyclonal populations of cells were cultured for 2 days and hECSIT expression was determined.

2.2.12 EMSA

EMSA was used to detect the presence of DNA-binding proteins in nuclear extracts. NFκB infrared dyes labeled oligonucleotides were purchased from Licor Biosciences.

2.2.12.1 Preparation of sub-cellular nuclear fractions

Following treatment cells were washed in PBS and resuspended in 1ml buffer A. Following centrifugation at 4ºC (21,000g for 10 min) supernatant was removed and cells were lysed in 20μl of Buffer A containing 0.1% (v/v) IgePal for 10 min on ice. Lysates were centrifuged at 21,000g for 2 minutes. Supernatants constituted cytosolic fractions and were stored at -20^{0}C.The remaining pellets were resuspended in 20μl of Buffer C and incubated on ice for 15'. Samples were then centrifuged at 21,000g for 10 min.The supernatants, constituting nuclear extracts were then transferred to 75μl of Buffer D. A Bradford assay was used to determine protein concentration and nuclear extracts were assayed for NFκB DNA binding activity as outlined in the following section.

2.2.12.2 EMSA Reaction

Nuclear extracts (5µg protein) were incubated with the following reaction mix:

10x Binding buffer	2µl
Poly (dI-dC) concentration	1µl
1% NP40	1µl
NFκB Oligo	1µl
Nuclear extract	5ug
Water	to 20ul

NFκB consensus oilgonucleotide:

5'-AGTTGAGGGGACTTTCCCAGGC-3'

3'-TCAACTCCCCTGAAAGGGTCCG-5'

Underlined nucleotides indicate binding sites for NFκB.

For competition assay unlabeled oligonucleotide containing the consensus NFκB sequence was added for 20 min prior to the addition of the IRDye labeled oligonucleotides. Incubations were performed in the dark for 1h at room temperature. Orange loading dye (2µl) was added to each sample and subjected to native gel electrophoresis on 5% acrylamide gels that had been pre-run for 30 min at 90V. Gels were then removed from glass plates and visualized using a Licor scanner.

2.2.13 ELISA

Cell supernatants were collected and stored at -20ºC until ELISA analysis. 96-well NUNC maxisorb plates were coated with the appropriate capture antibody and incubated overnight at room temperature with gentle agitation. Plates were washed three times with wash buffer (PBS with 0.05% (v/v) Tween-20) and dried by inverting the plates on tissue paper. Plates were blocked for 1 hour with PBS containing 1% (w/v) BSA. Plates were again washed three times and dried. Samples or standards (100µl) diluted in reagent diluent were added to each well. Standard concentration ranged from 0-2000pg/ml. Plates were incubated with samples and standards for 2h and were then washed three times. Detection antibody (100µl) (biotinylated) was diluted in reagent diluent was added to each well. Again plates were incubated for 2h and then washed. Streptavidin-HRP conjugate (100µl) was then added to each well. The plates were then incubated in the dark for 20 min and then the wash step was repeated. An aliquot (100µl) TMB solution was added to each well and again plates were incubated in the dark for 20 min. 50µl of H_2S0_4 was used to stop the reaction and the absorbance measured at 450nm using a ELx800TM microplate reader with Gen5 Data analysis software. The concentrations of cytokine in each sample were extrapolated from a standard curve that related absorbance to standard concentration. Standard samples were assayed in duplicate to generate the standard curve, while all samples were assayed in triplicate.

2.2.14 PCR Based Genotyping

PCR Amplification was performed on genomic DNA using GotoTaq DNA polymerase and specific primers to detect heterozygous/homozygous conventional *Ecsit* mice.

4192_62: CCATTTGCTGGAGTCTGTTCC

4192_63: AAATTCAGCACCTACATGGCAG

Control Primers: CD79B Control Allele

1260_1: GAGACTCTGGCTACTCATCC

1260_2: CCTTCAGCAAGAGCTGGGGAC

Flpe Transgene Primers:

1307_1: Flpe_as_GGCAGAAGCACGCTTATCG

1307_2: Flpe_s_GACAAGCGTTAGTAGGCACAT

PCR Reaction:

Genomic DNA	2µl
5X Buffer	5µl
$MgCl_2$	2µl
Primers (5µM)	1µl
dNTP mix (10nM each)	1µl
GotoTaq	0.15µl
PCR-grade water	to 25µl

For each target the samples were initially heated to 95ºC for 5'. This was followed by 35 cycles at 95ºC for 30s, at 60ºC for 30s and 72ºC for 1'. Samples were then incubated at 72ºC for 10' and stored at 4ºC. The PCR products were subjected to electrophoresis on a 1% (w/v) TAE agarose gel, containing ethidium bromide (5µg/ml).

2.2.15 Agarose Gel Electrophoresis

Agarose gels were prepared by suspending agarose in TAE (0.5X). This was then heated in a microwave until the agarose had completely dissolved. The solution was allowed to cool before Ethidium Bromide (5µg/ml) was added and the agarose was poured into the gel tray. Following solidification, agarose gels were covered and electrophoresed in TAE (1X). Samples were run simultaneously with molecular size markers with the range of the marker chosen to suit the particular sample size. Gels were electrophoresed at 100V for 30'. Nucleic acids were visualized under ultraviolet light (UV) (254nm) and images were acquired using the SynGene Gbox gel documentation system (Frederick, MD, USA).

2.2.16 Isolation of RNA and cDNA synthesis

2.2.16.1 Isolation of total RNA

Total RNA was extracted from cells using Trizol reagent as per manufacturer's instructions. The amount of isolated RNA was quantified by measuring the absorbance at wavelengths of 260nm and 280nm on a spectrophotometer, where an absorbance of 1 unit at 260nm is 40µg/ml. Pure RNA preparations have OD260/280 ratio of 1.8-1.9. Extracted RNA was stored at -80ºC.

2.2.16.2 Synthesis of first strand cDNA from messenger RNA (mRNA)

The Bioline Bioscript cDNA synthesis kit was used for generating full length first strand cDNA from total cellular RNA. RNA (2µg) was placed in nuclease free microcentrifuge tubes with 1µl (0.5µg/µl) of random primers and water to 13µl and incubated at 70ºC for 10'. The mixture was then chilled on ice and centrifuged briefly.

The following components were then added:

Bioscript Enzyme	0.5µl
5X Bioscript Enzyme Buffer	5µl
Water	to 20µl

The reaction mixture was then incubated at 42ºC for 1h followed by 10 min at 72ºC. Generated cDNA was stored at -20ºC for long-term storage.

2.2.17 Real Time PCR

A 25µl real-time PCR reaction was prepared in each optical tube as follows:

Template	4µl
SYBR green master mix (2x)	10µl
Primers (4mM)	2.5µl each
PCR Grade water	to 25µl

For each target the samples were initially heated to 95ºC for 15min for pre-denaturation. This was followed by 40 cycles at 95ºC for 30s, at 57ºC for 30s and at 72ºC for 45s. The PCR was conducted in a Applied Biosystems Step One PLUS real time PCR instrument. Integration of the fluorescent SYBR green into the PCR product was monitored after each annealing step. Amplification of one specific product was confirmed by melt curve analysis where a single melt curve peak eliminated the possibility of primer dimer association. For melt curve analysis to be performed the products were heated from 60ºC to 95ºC after the 40 cycles. The relative quantification of target gene expression was evaluated using the ΔCT method. The

ΔCT value was determined by subtracting the HPRT CT value for each sample from the target CT value. Fold change in the relative gene expression of each target was determined by calculating the $2^{-\Delta CT}$.

2.2.18 PBMC Isolation

Buffy coat blood packs from healthy donors were obtained from the Irish blood transfusion service. Buffy coats were diluted 1:1 with sterile PBS and transferred to a culture flask. 15ml of Lympho- prep was added to each of 3 Falcon tubes (50 ml). 35ml of the diluted blood was then layered slowly over the Lympho-prep at an angle. Falcon tubes were then centrifuged at 400 x g for 25 mins. Using a Pasteur pipette the top plasma layer of PBMCs were removed from each of the 3 tubes into a new 50 ml Falcon tube. The cells were then washed in PBS and centrifuged again at 800 x g for 10 mins. Cells were then resuspended in RPMI media and counted.

2.2.19 Sample preparation for mass spectrometry analysis

The indicated gel bands were first washed with deionised water (2 x 10 min) and the Coomassie Blue-stained band of interest was excised from the gels and placed into siliconised 1.5 ml Eppendorf tubes. The gel plug was then destained, desalted and washed as follows: Gel plugs were first washed with water and then with 50mM NH4HC3/acetonitrile 1:1 (v/v) for 15 min at 37^0C. The liquid was removed and enough acetonitrile was added to cover the gel plugs. Acetonitrile was removed and the gel plugs were rehydrated in 50mM NH_4HCO_3. After 5 min, an equal volume of acetonitrile was added. After 15 min of incubation all the liquid was removed and the gel plug was then dehydrated in 100% acetonitrile. The acetonitrile was removed and, the gel plug was then dried down for 30 min using a Heto type vacuum centrifuge from Jouan Nordic A/S (Allerod Denmark). Individual gel plugs were then rehydrated in enough digestion buffer (1mg of trypsin in 20ml of 50mM NH_4HCO_3) to cover the gel plug. More digestion buffer was added if all the initial volume had been absorbed by the gel pieces. The samples were then incubated at 37^0C for a period 4 h – overnight. The peptides generated by tryptic digestion were recovered by removing

supernatants from the digested gel plug. Further recovery was achieved by adding 30% acetonitrile/ 0.2% trifluroacetic acid to the gel plugs for 10 min at 37^0C with gentle agitation. The resulting supernatants were added to the initial peptide recovery following trypsin digestion. Exhaustive peptide recovery was achieved through the addition of 60% acetonitrile/0.2% trifluotoacetic acid to each plug for 10 min at 37^0C with gentle agitation. Supernatants were added to the peptide pool and the sample volume was reduced until dry through vacuum centrifugation. Samples were resuspended in 15ml of ultra-pure ddH2O and 0.1% formic acid for identification by ion trap LC/MS (Liquid Chromatography/ Mass Spectrometry) analysis.

The mass spectrometric analysis of peptides was carried out in the Proteomics Suite of the National University of Ireland, Maynooth with a Model 6340 Ion Trap LC/MS apparatus from Agilent Technologies (Santa Clara, CA). Excision, washing, destaining and treatment with trypsin, was performed by the above optimised method. Separation of peptides was performed with a nanoflow Agilent 1200 series system, equipped with a Zorbax 300SB C18 5mm, 4mm, 40 nl precolumn and a Zorbax 300SB C18 5 mm, 43mm x 75mm analytical reversed phase column using HPLC-Chip technology (Staples et al., 2009). The mobile phases utilized were A: 0.1% formic acid, B: 50% acetonitrile and 0.1% formic acid. Samples (5ml) were loaded into the enrichment column at a capillary flow rate set to 4ml/min with a mix of A and B at a ratio 19:1 (v/v).Tryptic peptides were eluted with a linear gradient of 10-90% solvent B over 15 min with a constant nano pump flow rate of 0.60ml/min. A 1min post time of solvent A was used to remove sample carry over. The capillary voltage was set to 2000 V and the flow and the temperature of the drying gas was 4ml/min and 300^0C, respectively. For protein identification, database searches were carried out with Mascot MS/MS Ion search (Matrix Science, London, UK).

2.2.20 Mitochondrial ROS measurement

Human PBMCs were isolated as outlined in section 2.2.18. Cells were plated at a density of 2 x 10^5. The following day cells were transfected with hECSIT specific siRNA as outlined in section 2.2.4.2. 48 hours after transfection cells were stimulated with LPS for 6hrs. Cells were then washed 3 times with warm PBS and stained with MitoSox (Invitrogen) at a final concentration of 2.5µM in OptiMEM for 30 minutes.

Cells were washed in PBS 3-5 times and cells were removed from plates resuspended in PBS containing 1% FBS and analysed by flow cytometry in the FL3 region.

2.2.21 DUB-Glo Protease Assay

DUB activity of recombinant full length hECSIT and C-terminal ECSIT was measures using the Promega DUB-Glo Protease Assay system. 50µl of DUB-Glo reagent was added to each well of a white 96-well plate containing 50µl of water, control or test sample. Samples were then mixed using a plate shaker at 300–500rpm for 30 seconds. Samples were then incubated at room temperature for 10-60 minutes. Luciferase measurements were then recorded using a luminometer plate reader after 10 min, 30 min and 60 min to determine DUB activity.

2.2.22 Statistical Analysis

Statistical analysis was performed using the Two-tailed Student's t-test where indicated. All statistical analysis was performed using the Prism 5 GraphPad software.

Chapter 3

Investigating the regulation and mechanism of hECSIT in TLR signalling

3.1 Introduction

Bacterial or viral infection leads to the activation of TLRs. Activation of these receptors leads to downstream signalling cascades within the cell that culminates in the activation of transcription factors such as NFκB and the IRFs, leading to production of pro-inflammatory cytokines and type 1 IFN. TLR4 has perhaps been the most widely study TLR and can initiate two signalling events know as the MyD88 dependent and MyD88 independent signalling pathways with the former resulting in activation of NFκB and the latter leading to the production of type 1 IFN. Other endosomal TLRs,, such as TLR3 respond to viral nucleic acids to produce type 1 IFN. TLRs are crucial for the eradication of infection however tight regulation of these signalling pathways are required to prevent damage and the manifestation of severe auto-immune conditions such as lupus and different types of cancer. Many regulators exist in the cell and serve to inhibit TLR pathways via the targeting of critical intracellular signalling adaptors such as TRAF6. TRAF6 ubiquitination leads to recruitment of TAK1 and the IKK complex which in turn phosphorylates IκB-α and activates NFκB. The creation of TRAF6 deficient mice revelaed the importance of TRAF6 in innate immunity. TRAF6 deficient mice have a severe deficiency in NFκB activation in response to IL-1β and LPS (Lomaga et al, 1999).

As discussed mECSIT was initially described as a TRAF6 interacting protein that bridged the latter to MEKK1 during TLR signalling. Overexpression of ECSIT was also demonstrated to activate NFκB whereas a truncated form of mECSIT, lacking the N-terminus, displayed dominant negative effects and strongly inhibited NFκB. Subsequent generation of an *Ecsit* knockout mouse revealed an embryonic lethal phenotype which resulted in death at E7.5 (Xiao et al, 2003). This phenotype was attributed to impaired mesoderm development and Bone Morphogenetic protein (BMP) signalling. The embryonic lethality of *Ecsit* $^{-/-}$ mice prevented further analysis of the *in vivo* role of *Ecsit*. In an attempt to further analyse the role of ECSIT Xiao *et al* used shRNA to knockdown the expression ECSIT. Knockdown of mECSIT resulted in impaired LPS induced NFκB activation. Survival of *Ecsit* $^{+/-}$ mice allowed for more detailed analysis of ECSITs functional role in vivo and identified mECSIT as a key signalling adaptor in mROS production during TLR signalling (West et al, 2011). Engagement of TLR4 and TLR2 results in recruitment of TRAF6 to the outer

mitochondrial membrane to facilitate the ubiquitination of mECSIT and subsequent production of mROS as demonstrated by reduced levels of mROS production in Ecsit$^{+/-}$ mice and TRAF6$^{-/-}$ mice. Surprisingly however, *Ecsit*$^{+/-}$ mice showed no deficiency in NFκB activation in response to TLR2 and TLR4. A mitochondrial role for murine ECSIT in the generation of ROS was of special interest considering an earlier report showing ECSIT to be an important regulator of mitochondrial complex 1 assembly during oxidative phosphorylation (Vogel et al, 2009).

To date there have been no published studies on the role of the human ortholog of ECSIT in TLR biology. The host laboratory for this thesis has previously cloned hECSIT and demonstrated functional differences between the murine and human forms of ECSIT. Over-expression studies suggested that hECSIT negatively regulates NFκB and this was associated with deubiquitination of TRAF6. The first section of this thesis aimed to further probe the regulatory role of hECSIT in IL-1R/TLR4 signalling and determine the mechanisms by which hECSIT is regulated and how it exerts its regulatory effect in these pro-inflammatory signalling pathways.

3.2 Results

3.2.1 Knockdown effect of hECSIT on LPS induced NFκB activation and mROS production

Previous work carried out in the author's host laboratory had identified hECSIT as a negative regulator of IL-1R/TLR4 signalling. These findings were mostly based on overexpression studies and the present study commenced with a characterisation of the effects of hECSIT knockdown on these pathways. U373 cells were initially transfected with control or ECSIT-specific siRNA and knockdown of hECSIT expression was confirmed by Western blotting (Fig. 3.1A). These cells were subsequently treated with LPS for various times. Knockdown of hECSIT with siRNA resulted in increased phosphorylation of IκB-α and more pronounced degradation of IκB-α in response to LPS espcially at longer time points post stimulation (Figure 3.1A). We next looked at activation of NFκB by characterising the binding of nuclear extracts to an oligonucleotide containing the NFκB recognition motif. U373 cells were transduced with lentiviral particles containing control or hECSIT-specific shRNA and cell lines were selected for stably integrated shRNA constructs. hECSIT expression was suppressed in cells stably expressing hECSIT shRNA (Fig. 3.1B). Cells were stimulated with LPS for the indicated times and nuclear extracts were assayed for NFκB oilgonucleotide binding. LPS induced a time dependent increase in the binding of nuclear extracts to the NFκB oligonucleotide and this was slightly enhanced in hECSIT knockdown cells (Figure 3.1B). Given that pro-inflammatory cytokines are primarily regulated by NFκB transcription factors we also measured LPS-induced expression of the cytokines IL-6 and IL-8 that are strongly regulated by NFκB. However knockdown of hECSIT resulted in no significant difference in LPS and IL-1 induced production of IL-6 (Figure 3.2).

A recent report had shown that ubiquitination of mECSIT by TRAF6 promotes accumulation of mECSIT at the outer mitochondrial membrane to promote the production of mROS during TLR4 and TLR2 signalling. Since murine and human ECSIT appear to have different functions in the NFκB pathway we investigated if hECSIT could mimic the ability of mECSIT to regulate Mitochondrial Reactive Oxygen Species (mROS) production. Human Peripheral Blood Mononuclear Cells

(PBMCs) were transfected with control or hECSIT specific siRNA and stimulated with LPS to promote production of mROS. Stimulation of human PBMCs with LPS resulted in a slight increase in mROS production in hECSIT knockdown cells (Figure 3.3A) as confirmed by an increase in mean fluorescent intensity in cells positively stained with the mROS specific stain MitoSox (Figure 3.3B). Knockdown of hECSIT was confirmed in whole cell lysates (Figure 3.3C). These results again suggest contrasting functions for murine and human ECSIT in that whereas the murine form mediates the production of mROS, hECSIT appears to counter-regulate its production.

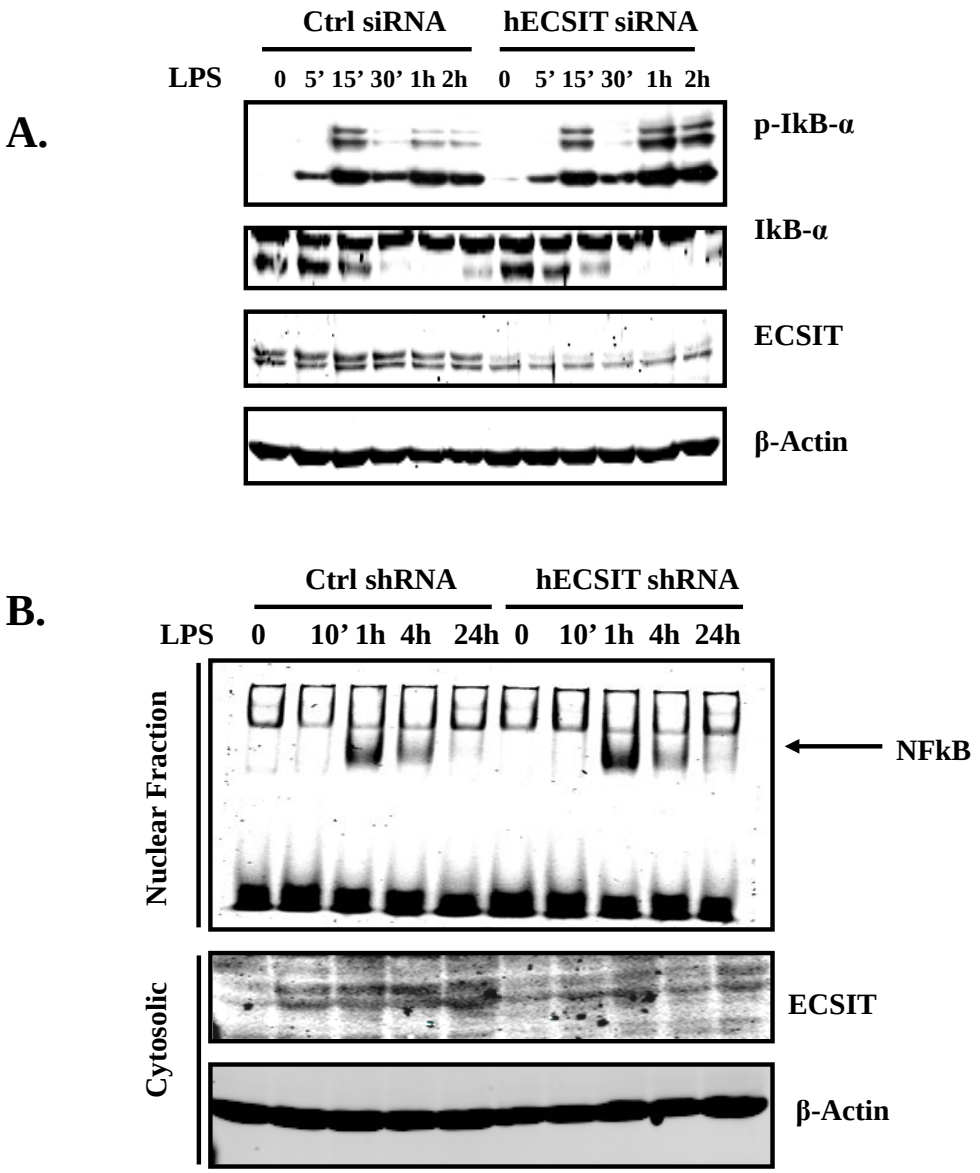

Figure 3.1 Knockdown effect of hECSIT on LPS induced NFκB activation

(A) U373 cells were transfected with hECSIT specific siRNA (30nm) or Control siRNA (30nm) for 48 hrs. Cells were then treated with LPS (100ng/ml) for the indicated times. Cells lysates were prepared and separated by SDS-PAGE followed by Immunoblotting for phosphorylated and total levels of IκB-α. Lysates were also probed for levels of ECSIT and β-Actin to confirm knockdown and equal loading. (B) U373 Cells were infected with Lentivirus containing constructs encoding control or hECSIT specific shRNA. Cells were grown in the presence of puromycin (8μg/ml) to select cells with stably integrated shRNA constructs. Selected cells were treated with LPS (100ng/ml) for the indicated times. Nuclear extracts were prepared and subsequently incubated with an Infra-Red labelled oligonucleotide containing an NFκB-binding motif and separated by native PAGE. Cytosolic extracts were probed for levels of hECSIT and β-Actin to confirm knockdown and equal loading respectively. Data shown is representative of 3 independent experiments.

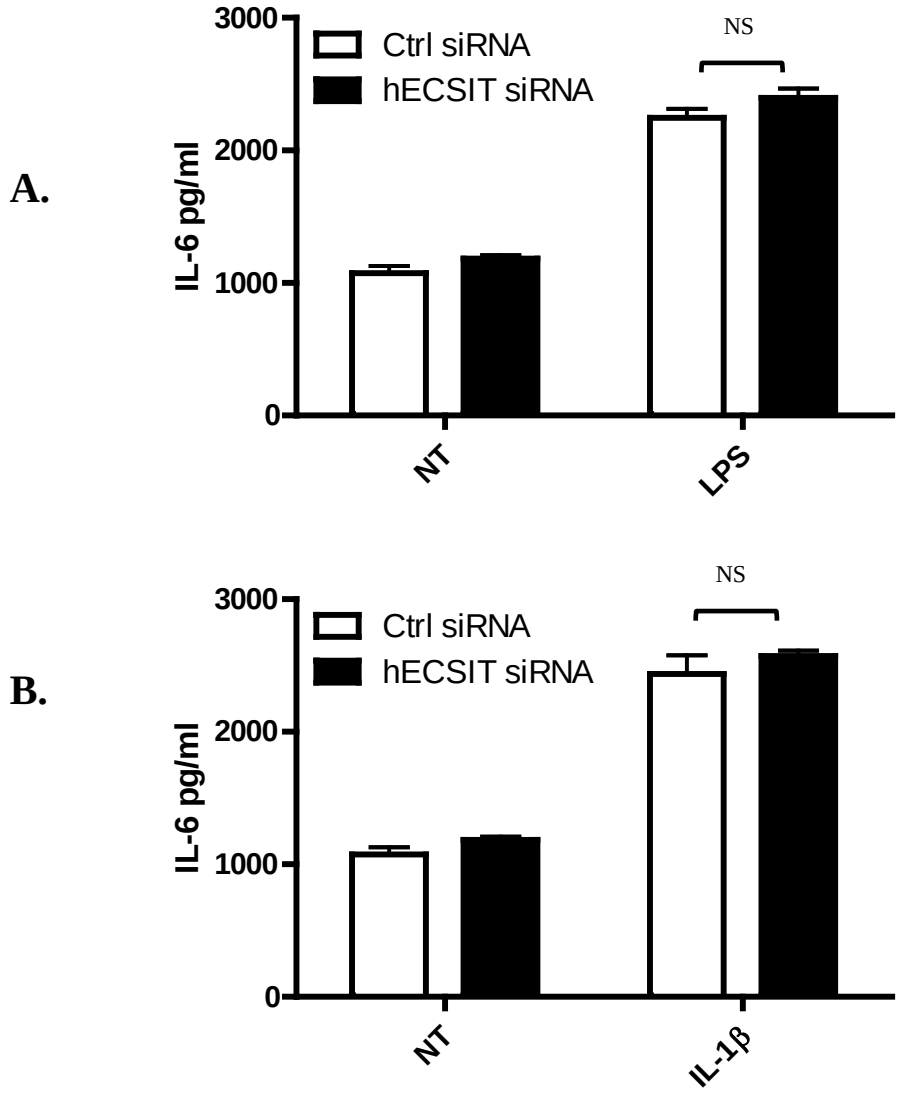

Figure 3.2 Knockdown effect of hECSIT on LPS and IL-1 induced IL-6 production

U373 Cells were transfected with hECSIT specific siRNA (30nm) or Control siRNA (30nm). 48 hours after transfection cells were stimulated with (A) LPS (100ng/ml) or (B) IL-1β (10ng/ml) for 24 hrs. Media from NT and LPS and IL-1β treated cells were analysed for levels of IL-6 by ELISA. Data shown represents the mean of 3 independent experiments; $p<0.05$.

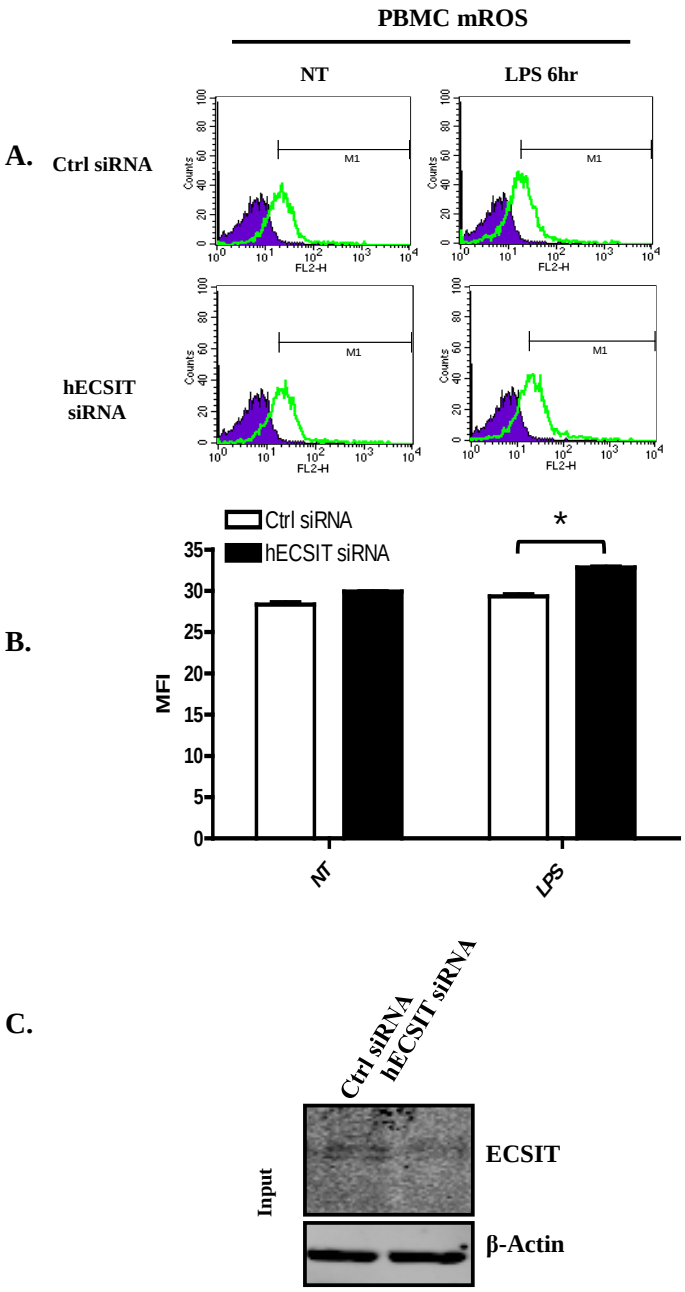

Figure 3.3 Knockdown of hECSIT enhances LPS-induced production of mROS

Healthy donor PBMCs were isolated by Ficoll -paque method and transfected with hECSIT specific siRNA (30nm) or Control siRNA (30nm). 24 hours later cells were re-transfected with siRNA as before. 48 hours after the first transfection cells were stimulated with LPS (100ng/ml) for 6hr. Cells were subsequently stained with MitoSox and analysed by flow cytometry (A) with data also displayed as mean fluorescent intensity (MFI) (B) Data represent mean +/- SD from triplicate samples from 3 independent experiments (C) Cell lysates were generated and probed for hECSIT and β-Actin to confirm knockdown and equal loading respectively; $p<0.05$.

3.2.2 hECSIT interacts with and regulates TRAF6 ubiquitination

Given that hECSIT appears to have roles that contrast to those of mECSIT we decided to probe the molecular basis to the hECSIT function by initially focussing on its protein interaction partners. mECSIT was initially described as a TRAF6 interacting protein in a yeast two hybrid study and was subsequently shown to promote the polyubiquitination of hECSIT during TLR signalling. Overexpression studies were initially performed to compare the ability of murine and human ECSIT to interact with TRAF6 with co-immunoprecipitation analysis showing that both forms of ECSIT are capable of interacting with TRAF6 (Fig. 3.4C). Co-immunoprecipitation studies were carried out to further investigate the possible interaction between hECSIT and TRAF6 at an endogenous level in response to TLR ligands using different cell lines. U373 cells treated with LPS resulted in a time-dependent interaction between hECSIT and TRAF6 as demonstrated by co-immunoprecipitation of TRAF6 with hECSIT (Figure 3.4A). IL-1 showed a similar ability to promote the interaction of TRAF6 and hECSIT in HeLa cells (Figure 3.4B). TRAF6 is an important E3 ligase in the activation of NFκB and mutation of the C70 residue in its RING domain results in loss of its E3 ligase activity and its ability to activate NFκB. TRAF6 can also undergo auto-ubiquitination at K124. We next assessed if these sites are important for the interaction between TRAF6 and hECSIT. Co-immunoprecipitation analysis showed that mutation of the C70 residue of TRAF6 resulted in reduced interaction between hECSIT and TRAF6 (Figure 3.5). However mutation of the K124 residue, the site for auto-ubiquitination, failed to affect this interaction (Figure 3.5). Interestingly the co-expression of hECSIT with TRAF6 leads to increased levels of hECSIT and the appearance of faster migrating anti-ECSIT immunoreactive bands possibly indicative of TRAF6-induced processing of hECSIT. However expression of hECSIT with the TRAF6 E3 ligase mutant, C70A, resulted in impaired phosphorylation and processing of hECSIT (Figure 3.5). Interestingly this was not apparent with mECSIT. In addition the putative processed form of hECSIT is less apparent when hECSIT is coexpressed with the TRAF6 mutant that lacks E3 ligase activity.

Given the interaction of hECSIT with TRAF6 in an E3 ligase dependent manner we next assessed if hECSIT could regulate the ubiquitination status of TRAF6. Thus hECSIT was knocked down in HEK293 cells with hECSIT-specific

siRNA and the ability of LPS to promote ubiquitination of TRAF6 was examined (Figure 3.6). LPS promoted the ubiquitination of TRAF6 in a time dependent manner However in knockdown cells TRAF6 ubiquitination was more prolonged. The increased ubiquitination of TRAF6 under conditions of ECSIT knockdown correlates with the observed enhanced activation of NFκB, and thus the regulatory effects of hECSIT on NFκB might be associated with its regulatory effects on the ubiquitination of TRAF6.

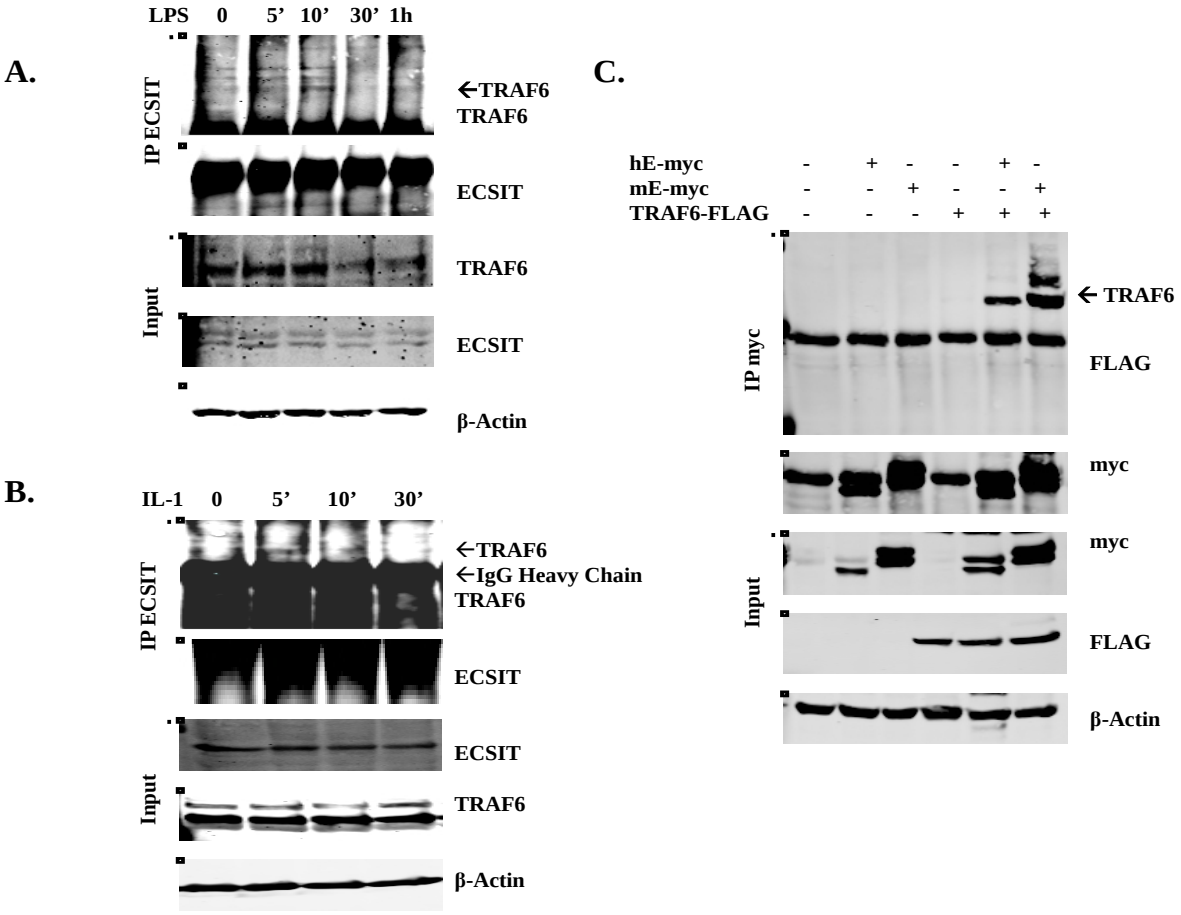

Figure 3.4 hECSIT interacts with TRAF6

(A) U373 cells were treated with LPS (100ng/ml). (B) HeLa cells were treated with IL-1β (10ng/ml) for the indicated times. Cell lysates were generated and a sample for whole cell lysates analysis was retained. The remaining lysates was immunoprecipitated using an anti-ECSIT antibody. Immunoprecipitates were subsequently assayed for co-precipitated TRAF6. The expression levels of ECSIT and TRAF6 in whole cell lysates (Input) were also assessed by western blotting. Cell lysates were generated and a sample for whole cell lysates analysis was retained. The remaining lysates was immunoprecipitated using an anti-ECSIT antibody. Immunoprecipitates were subsequently assayed for co-precipitated TRAF6. The expression levels of ECSIT and TRAF6 in whole cell lysates (Input) were also assessed by western blotting. (C) HEK293 cells were co-transfected with Empty vector (EV) pcDNA3.1 (1µg), myc-tagged hECSIT (1µg) or myc-tagged mECSIT (1µg) with or without FLAG-tagged TRAF6 (1µg). EV was used to normalize total amount of DNA transfected. 24 hrs post-transfection cell lysates were generated and immunoprecipitated with anti-myc antibody. Immunoprecipitates were then subject to SDS-PAGE and subsequently to western blotting using anti-FLAG antibody. Whole cell lysates were also analysed by western blotting using anti-FLAG and anti-Myc antibodies to confirm expression of TRAF6 and ECSIT constructs, respectively. Results are representative of 3 independent experiments.

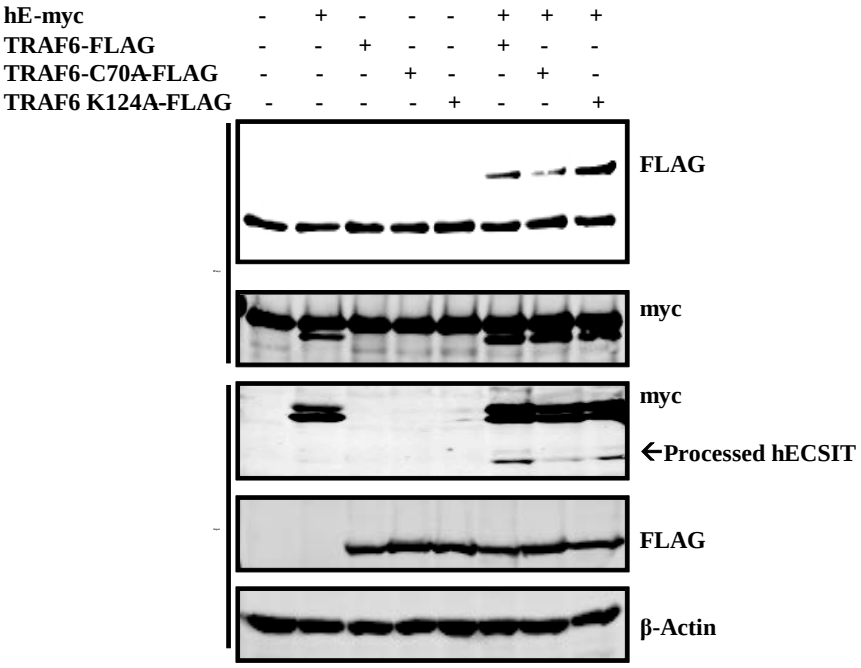

Figure 3.5 Mutation of the RING domain of TRAF6 reduces its interaction with hECSIT

HEK293 cells were co-transfected with Empty vector (EV) pcDNA3.1 (1µg), myc-tagged hECSIT (1µg) or with or without FLAG-tagged TRAF6 (1µg), TRAF6C70A (1µg) or TRAF6K124A (1µg). EV was used to normalize total amount of DNA transfected. 24 hrs post-transfection cell lysates were generated and immunoprecipitated with anti-myc antibody. Immunoprecipitates were then subject to SDS-PAGE and subsequently to western blotting using anti-FLAG antibody. Whole cell lysates were also analysed by western blotting using anti-FLAG and anti-Myc antibodies to confirm expression of TRAF6 and ECSIT constructs, respectively. Results are representative of 3 independent experiments.

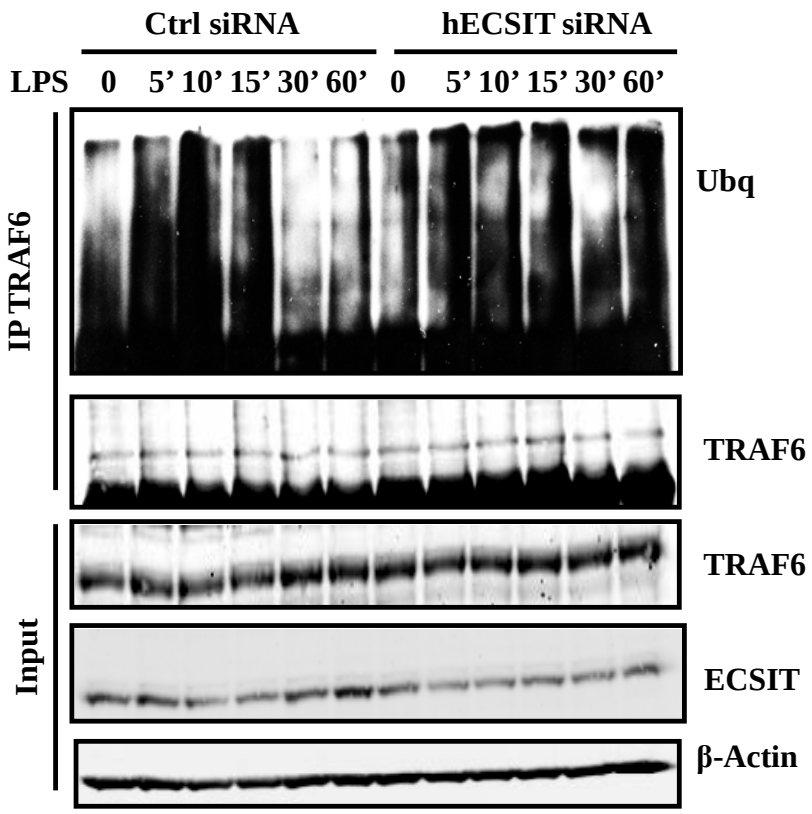

Figure 3.6 Knockdown of hECSIT prolongs LPS induced ubiquitination of TRAF6 in HEK293 cells

HEK293-TLR4 Cells were transfected with hECSIT specific siRNA (30nm) or Control siRNA (30nm). 48 hrs after transfection cells were then treated with LPS (100 ng/ml) for the indicated times. Cell lysates were generated and immunoprecipitated using anti-TRAF6 antibody. The immunoprecipitates were then assayed for ubiquitination and TRAF6 by immunoblotting using anti-ubiquitin and TRAF6 antibodies respectively. Expression levels of TRAF6, ECSIT and β-Actin were also assessed in cell lysates to confirm knockdown and equal loading, respectively of input samples prior to immunoprecipitation. Data shown is representative of 3 independent experiments.

3.2.3 TRAF6 and TAK1 promote, ubiquitination and processing of hECSIT

The identification of processed forms of hECSIT, when co-expressed with wild type TRAF6, led us to investigate if other signalling components in the NFκB pathway could similarly promote processing of hECSIT. TAK1 is an important kinase in the activation of NFκB and is a downstream effector of TRAF6 and, therefore we compared the ability of TRAF6 and TAK1 to induce processing of hECSIT. TAK1 activity requires the presence of its protein interaction partner TAB1, and when investigating the effects of TAK1, we also co-expressed TAB1. Expression of hECSIT with TAK1/TAB1 resulted in the appearance of a number of fast migrating anti-ECSIT immunoreactive bands and the profile of these bands was similar to when hECSIT was co-expressed with TRAF6 (Figure 3.7A). Furthermore, in these studies the co-expression of hECSIT with TRAF6 or TAK1 resulted in the appearance of a slower migrating form of hECSIT, and this may possibly represent modification by phosphorylation. In order to evaluate the physiological relevance of such putative phosphorylation or processing of ECSIT by signalling molecules like TRAF6 and TAK1, we immunoblotted for endogenous ECSIT in U373 cells that have been stimulated with LPS for various time periods. Stimulation with LPS resulted in a time-dependent increase in intensity of fast migrating anti-ECSIT immunoreactive bands (Fig 3.7B). We also provide further support that these bands represent processed forms of hECSIT since they are absent or greatly reduced in hECSIT knockdown cells (Figure 3.7B). Furthermore the hECSIT construct is tagged with a myc tag at the C-terminal end of the protein. Given the appearance of a faster migrating band when probed with an anti-myc antibody we concluded that the processed form of hECSIT is the C-terminal section of the protein and the potential processing sites lie in the N-terminal region of the sequence. Given that a previous report indicated TRAF6 to promote ubiquitination of mECSIT and that ubiquitination is sometimes a pre-requisite to protein processing, we next examined if TRAF6 can promote ubiquitination of hECSIT by measuring the ubiquitination status of immunoprecipitated hECSIT. The co-expression of hECSIT with increasing amounts of expression constructs encoding TRAF6 resulted in strong ubiquitination of hECSIT (Fig. 3.8B). Given that TAK1 can also promote processing of hECSIT we also demonstrate that TAK1 stimulates very strongly the ubiquitination of hECSIT (3.8A). It is also notable that TAK1 promotes the appearance of an ECSIT form that migrates

closely above the full length form and it is tempting to speculate that might be the result of TAK1 promoting the phosphorylation of hECSIT.

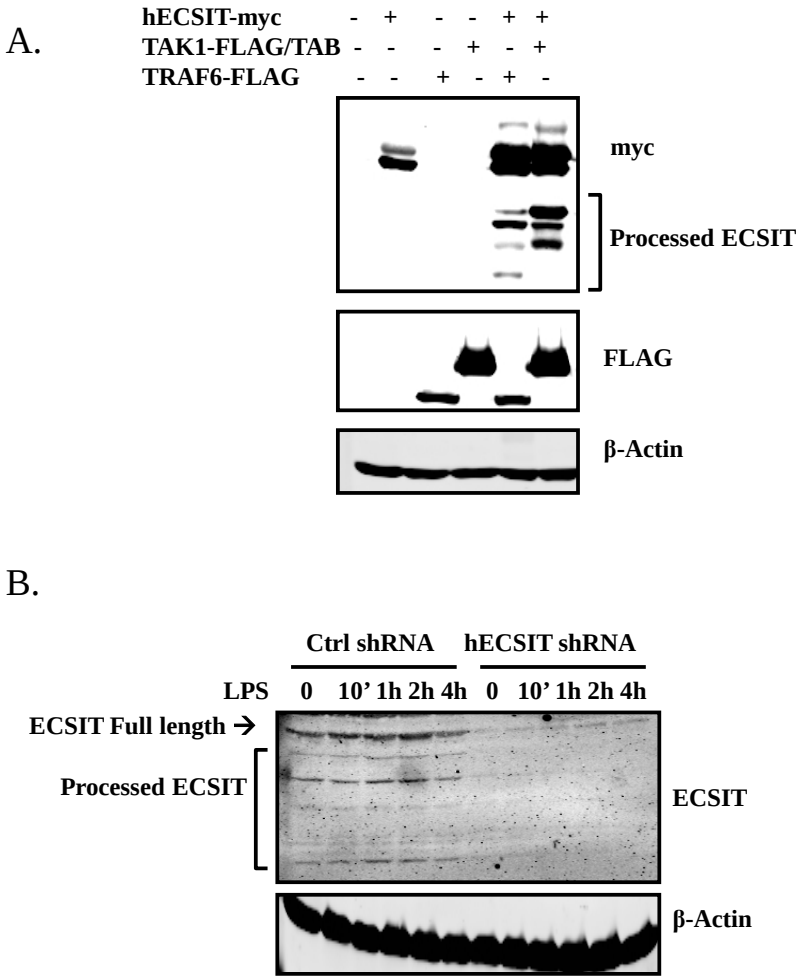

Figure 3.7 TRAF6 and TAK1 promote processing of hECSIT

(A) HEK293 cells were co-transfected with Empty vector (EV) pcDNA3.1 (1µg), myc-tagged hECSIT (1µg) with or without FLAG-tagged TRAF6 or TAK1 (1µg). EV was used to normalize total amount of DNA transfected. 24 hrs post-transfection cell lysates were analysed by western blotting using anti-FLAG and anti-Myc antibodies to assess levels of TAK1, TRAF6 and ECSIT , respectively. Results are representative of 3 independent experiments. (B) U373 Cells were infected with Lentivirus containing constructs encoding control or hECSIT specific shRNA. Cells were grown in the presence of puromycin (8µg/ml) to select cells with stably integrated shRNA constructs. Selected cells were treated with LPS (100ng/ml) for the indicated times. Cell lysates were subsequently generated and probed for processed hECSIT by western blotting using anti-ECSIT antibody. Data shown is representative of 3 independent experiments.

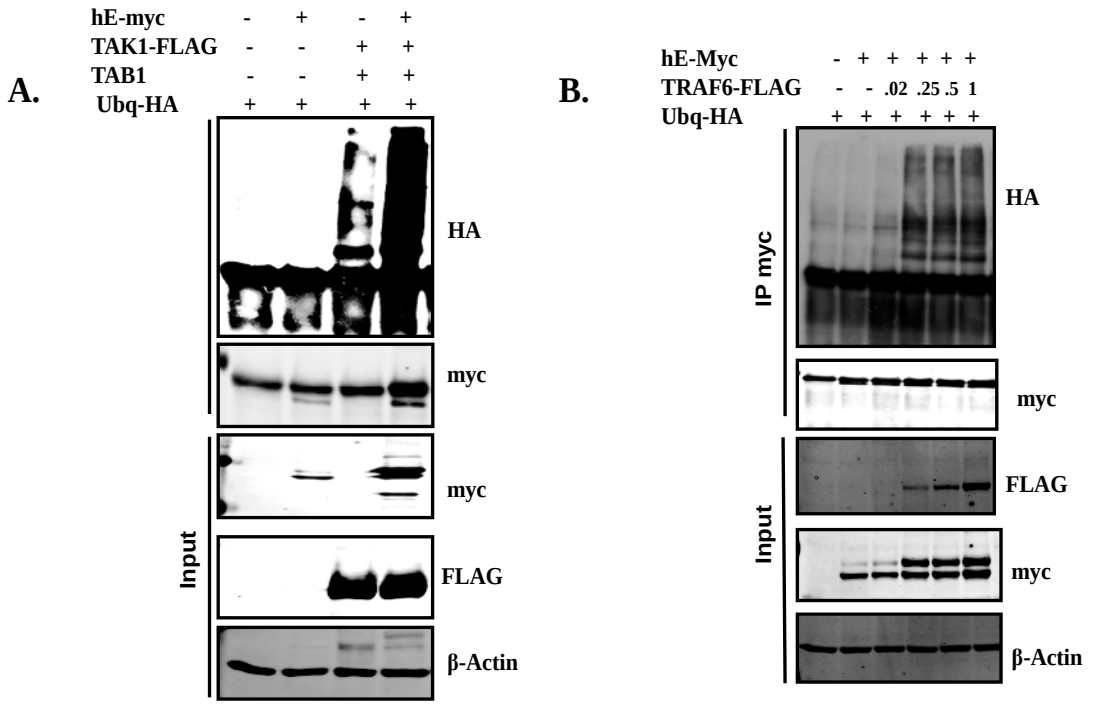

Figure 3.8 TAK1 and TRAF6 promote the ubiquitination of hECSIT

HEK293 cells were co-transfected with Empty vector (1µg), HA-Ubq (1µg), myc-tagged hECSIT (1µg) with or without FLAG-tagged TAK1 (1µg) and TAB1 (1µg). EV was used to normalize total amount of DNA transfected. 24 hrs post-transfection cell lysates were generated and immunoprecipitated using an anti-myc antibody. Immunoprecipitates were then subject to SDS-PAGE and subsequently to western blotting using anti-HA antibody. Whole cell lysates were also analysed by western blotting using anti-FLAG and anti-Myc antibodies to confirm expression of TAK1 and ECSIT constructs, respectively. (B) HEK293 cells were co-transfected with Empty vector (1µg), HA-Ubq (1µg), and myc-tagged hECSIT (1µg) with or without increasing concentrations of FLAG-tagged TRAF6 (0.025-1µg). EV was used to normalize total amount of DNA transfected. 24 hrs post-transfection cell lysates were generated and immunoprecipitated using an anti-myc antibody. Immunoprecipitates were then subject to SDS-PAGE and subsequently to western blotting using anti-HA antibody. Whole cell lysates were also analysed by western blotting using anti-FLAG and anti-Myc antibodies to confirm expression of TRAF6 and ECSIT constructs, respectively. Data shown is representative of 3 independent experiments.

3.2.4 hECSIT interacts with TAK1

Given the ability of TAK1 to potentially regulate the phosphorylation, ubiquitination and processing of hECSIT, we characterised the potential interaction between hECSIT and TAK1 using co-immunoprecipitation analysis. The interaction of TAK1 with hECSIT and mECSIT was initially investigated after transient transfection of expression constructs encoding both proteins in HEK293T cells. Myc-tagged hECSIT or mECSIT was co-expressed with FLAG-tagged TAK1/TAB1, immunoprecipitated with anti-myc antibody and probed for the presence of co-precipitated FLAG-tagged TAK1. As shown in Figure 3.9C both hECSIT and mECSIT interacted with TAK1. We next aimed to confirm interaction of endogenous forms of these proteins and characterise the potential regulatory effects of TLR signalling on such interactions. U373 cells were treated with LPS and immunoprecipitated with anti-ECSIT antibody. The subsequent precipitate was then analyzed for the presence of co-precipitated TAK1 by western blotting. LPS promoted the interaction of TAK1 with hECSIT in a time-dependent manner, as demonstrated by the co-immunoprecipitation of the two proteins (Figure 3.9A). Treatment of HeLa cells with IL-1β also resulted in the co-immunoprecipitation of hECSIT with TAK1 in a time dependent manner (Figure 3.9B). These data confirm that pro-inflammatory signalling pathways such as TLR4 and IL-1 promote the association of TAK1 with hECSIT and this may lead to the phosphorylation, ubiquitination and processing of hECSIT.

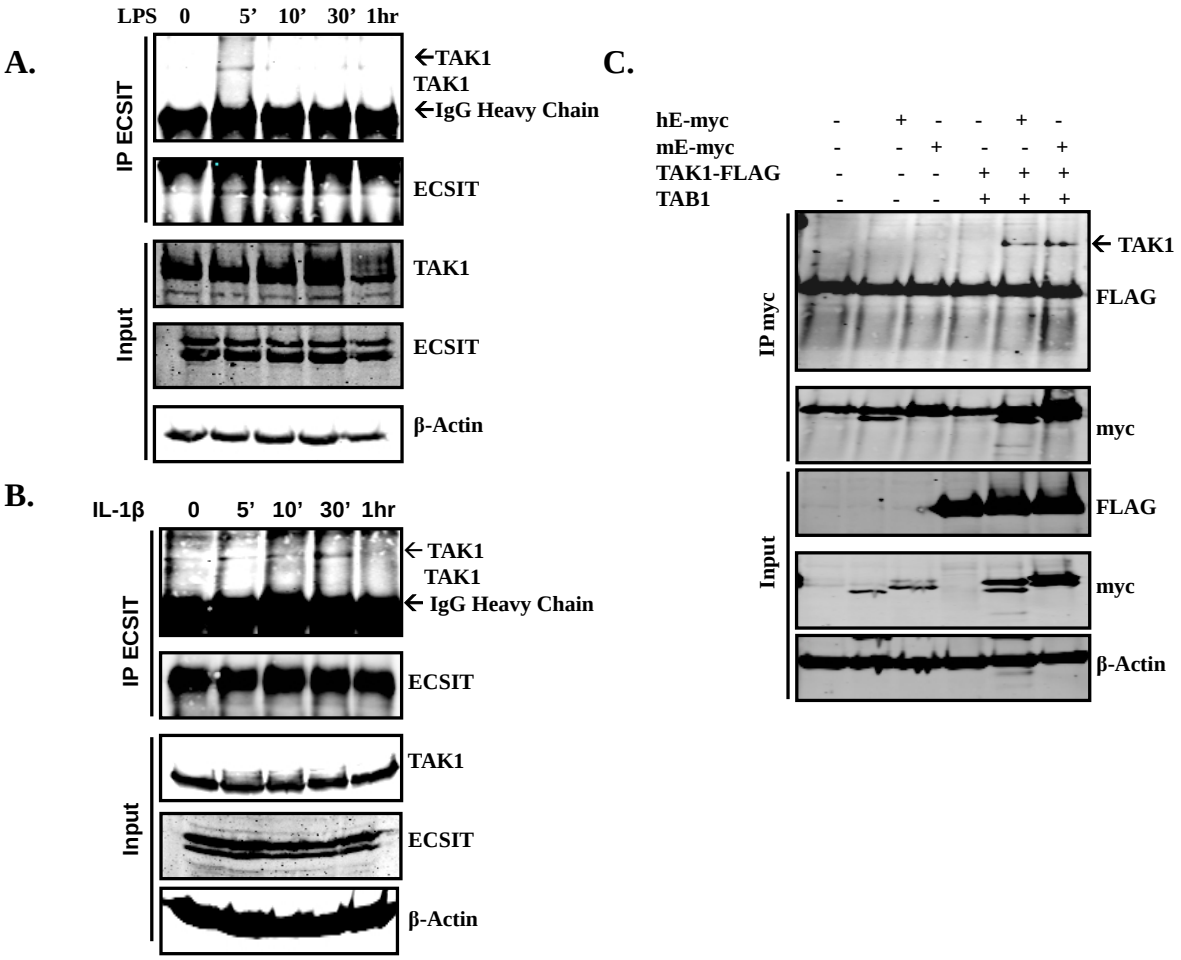

Figure 3.9 hECSIT interacts with TAK1

(A) U373 cells were treated with LPS (100ng/ml) for the indicated times. (B) HeLa cells were treated with IL-1β (10ng/ml) for the indicated times. Cell lysates were generated and a sample for whole cell lysates analysis was retained. The remaining lysates was immunoprecipitated using an anti-ECSIT antibody. Immunoprecipitates were subsequently assayed for co-precipitated TAK1. The expression levels of ECSIT and TAK1 in whole cell lysates (Input) were also assessed by western blotting. (C) HEK293 cells were co-transfected with Empty vector (EV) pcDNA3.1 (1µg), myc-tagged hECSIT (1µg) or myc-tagged mECSIT (1µg) with or without FLAG-tagged TAK1 (1µg). EV was used to normalize total amount of DNA transfected. 24 hrs post-transfection cell lysates were generated and immunoprecipitated with anti-myc antibody. Immunoprecipitates were then subject to SDS-PAGE and subsequently to western blotting using anti-FLAG antibody. Whole cell lysates were also analysed by western blotting using anti-FLAG and anti-Myc antibodies to confirm expression of TAK1 and ECSIT constructs, respectively. Data shown are representative of 3 independent experiments.

3.2.5 The Kinase activity and ubiquitination of TAK1 is required for the phosphorylation, ubiquitination and processing of hECSIT

We next began to investigate the direct role of TAK1 in regulating the various modifications of hECSIT. TAK1 facilitates the activation of NFκB and the MAP kinases via its kinase activity. The ubiquitination of TAK1 is also required in the activation of NFκB in response to IL-1β and TNF-α (Fan et al, 2009). We first analysed the role of, if any, the kinase activity of TAK1 in regulating the various modifications of hECSIT. To this end we employed the TAK1 inhibitor 5z-7-oxozeanol to block the kinase activity of TAK1. LPS stimulation of U373 cells resulted in hECSIT processing and this was dramatically reduced when cells were pre-treated with the TAK1 inhibitor (Figure 3.10A). Similarly HeLa cells, treated with IL-1β, also showed time-dependent processing of hECSIT and pre-treatment of cells with a TAK1 inhibitor blocked this IL-1β induced processing of hECSIT. The efficacy of the inhibitor was confirmed by demonstrating its ability to block IL-1-induced degradation of IκB-α in HeLa cells (Figure 3.10B). To further probe the moleclar basis to the importance of TAK1 kinase activity for ECSIT processing, an expression construct encoding a kinase dead form of TAK1 was assessed for its potential to interact with hECSIT. Kinase dead TAK1 failed to mimic its wild type counterpart in interacting with hECSIT (Figure 3.11A) and thus unsurprisingly did not induce the putative phosphorylation, processing (Figure 3.11A) or ubiquitination of hECSIT (Figure 3.11B). Both K158 and K209 have been described as putative ubiquitination sites in TAK1 (Fan et al, 2011) with the former identified as an important ubiquitination site for the activation of NFκB. Introduction of the TAK1-K158R mutation resulted in the loss of binding of TAK1 to hECSIT and lack of effect on the phosphorylation, processing (3.12A) and ubiquitination (3.12B) of hECSIT. Ubiquitination of K209 is dispensable for TAK1 mediated activation of NFκB and interestingly the K209R mutant form of TAK1 retained the ability, albeit to a slightly lesser effect, to interact with hECSIT and promote its various modifications. In order to confirm the potential phosphorylation of hECSIT by TAK1, lysates containing over-expressed hECSIT and TAK1 were incubated with or without the phosphatase CIP. However CIP treatment had no effect on this modification (Figure 3.13).

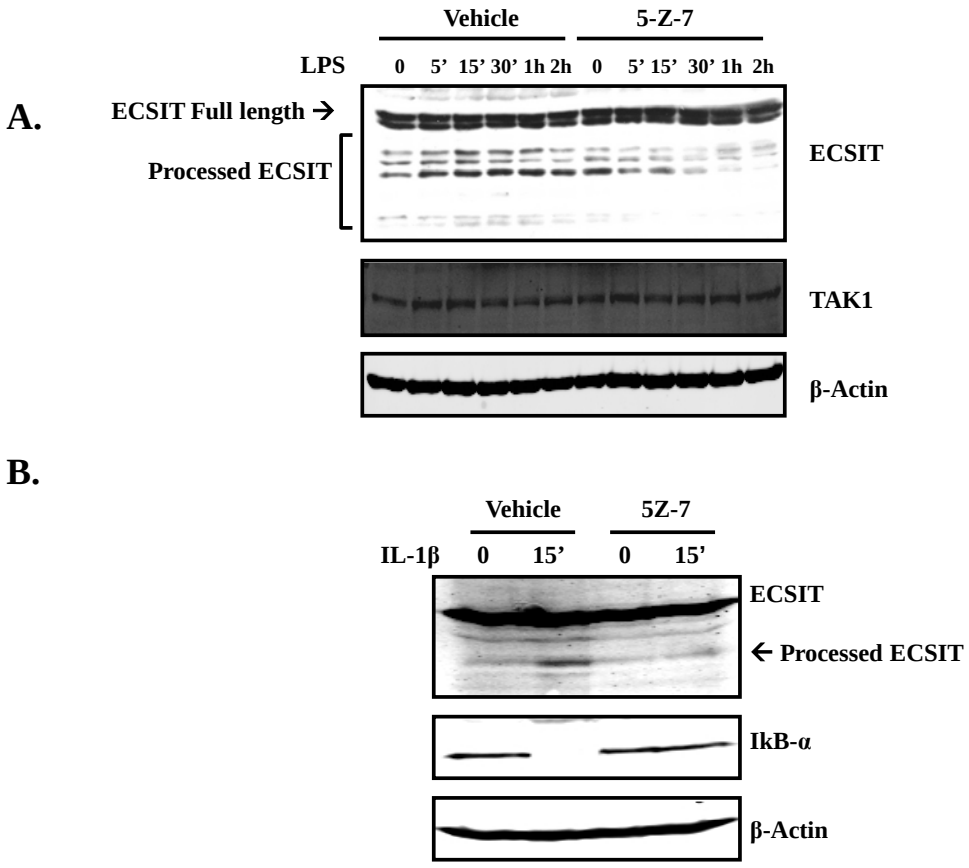

Figure 3.10 Inhibition of TAK1 blocks LPS and IL-1β induced processing of hECSIT

(A) U373 cells were pre-treated with 5Z-7-oxozeanol (20Mm) or DMSO (Vehicle) for 2hrs followed by treatment with LPS (100ng/ml) for the indicated times. Cell lysates were subsequently generated and probed for hECSIT using an anti-ECSIT antibody. (B) HeLa cells were pre-treated with 5Z-7-oxozeanol (20Mm) or DMSO (Vehicle) for 2hrs followed by treatment with IL-1β (10ng/ml) for the indicated times. Cell lysates were subsequently generated and probed for hECSIT using an anti-ECSIT antibody. Processed forms of hECSIT are indicated by arrows.

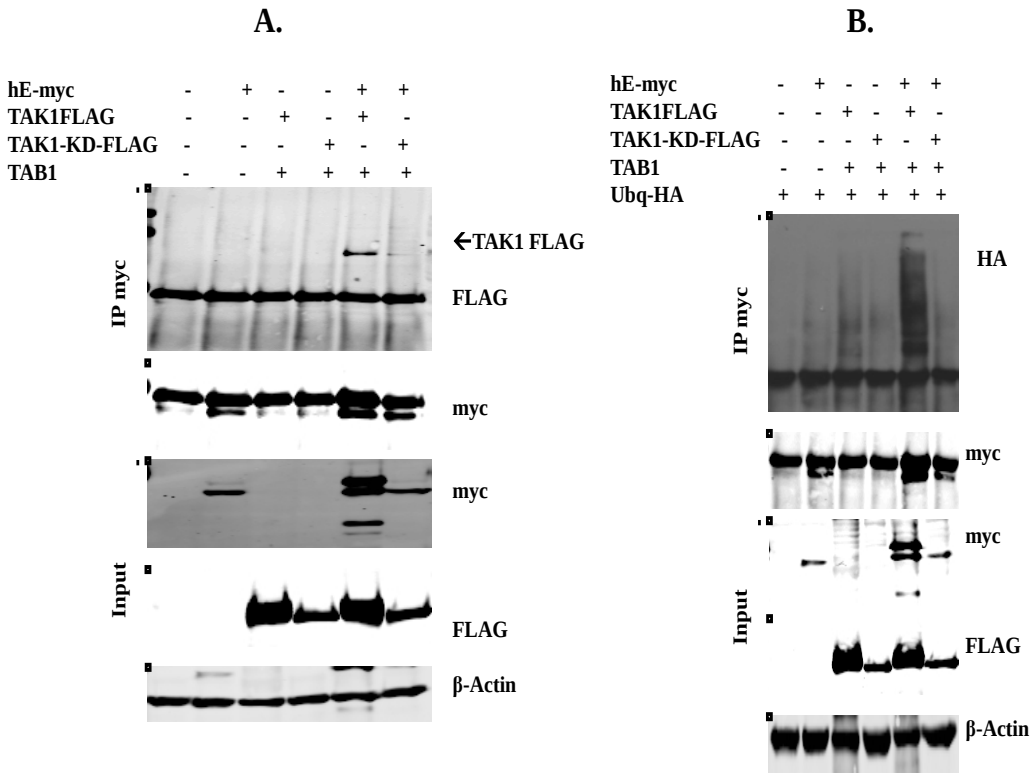

Figure 3.11 The kinase activity of TAK1 is required for its interaction with hECSIT and to manifest putative phosphorylation, processing and ubiquitination of hECSIT

(A) HEK293 cells were co-transfected with Empty vector (EV) pcDNA3.1 (1µg), myc-tagged hECSIT (1µg) with or without FLAG-tagged TAK1 (1µg) or Kinase dead TAK1 (1µg) and TAB1 (1µg). EV was used to normalize total amount of DNA transfected. 24 hrs post-transfection cell lysates were generated and immunoprecipitated with anti-myc antibody. Immunoprecipitates were then subject to SDS-PAGE and subsequently to western blotting using anti-FLAG antibody. Whole cell lysates were also analysed by western blotting using anti-FLAG and anti-Myc antibodies to confirm expression of TAK1 and ECSIT constructs, respectively. (B) HEK293 cells were co-transfected with Empty vector (1µg), HA-Ubq (1µg), myc-tagged hECSIT (1µg) with or without FLAG-tagged TAK1 (1µg) and TAB1 (1µg). EV was used to normalize total amount of DNA transfected. 24 hrs post-transfection cell lysates were generated and immunoprecipitated using an anti-myc antibody. Immunoprecipitates were then subject to SDS-PAGE and subsequently to western blotting using anti-HA antibody. Whole cell lysates were also analysed by western blotting using anti-FLAG and anti-Myc antibodies to confirm expression of TAK1 and ECSIT constructs, respectively. Data shown is representative of 3 independent experiments

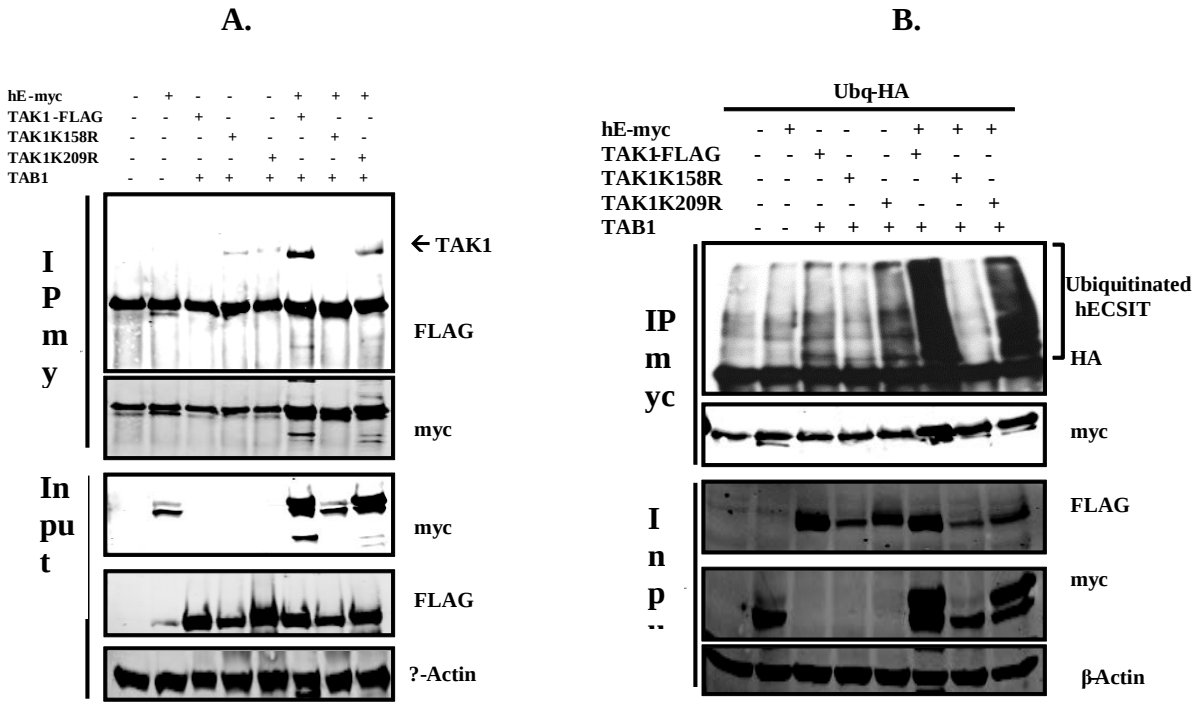

Figure 3.12 The K158 ubiquitination site of TAK1 is required for its binding to and modification of hECSIT

(A) HEK293 cells were co-transfected with Empty vector (EV) pcDNA3.1 (1µg), myc-tagged hECSIT (1µg) with or without FLAG-tagged TAK1 (1µg), TAK1-K158R or TAK1-K209R (1µg) and TAB1 (1µg). EV was used to normalize total amount of DNA transfected. 24 hrs post-transfection cell lysates were generated and immunoprecipitated with anti-myc antibody. Immunoprecipitates were then subject to SDS-PAGE and subsequently to western blotting using anti-FLAG antibody. Whole cell lysates were also analysed by western blotting using anti-FLAG and anti-Myc antibodies to confirm expression of TAK1 and ECSIT constructs, respectively. (B) HEK293 cells were co-transfected with Empty vector (1µg), HA-Ubq (1µg), myc-tagged hECSIT (1µg) with or without FLAG-tagged TAK1, TAK1-K158R or TAK1-K209R (1µg) and TAB1 (1µg). EV was used to normalize total amount of DNA transfected. 24 hrs post-transfection cell lysates were generated and immunoprecipitated using an anti-myc antibody. Immunoprecipitates were then subject to SDS-PAGE and subsequently to western blotting using anti-HA antibody. Whole cell lysates were also analysed by western blotting using anti-FLAG and anti-Myc antibodies to confirm expression of TAK1 and ECSIT constructs, respectively. Data shown is representative of 3 independent experiments.

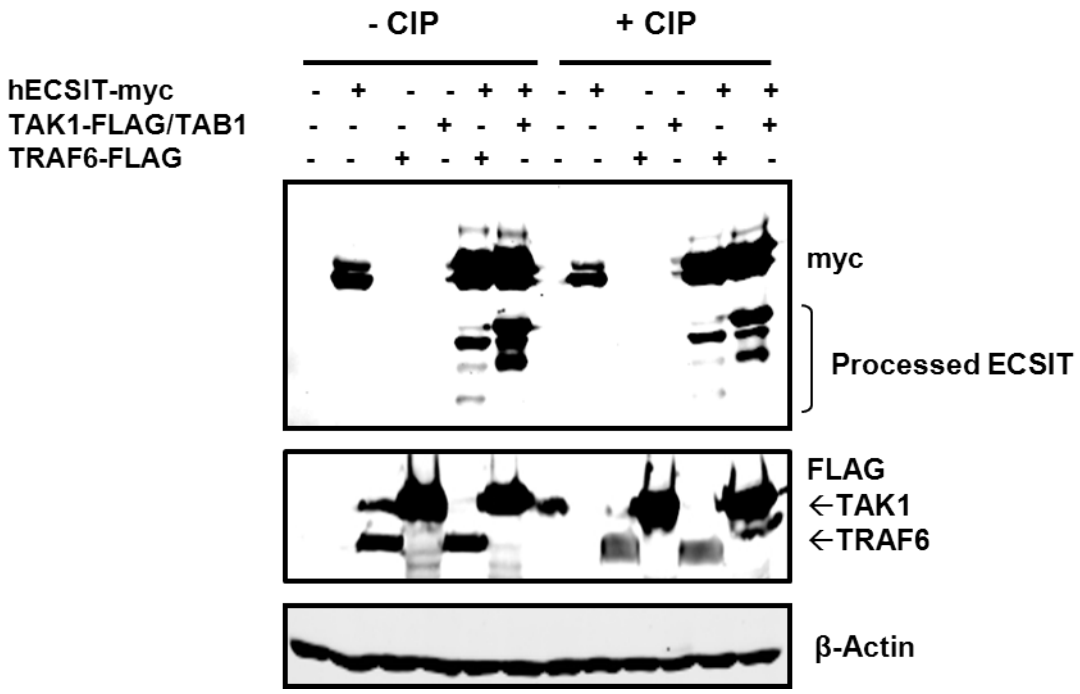

Figure 3.13 Phosphatase treatment of TAK1 induced hECSIT modification

HEK293 cells were co-transfected with Empty vector (EV) pcDNA3.1 (1µg), myc-tagged hECSIT (1µg) with or without FLAG-tagged TAK1 and TAB1 (1µg) or TRAF6 (1µg). EV was used to normalize total amount of DNA transfected. 24 hrs post-transfection cell lysates were generated and incubated at 37°C for 30 minutes with Calf Intestinal phosphatase (CIP). 4X sample buffer was then added to terminate the reaction. Samples were then subject to SDS-PAGE and subsequently to western blotting using anti-FLAG antibody. Whole cell lysates were also analysed by western blotting using anti-FLAG and anti-Myc antibodies to confirm expression of TAK1 and ECSIT constructs, respectively

3.2.6 Caspase 8 promotes the phosphorylation, ubiquitination and processing of hECSIT

From the previous results it was established that hECSIT is subjected to various forms of modification including extensive processing. The identification of TAK1 as the potential kinase and TRAF6 as the E3 ligase led us to search for a protease that could potentially process hECSIT. Caspase 8 is a widely studied protease that functions in most TLR pathways and has been shown to directly process proteins such as RIP1 and IRF3. Caspase 8 was initially shown to co-immunoprecipitate with hECSIT and this was independent of its caspase catalytic activty since the C360S point mutant form of caspase 8 was also capable of interacting with hECSIT . Caspase 8 also promoted the phosphorylation and processing of hECSIT however the Caspase 8-C360s mutant was unable to process hECSIT, although phosphorylation was not affected (Figure 3.14A). As Caspase 8 promoted phosphorylation of hECSIT we next addressed if caspase 8 could induce ubiquitination of hECSIT. Co-expression of hECSIT with Caspase 8 resulted in the ubiquitination of hECSIT. However, while Caspase 8-C360s retained its ability to promote phosphorylation of hECSIT it failed to induce the ubiquitination of hECSIT (Figure 3.14B). Bioinformatic analysis was also performed on the hECSIT protein sequence in order to identify possible Caspase recognition sites (Table 3.1) however the corresponding processed fragments did not correspond in size to any of the predicted processing sites.

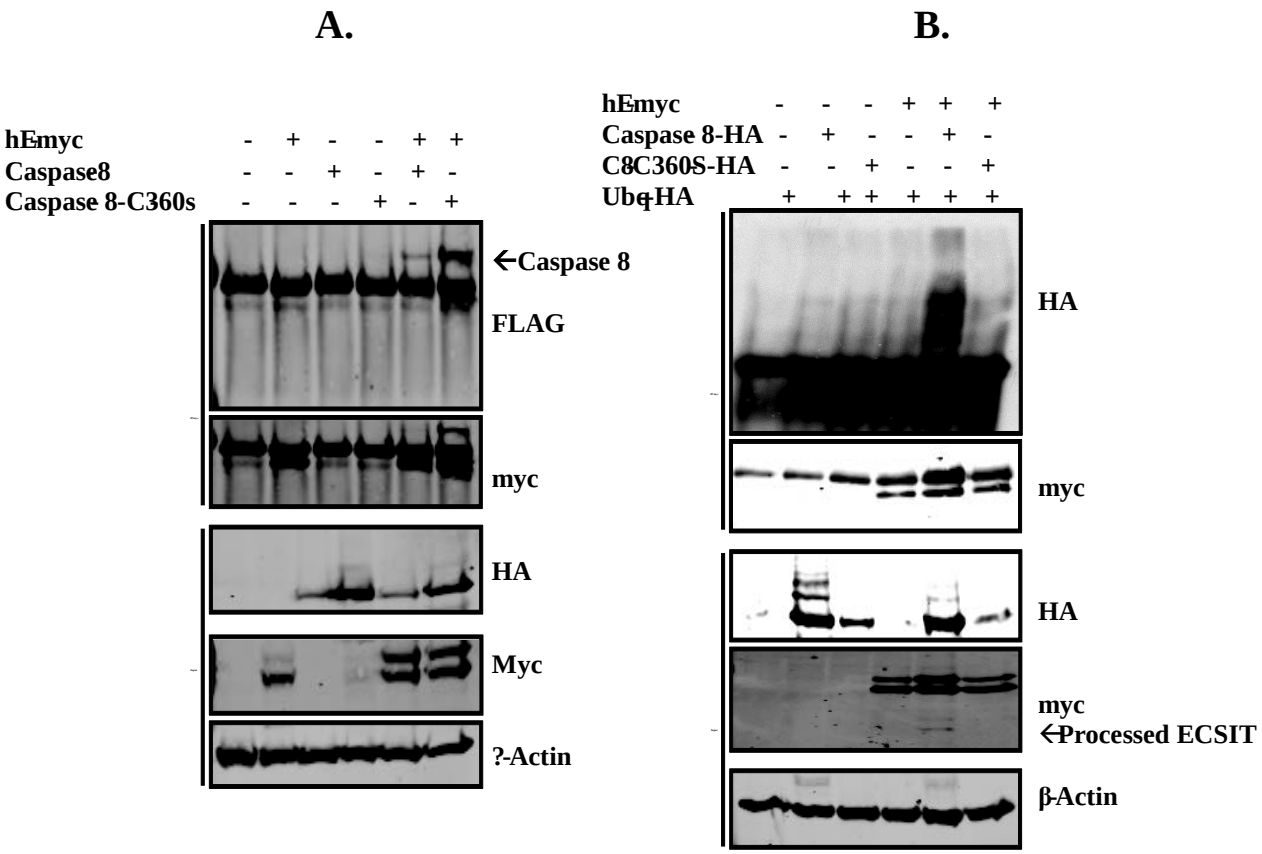

Figure 3.14 Caspase 8 promotes the phosphorylation, processing and ubiquitination of hECSIT through its catalytic cysteine residue

(A) HEK293 cells were co-transfected with Empty vector (EV) pcDNA3.1 (1µg), myc-tagged hECSIT (1µg) with or without HA-tagged Caspase 8 (1µg) or Caspase 8-C360S (1µg). EV was used to normalize total amount of DNA transfected. 24 hrs post-transfection cell lysates were generated and immunoprecipitated with anti-myc antibody. Immunoprecipitates were then subjected to SDS-PAGE and subsequently to western blotting using anti-HA antibody. Whole cell lysates were also analysed by western blotting using anti-HA and anti-Myc antibodies to confirm expression of TAK1 and ECSIT constructs, respectively. (B) HEK293 cells were co-transfected with Empty vector (1µg), HA-Ubq (1µg), myc-tagged hECSIT (1µg) with or without HA-tagged Caspase 8 (1µg) or Caspase 8-C360S (1µg). EV was used to normalize total amount of DNA transfected. 24 hrs post-transfection cell lysates were generated and immunoprecipitated using an anti-myc antibody. Immunoprecipitates were then subject to SDS-PAGE and subsequently to western blotting using anti-HA antibody. Whole cell lysates were also analysed by western blotting using anti-FLAG and anti-Myc antibodies to confirm expression of Caspase 8 and ECSIT constructs, respectively.

Sequence Name	ECSIT
Sequence	MSWVQ...QQGQS
Length of Sequence	431 residues
Predicted Sites (P4-P1)	DPVE-225
	DNYE-345
	DINE-350
	DHQE-418
Predicted Sites (P4-P2')	YGVE-123
	VERD-125
	EQME-169
	KETE-180
	DPVE-225
	MEPD-237
	EERE-316
	REVE-318
	ETPE-322
	DNYE-345
	YEFD-347
	DINE-350
	NEVE-352
	STRE-399
	DHQE-418
	QEED-420
	EEDD-421
Predicted Sites (P14-P10')	DPVE-225
	MEPD-237
	VFVE-288
	SGWD-342
	DNYE-345
	YEFD-347
	DINE-350
	EVEE-353
	STRE-399
	EEDD-421

Table 3.1 Bioinformatic analysis of hECSIT sequence for Caspase cleavage site

The sequence for hECSIT was analysed using the Uni-prot sortware for potenital caspase Aspartic Acid and Glutamic Acid recognition sites.

3.2.8 The C-terminus of hECSIT is inhibitory and contains both E3 ligase and DUB activity

We next aimed to characterise the processed forms of hECSIT that are apparent in response to TLR/IL-1R signalling or when co-expressed with TRAF6 or TAK1. As before, co-expression of myc-hECSIT with TAK1/TAB1 resulted in the migration of a number of processed hECSIT bands on a western blot (Figure 3.15A). An anti-myc antibody was used to immunoprecipitate the various forms of ECSIT and these were resolved by SDS-PAGE and Coomassie stained (Figure 3.15B). The processed form of hECSIT, represented by the band of highest intensity, was then excised and tryptically digested for LC/MS mass spectrometry analysis. Peptides corresponding to amino acids in the C-terminal section of hECSIT were identified (Figure 3.15C). Protein marker and mass spec coverage of the hECSIT sequence identified processed hECSIT to be a C-terminal myc tagged fragment , ~ 40kDa in size.

In order to understand the functional consequence of hECSIT processing truncation mutants incorporating processed hECSIT were generated. A previous study demonstrated that truncation of the N-terminus of mECSIT results in a dominant negative form that negatively regulates the NFκB pathway (Kopp et al, 1999). Thus a corresponding C-terminal (residues 266-431) mutant of hECSIT was generated and the residual N-terminal fragment (residues 1-265) was also made. In order to investigate the inhibitory effects of both truncation mutants NFκB luciferase reporter assays were used. Transfection of TRAF6 resulted in NFκB activation. While full length hECSIT slighly inhibited this activation, the C-terminal truncation mutant showed greater inhibitory effects whereas the N-terminal truncation mutant failed to affect TRAF6 induced activation of NFκB (Figure 3.16A). In order to confirm this effect a semi-rescue experiment was carried out using hECSIT specific siRNA. Treatment of HEK293-TLR4 cells with LPS resulted in an augmented NFκB response when hECSIT was knocked down however reconstitution of hECSIT with the C-terminal truncation mutated rescued the inhibitory effect resulting in decreased NFκB activation in response to LPS. In keeping with our previous data the N-terminal fragment failed to reconstitute the inhibitory effect (Figure 3.16B). These results suggested that hECSIT exerts its regulatory effect via its C-terminus and that the processing of hECSIT is required for it to inhibit TRAF6.

We next probed the molecular basis to the inhibitory effects of the C-terminal fragment. Given that ECSIT knockdown leads to enhanced TLR-induced ubiquitination of TRAF6 we hypothesised that the C-terminal fragment may possess deubiquitinating activity. In order to analyse deubiquitinating activity a recombinant protein encoding the C-terminal truncation mutant was generated and its purity and identify was confirmed by, coomassie staining, western blotting and mass spectrometry (Figure 3.17). DUB activity was analysed using a luciferase tagged DUB substrate. Incubation of recombinant full length hECSIT with the DUB substrate failed to show any DUB activity. However the recombinant C-terminal fragment of hECSIT exhibited strong DUB activity over the indicated incubation time-points (Figure 3.18A). As other DUB enzymes such as A20 also posess E3 ligase activity we assessed hECSIT for E3 ligase activity. Recombinant full length hECSIT or recombinant c-terminal hECSIT were incubated with the indicated ubiquitination reaction mix and assessed for their ability to generate polyubiquitin chains by probing for ubiquitin. Both full length and the C-terminal mutant of hECSIT had E3 ligase activity (Figure 3.18B). This indicated that the C-terminal processed fragment of hECSIT contains both E3 ligase and a cryptic DUB function that is only active when processed.

In order to confirm TRAF6 as a possible substrate for the DUB activity of processed hECSIT an *in vitro* ubiquitination reaction was carried out and the C-terminal fragment of hECSIT was assayed for its ability to deubiquitinate TRAF6. Recombinant TRAF6 was incubated with or without full length recombinant hECSIT or recombinant C-terminal hECSIT in the indicated ubiquitin reaction mix. Following a 2hr reaction TRAF6 was immunoprecipitated and levels of TRAF6 ubiquitination were analysed by probing the immuno-precipitates with an anti-ubiquitin antibody (Figure 3.19). Incubation of TRAF6 with C-terminal hECSIT resulted in the deubiquitination of TRAF6. This suggested that hECSIT is processed in order to activate the DUB activity of hECSIT and target TRAF6 for deubiquitination.

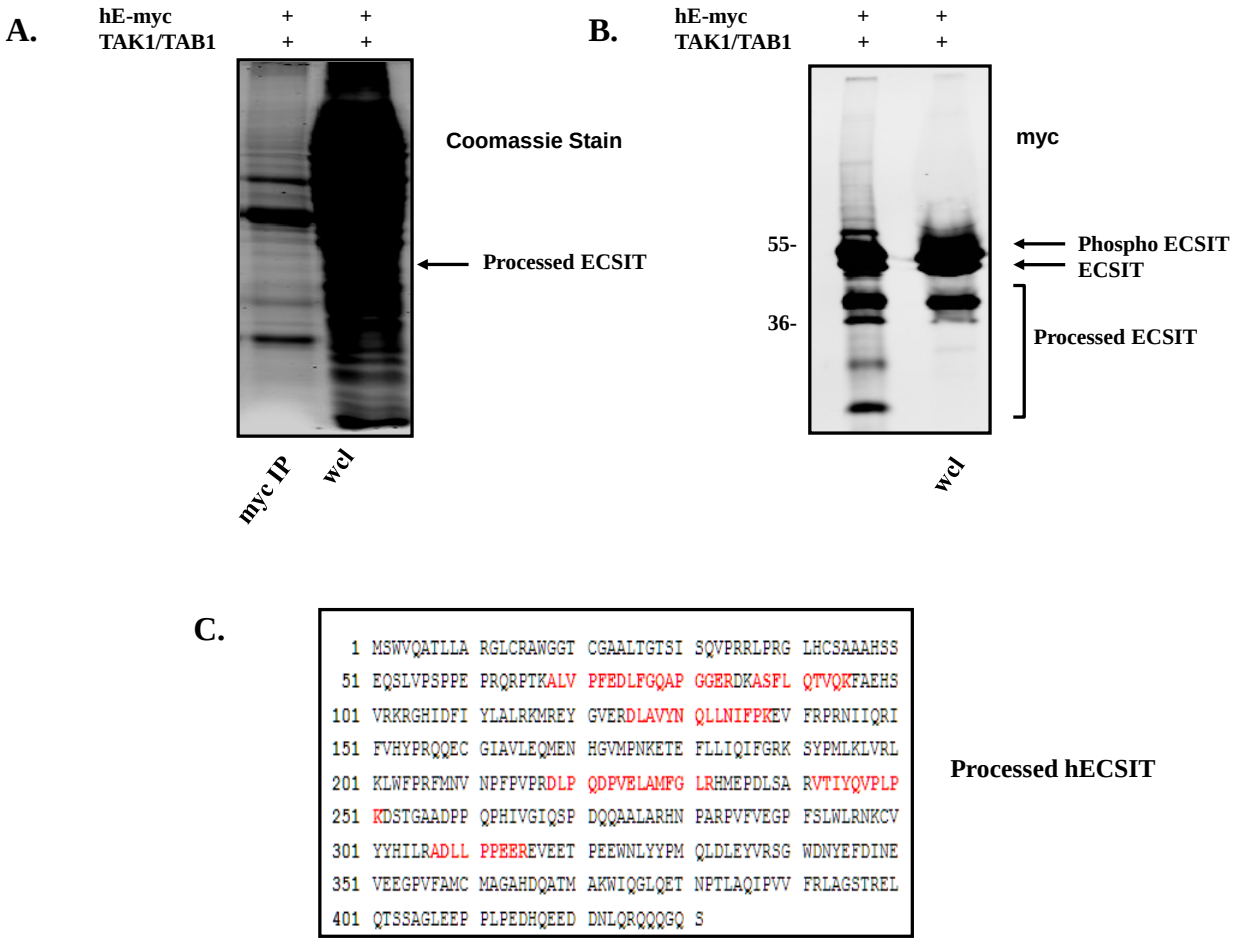

Figure 3.15 Identification of processed hECSIT

HEK293T cells were co-transfected with myc-tagged hECSIT (50µg) FLAG-tagged TAK1 (25µg) and TAB1 (25µg). 24 hrs post-transfection cell lysates were generated and immunoprecipitated with anti-myc antibody. Immunoprecipitates and whole cell lysates were then subject to SDS-PAGE and subsequently to western blotting using Coomassie staining (A) and anti-myc antibody (B). Processed hECSIT (Indicated by arrow) was then excised from the coomassie gel and subjected to tryptic digestion followed by LC-MS/MS. Mascot searches were determined using Swiss-Prot databases for the human genome.

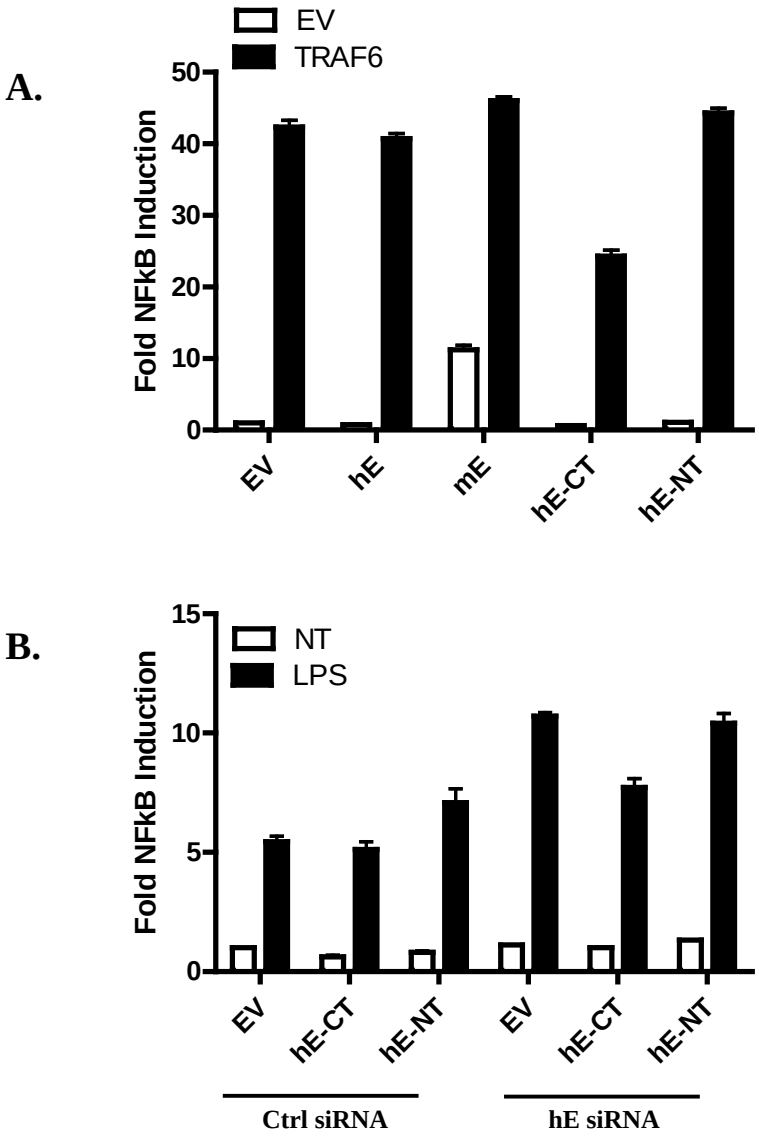

Figure 3.16 The C-terminus of hECSIT is more inhibitory than full length hECSIT

(A) HEK293 cells were co-transfected with NFκB firefly luciferase reporter construct (80ng), TK renilla (20ng) and myc-tagged hECSIT or mECSIT or the C-terminal or N-terminal of hECSIT (50ng) with or without FLAG-tagged TRAF6 (100ng). Empty Vector (EV) pcDNA3.1 was used to normalise total amount of DNA whilst TK Renilla was used to normalise for transfection efficiency. 24hr post-transfection cell lysates were generated the following day and assayed for firefly luciferase activity. (B) HEK293 cells were co-transfected with NFκB firefly luciferase reporter construct (80ng), TK Renilla (20ng) and hECSIT specific siRNA or Lamin control siRNA (10nM). 24 hrs post transfection the cells were transfected with EV, C-terminal or N-terminal hECSIT. 24 hours later cells were treated with LPS for 6 hrs. Cell lysates were then generated and assayed for firefly luciferase and renilla luciferase activity. Results represent mean +/- SD of triplicate determinations and is a representative of 3 independent experiments.

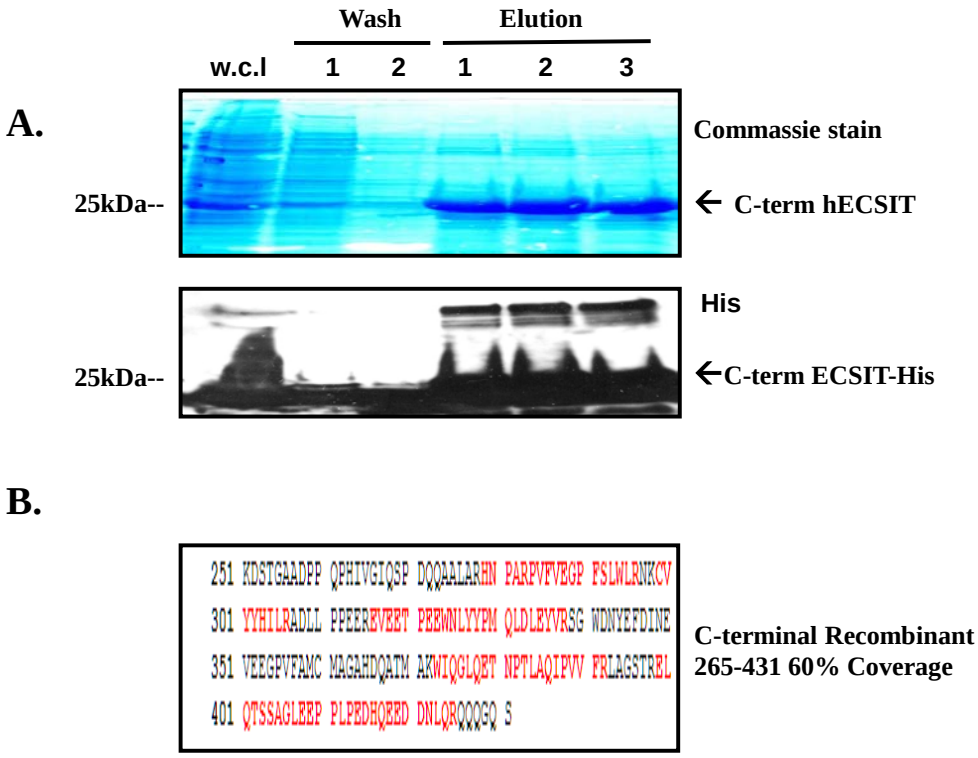

Figure 3.17 Generation and purification of recombinant C-terminus hECSIT

(A) His-tagged C-terminal hECSIT was purified from BL21 *E.coli* competent cells using Ni-NTA resin. Eluted protein was then subjected to SDS-PAGE followed by western blotting and Coomassie staining to determine protein purity (B). Bands from the Coomassie gel were then excised and trypticly digested and analysed using LC-MS/MS Agilent 6510 Ion trap technologies. Swiss-Prot database searches recovered 60% coverage of the C-terminus of hECSIT (C).

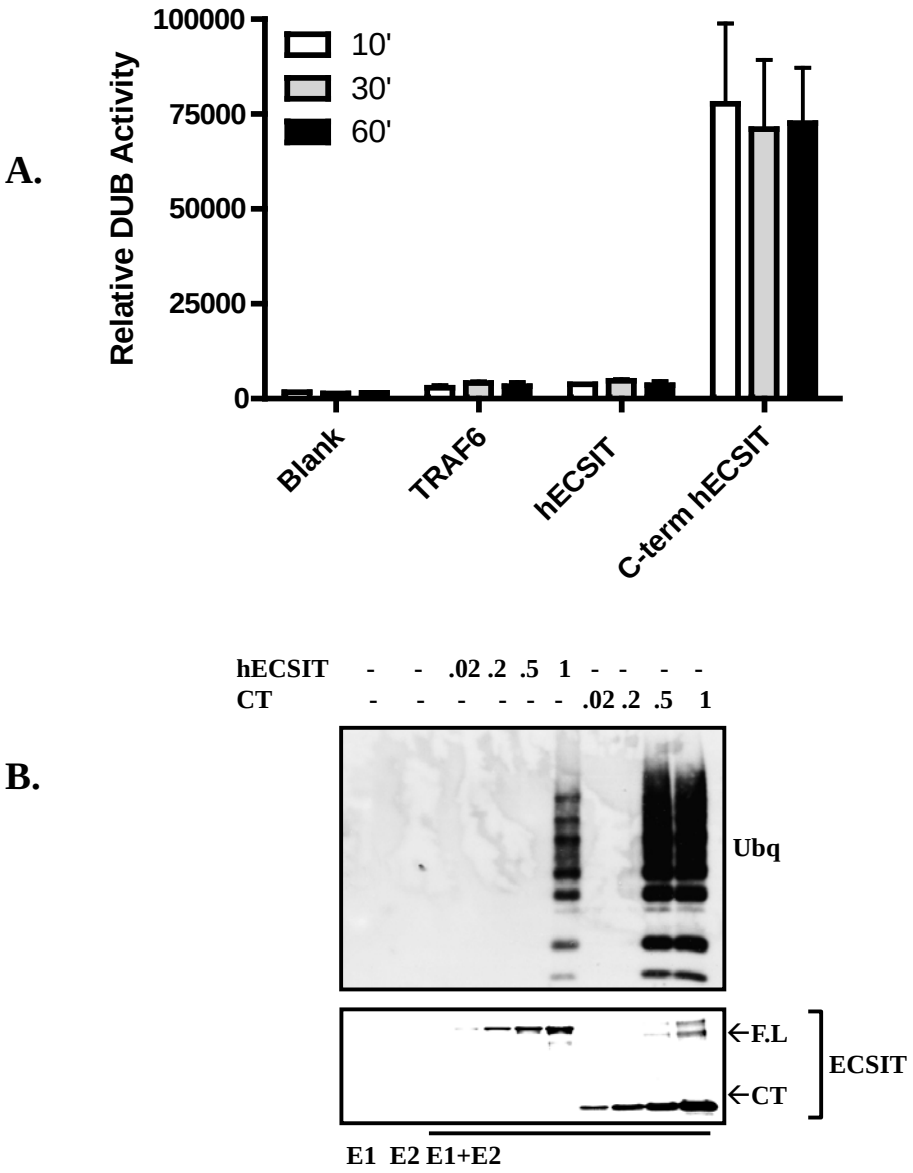

Figure 3.18 The C-terminus of hECSIT contains both DUB and E3 ligase activity

(A) Recombinant TRAF6, hECSIT and C-terminal hECSIT (1µg) were incubated with the DUB-Glo protease assay substrate. Luciferase activity was then measured after the indicated times to assess for DUB activity. (B) Increasing concentrations of recombinant hECSIT or recombinant c-term hECSIT (0.02-1µg) was incubated in a reaction mix containing Ubiquitin (2µg), E1 (50ng), E2 UbcH13/Uev1a (400ng), $MgCl_2$ (2mM), ATP (2Mm), protease inhibitor cocktail and H_20. Reactions were incubated at 37°C for 2hrs and terminated with 4x SDS sample buffer. Samples were then subjected to western blotting to analyse poly-ubiquitin chains and expression of hECSIT.

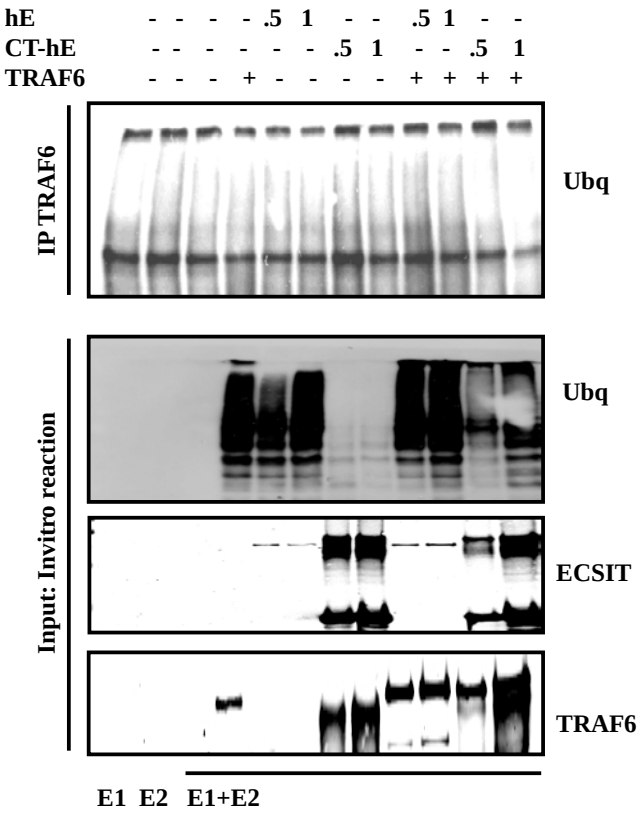

Figure 3.19 The C-terminus of hECSIT deubiquitinates TRAF6 *in vitro*

Recombinant TRAF6 was incubated with or without the indicated concentrations of recombinant hECSIT (0.5-1µg) or C-terminal hECSIT (0.5-1µg) in a reaction mix containing Ubiquitin (2µg), E1 (50ng), E2 UbcH13/Uev1a (400ng), $MgCl_2$ (2mM), ATP (2Mm), protease inhibitor cocktail and H_20. Reactions were incubated at 37°C for 2hrs and subsequently immunoprecipitated using anti-TRAF6 antibody. The immunoprecipitate was then assayed for TRAF6 ubiquitination by Immunoblotting for ubiquitin. Levels of TRAF3, ECSIT and ubiquitin were also assessed in the input by western blotting.

3.2.10 Mutation of a PEST-like sequence enhances the inhibitory effect of hECSIT

Analysis of the hECSIT sequence revealed a putative conserved PEST like sequence in the C-terminus. PEST sequence is a peptide sequence which is rich in Proline (P), Glutamic acid (E), Serine (S), and Threonine (T). This sequence is associated with proteins that have a short intracellular half-life; hence, the PEST sequence acts as a signal peptide for protein degradation. Given that this PEST sequence was located in the C-terminus we examined how mutation of the PEST sequence would affect the inhibitory capacity of hECSIT. Myc-tagged hECSIT E322A and myc-tagged hECSIT-E323A were assessed for their ability to interact with TRAF6. Co-immunoprecipitation experiments revealed that mutation of the hECSIT PEST sequence did not affect the interaction between hECSIT and TRAF6 with a comparable interaction observed between wild type hECSIT and hECSIT-E322 and hECSIT-E323 (Figure 3.20A). Given that mutation of the PEST sequence did not affect the interaction of TRAF6 and hECSIT we next sought to examine the capacity of the wild type hECSIT and the PEST mutants to deubiquitinate TRAF6. Co-transfection of TRAF6 with hECSIT resulted in greatly reduced ubiquitination of TRAF6 and this is consistent with the C-terminal region of hECSIT displaying DUB activity. Point mutant forms of the PEST sequences showed slightly greater levels of processing, at least for the E322A mutant, and this was associated with augmented inhibitory effects on the ubiquitination of TRAF6 (Figure 3.20B) further supporting an inhibitory role for the processed hECSIT forms.

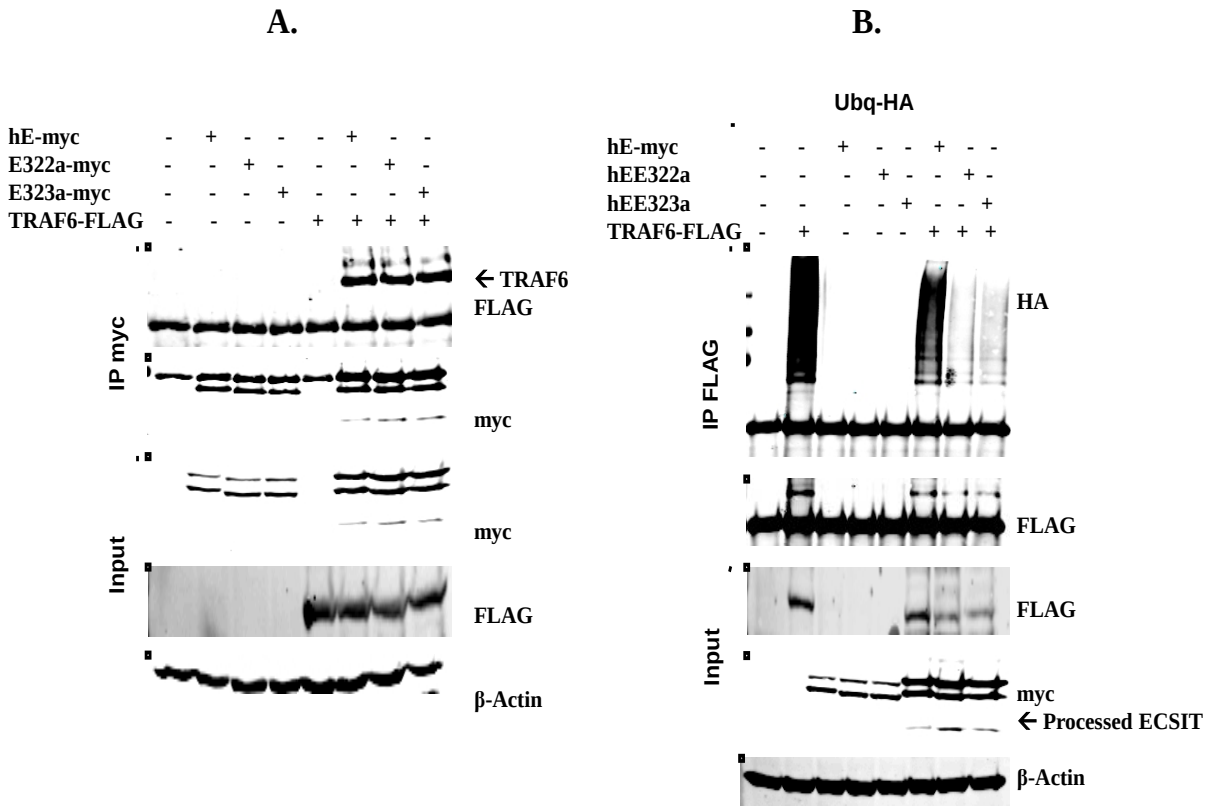

Figure 3.20 Mutation of a hECSIT PEST sequence enhances processing and TRAF6 deubiquitination

HEK293 cells were co-transfected with Empty vector (1µg), HA-Ubq (1µg), FLAG-tagged TRAF6 (1µg) with or without myc-tagged hECSIT (1µg) or hE-E322a (1µg) or hE-E323a (1µg). EV was used to normalize total amount of DNA transfected. 24 hrs post-transfection cell lysates were generated and immunoprecipitated using an anti-FLAG antibody. Immunoprecipitates were then subject to SDS-PAGE and subsequently to western blotting using anti-HA antibody. Whole cell lysates were also analysed by western blotting using anti-FLAG and anti-Myc antibodies to confirm expression of TRAF6 and ECSIT constructs, respectively.

3.2.11 Generation, genotyping and phenotyping of Humanised *ECSIT* mice

The embryonic lethality of *Ecsit* $^{-/-}$ mice has seriously hampered the elucidation of the physiological roles of ECSIT. Consequently heterozygous *Ecsi*t $^{+/-}$ mice have been used that show ~ 40% reduction in ECSIT expression in some cells relative to their wildtype counterparts. Given our initial findings that hECSIT appears to act as a negative regulator of TLR signalling and differs functionally from murine ECSIT we were keen to establish a model to allow for delineation of the physiological role of human ECSIT. To this end and towards the completion of the work for this thesis, we were successful in generating a knockin mouse in which the murine *Ecsit* gene was replaced by the human *ECSIT* gene. Such a humanised mouse was generated by Taconic Artemis using their homologous recombination technology and the Flpe transgene (Figure 3.21C). The Flpe transgene was subsequently removed by breeding the resulting *ECSIT* $^{+/-}$ mice with C57BL/6 mice during colony expansion. Mice were genotyped by PCR analysis of DNA isolated from ear punches.

Confirmation of gene-replacement was confirmed by RT-PCR and western blotting. Primers specific to both hECSIT and mECSIT were used to amplify ECSIT DNA isolated from MEFs. The use of genomic DNA from WT mice as template resulted in the amplification of a 241 bp fragment from the murine *Ecsit* allele whilst the presence of the human *ECSIT* allele generates a fragment of 349 bp. (Figure 3.21A). Protein expression was determined by generating cell lysates from MEF cells. Probing of lysates with an ECSIT specific polyclonal antobody showed expression of mECSIT in WT mice and expression of hECSIT in homozygote mice. Heterozygote mice expressed both mECSIT and hECSIT as indicated by arrows (Figure 3.21B).

Both heterozygous and homozygous ECSIT mice were viable however homozygote females were unable to carry a litter to full term and pregnancy in female mice resulted in miscarriage or fatality.

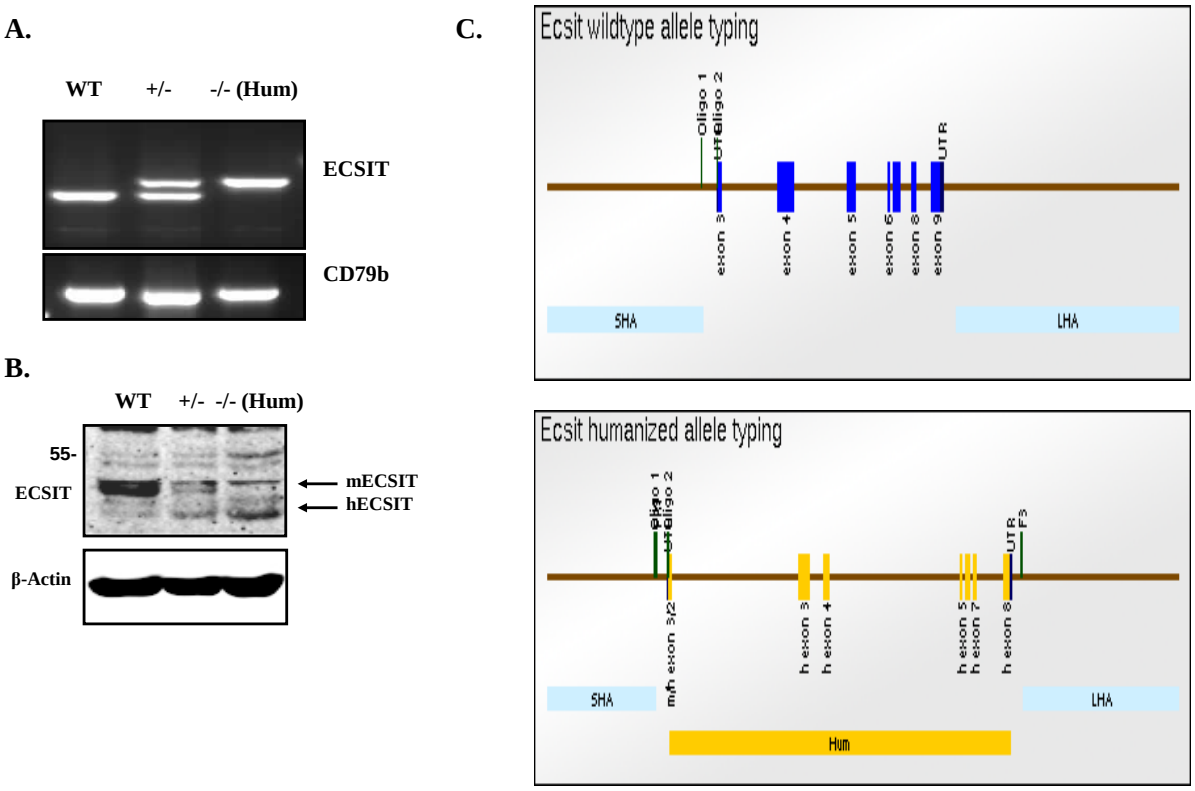

Figure 3.21 Generation and genotyping of Humanised ECSIT mice

(A) Genotyping was performed by PCR on genomic DNA from ear punches. Primers for the ECSIT gene differentiate between the wild type allele (WT) from the human allele in homozygote mice (-/- (Hum)) based on different fragment size. CD79b was used as the control allele. (B) MEFs were isolated from WT, *ECSIT*$^{+/-}$ and *ECSIT*$^{+/+}$ (Hum) embryos. Cell lysates were prepared and subjected to western blotting using anti-ECSIT and anti-β-Actin antibodies. (C) Diagram shows: the mouse ECSIT gene exons that were replaced with the hECSIT exons through homologous recombination.

3.2.11 Replacement of *Ecsit* with human *ECSIT* in a Humanised mouse model does not effect LPS and IL-1 induced activation of NFκB

As demonstrated previously siRNA and shRNA knockdown of hECSIT resulted in modest augmentation of NFκB in response to IL-1 and LPS indicating a potential negative inhibitory role for hECSIT in the NFκB pathway and an opposing function from its murine counterpart. In order to further assess the role of hECSIT in regulating NFκB primary MEF cells were isolated from WT and *ECSIT*$^{+/+\ (Hum)}$ embryos and treated with LPS and levels of IL-6 and Keratinocyte Chemoattractant (KC) were measured by ELISA. Replacement of *Ecsit* with *ECSIT* failed to effect LPS induced IL-6 and KC production (Figure 3.22). To further confirm this we analysed the intracellular activation markers of NFκB activation. Stimulation of MEF cells with LPS again failed to alter the NFκB response in humanised MEFs in comparison to their WT counterparts as demonstrated by normal levels of p-IκB-α and p-p65 in our humanised MEF cells (Figure 3.23). As hECSIT had been previously shown to also negatively regulate IL-1R signalling we analysed NFκB activation in response to IL-1β. As with LPS, no difference in levels of p-p65 and p-IκB-α were observed in humanised MEF cells treated with IL-1β in comparison to WT MEF cells (Figure 3.24). We next examined other intra-cellular read-outs in order to gain a functional understanding of hECSIT's mechanism of action.

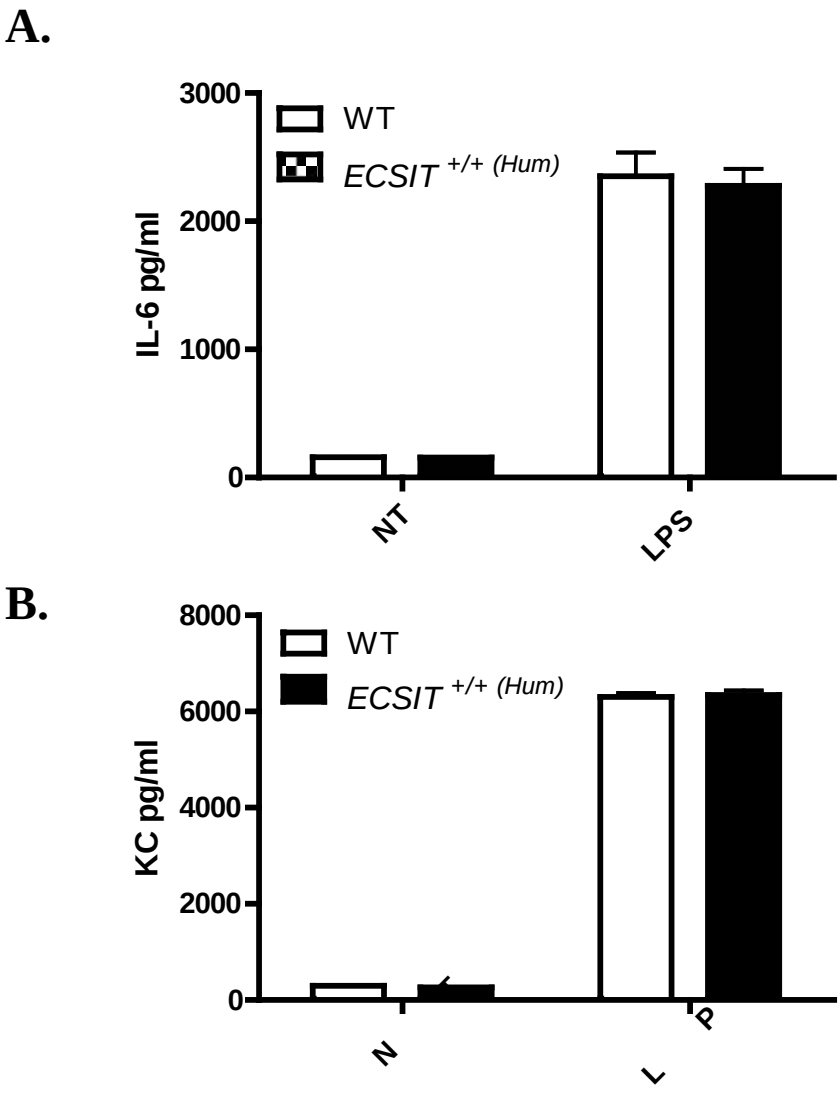

Figure 3.22 Replacement of *Ecsit* with *ECSIT* does not impair LPS induced expression of IL-6 and KC

MEFs were isolated from WT and *ECSIT* $^{+/+ (Hum)}$ embryos and treated with or without LPS (100ng/ml) for 24 hrs. NT and treated media were then assayed for levels of IL-6 (A) and KC (B) by ELISA. Data represents the mean +/- S.D of 3 independent experiments.

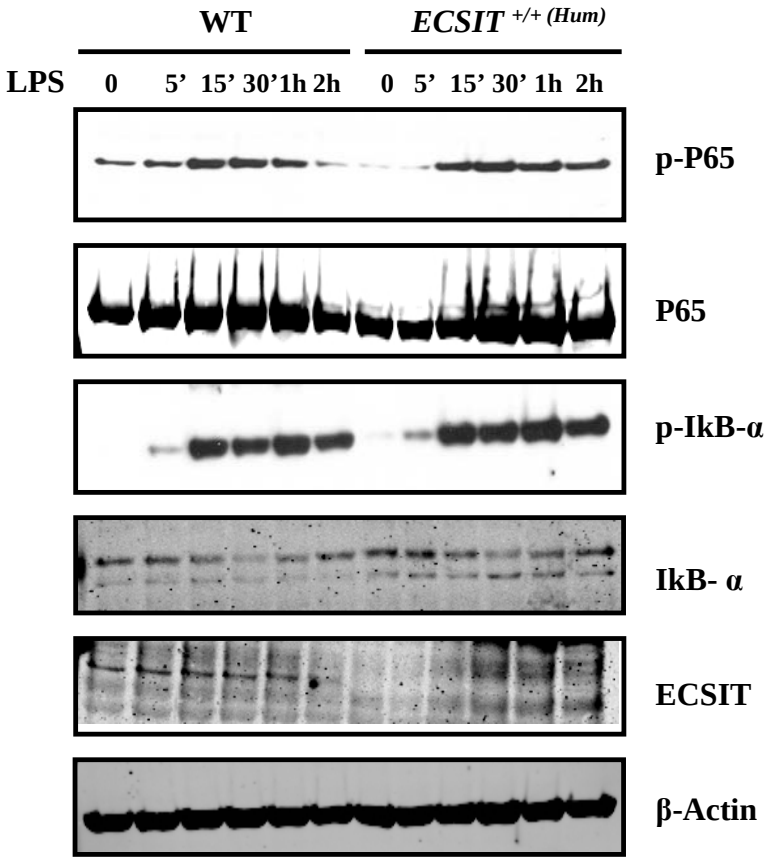

Figure 3.23 Replacement of *Ecsit* with *ECSIT* does not affect LPS induced NFκB activation

MEFs were isolated from WT and *ECSIT* $^{+/+ (Hum)}$ embryos and treated with or without LPS (100ng/ml) for the indicted times. Cell lysates were then prepared and immunoblotted for phosphorylated and total levels of P65 and IκB-α. Lysates were also probed for levels of ECSIT and β-Actin.

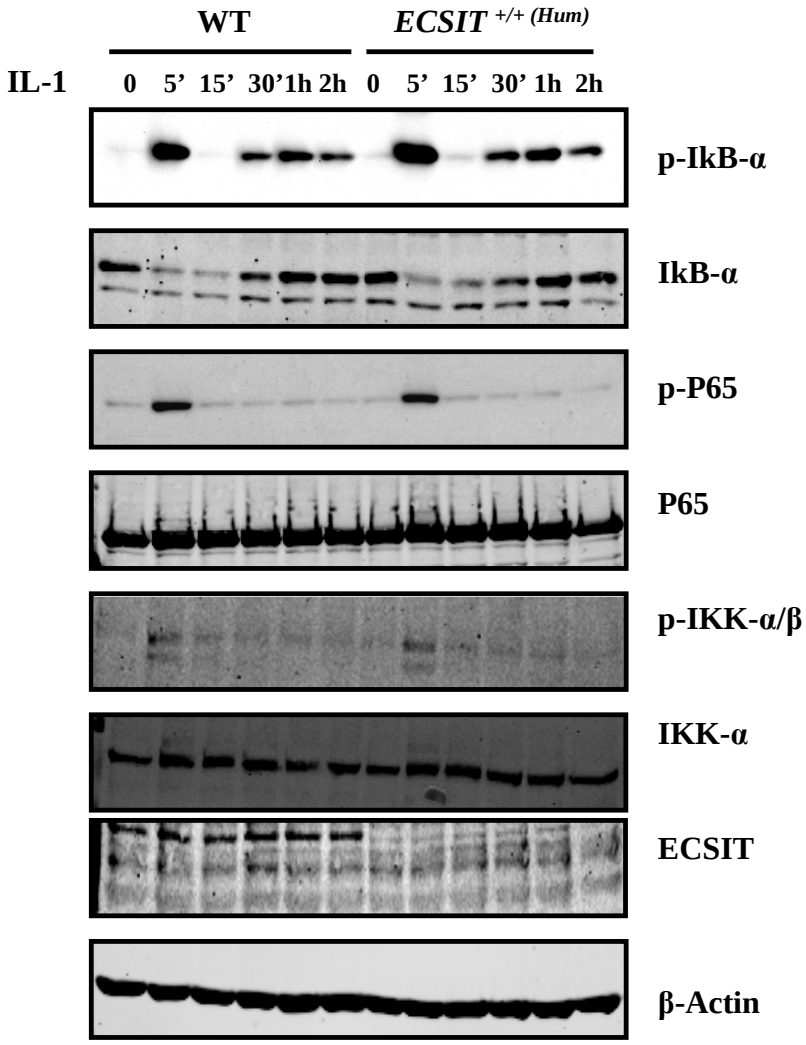

Figure 3.24 Replacement of *Ecsit* with *ECSIT* does not affect IL-1 induced NFκB activation

MEFs were isolated from WT and -/- (Hum) embryos and treated with or without IL-1 (10ng/ml) for the indicted times. Cell lysates were then prepared and immunoblotted for phosphorylated and total levels of P65 IκB-α and IKK-α. Lysates were also probed for levels of ECSIT and β-Actin.

3.2.12 hECSIT inhibits Inflammasome mediated IL-1β production

As discussed previously knockdown of hECSIT resulted in modest increases in NFκB, however production of mROS in response to LPS was also significantly enhanced when hECSIT was knocked down. As no difference in the IL-1/LPS NFκB response in our humanised model was observed we further analysed the effect of hECSIT on mROS production. mROS has been shown to function as a second signal for inflammasome assembly and IL-1β processng. In order to analyse the effect of hECSIT on this MEF cells were treated with LPS and ATP to drive inflammasome activation. WT MEFs treated with LPS and ATP for the indicated times resulted in induction of IL-1β production, however this was significantly attenuated in our *ECSIT* $^{+/+(Hum)}$ cells as demonstrated by lower levels of IL-1β measured by ELISA (Figure 3.25).

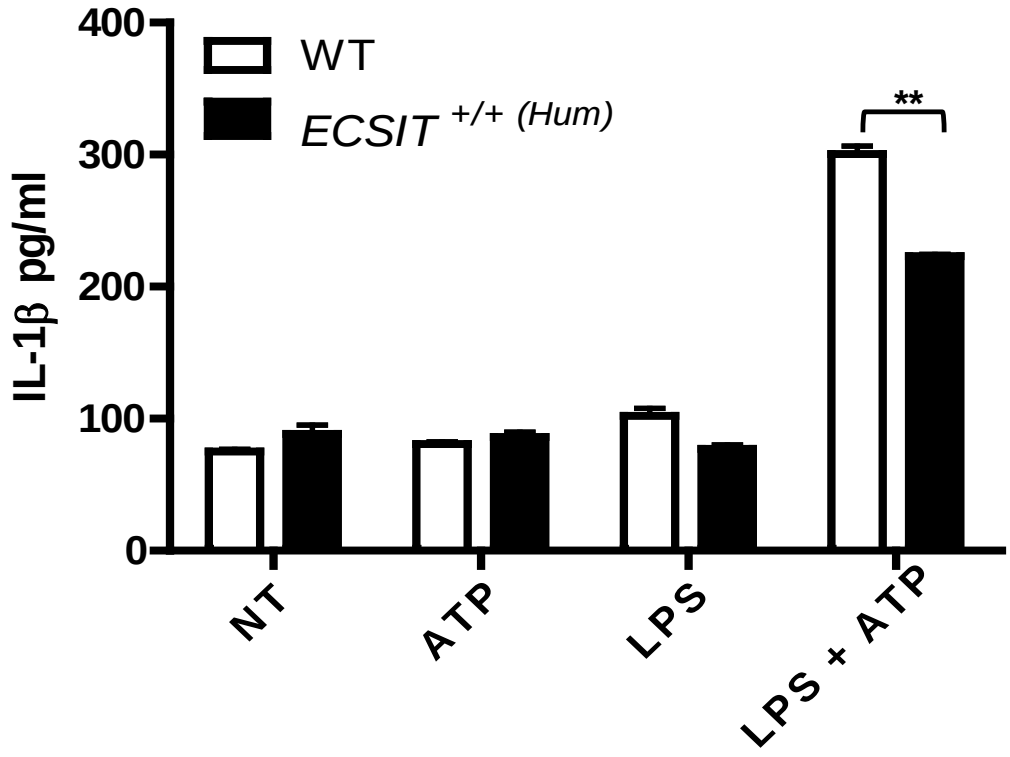

Figure 3.25 Replacement of *Ecsit* with *ECSIT* impairs Inflammasome induced IL-1β production

MEFs were isolated from WT and *ECSIT* $^{+/+ (Hum)}$ embryos and treated with or without LPS (100ng/ml) for 3hrs followed by ATP (100mM) for 1hr. NT and treated media were then assayed for levels of IL-1β by ELISA. Data represents the mean +/- S.D of 3 independent experiments; p=<0.01

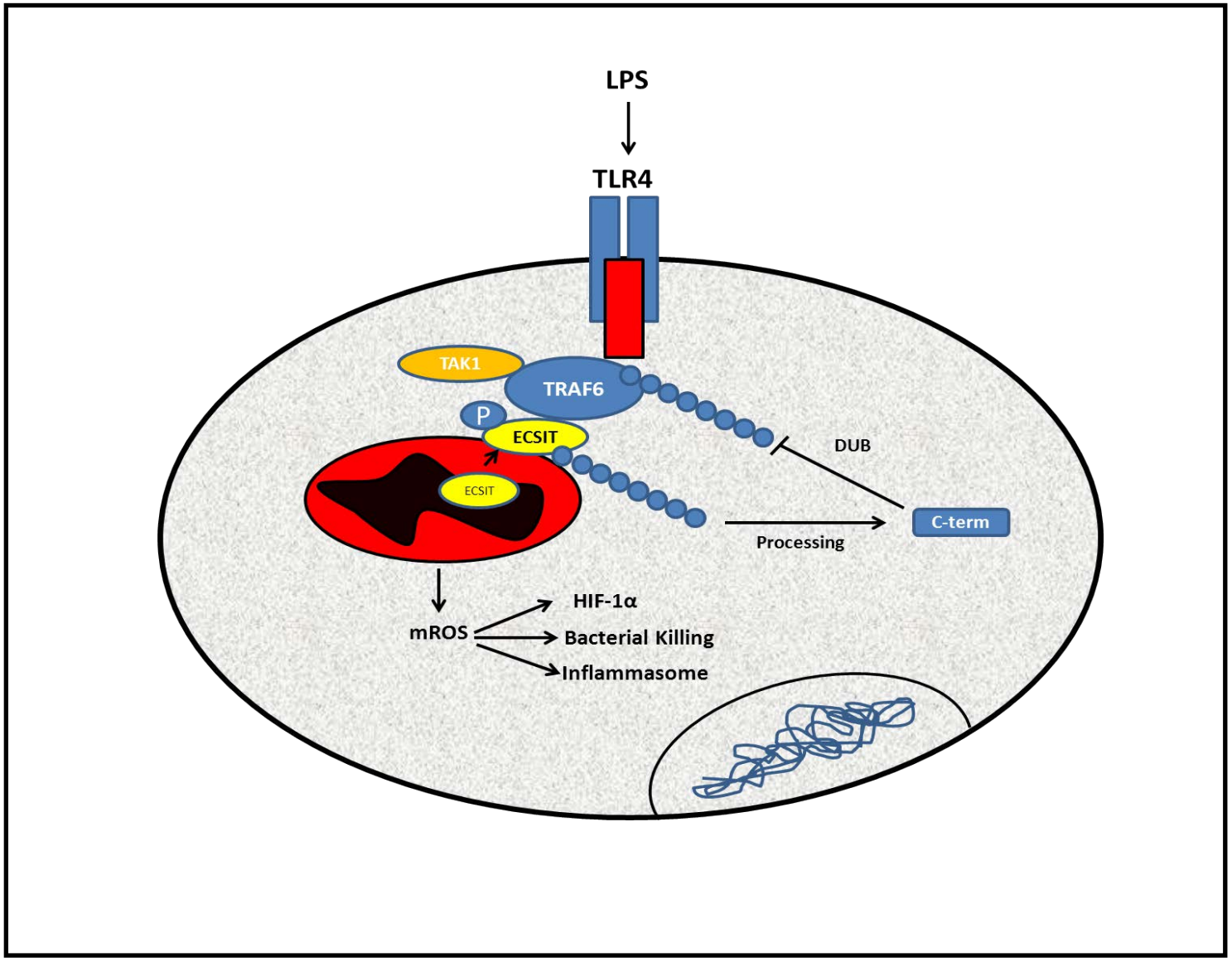

Figure 3.26 Schematic representation of hECSIT's regulatory effect in TLR4 signalling

Activation of TLR4 by LPS results in ECSIT phosphorylation, ubiquitination and processing. Processing of hECSIT results in an active DUB enzyme which can deubiquitinate TRAF6 in an auto-regulatory fashion.

3.3 Discussion

During infection TLRs function as the immune system's first line of defence. Activation of TLRs leads to the nuclear translocation of transcription factors such as NFκB and the IRFs which promote the production of pro-inflammatory cytokines and type 1 IFN. NFκB is a highly regulated transcription factor and many intracellular signalling intermediates promote or inhibit activation of NFκB. ECSIT was originally identified as a TRAF6 interacting protein in a yeast two hybrid study that positively regulated the activation of NFκB. Subsequent studies highlighted the importance of ECSIT in development as ECSIT knockout mice displayed a lethal embryonic phenotype. The production of heterozygote mice in a recent report identified ECSIT as a positive regulator of mROS production and showed ECSIT as a mitochondrial protein that linked TLR signalling to the outer membranes of the mitochondria. Currently there exists no published information on the role of the human orthologue of hECSIT in TLR signalling. The present study aimed to build on early findings from the author's host laboratory and especially focus on the mechanistic basis to the effects of hECSIT and an explanation for the functional differences between mECSIT and hECSIT.

As previously discussed knockdown of hECSIT modestly augmented NFκB activation in response to LPS. However the recently available information on mECSIT's role in mROS production prompted us to examine the potential role of hECSIT in mROS production. Knockdown of hECSIT in primary human cells resulted in augmented LPS induced mROS production. As hECSIT's effect on NFκB activation is marginal we speculate that augmented mROS may explain the indirect effect on NFκB as previous studies have shown that ROS can activate NFκB during cell stress responses (Ghosh and Karin, 2002). Given that over-expression of hECSIT results in the deubiquitination of TRAF6 we next looked at TRAF6 ubiquitination at an endogenous level. Knockdown of hECSIT resulted in prolonged ubiquitination of TRAF6 in response to LPS. However this effect was not mirrored by proinflammatory cytokine production. The ubiquitination of TRAF6 has been associated with other intracellular signalling pathways regulated by LPS, such as mROS (West et al, 2011) and autophagy (Shi and Kehrl, 2010). Also it has been suggested that free ubiquitin chains are sufficient to activate NFκB suggesting that TRAF6 may be dispensable for NFκB activation. As mentioned ECSIT has primarily been studied in the context of

mitochondrial function (Vogel et al 2007; West et al, 2011) and for the most part localises in the outer mitochondrial membranes. When TLRs are activated TRAF6 ubiquitination of mECSIT leads to its accumulation at the outer mitochondrial membrane (West et al, 2011). Therefore hECSIT may only temporally target a small proportion of TRAF6 at certain sub-cellular locations and hence no direct downstream effect is seen as a result of this. However the exact sub-cellular location of hECSIT in response to TLR ligands has yet to be analysed. This will need to be examined to confirm the latter hypothesis.

The conserved interaction shown between hECSIT and TRAF6 led us to investigate the post-translational modifications of hECSIT. TRAF6 over-expression induced various modifications of hECSIT, including putative phosphorylation and ubiquitination and processing of hECSIT, and we were keen to see if these various modifications were related and possibly regulated in a sequential manner. Given that TRAF6 triggers TAK1 activation we were especially keen to assess if TAK1 could reproduce the modifications of hECSIT that were effected by co-expression of TRAF6. We initially showed that both LPS and IL-1 induced a time-dependent interaction between TAK1 and hECSIT, and that co-expression of TAK1 was sufficient to trigger the various modifications of hECSIT. Mutational analysis revealed that both the kinase activity of TAK1 and ubiquitination of TAK1 are required for the processing of hECSIT. Kinase dead TAK1 is unable to activate NFκB and the MAP kinases and mutation of TAK1 at K158 also abrogates NFκB activation (Fan et al, 2011). This raised the possibility that processing of hECSIT first required the activation of NFκB to induce the auto-regulatory processing of hECSIT. To confirm this we utilised the pharmacological inhibitor 5z-7-oxozeanol to inhibit TAK1 kinase activity. In keeping with the previous data inhibition of TAK1 kinase activity impaired LPS and IL-1β induced processing of hECSIT. TAK1 inhibition also inhibited NFκB as demonstrated by reduced IκB-degradation in response to IL-1β. This indicated that the activation of NFκB was possibly required to drive the formation of the regulatory complex that was mediating the activation of hECSIT. Many similar negative feedback loops have been described previously and it is not unprecedented that hECSIT exerts its inhibitory effect in such a manner. Other kinases such as IKK-α have been attributed to inhibition of NFκB by activating negative regulators such as A20 (Shembade et al, 2010). Despite many attempts we were unable to show direct phosphorylation of hECSIT by recombinant TAK1 in an

in vitro system. This might be due to recombinant TAK1 lacking some pre-requisite for modification or an ancillary protein to manifest its kinase activity towards hECSIT. Furthermore, incubation of lysates containing phosphorylated hECSIT with the phosphatase CIP had no effect on levels of phosphorylated hECSIT. As this was done using an over-expression approach the levels of CIP used may not have been at a high enough threshold to reduce the overall level of phosphorylated hECSIT. However the possibility of another form of modification must also be considered and different approaches to identify the TAK1 mediated modification will be investigated in future experiments. An endogenous approach may give a clearer result. Given that TRAF6 had been previously described to ubiquitinate hECSIT we next aimed to identify a protease that was being recruited to process hECSIT. Caspase 8 induced processing of hECSIT; however the Caspase 8 catalytic mutant was unable to induce processing of hECSIT. The protease activity of Caspase 8 has a number of targets in TLR signalling including IRF3 (Sears et al, 2011), RIP1 (Rajput et al, 2011) and CYLD (O'Donnell et al, 2012). Bioinformatic analysis was also performed on the hECSIT sequence in order to find potential caspase recognition sites in the sequence. Whilst the Uni-Prot software predicted a number sites, the relative sizes of the processed site would not correspond to the processed ECSIT bands we have identified. Furthermore mutation of sites D74, D85, D108 and D125 to serine residues did not affect the ability of Caspase 8 to induce hECSIT processing (data not shown). A direct processing site will need to be determined in order to confirm the requirement for Caspase 8 in hECSIT processing.

We next aimed to understand the functional consequence of hECSIT processing. ECSIT has been shown to contain an N-terminal mitochondrial localisation sequence. It is possible that processing of hECSIT allows it to leave the mitochondrial membranes and exhibit its inhibitory effect on TRAF6. In support of this it has been previously shown that a truncated form of mECSIT lacking its N-terminus promotes a dominant negative effect on NFκB (Kopp et al, 1999). We therefore generated a truncated hECSIT construct based on the mECSIT truncation sequence to analyse its inhibitory function and enzymatic activity. The N-terminal truncation mutant, coding amino acids 261-431, exhibited a stronger inhibitory effect than the full length protein indicating that processing is required for hECSIT to carry out its inhibitory function. To confirm this we measured DUB activity and also E3 ligase activity of recombinant full length and C-terminal hECSIT. Surprisingly the C-

terminus of hECSIT contained both E3 ligase and DUB activity and the C-terminal hECSIT mutant was able to directly deubiquitinate TRAF6 *in vitro*. Such roles have also been extensively described for A20 where both E3 ligase and activity are utilised by A20 to inhibit TLR and TNF signalling. It is possible that the processing of hECSIT results in it exiting the mitochondria thereby allowing it deubiquitinate TRAF6. As hECSIT is also heavily ubiquitinated it is possible that multiple linkages such as K63 and K48 ubiquitination, control the stability of hECSIT and hence its functional effects. Identification of a direct catalytic residue required for this DUB activity or ubiquitinated lysine residues will confirm the latter. Also sub-cellular localisation studies utilising confocal microscopy or protein fractionation after stimulation with TLR ligands would give us a greater understanding of hECSIT's function. As mentioned, hECSIT also exhibited E3 ligase activity. Thus far we have not identified a substrate for this. However, analysis of hECSIT in other signalling pathways may reveal targets for its E3 ligase function.

Analysis of the hECSIT sequence also revealed a PEST-like sequence in the C-terminus of hECSIT. Given the importance of these sequences in signalling for protein degradation we were interested in what effects mutation of this domain would have on the stability of processed hECSIT. Mutation of two glutamic acid residues increased the stability and expression of processed hECSIT. And as a result the PEST mutant was more efficient at deubiquitinating TRAF6. Identification of these sites may prove useful in the development of any hECSIT based therapeutics and it will be of interest to analyse hECSIT peptides containing these mutants *in vivo* to assess their half- life and therapeutic potential.

Given our data appears to show that hECSIT plays a functionally opposing role to its murine orthologue in conjunction with the lethal phenotype of ECSIT-deficient mice, the use of ECSIT knockout mice is of limited value in studying the role of hECSIT at a physiological level. To overcome this limitation, mice were humanised at the Ecsit locus. Unfortunately these mice were generated towards the end of the present study and thus with time limitations, it is only possible to present early studies from these mice. The humanised mice were viable and displayed normal development. However upon colony expansion homozygote female mice were unable to carry a litter to full term. All homozygote pregnancies resulted in miscarriage or death which suggests that hECSIT cannot completely compensate for the loss of mECSIT during gestation. However heterozygous female mice crossed with

homozygote male mice display no defect in reproducing. Further pathological analysis of the humanised mice will be required to identify the exact problem. We are now continuing to analyse this phenotype through pathology and histology. In keeping with previous data on *Ecsit* $^{+/-}$ mice, our humanised model also displayed no effect on NFκB in response to LPS. As mROS has been linked to inflammasome activation (Menu et al, 2012), we next examined IL-1β production. As IL-1β production in our humanised cells was impaired we can speculate that this is perhaps as a result of lower mROS production in response to LPS. The difficulty in breeding the humanised mice has imposed many limitations on the number of experiments performed. mROS production is primarily associated with macrophages and low animal numbers has thus far limited us to ex-vivo experiments in MEF cells. Analysis of mROS in macrophages from our humanised mice will need to be conducted to further confirm this finding.

This study further highlights hECSIT as a negative regulator of TLR signalling and has identified a novel intricate mechanism to explain the difference in function observed between hECSIT and mECSIT. Further *in vivo* work and analysis of hECSIT in other innate signalling pathways will help in further elucidation of the physiological and pathological roles of hECSIT. It will also be of interest to explore if any natural occurring defective forms or expression of hECSIT may provide a genetic basis to some cases of chronic inflammatory diseases and cancer observed through dysregulated TLR signalling.

Chapter 4

Investigating the role of hECSIT inTLR3 signalling

4.1 Introduction

TLRs represent the immune systems first defence to invading pathogens by activating downstream transcription factors such as NFκB that promotes the production of pro-inflammatory cytokines and IFNs to trigger an immune response to eliminate infection (Moynagh, 2005). Most TLRs use the MyD88-dependent pathway to activate NFκB but TLR4 can additionally deploy other protein adaptors, TRIF and TRAM, to trigger a MyD88-independent pathway that also activates NFκB (Yammamoto et al, 2002). Uniquely TLR3, an endosomal anti-viral TLR, uses TRIF as its exclusive adaptor protein. TRIF recruits the adaptor kinase RIP1 to trigger downstream TAK1 and IKK-mediated activation of NFκB (Cusson-Hermance et al, 2005; Meylan et al, 2004). TRAF6 has also been reported to play a role in TRIF mediated activation of NFκB (Sasai et al, 2010). However other studies have concluded that TRAF6 is dispensable for TLR3 signalling (Jiang et al, 2004). Such a discrepancy in relation to the role of TRAF6 may be due to cell specific roles for TRAF6 and/or functional redundancy of TRAF6 with other members of the TRAF family (Sato et al, 2003). Alternatively TLR3 can also activate the transcription of type 1 IFN through the multifunctional adaptor TRAF3 (Liu and Chen, 2011). TRAF3 has been extensively studied in the regulation of TLR3 signalling. TRAF3 forms a complex with TANK, NEMO and TBK1 (Oganesyan et al, 2006). NEMO is required for the activation of both IKK and TBK1 in response to viral infection, and mutations disrupting the binding of NEMO to polyubiquitin chains impair the activation of the latter kinases (Zhao et al, 2007). It has been proposed that auto-ubiquitination of TRAF3 is required for downstream activation of TBK1 however TRAF3 deficient cells only exhibit a partial defect in producing IFNβ following viral infection (Zeng et al, 2009). However a recent study revealed a loss of function mutation (R118W) in patients which resulted in impaired IFN production in response to viral infection (Perez de Diego et al, 2010). Such a discrepancy in the role of TRAF3 can perhaps be attributed to its range of functions which vary dependent on cell type, its subcellular localization and its modification by ubiquitin. Many studies are now utilizing conditional knock-out models to study the role of TRAF3 in a cell specific manner. The activation of TLR4 results in the degradation of TRAF3 which is facilitated by the K48 ubiquitination of TRAF3 by cIAP1. When TRAF3 is degraded it releases TAK1 and the MAP kinase pathway is activated (Tseng et al, 2009).The ability of

TRAF3 to positively regulate IFN production and negatively regulate P38 and JNK activation is attributed to the compartmentalization of the activated TLR. TRAF3 dependent activation of the IFN response is initiated from signalling complexes that are assembled by the adaptor TRIF at an endosomal location. Signalling complexes assembled by MyD88 are located at the plasma membrane. In the endosome TRAF3 is able to positively regulate the production of type 1 IFN however at plasma membrane locations, TRAF3 negatively regulates MAP kinase signalling by sequestering TAK1 (Barton et al, 2009).

In addition to the negative regulation of the MAP kinases TRAF3 also functions as a negative regulator of non-canonical NFκB activation. TRAF3 is constitutively bound to NIK in resting cells and upon *de novo* synthesis; NIK is immediately bound by TRAF3 and targeted for ubiquitin-proteasome mediated degradation (Liao et al, 2004). Further investigation also revealed a role for cIAPs and TRAF2 in TRAF3 regulation of NIK. Following stimulation of the non-canonical pathway cIAP is K63 ubiquitinated by TRAF2 which enhances cIAPs E3 ligase affinity for TRAF3 which results in its K48 ubiquitination and subsequent degradation (Xiao et al, 2004). It was later shown that TRAF3 acts a molecular bridge between cIAP and NIK which allows NIK to interact with cIAP (Vallabhapurapu et al, 2008). When TRAF3 is degraded newly synthesized NIK is no longer able to interact with the cIAP-TRAF2 complex and is free to autophosphorylate and activate the IKK complex (Zarnegar et al, 2008) followed by the processing of p100 (Cheng et al, 2008). This mechanism is highlighted in TRAF3 $^{-/-}$ B-cells which contain high levels of NIK and exhibit constitutive p100 processing which can be blocked in a TRAF3 NIK double $^{-/-}$ (Gardam et al, 2008).

A recent study has implicated mECSIT as a positive regulator of IRF3/7 activation however as this study was carried out independent of any pathway specific ligand or endogenous analysis the precise role of mECSIT in this pathway has yet to be established. The present study aimed to analyse the role of hECSIT in anti-viral signalling by studying the TLR3 pathway. Through a combination of knockdown methods and our humanised mouse model we show an evolutionary diverged role for hECSIT and mECSIT in TLR3 signalling and provide a mechanistic basis for this difference. Activation of TLR3 signalling induces the phosphorylation and subsequent processing of hECSIT in a TAK1 dependent manner. This critical activation step allows hECSIT to associate with and facilitate the polyubiquitination of TRAF3 thus

inhibiting the ability of the latter to promote activation of NFκB and the IRFs. These findings reveal hECSIT as an important regulator of TLR3 signalling limiting the activation of NFκB and IRFs.

4.2 Results

4.2.1 hECSIT negatively regulates TLR3 signalling

Following on from our initial study of the role of hECSIT in TLR4 signalling we were interested to explore the role of hECSIT in other innate immune signalling pathways, in particular anti-viral signalling pathways. As previously discussed we have identified hECSIT as a negative regulator of TLR4/IL-1R signalling. To investigate the potential regulatory role of hECSIT in TLR3 signalling an initial combination of siRNA and over-expression studies in HEK293-TLR3 cells were performed. Gene reporter assays using IRF3, IRF7 and RANTES driven luciferase tagged promoters were used to investigate the possibility of divergent roles between hECSIT and mECSIT and their functional role in TLR3 signalling. Over-expression of hECSIT resulted in inhibition of polyriboinosinic: polyribocytidylic acid (Poly (I:C)), the TLR3 agonist, induced expression of reporter gene constructs regulated by IRF3, IRF7 and the RANTES promoter. In contrast over-expression of mECSIT augmented the ability of Poly (I:C) to active these transcription factors and promoter (Figure 4.1). To further confirm the divergent inhibitory roles of hECSIT and mECSIT in TLR3 signalling that were indicated from these overexpression studies, these pathways were also studied in hECSIT knockdown cells. Co-transfection of an IRF3-dependent luciferase reporter construct with hECSIT specific siRNA, to suppress the expression of hECSIT resulted in enhanced IRF3 activation in response to Poly (I:C) (Figure 4.2A). A similar augmentation of TLR signalling was observed with reporter gene constructs regulated by IRF7 (Figure 4.2B) and NFκB (Figure 4.2D). Given these effects on IRFs and NFκB we also probed the effect of hECSIT on a naturally occurring promoter that is regulated by both NFκB and IRFs and show that hECSIT knockdown potentiates TLR3-induced activation of the RANTES promoter (Figure 4.2C).

We next examined the role of hECSIT in regulating the expression of type 1 IFNs since they are strongly regulated by TLR3 and the downstream activation of NFκB and IRFs. Using a type 1 IFN-reporter cell line as a bioassay system, the TLR3 agonist Poly (I:C), induced increased levels of type 1 IFN when hECSIT was knocked down (Figure 4.3A).The knockdown of hECSIT in these studies was confirmed by western blot (Figure 4.3C).

We were keen to confirm that the above enhancing effects of hECSIT knockdown on Poly (I:C) signalling was not an artifact of HEK293-TLR3 cells or of the siRNA-mediated knockdown approach. To this end U373 cells were transduced with lenti-virus to stably express hECSIT-specific shRNA and knockdown hECSIT expression. Knockdown of hECSIT was confirmed by RT-PCR (Figure 4.3C). Cells were stimulated with Poly (I:C) for the indicated time and assayed for the induction of IFNβ and RANTES mRNA. Again, the expression levels of these IRF- regulated genes, in response to Poly (I:C) were significantly enhanced under conditions of hECSIT knockdown consistent with our earlier findings from over-expression and siRNA knockdown analysis that indicated hECSIT to be a negative regulator of expression of type 1 IFN and related genes in response to Poly(I:C).

We next addressed if the regulatory effects of hECSIT on expression of type 1 IFNs and related genes also applied in our humanised murine model. MEF cells from *ECSIT* $^{+/+\ (Hum)}$ were stimulated with Poly (I:C) for the various times and assayed for mRNA levels of IL-6 (Figure 4.5A), RANTES (Figure 4.5B) and IFNβ (Figure 4.5C). The efficacy of Poly (I:C) in inducing IL-6, RANTES and IFNβ was lower in cells from mice containing human *ECSIT* alleles relative to cells from mice containing the murine counterparts. ELISA analysis to assay protein levels of IL6 and IFNβ further confirmed this reduced efficacy of Poly (I:C) in cells from mice humanized at the *ECSIT* locus Poly (I:C) (Figure 4.6). From the data above it is clear that hECSIT is effecting the transcriptional activation of Poly (I:C) induced NFκB and IRF responsive genes. To further analyse these effects levels of phosphorylated intracellular signalling mediators were analysed in response to Poly (I:C). As mentioned TLR3 signalling results in the activation of NFκB and the IRFs mediated by the adaptors RIP1 and TRAF3, respectively. The TAK1 and IKK complex are the major drivers of MAP kinase and NFκB activation whereas TBK1 and IKKi mediate the activation of the transcription factors IRF3 and IRF7. Suppression of hECSIT in HEK293-TLR3 cells resulted in increased levels of Poly (I:C) induced phosphorylated TBK1 and IRF3 (Figure 4.7). In keeping with these findings MEF cells derived from our -/- (Hum) mice exhibited a lower level of phosphorylated TBK1 and IRF3. Lower levels of Poly (I:C) induced p-IκB-α were also observed in response to Poly (I:C) (Figure 4.8). These ex vivo studies are consistent with the earlier cell-based approaches demonstrating an important role for hECSIT in limiting type 1 IFN and

pro-inflammatory gene expression. Thus hECSIT serves an important regulatory function in controlling anti-viral signalling.

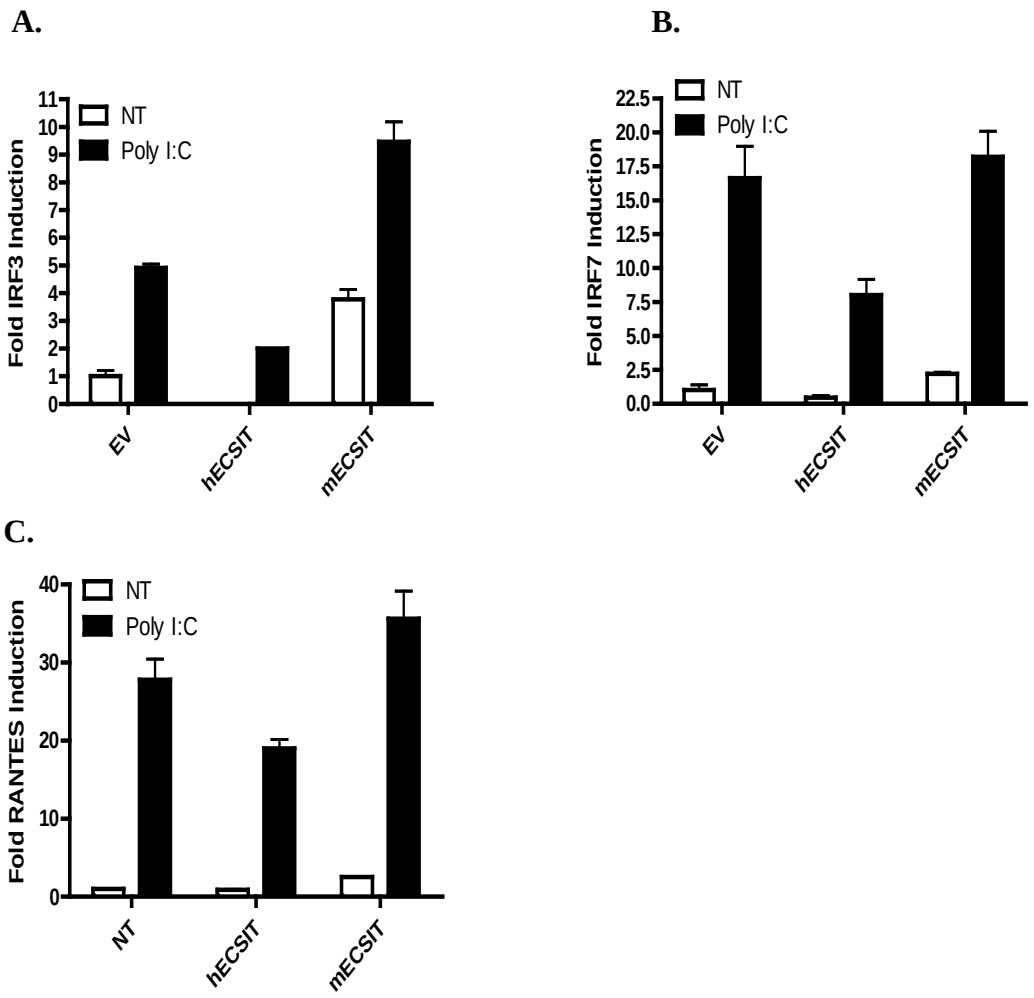

Figure 4.1 Differential effects of hECSIT and mECSIT on TLR3 signalling

HEK293-TLR3 cells were co-transfected with pFA (30ng) IRF3 (A) or pFA IRF7 (30ng) (B) with pFR luciferase reporter construct (60ng) or RANTES promoter-regulated firefly luciferase reporter construct (C) (80ng), TK renilla (20ng) and myc-tagged hECSIT or mECSIT (1µg). Empty Vector (EV) pcDNA3.1 was used to normalise total amount of DNA whilst TK renilla was used to normalise for transfection efficiency. 24 hrs post transfection the cells were treated with Poly (I:C) (25µg/ml) for a further 24 hr. Cell lysates were generated 48 hrs after transfection and assayed for firefly luciferase and renilla luciferase activity. Results represent mean +/- SD of triplicate determinations and is representative of 3 independent experiments.

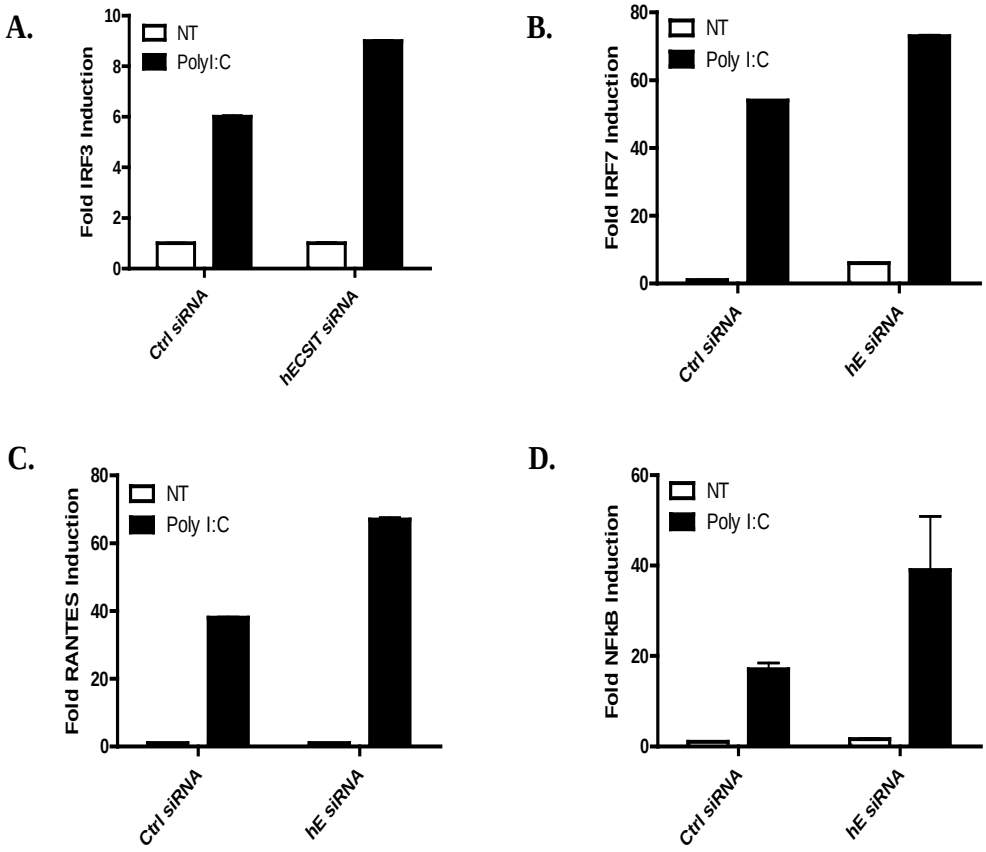

Figure 4.2 Knockdown of hECSIT enhances Poly (I:C) induced activation of IRF3, IRF7, NFκB and the RANTES promoter

HEK293-TLR3 cells were co-transfected with pFA (30ng) IRF3 (A) or pFA IRF7 (30ng) (B) with pFR luciferase reporter construct (60ng) or RANTES (C) or NFκB (D) firefly luciferase reporter construct (80ng) and TK renilla (20ng) reporter construct with hECSIT specific siRNA or Lamin control siRNA (10nM). 24 hrs post transfection the cells were treated with Poly (I:C) (25µg/ml) for a further 24 hr. Cell lysates were generated 24 hrs later and assayed for firefly luciferase and renilla luciferase activity. Results represent mean +/- SD of triplicate determinations and is an average of 3 independent experiments.

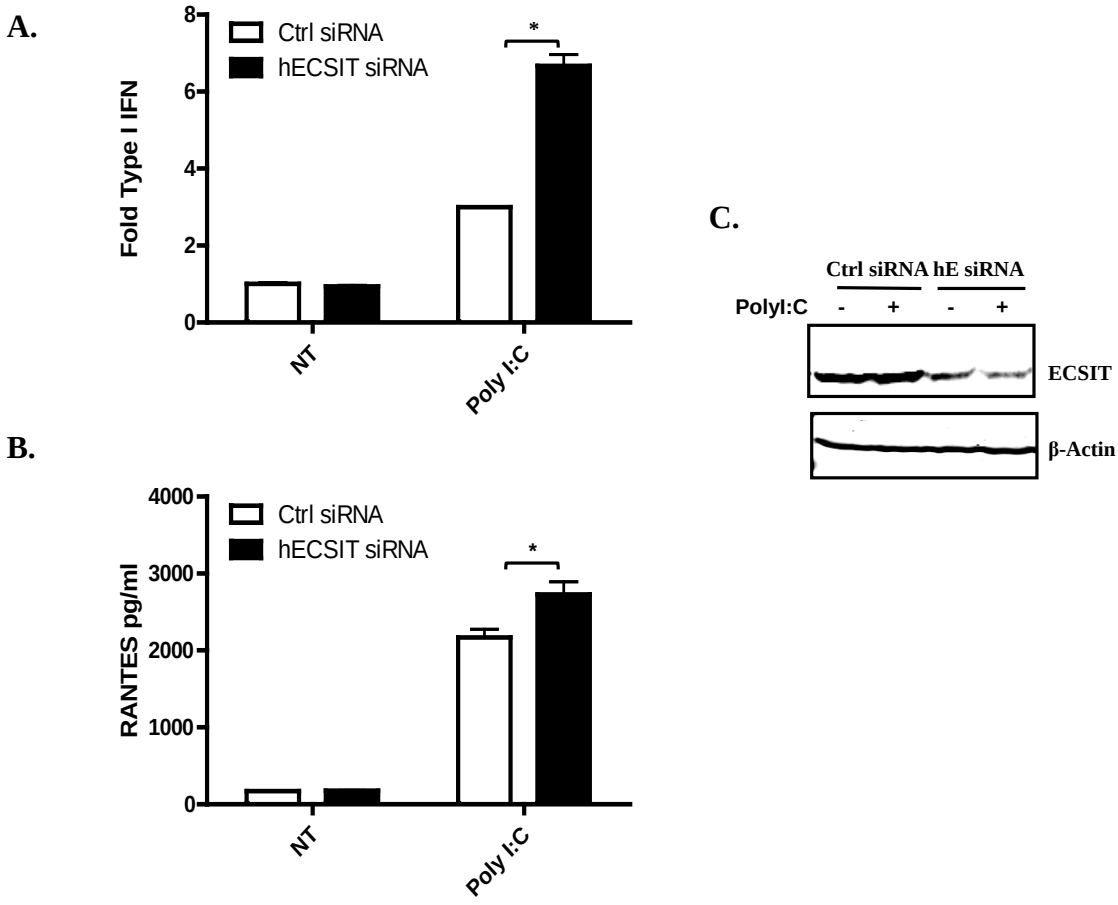

Figure 4.3 siRNA-mediated knockdown of hECSIT enhances Poly (I:C) induced expression of IFN and RANTES in HEK-TLR3 cells.

HEK293-TLR3 Cells were transfected with hECSIT specific siRNA (30nm) or Control siRNA (30nm). 48 hours after transfection cells were stimulated with Poly (I:C) (205µg/ml) for 24 hrs. Media from Non-treated and TNF treated cells were analysed for (A) type 1 IFN by bioassay and (B) RANTES levels by ELISA. Data shown represents the mean of 3 independent experiments. *$p < 0.05$. (C) Cell lysates were probed for expression levels of hECSIT and β-Actin by western blot.

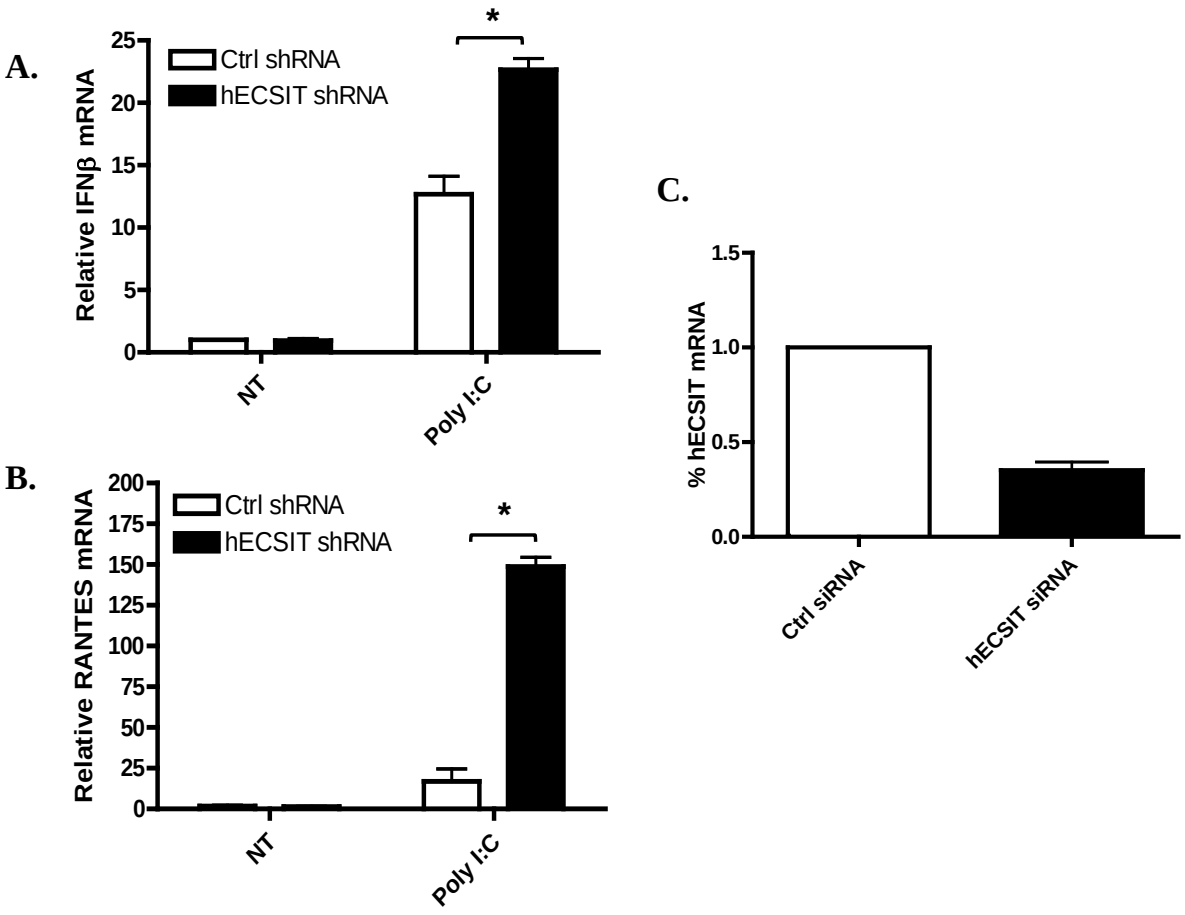

Figure 4.4 shRNA-mediated knockdown of hECSIT enhances Poly (I:C) induced expression of IFNβ and RANTES mRNA in U373 cells

U373 Cells were infected with Lentivirus containing constructs encoding control or hECSIT specific shRNA. Cells were grown in the presence of puromycin (8µg/ml) to select cells with stably integrated shRNA constructs. Selected cells were treated with Poly (I:C) (25µg/ml) for 6 hrs. mRNA expression levels of IFNβ (A) and RANTES (B) were measured by quantitative RT-PCR and expressed relative to expression levels in unstimulated control siRNA cells. Data represents the average of 3 independent experiments; $p<0.05$. (C) mRNA expression levels of hECSIT were measured by quantitative RT-PCR to confirm knockdown.

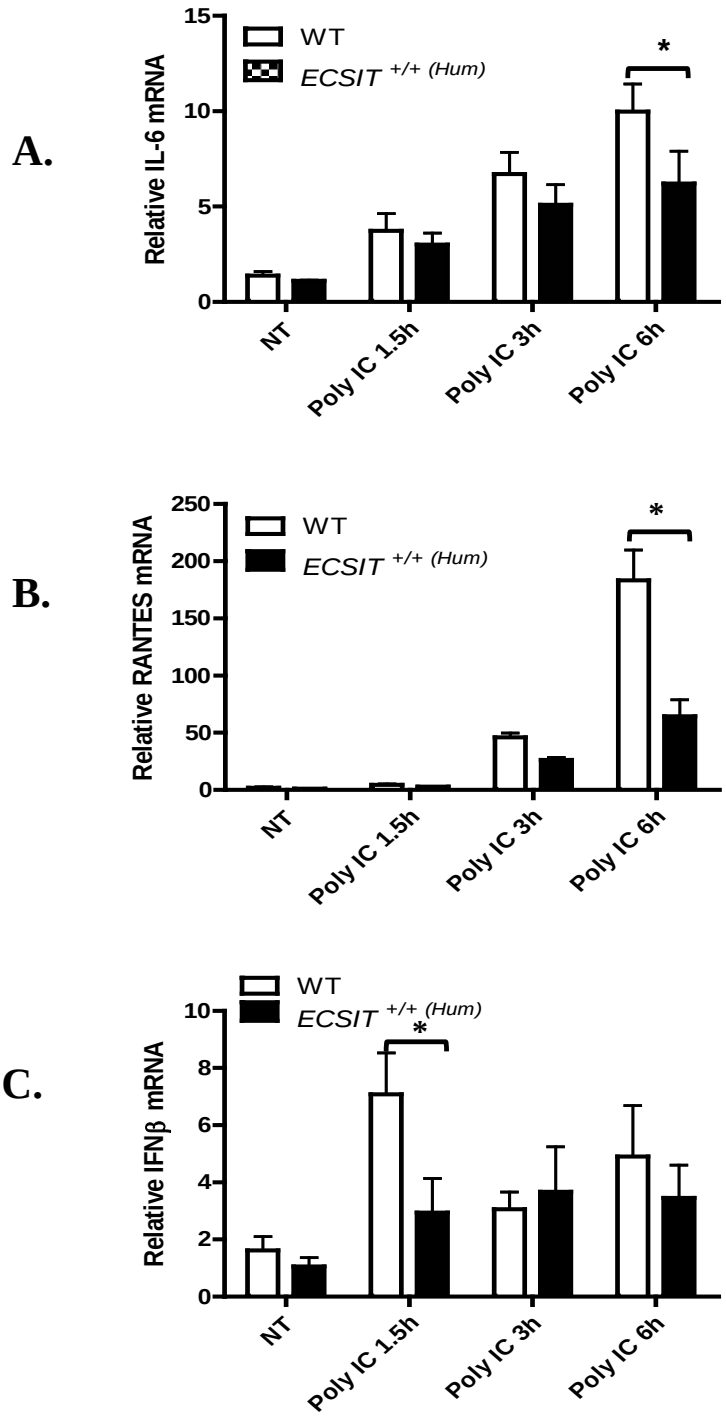

Figure 4.5 Replacement of *Ecsit* with *ECSIT* inhibits Poly (I:C) induced production of IL-6, RANTES and IFNβ

MEFs were isolated from WT and *ECSIT* $^{+/+ (Hum)}$ embryos and were treated with Poly (I:C) (25μg/ml) for the indicated times. mRNA expression levels of IL-6 (A) RANTES (B) and IFNβ (C) were measured by quantitative RT-PCR and expressed relative to expression levels in unstimulated WT cells. Data represents the average of 3 independent experiments; $p<0.05$

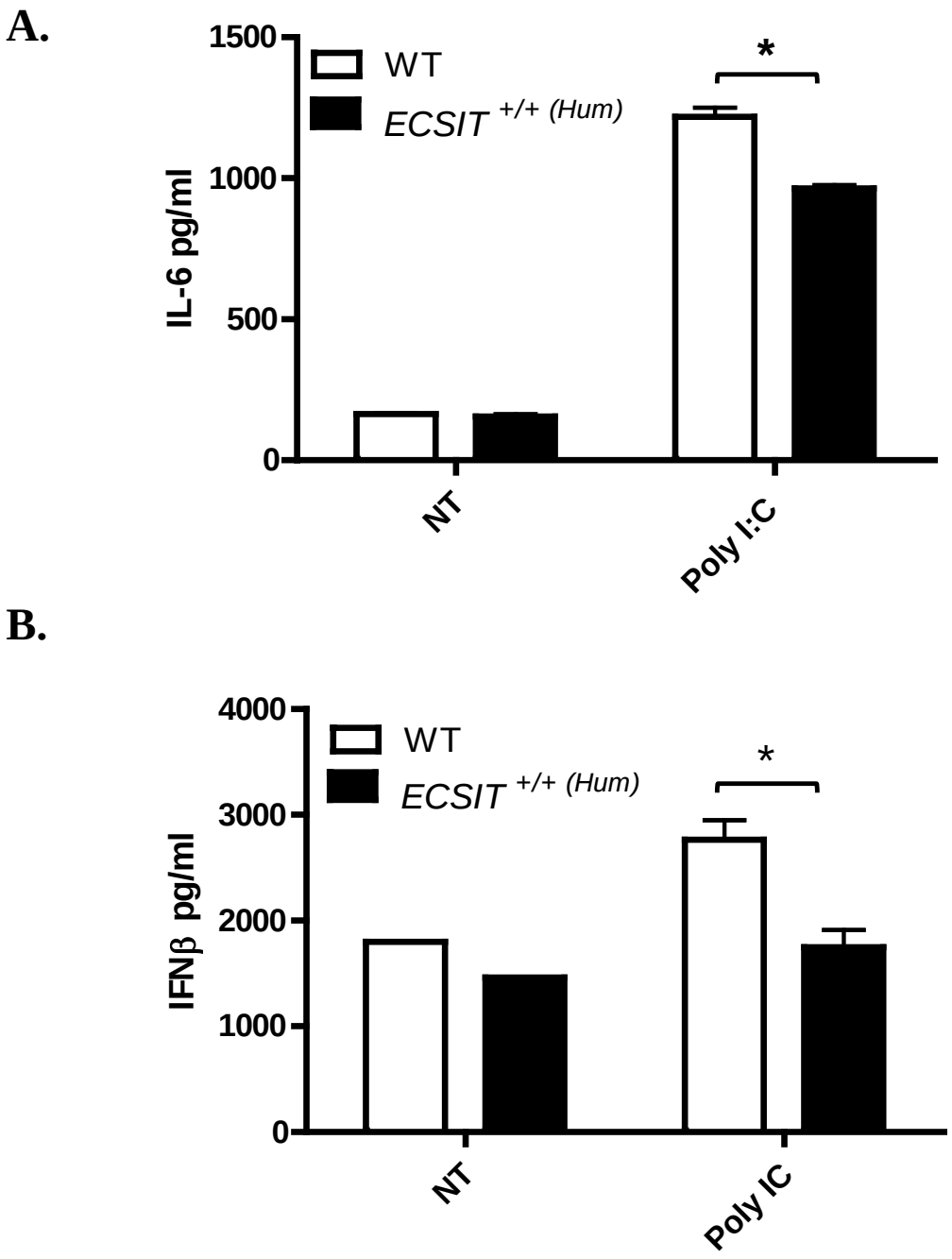

Figure 4.6 Replacement of *Ecsit* with *ECSIT* inhibits Poly (I:C) induced IL-6 and IFNβ production

MEFs were isolated from WT and *ECSIT* $^{+/+ (Hum)}$ embryos and were treated with Poly (I:C) (25μg/ml) for 24 hrs. Media from Non-treated and Poly (I:C) (25μg/ml) treated cells were analysed for levels of IL-6 (A) and IFNβ (B) by ELISA. Data represents the average of 3 independent experiments; $p<0.05$

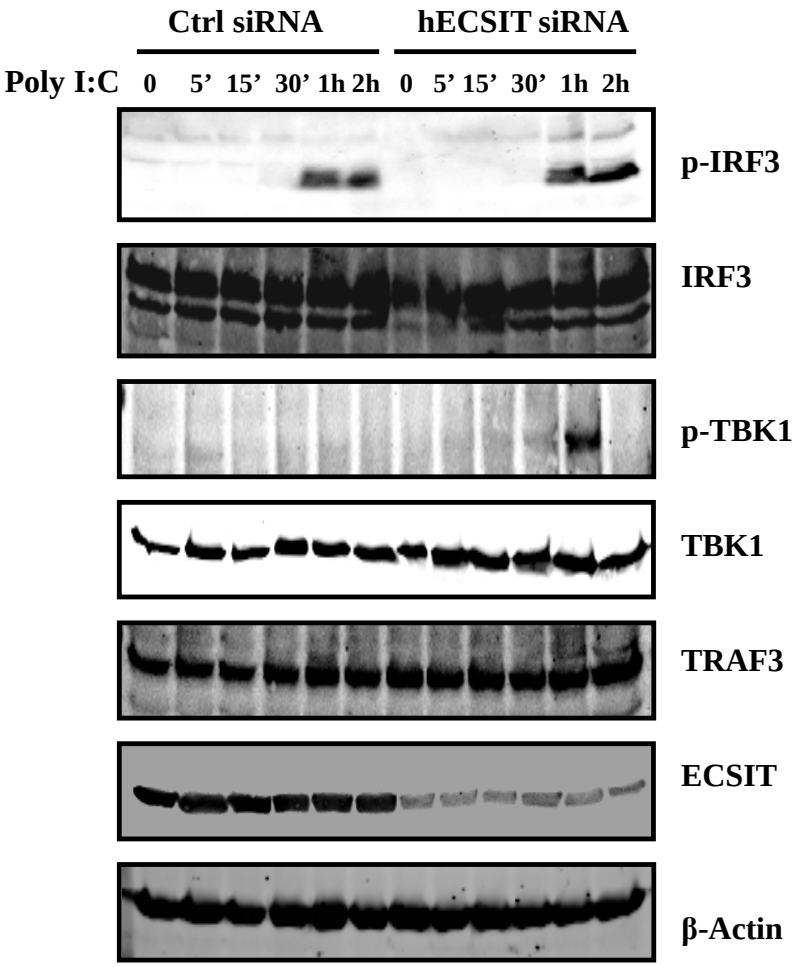

Figure 4.7 Knockdown of hECSIT increases Poly (I:C) induced IRF3 and TBK1 phosphorylation

HEK293-TLR3 cells were transfected with hECSIT specific siRNA (30nm) or Control siRNA (30nm) for 48 hrs. Cells were then treated with Poly (I:C) (25μg/ml) for the indicated times. Cells lysates were prepared and separated by SDS-PAGE followed by Immunoblotting for phosphorylated and total levels of IRF3 and TBK1. Lysates were also probed for levels of TRAF3, ECSIT and β-Actin to confirm knockdown and equal loading.

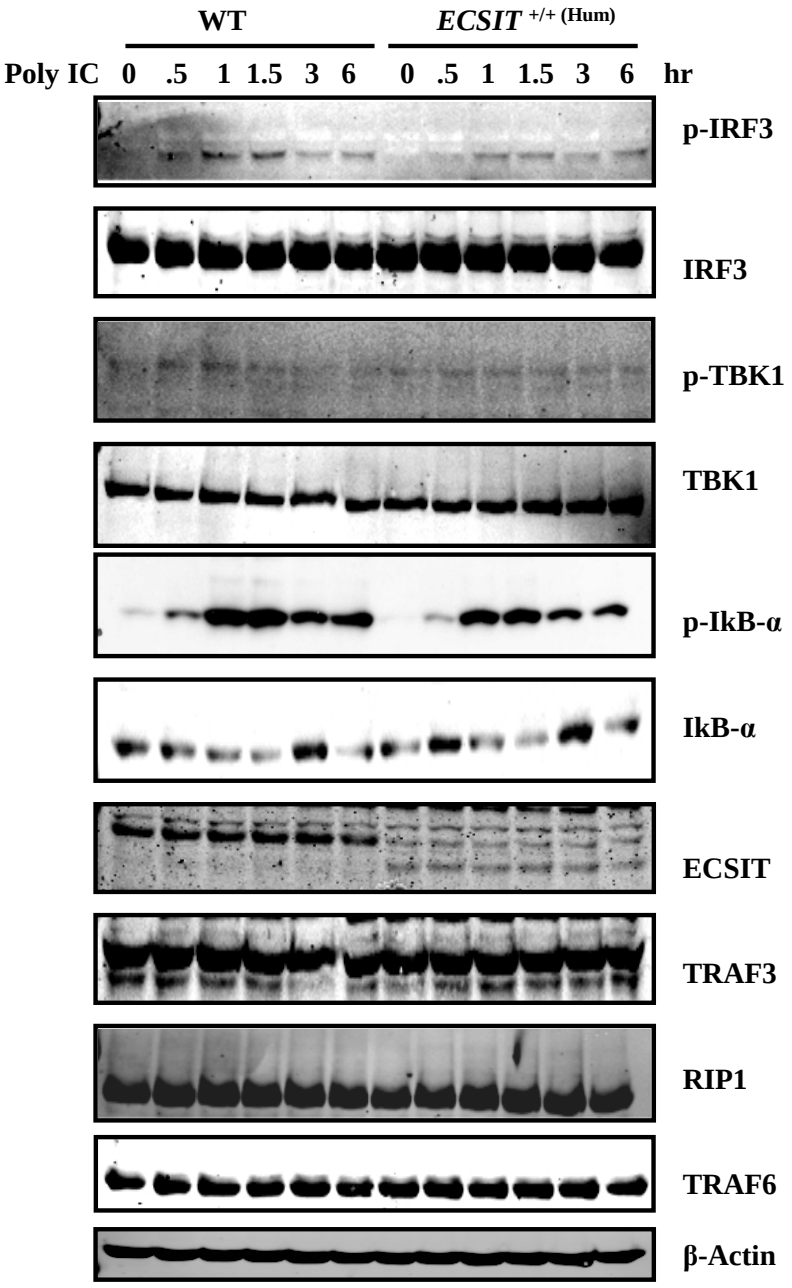

Figure 4.8 Replacement of *Ecsit* with *ECSIT* inhibits Poly (I:C) induced IRF3 and TBK1 phosphorylation

MEFs were isolated from WT and *ECSIT* $^{+/+ (Hum)}$ embryos and were treated with Poly (I:C) (25μg/ml) for the indicated times. Cells lysates were prepared and separated by SDS-PAGE followed by Immunoblotting for phosphorylated and total levels of IRF3, TBK1 and IκB-α. Lysates were also probed for levels of TRAF3, TRAF6 and RIP1. Levels of ECSIT and β-Actin were analysed to confirm genotyping and equal loading.

4.2.2 hECSIT interacts with TRAF3

We next probed the mechanism by which hECSIT can target the TLR3 pathway. As discussed TRAF3 is a multi-functional signalling adaptor in the TLR3 pathway and regulates both the IFN response and non-canonical activation of NFκB. The ubiquitination of TRAF3 plays important roles in the activation of the IRFs and the auto-ubiquitination of TRAF3 has been described as a prerequisite for phosphorylation of TBK1. Given the importance of TRAF3 in TLR3 signalling, coupled to our previous data demonstrating the E3 ligase activity and DUB activity of hECSIT, TRAF3 was examined as a potential target for hECSIT. Co-immunoprecipitation studies were carried out to investigate the possible interaction between hECSIT and TRAF3. HEK293-TLR3 cells were treated with Poly (I:C) for the indicated times and immunoprecipitated with anti-ECSIT. The subsequent precipitate was then analysed for the presence of co-precipitated TRAF3 by western blotting. Poly (I:C) promoted the interaction of TRAF3 with hECSIT in a time-dependent manner, as demonstrated by the co-immunoprecipitation of the two proteins (Figure 4.9A). We next investigated the regions of hECSIT that are important in facilitating its interaction with TRAF3. Myc-tagged hECSIT or the previously described N- and C-terminal truncation mutants were co-expressed with FLAG-tagged TRAF3, immunoprecipitated with anti-myc antibody and probed for the presence of co-precipitated FLAG-tagged TRAF3. As shown in Figure 4.9B hECSIT interacted with TRAF3 and this appears to be mediated by its C-terminal region since the C-terminal but not N-terminal truncation mutant of hECSIT interacted with TRAF3. Interestingly mECSIT also showed association with TRAF3.

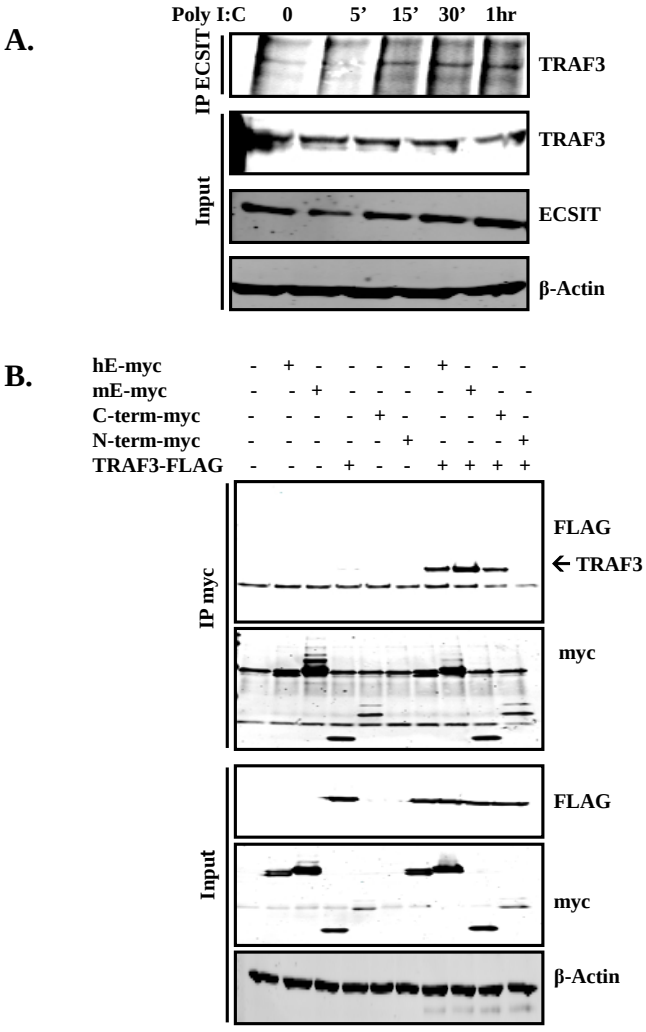

Figure 4.9 hECSIT interacts with TRAF3

(A) HEK293-TLR3 cells were treated with Poly (I:C) (25µg/ml) for the indicated times. Cell lysates were generated and a sample for whole cell lysates analysis was retained. The remaining lysates was immunoprecipitated using an anti-ECSIT antibody. Immunoprecipitates were subsequently assayed for co-precipitated TRAF3. The expression levels of ECSIT and TRAF3 in whole cell lysates (Input) were also assessed by western blotting. (B) HEK293 cells were co-transfected with Empty vector (EV) pcDNA3.1 (1µg), myc-tagged hECSIT (1µg) or myc-tagged mECSIT (1µg) or C-terminal hECSIT (1µg) or N-terminal hECSIT (1µg) with or without FLAG-tagged TRAF3 (1µg). EV was used to normalize total amount of DNA transfected. 24 hrs post-transfection cell lysates were generated and immunoprecipitated with anti-myc antibody. Immunoprecipitates were then subject to SDS-PAGE and subsequently to western blotting using anti-FLAG antibody. Whole cell lysates were also analysed by western blotting using anti-FLAG and anti-Myc antibodies to confirm expression of RIP1 and ECSIT constructs, respectively. Results are representative of 3 independent experiments.

4.2.3 hECSIT Ubiquitinates TRAF3

As hECSIT interacts with TRAF3 in response to Poly (I:C) stimulation we next probed the functional consequence of this interaction by measuring the ubiquitination of TRAF3. We were especially interested in the ubiquitination of TRAF3 given its importance in mediating the activation of the IRF transcription factors. Given that hECSIT possesses both E3 ligase and DUB activity the effect of hECSIT on TRAF3 ubiquitination was investigated.

Firstly an over-expression system was utilised to analyse the possible differential effects of mECSIT and hECSIT on TRAF3 ubiquitination. Myc-tagged hECSIT or mECSIT were co-transfected with FLAG-tagged TRAF3 and HA-ubiquitin. FLAG-tagged TRAF3 was immunoprecipitated and probed for ubiquitination using an anti-HA antibody. Co-expression of hECSIT or mECSIT resulted in an increase in the levels of TRAF3 ubiquitination (Figure 4.10A). To investigate this effect at an endogenous level TRAF3 ubiquitination was measured in cells where hECSIT expression was suppressed. Poly(I:C) induced strong ubiquitination of TRAF3 in a time-dependent manner but knockdown of hECSIT with hECSIT-specific siRNA resulted in greatly reduced ubiquitination of TRAF3 in response to Poly (I:C) compared with cells transfected with control siRNA (Figure 4.10B). These findings suggest that ECSIT acts as important mediator of TRAF3 ubiquitination in the TLR3 pathway.

We next compared the TLR3-induced ubiquitination of TRAF3 in MEF cells from ECSIT humanized mice and wild type mice. Stimulation of humanised MEF cells with Poly (I:C) resulted in an increase in TRAF3 ubiquitination when compared with WT cells (Figure 4.11). We next examined the capacity of hECSIT to directly ubiquitinate TRAF3 by using an *in vitro* ubiquitination assay and measuring the ubiquitination of recombinant TRAF3 in the presence of recombinant hECSIT. Incubation of recombinant TRAF3 with increasing concentrations of recombinant hECSIT and the indicated E1 and E2 enzymes resulted in a dose-dependent increase in TRAF3 ubiquitination as indicated by the appearance of high molecular weight forms of TRAF3 in anti-TRAF3 immunoblotting of reactions (Figure 4.12). To further confirm this TRAF3 was immunoprecipitated from the reaction to remove all associated reaction components. Immunoprecipitated TRAF3 was then assayed for levels of ubiquitination, which also showed increased levels of TRAF3 ubiquitination

when hECSIT was present (Figure 4.12). In conjunction with the earlier cell line and ex *vivo* approaches these findings provide strong support for hECSIT acting as a novel, direct E3 ligase for TRAF3.

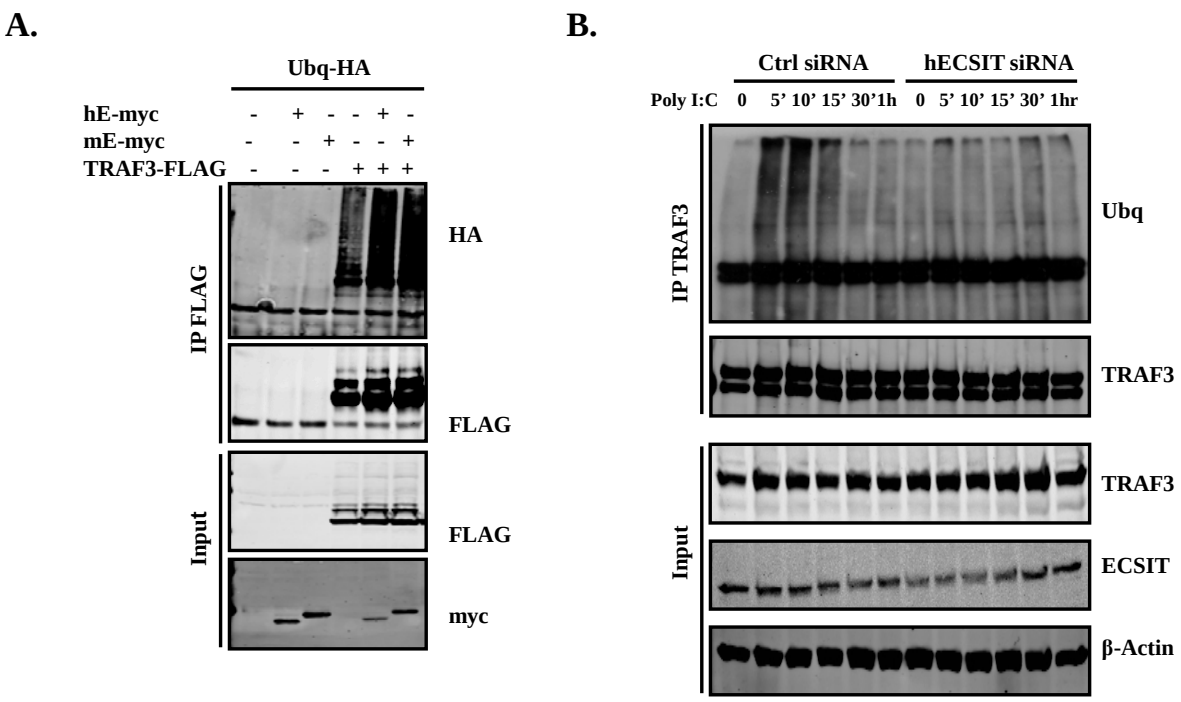

Figure 4.10 hECSIT promotes the ubiquitination of TRAF3

HEK293 cells were co-transfected with Empty vector (1µg), HA-Ubq (1µg), myc-tagged hECSIT (1µg) or myc-tagged mECSIT (1µg) with or without FLAG-tagged RIP1 (1µg). EV was used to normalize total amount of DNA transfected. 24 hrs post-transfection cell lysates were generated and immunoprecipitated using an anti-FLAG antibody. Immunoprecipitates were then subject to SDS-PAGE and subsequently to western blotting using anti-HA antibody. Whole cell lysates were also analysed by western blotting using anti-FLAG and anti-Myc antibodies to confirm expression of RIP1 and ECSIT constructs, respectively. (B) HEK293-TLR3 Cells were transfected with hECSIT specific siRNA (30nm) or Control siRNA (30nm). 48 hrs after transfection cells were then treated with Poly (I:C) (25µg/ml) for the indicated times. Cell lysates were generated and immunoprecipitated using anti-TRAF3 antibody. The immunoprecipitate was then assayed for TRAF3 ubiquitination and immunoprecipitated TRAF3 by Immunoblotting for ubiquitin and TRAF3 respectively. Expression levels of TRAF3, ECSIT and β-Actin were also assessed in the input by western blotting. Data shown is representative of 3 independent experiments.

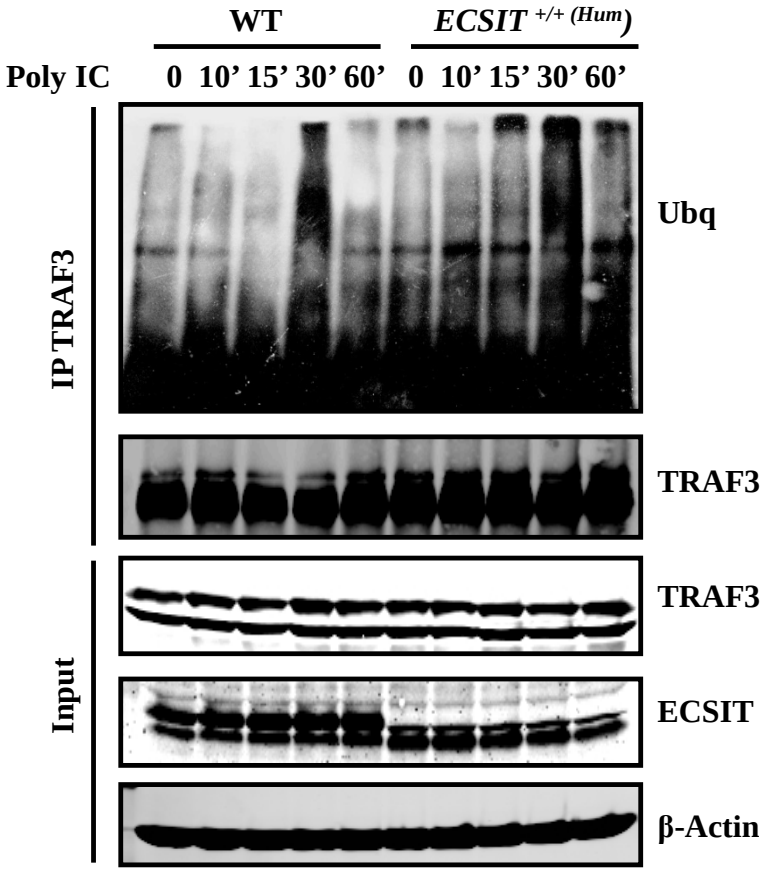

Figure 4.11 Replacement of mECSIT with hECSIT enhances Poly (I:C) induced TRAF3 ubiquitination

MEFs were isolated from WT and *ECSIT* $^{+/+ (Hum)}$ embryos and were treated with Poly (I:C) (25μg/ml) for the indicated times. Cell lysates were generated and immunoprecipitated using anti-TRAF3 antibody. The immunoprecipitate was then assayed for TRAF3 ubiquitination and immunoprecipitated TRAF3 by immunoblotting for Ubiquitin and TRAF3 respectively. Expression levels of TRAF3, ECSIT and β-Actin were also assessed in the input by western blotting. Data shown is representative of 3 independent experiments.

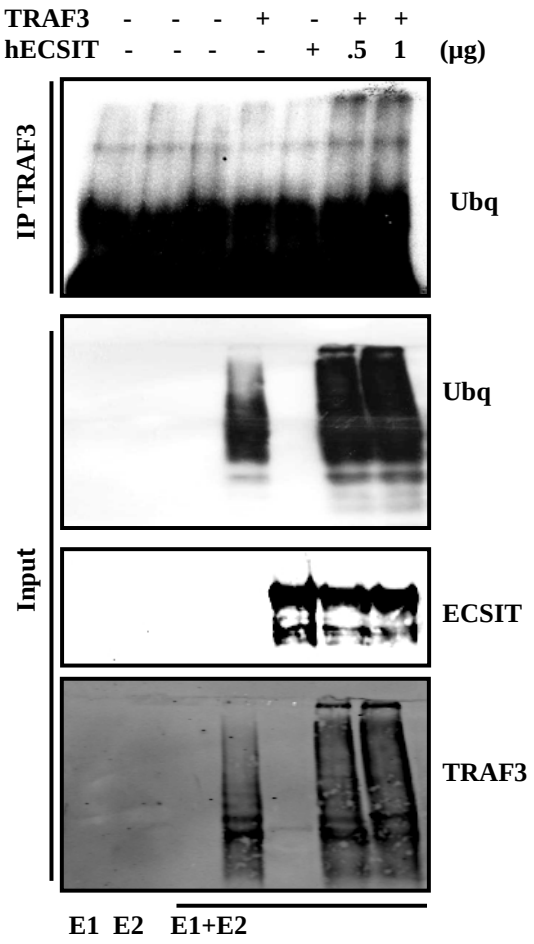

Figure 4.12 hECSIT Ubiquitinates TRAF3 *in vitro*

Recombinant TRAF3 was incubated with or without the indicated concentrations of recombinant hECSIT (0.5-1µg) in a reaction mix containing Ubiquitin (2µg), E1 (50ng), E2 UbcH13/Uev1a (400ng), $MgCl_2$ (2mM), ATP (2Mm), protease inhibitor cocktail and H_20. Reactions were incubated at 37°C for 2hrs and subsequently immunoprecipitated using anti-TRAF3 antibody. The immunoprecipitate was then assayed for TRAF3 ubiquitination by immunoblotting for ubiquitin. Levels of TRAF3, ECSIT and ubiquitin were also assessed in the input by western blotting. Data shown is representative of 3 independent experiments.

4.2.4 hECSIT is processed in response to Poly (I:C)

As previously demonstrated TAK1 promotes the formation of modified and processed forms of hECSIT in response to IL-1 and LPS that possesses both E3 ligase and DUB activity. In order to determine if hECSIT is similarly regulated by TAK1 in the context of TLR3 signalling we initially assessed if hECSIT can associate with TAK1 upon TLR3 stimulation. Poly (I:C) promoted the interaction of TAK1 and hECSIT in a time dependent manner in HEK293-TLR3 cells as shown by co-immunoprecipitation of TAK1 and hECSIT (Figure 4.13A). As hECSIT interacted with TAK1 in response to Poly (I:C) we next assessed the ability of Poly (I:C) to induce TAK1 dependent phosphorylation and processing of hECSIT using the pharmacological TAK1 inhibitor 5Z-7-oxozeanol. THP1 cells stimulated with Poly (I:C) resulted in putative phosphorylation and processing of hECSIT. However pre-treatment of THP1 cells with the TAK1 inhibitor resulted in inhibition of hECSIT phosphorylation and processing (Figure 4.13B). In order to determine the functional consequence of hECSIT processing in response to Poly (I:C) a truncated expression construct encoding the C-terminus of hECSIT was used as a model to represent the processed form of hECSIT. IFNβ-luciferase reporter assays revealed that in response to Poly (I:C) the C-terminus of hECSIT was more inhibitory than the full length hECSIT and the N-terminus of hECSIT (Figure 4.19A).

These data are consistent with a model where Poly (I:C) induces TAK1 dependent phosphorylation and processing of hECSIT to enhance its E3 ligase activity and facilitate the ubiquitination of TRAF3 to inhibit TLR3 signalling. This represents a novel mechanism by which hECSIT can exert its inhibitory effect on innate immune signalling and identifies TRAF3 as the first substrate for the E3 ligase function of hECSIT.

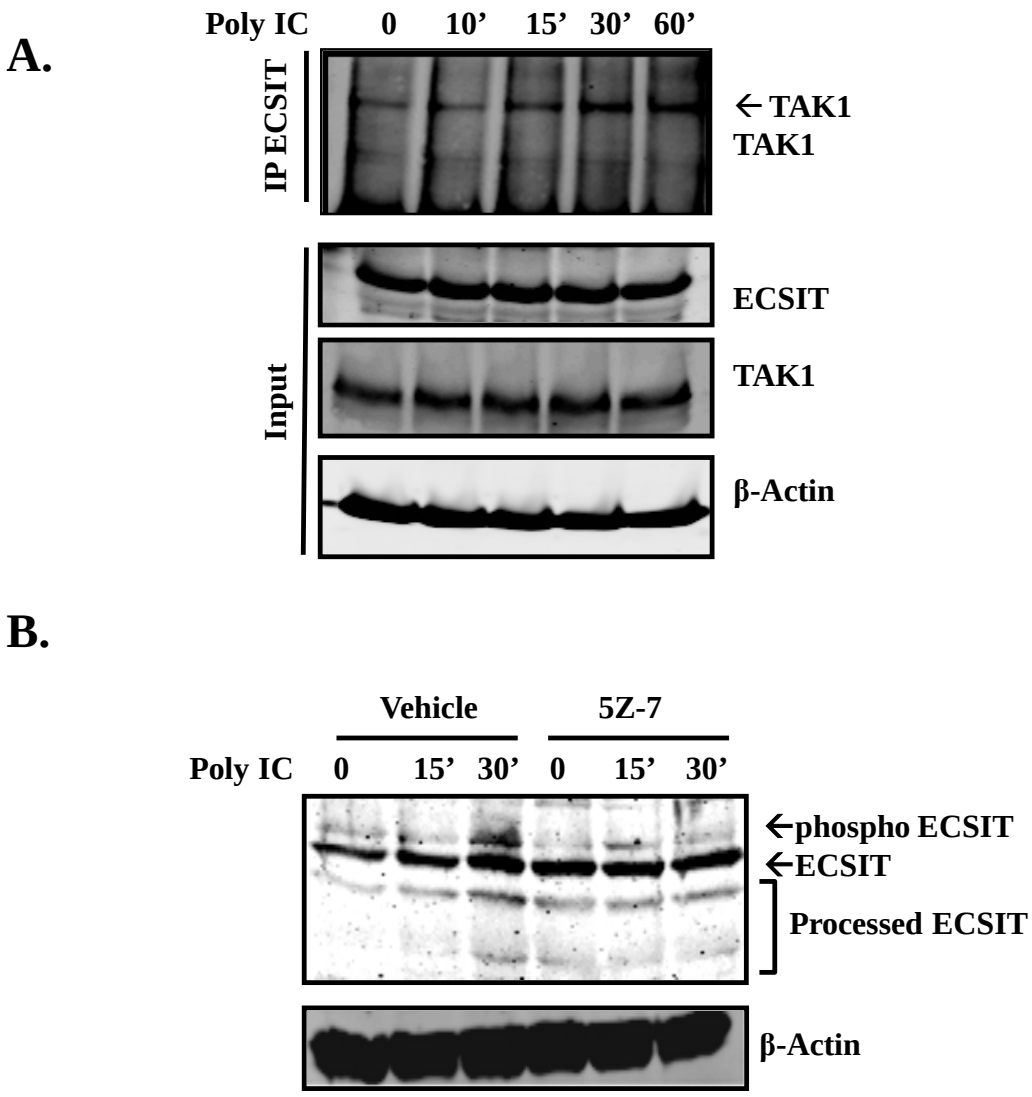

Figure 4.13 TAK1 promotes phosphorylation and processing of hECSIT in response to Poly (I:C)

(A) HEK293-TLR3 cells were treated with Poly (I:C) (25μg/ml) for the indicated times. Cell lysates were generated and a sample for whole cell lysates analysis was retained. The remaining lysates was immunoprecipitated using an anti-ECSIT antibody. Immunoprecipitates were subsequently assayed for co-precipitated RIP1 and ECSIT. The expression levels of ECSIT and RIP1 in whole cell lysates were also assessed by western blotting. (B) THP1 cells were pre-treated for 2 hrs with vehicle DMSO and 5z-7-oxozeanol (20Mm). Cells were then treated with Poly (I:C) (25μg/ml) for the indicated times. Cell lysates were generated and subjected to SDS-PAGE and probed by Immunoblotting for expression levels of ECSIT and β-Actin. Processed ECSIT is indicated by arrows.

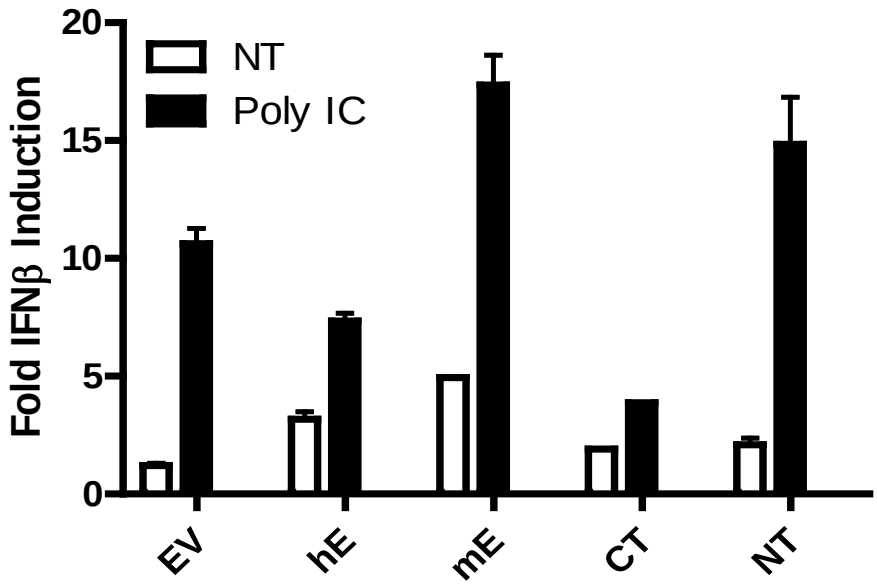

Figure 4.14 The C-terminus of hECSIT inhibits Poly (I:C) induced IFNβ activation

HEK293-TLR3 cells were co-transfected with IFNβ firefly luciferase reporter construct (80ng), TK renilla (20ng) and myc-tagged hECSIT or mECSIT or the C-terminal amino acids 261-435 (CT) or N-terminal of hECSIT amino acids 1-260 (NT) (100ng). Empty Vector (EV) pcDNA3.1 was used to normalise total amount of DNA whilst TK renilla was used to normalise for transfection efficiency. 24hr post-transfection the cells were treated with Poly (I:C) (25µg/ml). Cell lysates were generated the following day and assayed for firefly luciferase activity. Results represents mean +/- SD of triplicate determinations and is representative of 3 independent experiments.

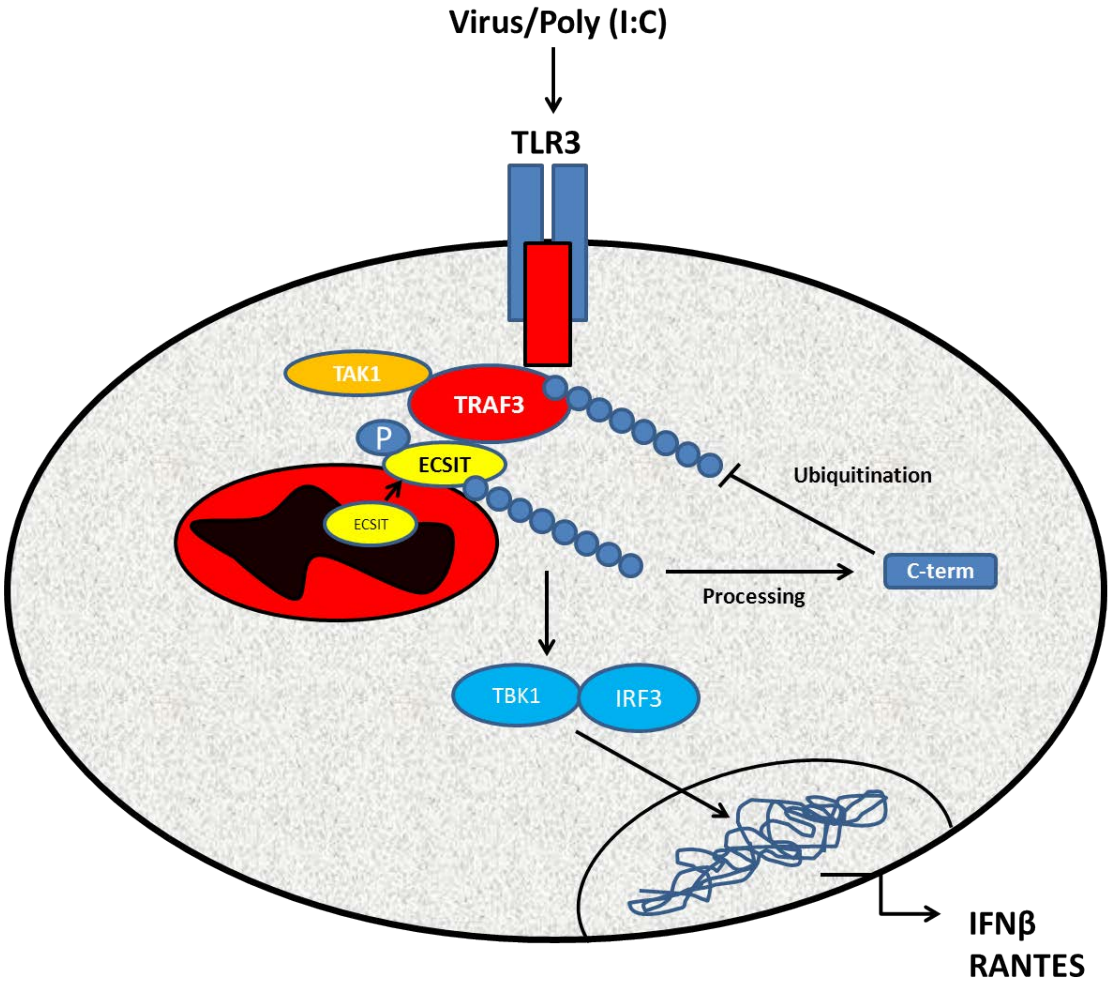

Figure 4.15 Schematic representation of hECSIT's regulatory effect in the TLR3 pathway

Activation of the TLR3 pathway results in the processing of hECSIT activating its E3 ligase activity. Direct ubiquitination of TRAF3 by hECSIT results in inhibition of the IRFs and NFκB

4.3 Discussion

In the previous chapter it was shown that the induction of TLR4 and IL-1R signalling results in the likely processing of hECSIT into an inhibitory form which reveals a cryptic DUB activity leading to the deubiquitination of TRAF6 and negative regulatory effects on the NFκB pathway and mROS production. It was also shown that the C-terminus of hECSIT also possessed E3 ligase activity. To investigate the role of hECSIT in anti-viral signalling we assessed its potential regulatory function in TLR3 signalling. The production of Type 1 IFN is tightly regulated to prevent excessive inflammation and auto-immunity after viral infection is eliminated (Gao et al, 2011). Many DUB enzymes and E3 ligases regulate this response such as A20, CYLD and DUBA (Zhang et al, 2008; Mankouri et al, 2010) the latter targeting the deubiquitination of TRAF3. In this study we have identified hECSIT as a novel regulator of TLR3 signalling. We propose that TLR3 signalling results in the activation of the E3 ligase function of hECSIT via a TAK1-dependent cross-regulatory mechanism, thus facilitating its interaction with TRAF3 and the ubiquitination of the latter. We propose that this ubiquitination step results in inhibition of TRAF3 in the cell leading to inhibition of type 1 IFN expression. In addition to uncovering a new regulatory mechanism in TLR3 signalling the findings also highlight TRAF3 as the first substrate for the E3 ligase function of hECSIT.

mECSIT has recently been identified as a positive regulator of IRF3 and IRF7 pathways (Kondo et al, 2012) although no definitive mechanistic role has been attributed to mECSIT in the TLR3 pathway. However, consistent with previous positive regulatory roles for mECSIT we demonstrate a positive role for mECSIT in Poly (I:C) induced activation of IRFs. However, hECSIT negatively regulates this pathway as demonstrated in our knockdown systems and our animal model. The availability of our humanised model allowed us to assess the physiological role of hECSIT in the TLR3 pathway. Replacing mECSIT with hECSIT resulted in attenuated IFN but also NFκB responses. Whilst TRAF3 had been our lead target thus far, the abrogated NFκB response shown in our primary cells cannot be explained by the targeting of TRAF3. However as hECSIT has dual DUB/E3 ligase activity it may also have dual targets in this pathway. As TRAF6 has been previously identified as a target for hECSIT and is required for both Poly (I:C) induced NFκB and IRF7

activation (Sasai et al, 2010; Siednienko et al, 2012) it will be interesting to examine the possibility of hECSIT also regulating TRAF6 in response to Poly (I:C).

A number of studies have identified various E3 ligases that target TRAF3 for ubiquitination to either inhibit or enhance the function of the latter. cIAP1/2 have been implicated in TRAF3 ubiquitination in TLR3 and TLR4 signalling as has Triad3a in RIG-I signalling. TRAF3 undergoes biphasic ubiquitination following viral infection. Early after infection, K63-linked polyubiquitination of TRAF3 contributes to IFN signalling while at later times after infection, TRAF3 undergoes K48-linked polyubiquitination mediated by Triad3a which results in the degradation of TRAF3. Here we propose hECSIT as a novel E3 ligase for TRAF3 in controlling the production of type 1 IFN. As we were unable to determine the exact ubiquitin linkage owing possibly due to E2 specificity further experimentation using a wider range of E2 enzymes will perhaps uncover the exact mechanism. TRAF3 ubiquitination is an important factor in TRAF3-mediated signalling as demonstrated by the number of E3 ligases that target TRAF3. However the specific lysine residues in TRAF3 that act as ubiquitination sites have yet to be identified. Mutational analysis of these sites and precise genetic models utilising knock-in site-specific mutations on putative ubiquitination sites, will be necessary for unequivocal conclusions about the exact role of TRAF3 ubiquitination. Furthermore the identification of a direct lysine residue where hECSIT ubiquitinates TRAF3 will be required to further understand this mechanism.

Consistent with our previous data hECSIT is also processed in response to Poly (I:C) in a TAK1 dependent manner. Such cross-regulation is not unprecedented as the TLR3 pathway is also targeted by the TIR adaptors Mal and MyD88 to inhibit IFNβ and RANTES production (Siednienko et al, 2010; Siednienko et al, 2011). Additionally the NFκB subunits Rel B and c-Rel can also induce the transcriptional repressor YY1 to inhibit TLR3 induced IFNβ production (Siednienko et al, 2011b). It is likely that TAK1-induced phosphorylation of hECSIT serves as an important pre-requisite for hECSIT processing as evident by the C-terminus containing both the E3 and DUB activity. Similarly the DUB enzyme DUBA also requires a phosphorylation event to manifest its DUB activity (Huang et al, 2012). Phosphorylation-dependent E3 ligase function has also been described. The catalytic activity of the Pellino proteins is strongly enhanced by phosphorylation (Ordureau et al, 2008) and in the context of anti-viral signalling Pellino 1 is activated by the kinases TBK1 and IKKi (Smith et al,

2010). As hECSIT can negatively regulate the TLR3 pathway it will also be of interest to examine its role, if any, in RIG-I signalling. It was been recently shown that mECSIT can interact with MAVS when over-expressed (Kondo et al, 2012). Given its mitochondrial localisation ECSIT could also be an important regulator of RLR signalling. Although more studies will be required to delineate the precise molecular mechanisms involved, this present study shows that TAK1 co-operates with hECSIT to restrict the TLR3 pathway.

Chapter 5

Investigating the role of hECSIT in TNF-α Signalling

5.1 Introduction

Inflammation is an essential component of innate immunity and the host response to infection. In response to viral or bacterial infection innate cells produce potent pro-inflammatory cytokines such as TNF-α and IL-1ß which trigger the inflammatory response (Serhan et al, 2008). TNF-α initiates a complex cascade of signaling events that lead to the induction of proinflammatory cytokines, cell proliferation, and differentiation or programmed cell death (Chen and Goeddel, 2002). The binding of TNF to its receptor TNFR1 leads to association of TNF-R1 associated death domain protein (TRADD) (Hsu et al, 1995) with the receptor complex followed by recruitment of FAS associated death domain protein (FADD), TRAF2 and RIP1 (Hsu et al, 1996). Whilst FADD can trigger activation of Caspase 8 leading to cell apoptosis (Wilson et al, 2009) TRAF2, cIAP1 and RIP1 mediate the activation of NFκB and MAP kinase in response to TNF-α (Karin and Gallagher, 2009) Alternatively inhibition of caspase activity can lead to the formation of the necroptosome, or programmed necrosis via the interaction of RIP1 and RIP3 to form the 'Ripoptosome' (Imre et al, 2011). The ubiquitination of RIP1 facilitates the recruitment of IKK complexes (Ea et al, 2006). The subject of RIP1 ubiquitination has been under much scrutiny in recent years and a number of E3 ligases have been implicated in the ubiquitination of RIP1 including TRAF2 (Lee et al, 2004, Wertz et al, 2004) (Yammato et al, 2006), the cellular inhibitor of apoptosis proteins (cIAPs) (Bertrand et al, 2005) and more recently LUBAC (Haas et al, 2009). K63-linked ubiquitination of RIP1 functions as a major cytoprotective effect. Linear ubiquitination of RIP1 has also been shown to inhibit the induction of apoptosis (Tokunaga and Iwai, 2011). Conversely disruption of RIP1 ubiquitination converts RIP1 into a death inducing protein via its interaction with Caspase 8 (O'Donnell and Ting 2010). Caspase 8 mediated cleavage of RIP1 prevents RIP1 induced NFκB activation, biasing the TNF pathway towards cell apoptosis (Lin et al, 1999). In the absence of caspase activity the phosphorylation of RIP1 by RIP3 promotes the assembly of the ripoptosome to induce necrosis. RIP1 has also been implicated in TLR signaling and IKK activation in response to signaling by the TLR3 and TLR4 adaptor TRIF (Cusson-Hermance et al., 2005; Meylan et al., 2004). A recent study has also described RIP1 as dual positive and negative regulator of RIG-I signaling (Rajput et al, 2011). RIP1 was shown to promote the activation of IRF3 downstream of RIG-I.

However this action was blocked following cleavage of RIP1 by Caspase-8 which converted RIP1 into an inhibitor of RIG-I signalling. This cleavage of RIP1 by Caspase-8 is ubiquitin dependent and Caspase 8 fails to cleave a form of RIP1 in which the ubiquitination site of lysine 377 has been mutated (Rajput et al, 2011).

A number of negative regulators of TNF signaling target RIP1 to inhibit NFκB activation and apoptosis. A20 is one such negative regulator and functions as a dual ubiquitin editing enzyme towards RIP1 (Wertz et al, 2004). RIP1 ubiquitination is also regulated by Triad3a (Fearns et al, 2006), Cezanne (Enesa et al, 2008) and CYLD (Wright et al, 2007) which all serve to inhibit NFκB. From these studies it is evident that RIP1 is a central target in the inhibition of the TNF-α signal. To this end it seemed appropriate to investigate if hECSIT, a novel E3 ligase/DUB enzyme, plays a regulatory role in the TNF-α pathway. The function of murine ECSIT has been previously demonstrated not to be involved in the regulation of TNF-α signalling. However the emergence of hECSIT being functionally different to its murine orthologue in TLR/IL-1R signalling prompted us to investigate other pathways activated during innate immune signalling. During TLR/IL-1R signalling hECSIT becomes activated via processing into an active form. This processed form is induced by the co-operative kinase activity of TAK1 and the protease activity of caspase 8, 2 proteins which are critical in the activation of NFκB and induction of apoptosis in the TNF-α pathway. Following on from our study in TLR/IL-1R signalling we decided to investigate the role of ECSIT and the processed subunit in the TNF-α pathway utilizing siRNA/shRNA methods in conjunction with our humanised animal model. As discussed mECSIT has been shown not to function in the TNF pathway. However no role for hECSIT in TNF signaling has been reported. This chapter aimed to characterize the role of hECSIT in the TNF-α pathway and to investigate the mechanistic basis of any such regulatory effects.

5.2 Results

5.2.1 hECSIT negatively regulates TNF-α induced NFκB activation and Apoptosis

Previous reports had indicated that mECSIT failed to play a role in the TNF pathway. To investigate the potential regulatory role of hECSIT in TNF-α signalling an initial combination of siRNA and over-expression studies in HEK293 cells were used. Co-transfection of an NFκB-dependent luciferase reporter construct with control siRNA or hECSIT-specific siRNA to suppress hECSIT expression resulted in enhanced NFκB activation in response to TNF-α (Figure 5.1A). To analyse this further hECSIT or mECSIT expression constructs were co-transfected with an NFκB-dependent luciferase reporter construct. Over-expression of hECSIT inhibited TNF-α induced NFκB activation whereas mECSIT promoted the activation of NFκB (Figure 5.1B)

To further analyse the role of hECSIT in regulating this pathway the HeLa cell system was used, a cell line well documented for potent TNF-α responses. HeLa cells were transfected with hECSIT specific siRNA. Knockdown was confirmed at a protein and mRNA level (Figure 5.2B, C). Activation of NFκB by TNF-α promotes the production of cytokines such as IL-6 and IL-8. Knockdown of hECSIT in HeLa cells enhanced the production of IL-6 after TNF-α treatment, as measured by ELISA (Figure 5.2C). This was further confirmed at an mRNA level by quantitative RT-PCR(Figure 5.3). The regulatory of hECSIT on TNF-α signalling was also assessed in primary MEF cells where mECSIT had been replaced with hECSIT. Replacing mECSIT with hECSIT resulted in decreased levels of IL-6 and KC in response to TNF-α (Figure 5.4). These data indicated that hECSIT has the capacity to negatively regulate TNF-induced expression of pro-inflammatory genes. To probe the target for such a regulatory role, the effects of hECSIT knockdown on TNF induced intracellular signalling were examined. siRNA-mediated suppression of hECSIT expression in HeLa cells resulted in increased levels of phosphorylated TAK1, IKK and IκB-α in response to TNF-α relative to cells transfected with control siRNA (Figure 5.5). This was also confirmed in U373 cells in which shRNA-mediated knockdown of hECSIT resulted in enhanced TNF-induced phosphorylation of TAK1, IKK and IκB-α, the latter being coincident with prolonged degradation of IκB (Figure 5.6). TNF-α is also a potent activator the MAP kinases P38 and JNK and whilst suppression of hECSIT in HeLa cells failed to enhance TNF-α induced

phosphorylation of p38, reduced levels of hECSIT were associated with modest enhancement of TNF-induced phosphorylation of JNK (Figure 5.7)

In addition to its widely characterised role in activating NFκB, TNF is also well known to regulate various forms of cell death. Again the HeLa cell and U373 cell systems were used in conjunction with siRNA and shRNA-mediated knockdown of hECSIT to assess it potential regulatory role in TNF-α induced apoptosis. TNF is cytoprotective under circumstances in which it activates NFκB to induce anti-apoptotic genes. However in the presence of protein synthesis inhibitors, like cyclohexamide, these anti-apoptotic genes are not expressed leading to caspase-mediated activation of the apoptotic programme. Thus treatment of U373 cells with TNF-α and cyclohexamide caused the cells to become rounded and detach from the cell culture plate and this was associated with increased apoptosis as measured by increases cleavage of PARP (Fig. 5.8A). However the number of rounded and detached cells and levels of cleaved PARP increased when hECSIT expression was suppressed by hECSIT specific shRNA (Figure 5.8A). This was further confirmed in HeLa cells where reduced expression of hECSIT led to increased cleavage of PARP in response to co-treatment of TNF-α and cyclohexamide. Furthermore an increase in RIP1 ubiquitination was also observed (Figure 5.8B).

The above findings, utilizing independent approaches to suppress hECSIT function in different cell lines in combination with a murine model to address the functional difference between hECSIT and its murine orthologue, provide strong evidence to suggest that hECSIT plays a key role in regulating the various signalling pathways that are triggered by TNF-α.

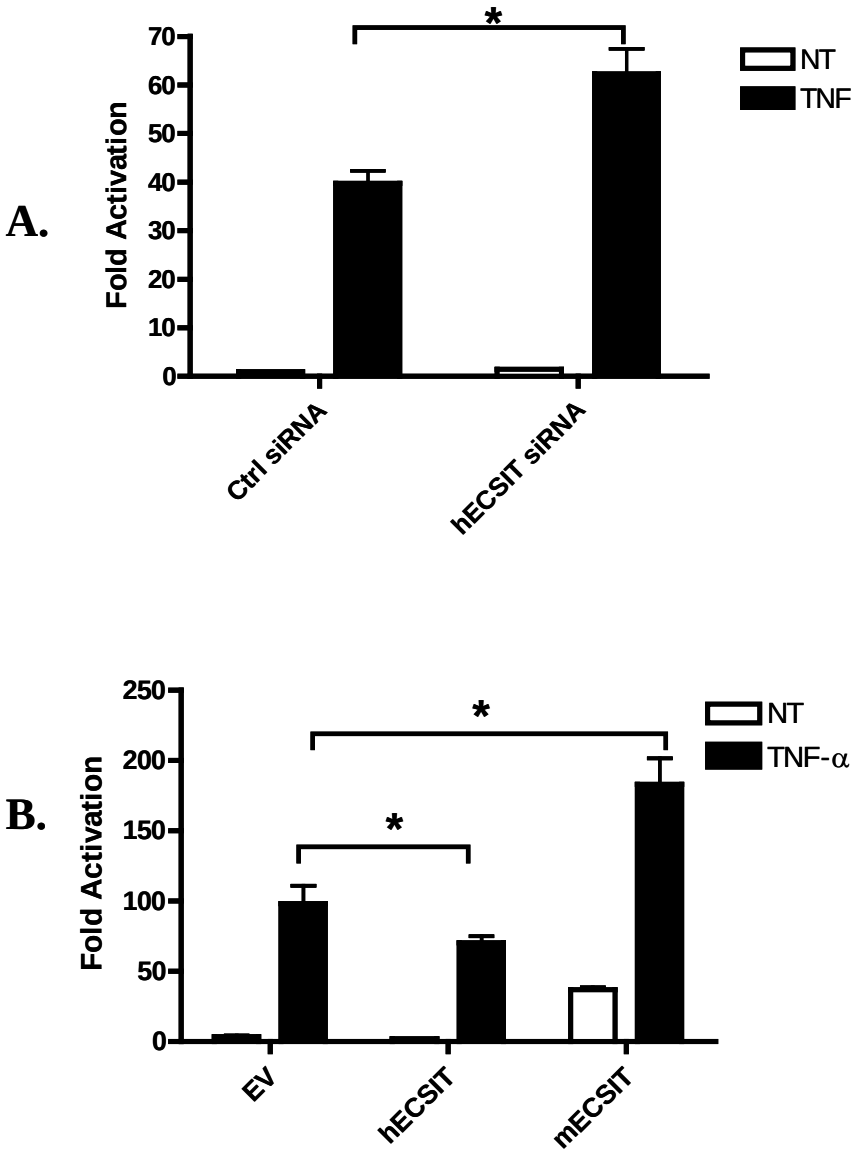

Figure 5.1 Differential effects of hECSIT and mECSIT on TNF induced activation of NFκB

(A) HEK293 cells were co-transfected with NFκB firefly luciferase reporter construct (80ng), TK renilla (20ng) and hECSIT specific siRNA or Lamin control siRNA (10nM). 24 hrs post transfection the cells were treated with TNF-α (50ng) for a further 24 hr. Cell lysates were generated 48 hrs after transfection and assayed for firefly luciferase and renilla luciferase activity. Results represent mean +/- SD of triplicate determinations and is an average of 3 independent experiments. (B) HEK293 cells were co-transfected with NFκB firefly luciferase reporter construct (80ng), TK renilla (20ng) and myc-tagged hECSIT or mECSIT (100ng). Empty Vector (EV) pcDNA3.1 was used to normalise total amount of DNA whilst TK renilla was used to normalise for transfection efficiency. 24hr post-transfection the cells were treated with TNF-α (50ng). Cell lysates were generated the following day and assayed for firefly luciferase activity. Data shown represents the mean of 3 independent experiments. *$p < 0.05$.

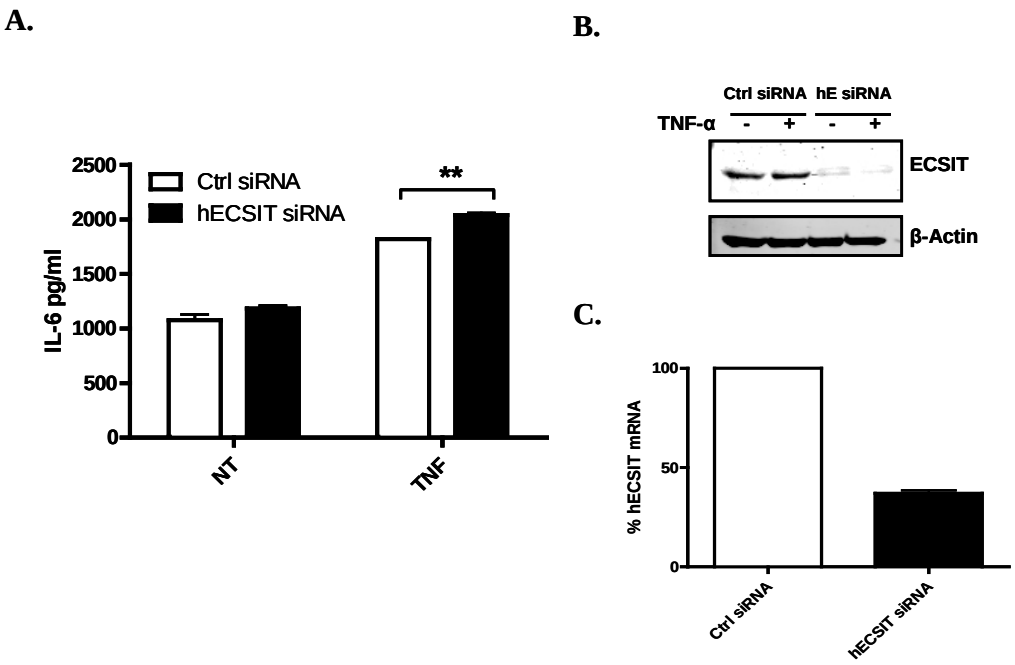

Figure 5.2 hECSIT knockdown enhances TNF induced expression of IL-6

U373 Cells were transfected with hECSIT specific siRNA (30nm) or Control siRNA (30nm). 48 hours after transfection cells were stimulated with TNF-α (50ng/ml) for 24 hrs. (A) Media from Non-treated and TNF treated cells were analysed for IL-6 levels by ELISA. Data shown represents the mean of 3 independent experiments. **p< 0.01. (B) Cell lysates were probed for expression levels of hECSIT and β-Actin. (C) RNA was extracted 48 hrs post-transfection and analysed by quantitative RT-PCR for levels of hECSIT mRNA.

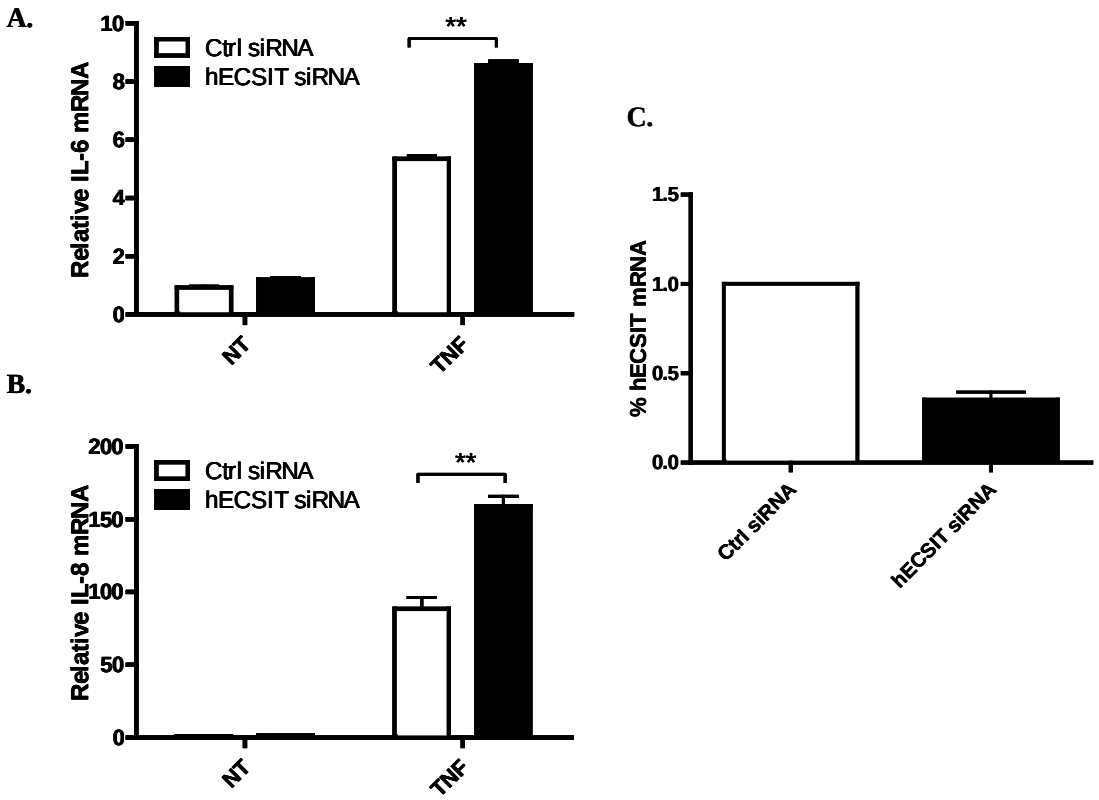

Figure 5.3 hECSIT knockdown enhances TNF induced IL-6 and IL-8 mRNA

HeLa Cells were transfected with hECSIT specific siRNA (30nm) or Control siRNA (30nm). 48 hrs after transfection cells were stimulated with TNF-α (50ng/ml) for 6 hrs. (A,B) mRNA expression levels of IL-6 and IL-8 were measured by quantitative RT-PCR and expressed relative to expression levels in unstimulated control siRNA cells. Data represents the average of 3 independent experiments; $p<0.01$. (C) mRNA expression levels of hECSIT were measured my quantitative RT-PCR.

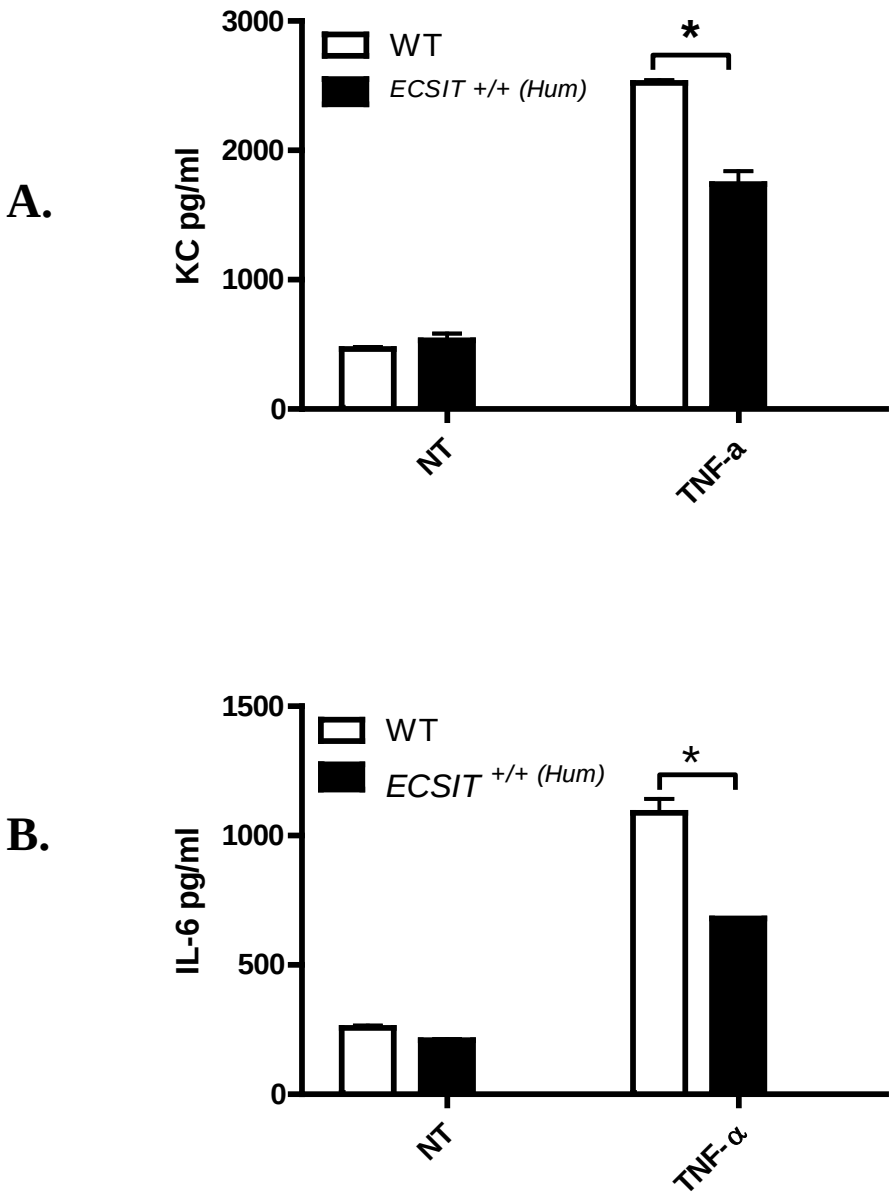

Figure 5.4 Replacement of *Ecsit* with *ECSIT* inhibits TNF induced production of IL-6 and KC

MEFs were isolated from WT and *ECSIT* $^{+/+ (Hum)}$ embryos and were treated with murine TNF-α (25ng/ml) for 24 hrs. Media from non-treated and treated cells were assayed for levels of IL-6 (A) and KC (B) by ELISA. Data represent the mean of 3 independent experiments; $p<0.05$.

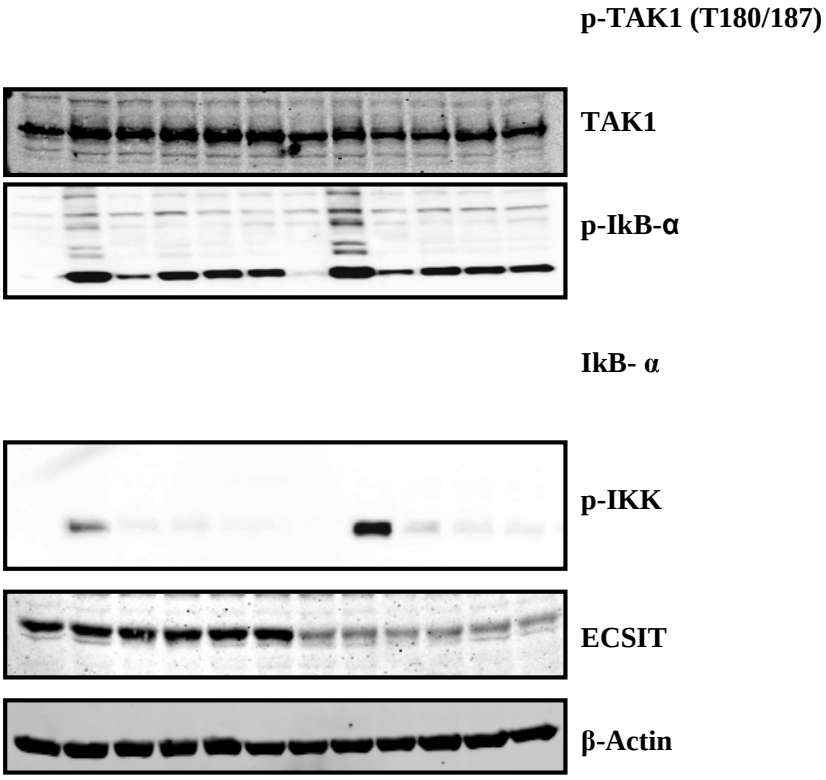

Figure 5.5 hECSIT knockdown enhances TNF induced NFκB activation in HeLa cells

HeLa cells were transfected with hECSIT specific siRNA (30nm) or Control siRNA (30nm) for 48 hrs. Cells were then treated with TNF-α (50ng/ml) for the indicated times. Cells lysates were prepared and separated by SDS-PAGE followed by Immunoblotting for phosphorylated and total levels of TAK1, IκB-α and IKK-α. Lysates were also probed for levels of ECSIT and β-Actin to check knockdown and equal loading.

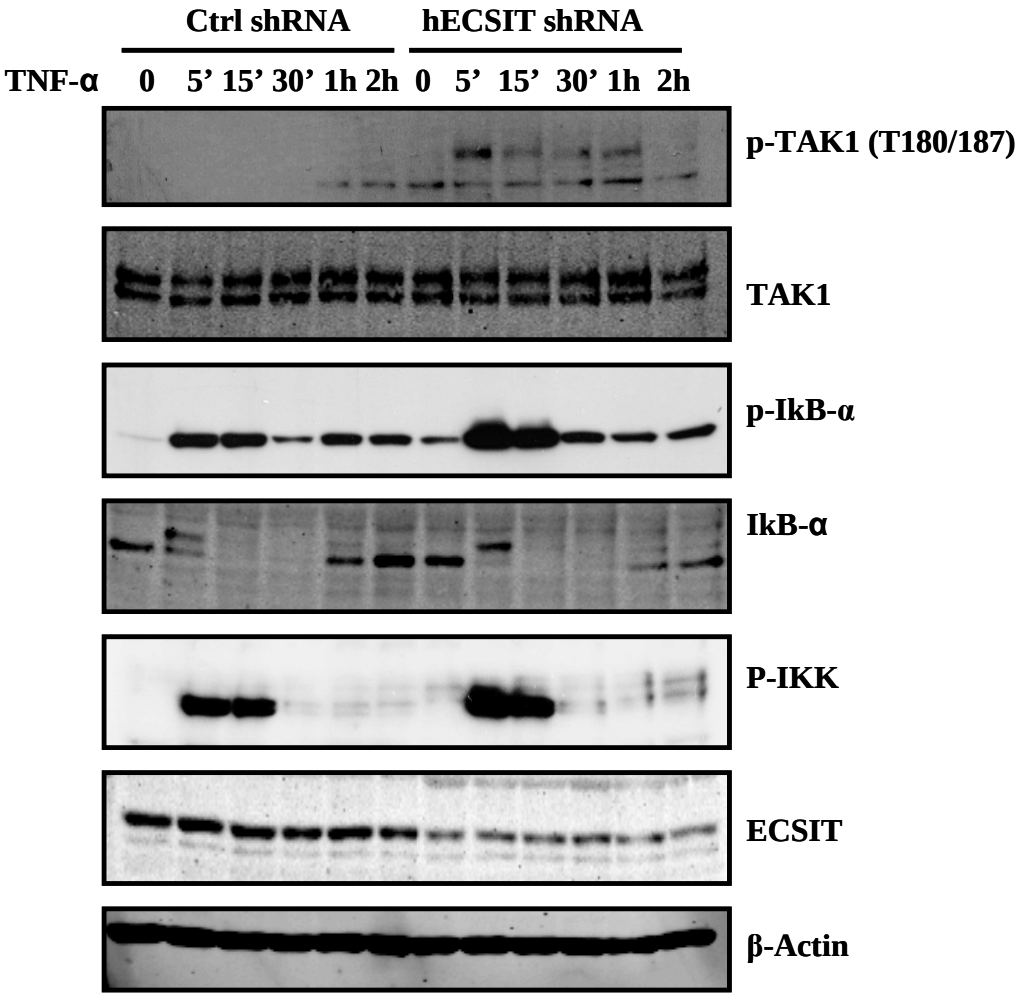

Figure 5.6 Knockdown of hECSIT enhances TNF induced NFκB activation in U373 cells

U373 Cells were infected with Lentivirus containing constructs encoding control or hECSIT specific shRNA. Cells were grown in the presence of puromycin (8μg/ml) to select cells with stably integrated shRNA constructs. Selected cells were treated with TNF-α (50ng/ml) for the indicated times. Cell lysates were prepared separated by SDS-PAGE followed by Immunoblotting for phosphorylated and total levels of TAK1, IκB-α and IKK-α. Lysates were also probed for levels of ECSIT and β-Actin to check knockdown and equal loading.

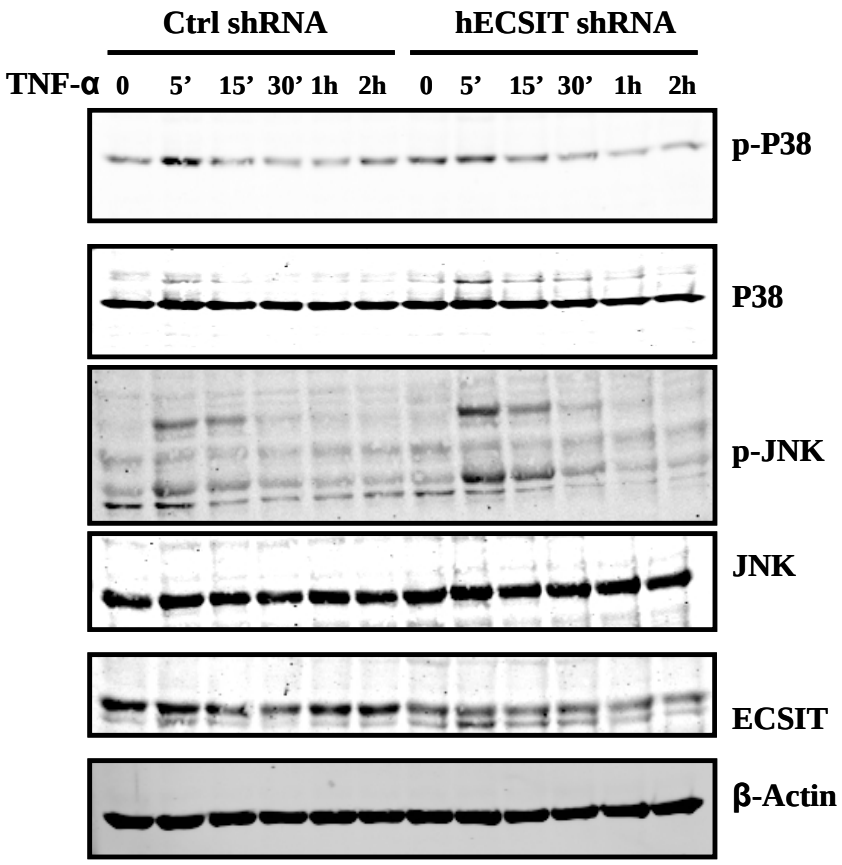

Figure 5.7 Knockdown of hECSIT enhances TNF induced JNK activation

U373 Cells were infected with Lentivirus containing constructs encoding control or hECSIT specific shRNA. Cells were grown in the presence of puromycin (8μg/ml) to select cells with stably integrated shRNA constructs. Selected cells were treated with TNF-α (50ng/ml) for the indicated times. Cell lysates were prepared separated by SDS-PAGE followed by Immunoblotting for phosphorylated and total levels of P38 and JNK. Lysates were also probed for levels of ECSIT and β-Actin to check knockdown and equal loading.

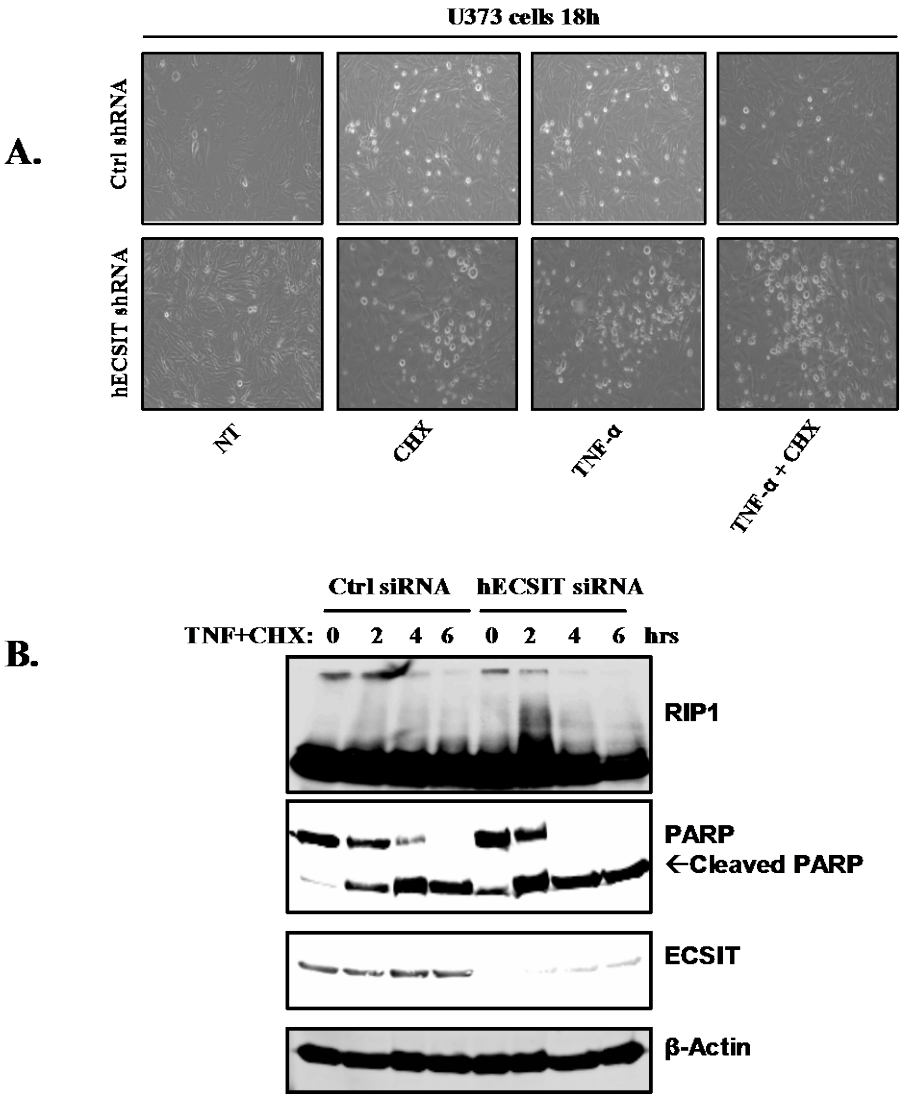

Figure 5.8 Knockdown of hECSIT sensitizes cells to TNF-α induced apoptosis

(A) U373 Cells were infected with Lentivirus containing constructs encoding control or hECSIT specific shRNA. Cells were grown in the presence of puromycin (8µg/ml) to select cells with stably integrated shRNA constructs. Selected cells were treated with or without TNF-α (50ng/ml) and CHX (10µg/ml) for the indicated times. Cells were then photographed using a phase contrast microscope (20µm). (B) HeLa Cells were transfected with hECSIT specific siRNA (30nm) or Control siRNA (30nm). 48 hrs after transfection cells were then treated with TNF-α (50ng/ml) and CHX (10µG/ml) for

the indicated times. Cell lysates were generated and separated by SDS-PAGE and were probed by Immunoblotting for expression levels of RIP1, cleaved PARP, ECSIT and β-Actin.

5.2.2 hECSIT interacts with RIP1

Given the ability of hECSIT to regulate TNF-α induced NFκB activation, we next characterized the ability of hECSIT to interact with the individual protein components of the TNF-α pathway. RIP1 acts as a central signalling adaptor in the TNF pathway and regulates both the NFκB and apoptotic arms of the pathway. RIP1 function is heavily regulated by its ubiquitination status. Given the earlier data indicating that hECSIT contains both E3 ligase and DUB activity, RIP1 was examined as a potential target for hECSIT. Co-immunoprecipitation studies were carried out to investigate the possible interaction between hECSIT and RIP1. U373 cells were treated with TNF-α and immunoprecipitated with anti-ECSIT antibody. The subsequent precipitate was then analyzed for the presence of co-precipitated RIP1 by western blotting. TNF-α promoted the interaction of RIP1 with hECSIT in a time-dependent manner, as demonstrated by the co-immunoprecipitation of the two proteins (Figure 5.9A). Treatment of HEK293 cells also resulted in the co-immunoprecipitation of hECSIT with RIP1 in a time dependent manner (Figure 5.9B). The interaction of RIP1 with hECSIT and mECSIT was also investigated after transient transfection in HEK293T cells. Myc-tagged hECSIT or mECSIT was co-expressed with FLAG-tagged RIP1, immunoprecipitated with anti-myc antibody and probed for the presence of co-precipitated FLAG-tagged RIP1. As shown in Figure 5.9C both hECSIT and mECSIT interacted with RIP1. These data suggests the regulatory role of hECSIT on TNF-α induced NFκB activation is achieved by targeting RIP1.

Figure 5.9 hECSIT Interacts with RIP1

HeLa cells (A), HEK293 cells (B) were treated with TNF-α (50ng/ml) for the indicated times. Cell lysates were generated and a sample for whole cell lysates analysis was retained. The remaining lysates was immunoprecipitated using an anti-ECSIT antibody. Immunoprecipitates were subsequently assayed for co-precipitated RIP1 and ECSIT. The expression levels of ECSIT and RIP1 in whole cell lysates (Input) were also assessed by western blotting. (C) HEK293 cells were co-transfected with Empty vector (EV) pcDNA3.1 (1µg), myc-tagged hECSIT (1µg) or myc-tagged mECSIT (1µg) with or without FLAG-tagged RIP1 (1µg). EV was used to normalize total amount of DNA transfected. 24 hrs post-transfection cell lysates were generated and immunoprecipitated with anti-myc antibody. Immunoprecipitates were then subject to SDS-PAGE and subsequently to western blotting using anti-FLAG antibody. Whole cell lysates were also analyzed by western blotting using anti-FLAG and anti-Myc antibodies to confirm expression of RIP1 and ECSIT constructs, respectively. Results are representative of 3 independent experiments.

4.2.3 hECSIT negatively regulates the ubiquitination of RIP1

As hECSIT interacts with RIP1 in response to TNF-α we next probed the functional consequence of this interaction by measuring the ubiquitination of RIP1. We were especially interested in the ubiquitination of RIP1 given that it is prone to an array of ubiquitin modifications and is tightly regulated by a number of deubiquitinating enzymes. Given that hECSIT possesses both E3 ligase and DUB activity the effect of hECSIT on RIP1 ubiquitination was examined. Analysis of the effect of hECSIT and mECSIT on RIP1 ubiquitination was initially investigated in HEK293T cells by transient transfection. Myc-tagged hECSIT or mECSIT were co-transfected with FLAG-tagged RIP1 and HA-ubiquitin. Immunoprecipitated RIP1 was probed for ubiquitination using an anti-HA antibody. Expression of hECSIT resulted in inhibition of RIP1 ubiquitination whereas expression of mECSIT resulted in enhanced RIP1 ubiquitination (Figure 5.10). This suggested hECSIT was negatively regulating the pathway at the level of ubiquitination. To investigate this effect at an endogenous level RIP1 ubiquitination was measured in cells where hECSIT expression was suppressed. Knockdown of hECSIT with hECSIT-specific siRNA resulted in increased ubiquitination of RIP1 in response to TNF-α in HEK293 cells (Figure 5.11). This was also observed in HeLa cells (Figure 5.12). To further validate the above conclusion that hECSIT knockdown enhanced TNF-induced RIP1 ubiquitination we used U373 cells stably expressing hECSIT specific shRNA to demonstrate the effect was independent of cell line or knockdown method. Knockdown of hECSIT in U373 cells also showed an increase in RIP1 ubiquitination in response to TNF-α (Figure 5.13). Since K63 linked polyubiquitination of RIP1 is usually associated with triggering of downstream activation of NFκB we especially focused on the potential of hECSIT to regulate K63-linked ubiquitination of RIP1. Knockdown of hECSIT in HeLa cells resulted in enhanced TNF-induced K63-linked ubiquitination of RIP1 and this is consistent with the earlier described augmentation of TNF-induced activation of NFκB under these conditions (Figure 5.14)

Given the differential effects of murine and human ECSIT in the TNF pathway we next characterised the ubiquitination of RIP1 in MEFs from WT mice and in ECSIT humanized mice. TNF induced ubiquitination of RIP1 in wild type MEFs but the efficacy of TNF was reduced in corresponding ECSIT humanised MEFs. Stimulation of ECSIT humanised MEF cells resulted in a decrease in RIP1

ubiquitination when compared to WT MEFs (Figure 5.15). In conjunction with the earlier cell line approaches these findings provides strong support for hECSIT acting as a novel regulator of RIP1 ubiquitination. As mentioned RIP1 is ubiquitinated by a number of E3 ligases such as TRAF2 and cIAP1. We assessed if hECSIT was capable of targeting any of these E3 ligases. HEK293T cells were transiently transfected with myc-tagged hECSIT or mECSIT or FLAG-tagged TRAF2 or cIAP1. The latter 2 proteins were immunoprecipitated using an anti-FLAG antibody and immuoprecipitates were probed for co-precipitated ECSIT by western blot. However both hECSIT and mECSIT did not interact with TRAF2 (Figure 5.16A) or cIAP1 (Figure 5.16B) and thus hECSIT might act directly on RIP1 to effect its de-ubiquitination.

These findings, employing independent approaches to suppress hECSIT expression in different cell lines, over-expression studies and primary humanised cells provide strong evidence that hECSIT plays a key role in regulating RIP1 ubiquitination in response to TNF-α.

hE-myc	-	+	-	-	+	-
mE-myc	-	-	+	-	-	+
RIP1-FLAG	-	-	-	+	+	+
Ubq-HA	+	+	+	+	+	+

Figure 5.10 Differential effects of hECSIT and mECSIT on RIP1 ubiquitination

HEK293 cells were co-transfected with Empty vector (1µg), HA-Ubq (1µg), myc-tagged hECSIT (1µg) or myc-tagged mECSIT (1µg) with or without FLAG-tagged RIP1 (1µg). EV was used to normalize total amount of DNA transfected. 24 hrs post-transfection cell lysates were generated and immunoprecipitated using an anti-FLAG antibody. Immunoprecipitates were then subject to SDS-PAGE and subsequently to western blotting using anti-HA antibody. Whole cell lysates were also analyzed by western blotting using anti-FLAG and anti-Myc antibodies to confirm expression of RIP1 and ECSIT constructs, respectively. Results are representative of 3 independent experiments.

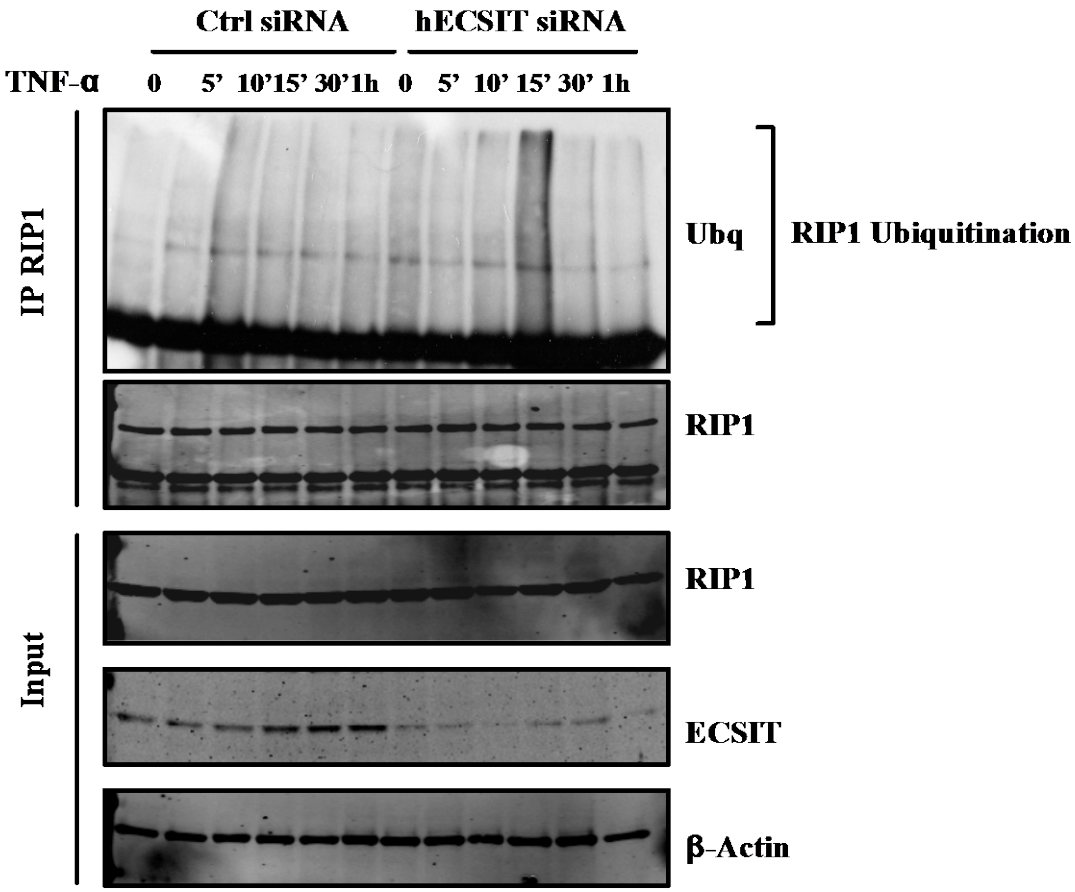

Figure 5.11 Knockdown of hECSIT enhances TNF induced RIP1 ubiquitination in HEK293 cells

HEK293 Cells were transfected with hECSIT specific siRNA (30nm) or Control siRNA (30nm). 48 hrs after transfection cells were then treated with TNF-α (50ng/ml) for the indicated times. Cell lysates were generated and immunoprecipitated using anti-RIP1 antibody. The immunoprecipitate was then assayed for RIP1 ubiquitination and immunoprecipitated RIP1 by Immunoblotting for ubiquitin and RIP1 respectively. Expression levels of RIP1, ECSIT and β-Actin were also assessed in the input by western blotting.

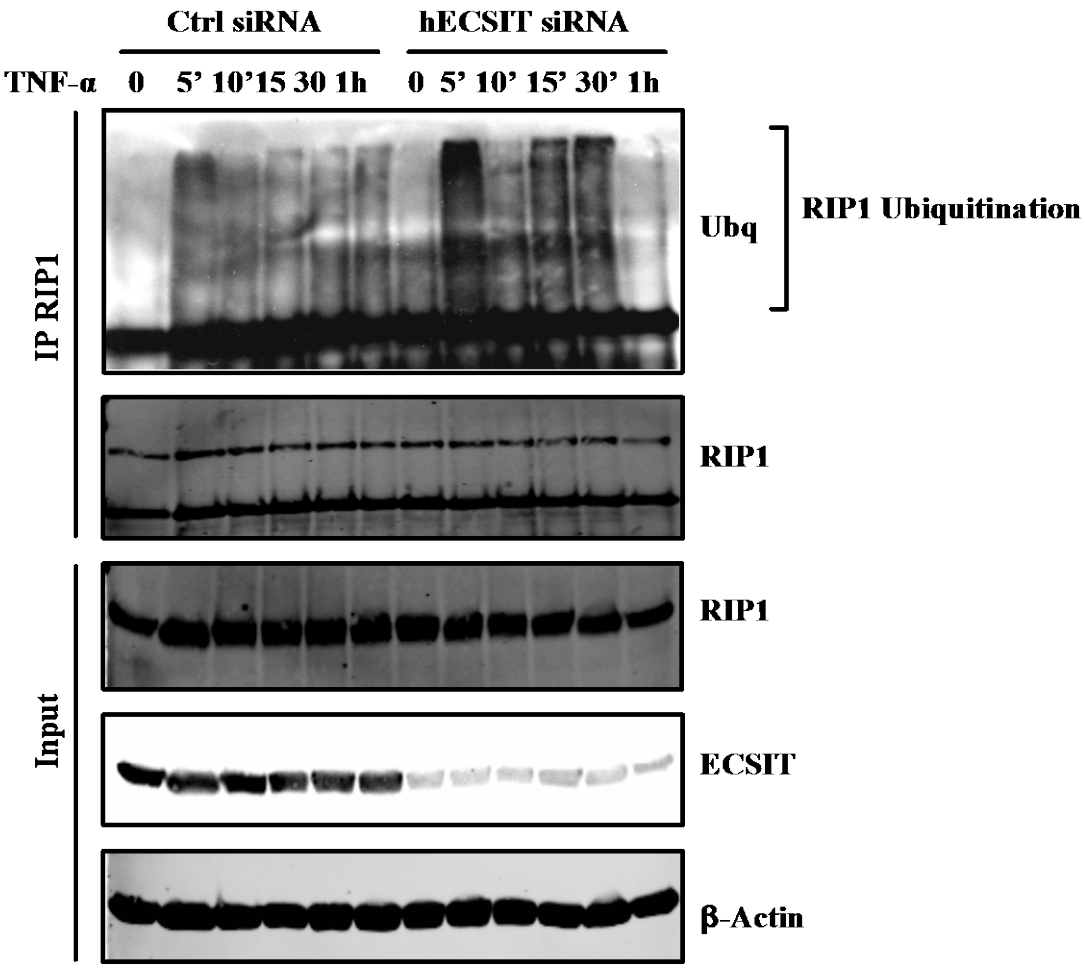

Figure 5.12 Knockdown of hECSIT enhances TNF induced RIP1 ubiquitination in HeLa cells

HeLa Cells were transfected with hECSIT specific siRNA (30nm) or Control siRNA (30nm). 48 hrs after transfection cells were then treated with TNF-α (50ng/ml) for the indicated times. Cell lysates were generated and immunoprecipitated using anti-RIP1 antibody. The immunoprecipitate was then assayed for RIP1 ubiquitination and immunoprecipitated RIP1 by Immunoblotting for ubiquitin and RIP1 respectively. Expression levels of RIP1, ECSIT and β-Actin were also assessed in the input by western blotting.

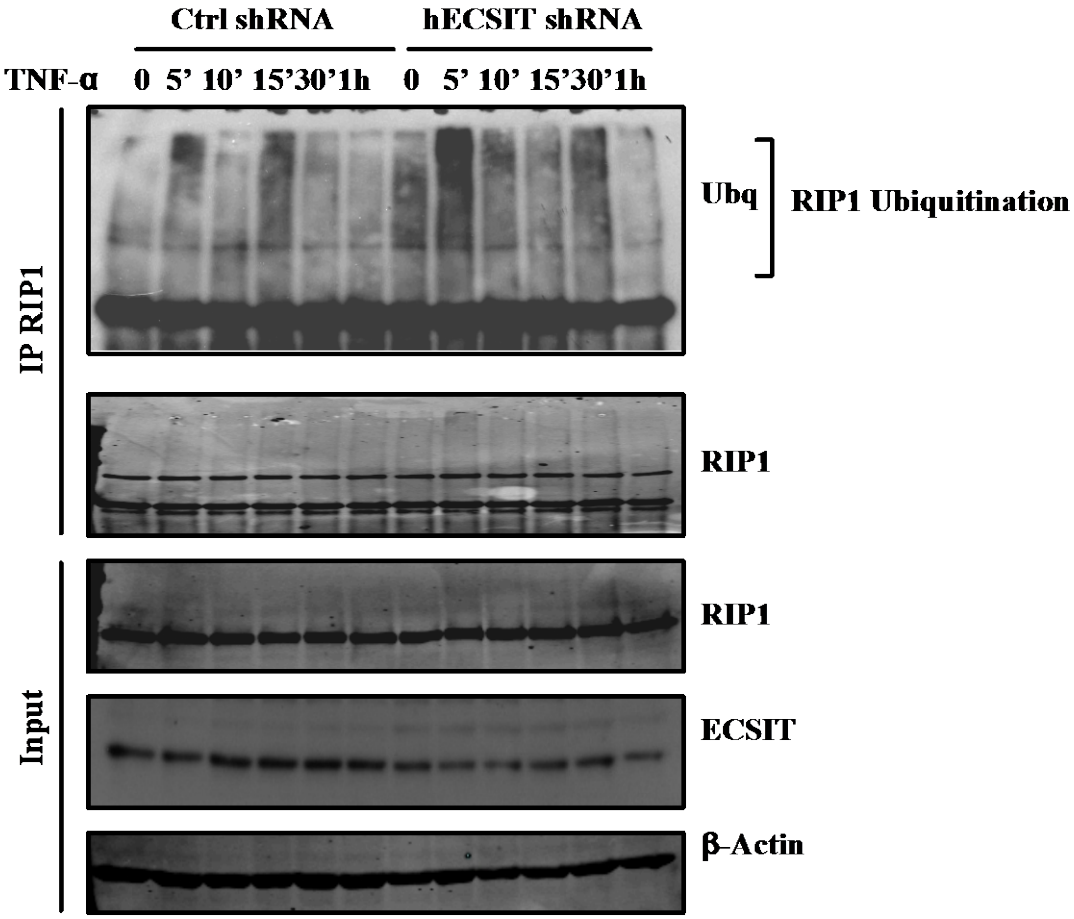

Figure 5.13 Knockdown of hECSIT enhances TNF induced RIP1 ubiquitination in U373 cells

U373 Cells were infected with Lentivirus containing constructs encoding control or hECSIT specific shRNA. Cells were grown in the presence of puromycin (8µg/ml) to select cells with stably integrated shRNA constructs. Selected cells were treated with TNF-α (50ng/ml) for the indicated times. Cell lysates were generated and immunoprecipitated using anti-RIP1 antibody. The immunoprecipitate was then assayed for RIP1 ubiquitination and immunoprecipitated RIP1 by Immunoblotting for ubiquitin and RIP1 respectively. Expression levels of RIP1, ECSIT and β-Actin were also assessed in the input by western blotting..

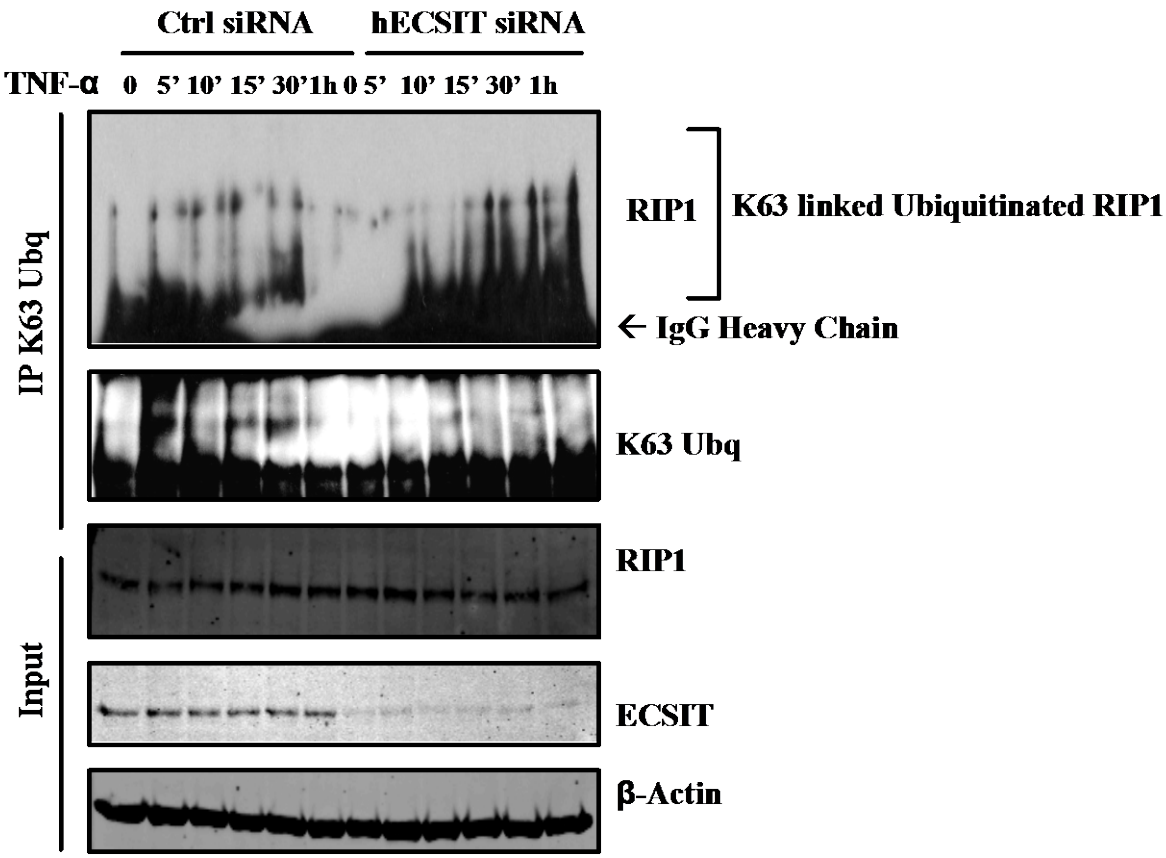

Figure 5.14 Knockdown of hECSIT enhances TNF induced K63-linked ubiquitination of RIP1

HeLa Cells were transfected with hECSIT specific siRNA (30nm) or Control siRNA (30nm). 48 hrs after transfection cells were then treated with TNF-α (50ng/ml) for the indicated times. Cell lysates were generated and immunoprecipitated using anti-K63 antibody. The immunoprecipitate was then assayed for K63- linked RIP1 ubiquitination and immunoprecipitated K63 ubiquitin chains by Immunoblotting for RIP and K63 respectively. Expression levels of RIP1, ECSIT and β-Actin were also assessed in the input by western blotting.

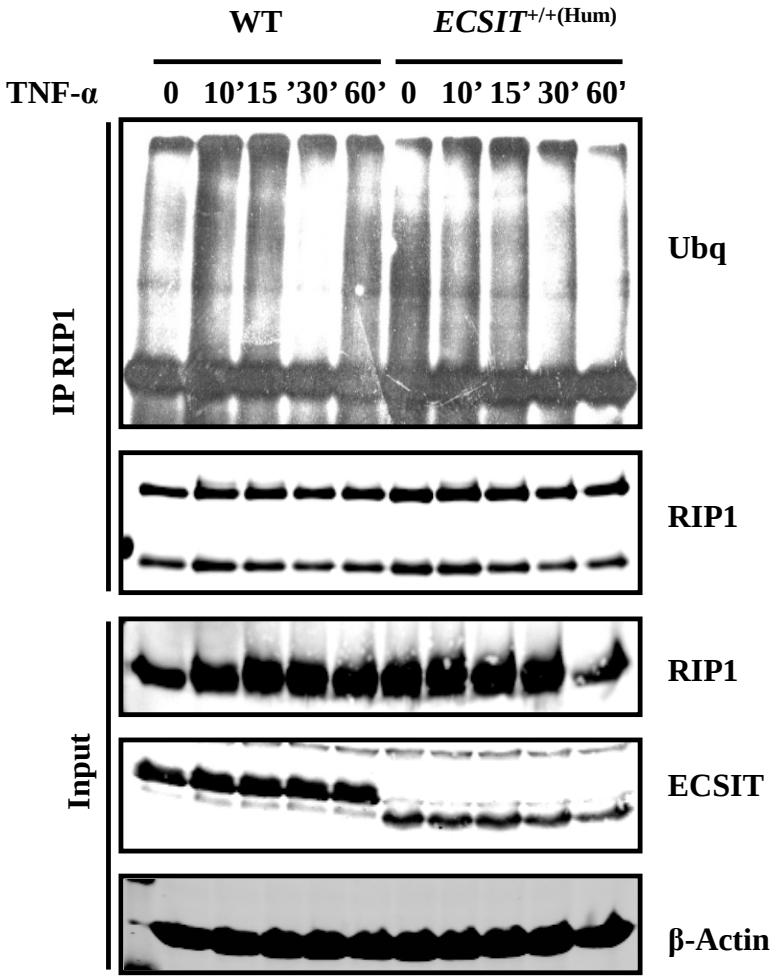

Figure 5.15 Replacement of *Ecsit* with *ECSIT* inhibits TNF induced RIP1 ubiquitination

MEFs were isolated from WT and *ECSIT* $^{+/+\ (Hum)}$ embryos and were treated with murine TNF-α (25ng/ml) for the indicated times. Cell lysates were generated and immunoprecipitated using anti-RIP1 antibody. The immunoprecipitate was then assayed for RIP1 ubiquitination and immunoprecipitated RIP1 by Immunoblotting for Ubq and RIP1 respectively. Expression levels of RIP1, ECSIT and β-Actin were also assessed in the input by western blotting.

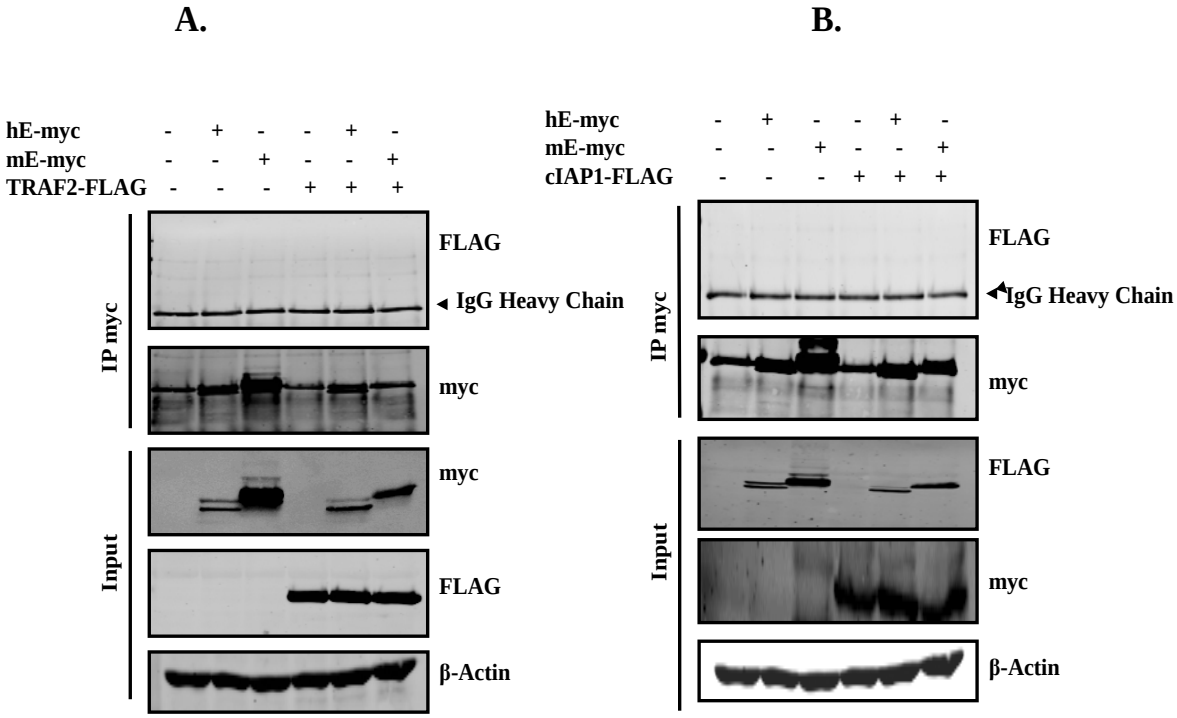

Figure 5.16 hECSIT and mECSIT do not interact with TRAF2 and cIAP1

HEK293 cells were co-transfected with Empty vector (EV) pcDNA3.1 (1µg), myc-tagged hECSIT (1µg) or myc-tagged mECSIT (1µg) with or without FLAG-tagged TRAF2 (1µg) (A) or cIAP1 (B). EV was used to normalize total amount of DNA transfected. 24 hrs post-transfection cell lysates were generated and immunoprecipitated with anti-myc antibody. Immunoprecipitates were then subject to SDS-PAGE and subsequently to western blotting using anti-FLAG antibody. Whole cell lysates were also analyzed by western blotting using anti-FLAG and anti-Myc antibodies to confirm expression of TRAF2 and ECSIT constructs, respectively. Results are representative of 3 independent experiments.

4.2.4 hECSIT is processed in response to TNF-α

We next addressed the potential mechanism by which hECSIT was mediating its regulatory effect on RIP1 ubiquitination. We have earlier shown data that suggest that in context of TLR4 and IL-1 signalling, hECSIT is processed in a TAK1 kinase-dependent manner to produce a C terminal fragment(s) with DUB activity. We assessed if hECSIT undergoes similar TAK1-dependent processing in response to TNF-α. Thus hECSIT protein expression was assayed by Western blotting in lysates from cells that had been treated with TNF-α in the absence or presence of the TAK1 inhibitor 5Z-7-oxozeanol and the caspase inhibitor Z-VAD-FMK. Treatment of THP1 cells with TNF-α resulted in the appearance of fast migrating forms of hECSIT consistent with hECSIT processing (Figure 5.17A). However upon pre-treatment of these cells with 5Z-7-oxozeanol or Z-VAD-FMK, the levels of processed hECSIT in response to TNF were greatly decreased (Figure 5.17A). Since under conditions of protein synthesis blockade, TNF-α can induce apoptosis we were also keen to characterise hECSIT processing under conditions of TNF induced apoptosis. Co-treatment of HeLa cells with TNF-α and CHX resulted in increased processing of hECSIT when compared to TNF-α treatment alone. However pre-treatment with 5Z-7-oxozeanol also resulted in decreased levels of processed hECSIT during apoptosis. The latter was confirmed by increased levels of cleaved PARP (Figure 5.17B). As shown previously hECSIT interacts with TAK1 in response to LPS and IL-1.We thus probed the association of hECSIT with TAK1 in response to TNF-α. Using co-immunoprecipitation hECSIT was found to associate with TAK1 in response to TNF-α in both U373 (Figure 5.18A) and HeLa cells (Figure 5.18B). Interestingly the co-precipitated forms of TAK1 manifested as multiple bands and a laddering pattern potentially indicative of varying levels of ubiquitination and the possibility that ubiquitinated forms of TAK1 interact with hECSIT. In order to determine the functional consequence of hECSIT processing in response to TNF-α a truncated expression construct encoding processed hECSIT was used as a model to analyse the inhibitory function of processed hECSIT in TNF signalling. NFκB reporter assays reveled that in response to TNF-α the C-terminus of hECSIT was more inhibitory than full length hECSIT (Figure 5.19A). This was further confirmed by a semi-rescue approach whereby HEK293T cells knocked down with hECSIT specific siRNA followed by transfection of the C-terminus or N-terminus revealed that only the C-

terminus, representing the processed form could rescue the inhibitory effect (Figure 5.19B)

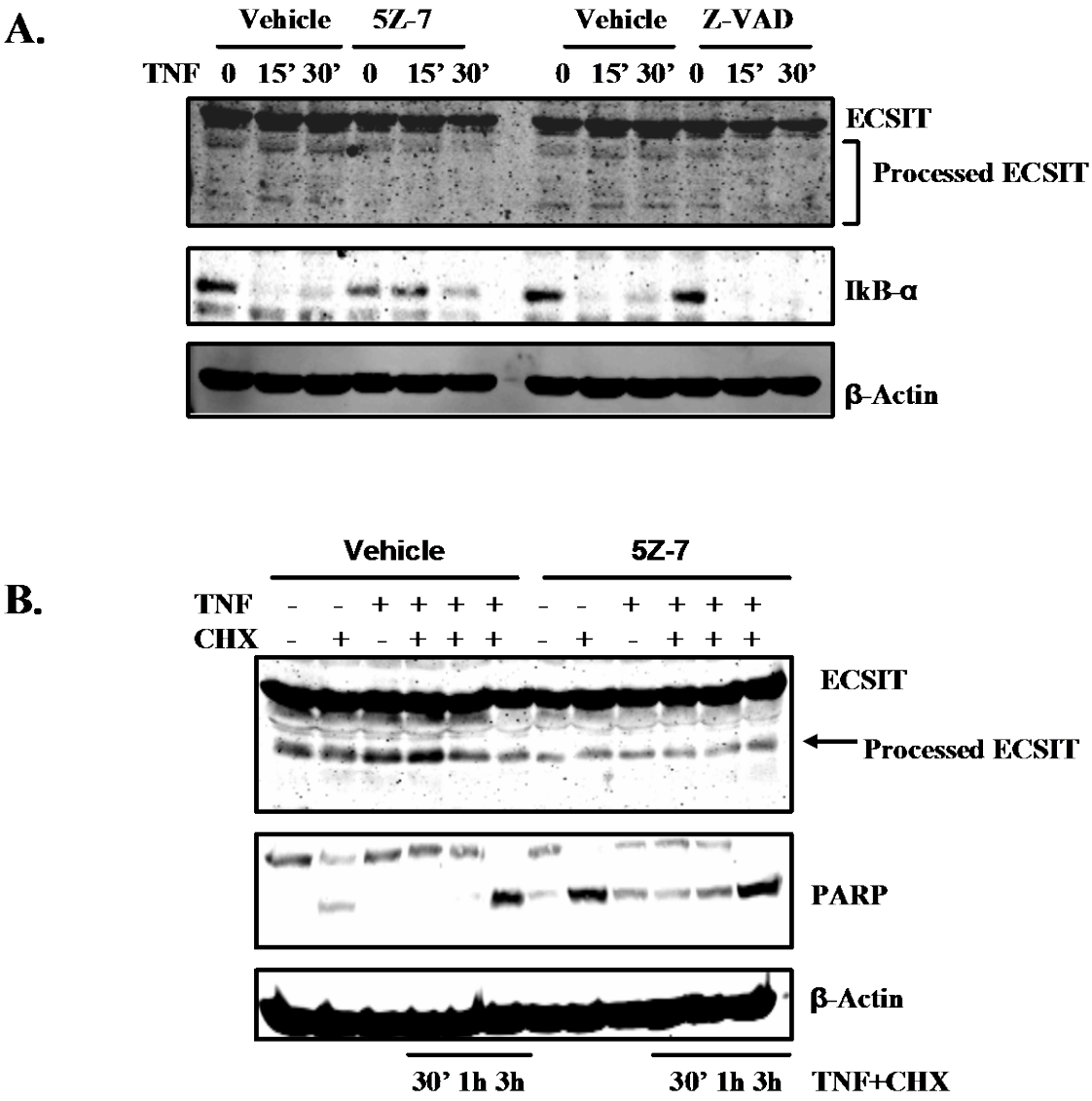

Figure 5.17 TNF-α promotes the processing of ECSIT in a TAK1 and Caspase dependent manner

(A) THP1 cells were pre-treated for 2 hrs with vehicle DMSO and 5z-7-oxozeanol (20Mm) or Z-VAD-FMK (10Mm). Cells were then treated with TNF-α (50ng/ml) for the indicated times. Cell lysates were generated and subjected to SDS-PAGE and probed by Immunoblotting for expression levels of ECSIT, IκB-α and β-Actin. Processed ECSIT is indicated by arrows. (B) HeLa cells were pre-treated for 2 hrs with vehicle DMSO or 5z-7-oxozeanol (20mM). Cells were then treated with TNF-α (50ng/ml) with or without cyclohexamide (10ug/ml) for the indicated times. Cell lysates were generated and subjected to SDS-PAGE and probed by Immunoblotting for expression levels of ECSIT, cleaved PARP and β-Actin. Processed ECSIT is indicated by arrows.

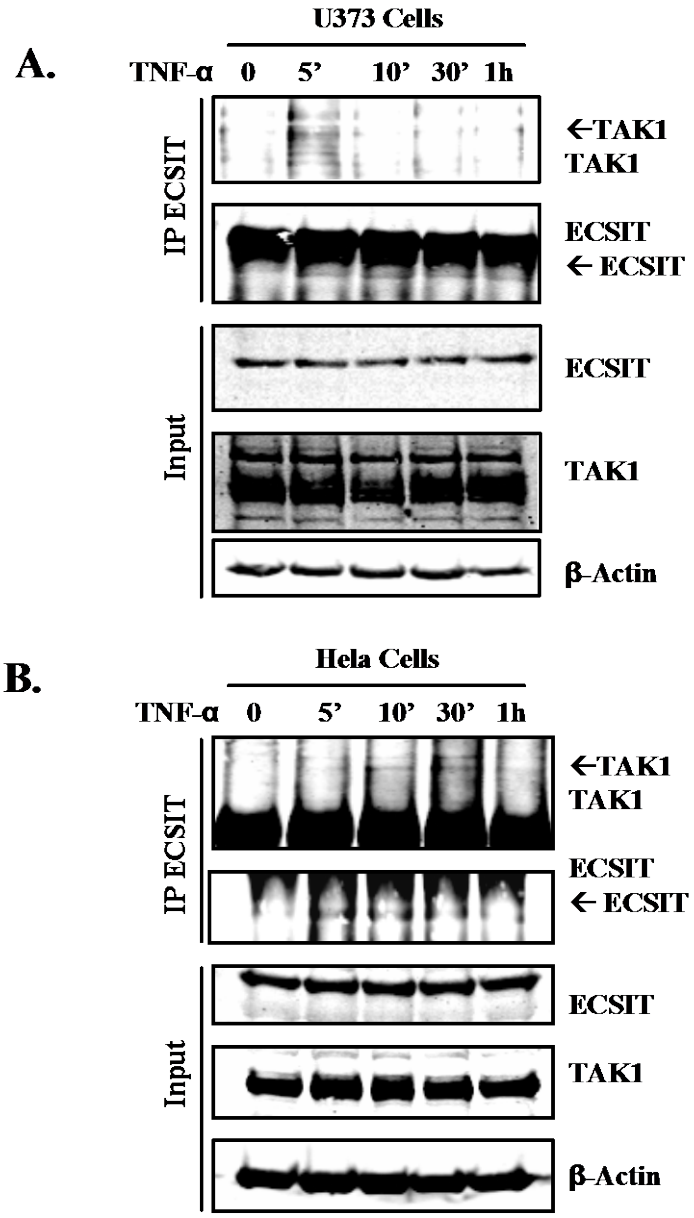

Figure 5.18 hECSIT interacts with TAK1 in response to TNF-a

U373 cells (A) and HeLa cells (B) were treated with TNF-α (50ng/ml) for the indicated times. Cell lysates were generated and a sample for whole cell lysates analysis was retained. The remaining lysates was immunoprecipitated using an anti-ECSIT antibody. Immunoprecipitates were subsequently assayed for co-precipitated RIP1 and ECSIT. The expression levels of ECSIT and RIP1 in whole cell lysates were also assessed by western blotting.

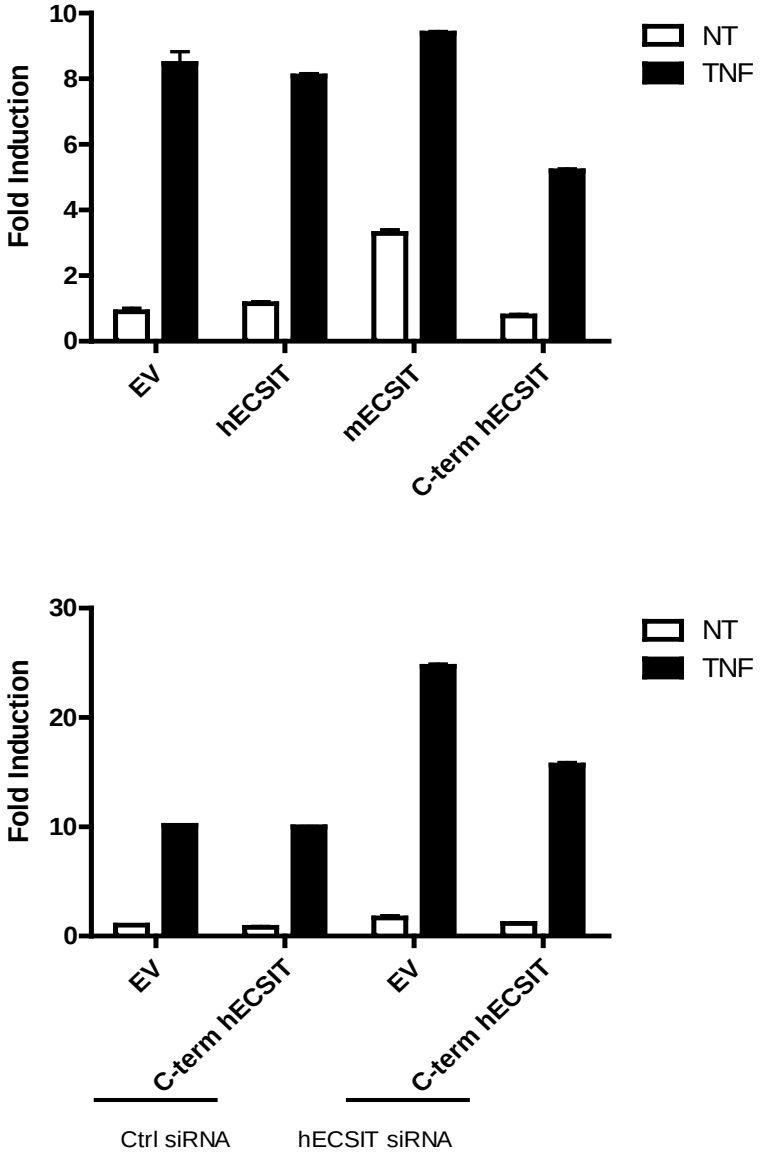

Figure 5.19 The C-terminus of hECSIT inhibits TNF induced NFκB activation

(A) HEK293 cells were co-transfected with NFκB firefly luciferase reporter construct (80ng), TK renilla (20ng) and myc-tagged hECSIT or mECSIT or the C-terminal or N-terminal of hECSIT (100ng). Empty Vector (EV) pcDNA3.1 was used to normalise total amount of DNA whilst TK renilla was used to normalise for transfection efficiency. 24hr post-transfection the cells were treated with TNF-α (50ng). Cell lysates were generated the following day and assayed for firefly luciferase activity. (B) HEK293 cells were co-transfected with NFκB firefly luciferase reporter construct (80ng), TK renilla (20ng) and hECSIT specific siRNA or Lamin control siRNA (10nM). 24 hrs post transfection the cells were transfected with EV, C-terminal or N-terminal hECSIT.24 hours later cells were treated with TNF-α for 6 hrs. Cell lysates were then generated and assayed for firefly luciferase and renilla. luciferase activity. Results represent mean +/- SD of triplicate determinations and is a representative of 3 independent experiments.

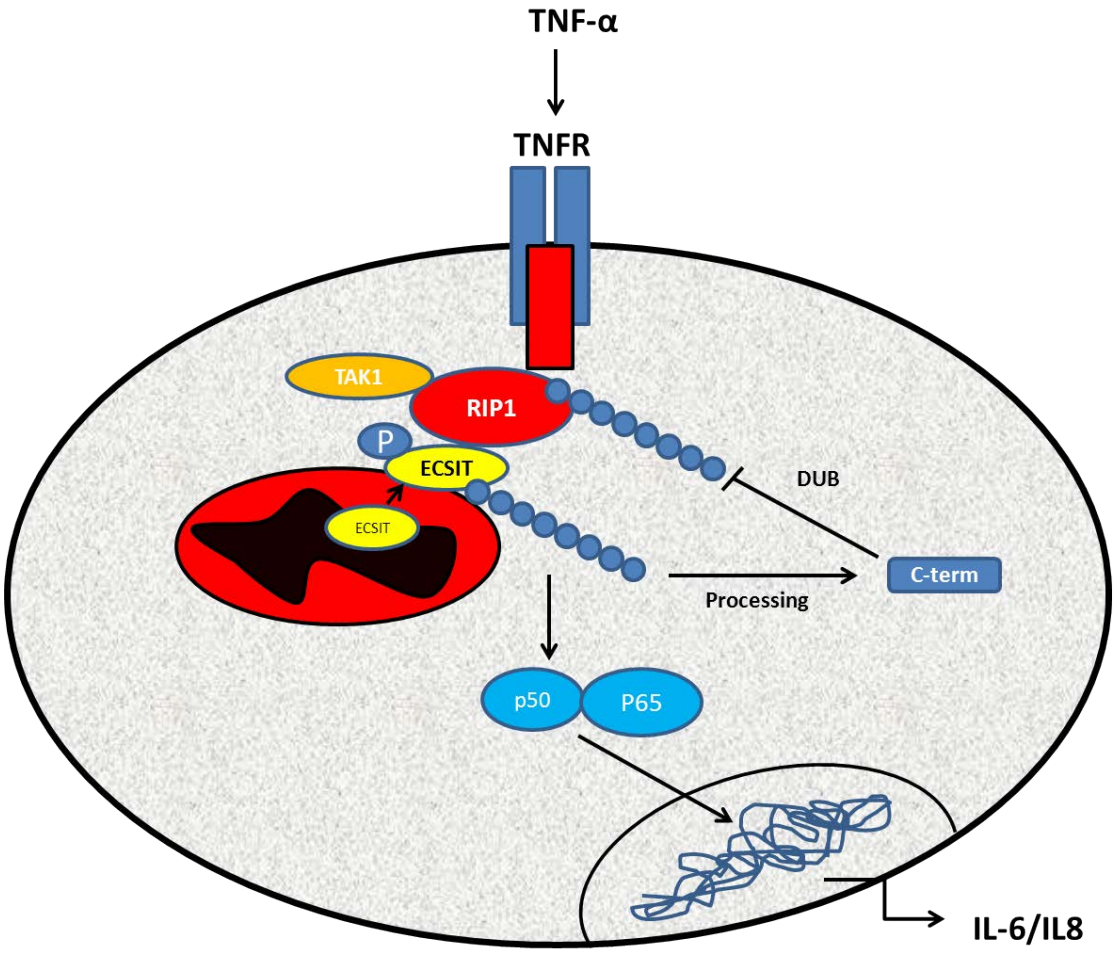

Figure 5.20 Schematic representation of hECSIT's regulatory effect in TNF signalling

Activation of the TNF pathway results in the ubiquitination of RIP1 for the downstream activation of NFκB. Processing of hECSIT results in an active deubiquitinating enzyme which targets RIP1 for deubiquitination to inhibit NFκB.

5.3 Discussion

This study highlights a critical role for hECSIT in the regulation of TNF-α induced NFκB activation and apoptosis. The initial suggestion of such a role arose from our cell line studies in which hECSIT knockdown augmented NFκB activation and sensitised cells to apoptosis in response to TNF-α. The physiological relevance of hECSIT in the TNF-α pathway was confirmed by the generation of humanised mice, where mECSIT was replaced with hECSIT, with cells from these mice displaying reduced activation of NFκB in response to TNF-α relative to wild type cells. Furthermore the differential effects of murine and human ECSIT function were also seen in TNF signalling.

hECSIT was initially assessed for its ability to regulate NFκB in response to TNF-α. mECSIT and hECSIT had opposing effects on NFκB where the latter strongly inhibited the TNF-α pathway. The murine orthologue mECSIT has been previously shown not to function in TNF signalling (Kopp et al, 1999) however our data would suggest a positive role for mECSIT in the pathway, a role consistent with functions in other pathways. Knockdown of hECSIT resulted in an enhanced NFκB response in cell lines as demonstrated by higher levels of cytokine production and phosphorylation of p-IκB-α and pIKK-β. This effect on NFκB was also observed in our animal model when mECSIT was replaced by hECSIT. Given that NFκB acts to counter regulate the apoptotic pathway by the induction of anti-apoptotic proteins it was of interest to examine if hECSIT could exert its regulatory effects on NFκB by affecting apoptosis. However the increased levels of apoptosis that are observed in hECSIT-knockdown cells cannot be attributed to impaired NFκB function and the augmented NFκB response in these cells does not provide any protective effect against TNF-α induced apoptosis. A similar effect has been shown in A20 deficient cells which have uncontrolled NFκB response whilst also being highly sensitive to an apoptotic stimulus (Shembade et al, 2009). Polymorphisms in A20 have also been linked to many inflammatory autoimmune diseases in humans (Coornaert et al, 2008) and expression of A20 is also upregulated in many forms of cancer and has been shown to have an important survival function in breast cancer (Vendrell et al, 2007). A20 has also been identified as a susceptibility locus for rheumatoid arthritis, SLE, type 1 diabetes, inflammatory bowel disease, celiac disease, psoriasis and coronary heart disease (Harhaj and Dixit, 2012). Given the similarities in function between A20

and hECSIT it would be interesting to investigate the expression levels of hECSIT in tumour cells and tissue from patients from the aforementioned conditions which would perhaps help explain the discrepancy between augmented NFκB activation and increased cell death when hECSIT is absent. However further analysis of the apoptotic response will need to be assessed and quantified in our knockdown systems and humanised model before a definitive role for hECSIT can be fully established in the apoptotic arm of the TNF-α pathway.

In order to further examine the negative role of hECSIT in the TNF pathway we looked for hECSIT interaction partners in response to TNF-α. We show that hECSIT can interact with RIP1 in a TNF dependent manner resulting in the decreased ubiquitination of RIP1 as evidenced by the complementary approaches of hECSIT knockdown and overexpression. Furthermore reduced levels of RIP1 ubiquitination in response to TNF-α were also observed in cells from our humanised mice. The ubiquitination of RIP1 by E3 ligases, such as TRAF2 and cIAP1, has traditionally been associated with promoting the activation of NFκB and blocking DISC formation by inhibiting the binding of RIP1 to FADD and Caspase 8 (Bertrand et al, 2008). We thus considered the possibility that the deubiquitination of RIP1 by hECSIT may allow RIP1 to interact with caspase 8 and FADD to promote apoptosis. However knockdown of hECSIT in HeLa and U373 cells resulted in increased levels of apoptosis in response to TNF-α and CHX indicating a role for hECSIT in suppressing apoptosis. As well as deubiquitination A20 can also mediate the K48-linked ubiquitination of RIP1 following TNF activation. As hECSIT has both E3 and DUB activity it is also possible hECSIT regulates RIP1 via K48 ubiquitination or another obscure linkage. Furthermore it is also possible that like A20, hECSIT has the ability to interchange K63 linked ubiquitin chains for K48 linked ubiquitin chains. A more comprehensive screen of E2 enzymes in vitro may give a better understanding for the types of ubiquitin chains hECSIT can produce and regulate. However as expression or knockdown of hECSIT had no effects on the expression levels of RIP1 it is more likely deubiquitination. RIP1 is subject to multiple forms of ubiquitination and regulators such as A20 and CYLD control these modifications via ubiquitination and deubiquitination. Like these regulators hECSIT exerts its regulatory effect via the deubiquitination of RIP1 however a direct catalytic residue in the sequence of hECSIT will need to be determined in order to confirm this DUB effect and eliminate the possibility of another mechanism.

In the previous chapter hECSIT was shown to mediate its regulatory effects in TLR signalling in a manner involving TRAF6, TAK1 and caspase 8 resulting in the possible phosphorylation, ubiquitination and processing of hECSIT into a functional inhibitory protein. The formation of such a complex in the TNF pathway is not unprecedented and many examples of similar regulatory complexes in this signalling pathway have been described. Such studies have highlighted a number of regulatory complexes in the TNF-α pathway involving the deubiquitinating enzymes A20 (Shembade et al, 2009) and CYLD (Ahmed et al, 2011). A20 functions in the context of a multi-protein complex consisting of A20, TAX1BP1 and the E3 ligases Itch and RNF11 (Harhaj and Dixit, 2012) whose interactions are formed through conserved PPxY and WW domains. CYLD also utilises the E3 ligase Itch through conserved PPxY domains to mediate the deubiquitination and subsequent K48-linked ubiquitination of TAK1 (Ahmed et al, 2011). The assembly of the A20 complex is dependent on a critical phosphorylation step whereby IKK-α directly phosphorylates TAX1BP1. In a similar manner hECSIT also forms a complex with TAK1 and caspase 8 and undergoes phosphorylation and processing during TNF-α signalling. While we propose hECSIT is phosphorylated in response to TNF-α we were unable to show this at an endogenous level owing possibly to cell responses and relative abundance. However as phosphorylation might be a pre-requisite for hECSIT processing, lower levels of TNF-α induced processing are seen in the presence of a TAK1 inhibitor. Identification of the hECSIT phosphorylation sites and generation of a phospho antibody will allow us to further study this modification in a ligand dependent manner. A similar result was observed with the caspase 8 inhibitor Z-VAD-FMK. Caspase 8 has been widely studied in the TNF-α pathway and has regulatory functions in apoptosis, necrosis but also functions in the RIG-I pathway (Rajput et al, 2011). Caspase 8 cleaves RIP1 during apoptosis and also inhibits necrosis by blocking the interaction of RIP1 and RIP3. The protease activity of caspase 8 also extends to the RIG-I pathway where processing of RIP1 by caspase 8 inhibits pathway activation and converts RIP1 into an inhibitor. As previously shown the catalytic mutant is unable to process hECSIT. Defining A direct caspase 8 processing site in the hECSIT sequence will give a greater understanding of the interaction between Caspase 8 and hECSIT during TNF signalling.

In summary the present findings highlight hECSIT as a new regulator of TNF-α signalling and strongly indicate it may play an important role in terminating both the

NFκB and apoptotic response to TNF-α. The present study also further confirms a key functional difference between two evolutionary conserved proteins, hECSIT and mECSIT and sheds more light on the complex system of TNF-α signalling by proposing a novel regulatory complex within the pathway. Whilst most studies have focused on the role of ECSIT in TLR mitochondrial signalling this present study extends the role of ECSIT beyond these pathways.

Chapter 6 Concluding Remarks

6.1 Concluding Remarks

The current study has identified hECSIT as a negative regulator of TLR and TNF-α signalling. Through the targeting of TRAF6, TRAF3 and RIP1, hECSIT utilises its DUB and E3 activity to attenuate innate immune signalling pathways. In addition to its dual ubiquitin editing function hECSIT under-goes a unique activation step through the co-operation of 3 multi-functional signalling intermediates, TAK1, TRAF6, and Caspase 8 which results in its processing. Whilst ECSIT's regulatory function centres on ubiquitination of its targets, its E3 ligase function and DUB function add additional complexity to elucidating its complete role. As discussed TLR4 signalling results in the processing of hECSIT into an active DUB enzyme which can negatively regulate TRAF6. Similarly TNF signalling also promotes processing of hECSIT in order to regulate RIP1 ubiquitination. Conversely during anti-viral responses hECSIT directly ubiquitinates TRAF3 resulting in inhibition of the type 1 IFN response. Thus far in this study we have been unable to identify a direct catalytic domain of hECSIT to explain these dual roles; however truncation experiments have demonstrated that the E3 ligase domain and DUB domain are both found in the C-terminal section of the protein. Given that hECSIT contains an N-terminal mitochondrial localisation sequence is possible that processing of hECSIT allows translocation of hECSIT to the cytoplasm where it can engage with its targets. Further work characterising its subcellular localisation and more specifically expression levels within different organs will allow us to understand the definitive in vivo role of hECSIT. Whilst no large scale studies have been carried out in patient disease cohorts, some screening studies have identified novel interactions for *ECSIT*.

The complexity of *ECSIT* function has been demonstrated by the lethal phenotype and the evolutionary functional difference we have shown between hECSIT and mECSIT. These complexities have slowed down the elucidation of the exact physiological role of *ECSIT*. The subcellular localisation of *ECSIT* has to date been the focus of the majority of *ECSIT* based studies. Many studies analysing the role of ECSIT have focussed on mitochondrial function. The mitochondrion is the energy centre of the cell and many diseases have impaired mitochondrial function. Parkinson's disease, diabetes, ataxia, multiple sclerosis and Alzheimer's disease all have impaired mitochondrial function. The lethal phenotype of the *ECSIT* mouse and the inability of *hECSIT* to completely compensate for the loss of *mECSIT* is perhaps

testament to the function of the mitochondria and the importance of *ECSIT* in development and the life cycle of the mitochondria. A recent study has flagged *ECSIT* as a potential dysregulated protein in the onset of Alzheimer's disease. Although an altered *ECSIT* gene expression has not been reported in AD patients to date, its expression is significantly up-regulated in Huntington's patients (Borovecki et al, 2005). This gives further support to the hypothesis that *ECSIT* might modulate the energetic requirements upon inflammatory response by regulating the rate of complex I synthesis (Vogel et al, 2007). Analysis of the expression levels of *ECSIT* in patients suffering from these diseases and potential protein interaction within these pathways would possibly highlight novel roles for *ECSIT* in the cell and lead to the targeting of *ECSIT* therapeutically.

TLR signalling is dependent on negative regulators to prevent excessive signalling and cytokine production. Exacerbated immune system activation has been attributed to cancer progression and auto-immune diseases such as Lupus. It will be of interest to identify possible SNPs and loss of function mutations in the *hECSIT* gene from patients suffering from these diseases. Furthermore utilisation of our humanised animal model to study the exact roles of *hECSIT* and *mECSIT* in these disease states will give us a greater understanding of *ECSIT's* physiological role.

The presented findings thus highlight a new novel regulator of innate immune signalling. Activation of these pathways promotes an auto-regulatory mechanism which results in the processing of hECSIT into an active protein. Through the targeting of TRAF6, RIP1 and TRAF3 hECSIT can attenuate signalling via its dual ubiquitin editing function. These effects promote hECSIT as a potential therapeutic target for diseases caused by dysregulated innate immune signalling pathways.

Chapter 7 References

References

Ahmad-Nejad P, H. H., Rutz M, Bauer S, Vabulas RM, Wagner H. (2002). "Bacterial CpG-DNA and lipopolysaccharides activate Toll-like receptors at distinct cellular compartments." Eur J Immunol **32**(7): 1958-1968.

Barton GM, K. J. (009). "A cell biological view of Toll-like receptor function: regulation through compartmentalization." Nat Rev Immunol **9**: 535-542.

Belgnaoui SM, P. S., Samuel S, Goulet ML, Sun Q, Kikkert M, Iwai K, Dikic I, Hiscott J, Lin R. (2012). "Linear Ubiquitination of NEMO Negatively Regulates the Interferon Antiviral Response through Disruption of the MAVS-TRAF3 Complex." Cell Host Microbe **12**(2): 211-222.

Berrington WR, M. M., Khadge S, Sapkota BR, Janer M, Hagge DA, Kaplan G, Hawn TR. (2010). "Common polymorphisms in the NOD2 gene region are associated with leprosy and its reactive states." J Infect Dis **201**: 1422-1435.

Bertrand MJ, M. S., Dickson KM, Ho WC, Boudreault A, Durkin J, Gillard JW, Jaquith JB, Morris SJ, Barker PA. (2008). "cIAP1 and cIAP2 facilitate cancer cell survival by functioning as E3 ligases that promote RIP1 ubiquitination." Mol Cell **30**: 689-700.

Bhoj VG, C. Z. (2009). "Ubiquitylation in innate and adaptive immunity." Nature **458**(7237): 430-437.

Bianchi K, M. P. (2009). "A tangled web of ubiquitin chains: breaking news in TNF-R1 signaling." Molecular cell **36**(5): 736-742.

Biron CA, N. K., Pien GC, Cousens LP, Salazar-Mather TP. (1999). "Natural killer cells in antiviral defense: function and regulation by innate cytokines." Annu Rev. Immunol **17**: 189-220.

Blasius AL, B. B. (2010). "Intracellular Toll like Receptors." Immunity **32**: 305-315.

Boneca IG, D. O., Cabanes D, Nahori MA, Sousa S, Lecuit M, Psylinakis E, Bouriotis V, Hugot JP, Giovannini M, Coyle A, Bertin J, Namane A, Rousselle JC, Cayet N, Prévost MC, Balloy V, Chignard M, Philpott DJ, Cossart P, Girardin SE. (2007). "A critical role for peptidoglycan N-deacetylation in Listeria evasion from the host innate immune system." PNAS **104**: 997-1002.

Boone DL, T. E., Lee EG, Ahmad RC, Wheeler MT, Tsui C, Hurley P, Chien M, Chai S, Hitotsumatsu O, McNally E, Pickart C, Ma A. (2004). "The ubiquitin-modifying enzyme A20 is required for termination of Toll-like receptor responses." Nature Immunology **5**(10): 1052-1060.

Butler MP, H. J., Moynagh PN. (2007). "Kinase-active interleukin-1 receptor-associated kinases promote polyubiquitination and degradation of the Pellino family:

direct evidence for PELLINO proteins being ubiquitin-protein isopeptide ligases." Journal of Biological Chemistry **282**(41): 29729-29737.

Chang M, J. W., Sun SC (2009). "Peli1 facilitates TRIF-dependent Toll-like receptor signaling and proinflammatory cytokine production." Nature Immunology **10**(10): 1089-1095.

Chang M, J. W., Sun SC. (2009). "Peli1 facilitates TRIF-dependent Toll-like receptor signaling and proinflammatory cytokine production." Nat Immunol **10**(10): 1089-1095.

Chen G, G. D. (2002). "TNFR1 Signalling: A beautiful pathway." Science **296**(5573): 1634-1635.

Chen, Z., Gibson, T.B., Robinson, F., Silvestro, L., Pearson, G., Xu, B., Wright, A., Vanderbilt, C., and Cobb, M.H. (2001). "MAP Kinases." Chem Rev **101**: 2449-2476.

Crosetto N, B. M., Dikic I. (2006). "Ubiquitin hubs in oncogenic networks." Mol Cancer Res **4**(12): 899-904.

Dynek JN, G. T., Dueber EC, Fedorova AV, Izrael-Tomasevic A, Phu L, Helgason E, Fairbrother WJ, Deshayes K, Kirkpatrick DS, Vucic D. (2010). "c-IAP1 and UbcH5 promote K11-linked polyubiquitination of RIP1 in TNF signalling." EMBO **29**(24): 4198-4209.

Ea CK, D. L., Xia ZP, Pineda G, Chen ZJ. (2006). "Activation of IKK by TNFalpha requires site-specific ubiquitination of RIP1 and polyubiquitin binding by NEMO. Ea CK, Deng L, Xia ZP, Pineda G, Chen ZJ." Mol Cell **22**(2): 245-257.

Elinav E, S. T., Henao-Mejia J, Flavell RA. (2011). "Regulation of the antimicrobial response by NLR proteins." Immunity **34**(5): 665-679.

Enesa K, Z. M., Chaudhury H, Luong le A, Rawlinson L, Mason JC, Haskard DO, Dean JL, Evans PC (2008). "NF-kappaB suppression by the deubiquitinating enzyme Cezanne: a novel negative feedback loop in pro-inflammatory signaling." Journal of Biological Chemistry **283**(11): 7036-7045.

Evans PC, S. T., Lai MJ, Williams MG, Burke DF, Heyninck K, Kreike MM, Beyaert R, Blundell TL, Kilshaw PJ. (2003). "A novel type of deubiquitinating enzyme." Journal of Biological Chemistry **278**(25): 23180-23186.

Fan Y, Y. Y., Mao R, Zhang H, Yang J. (2011). "TAK1 Lys-158 but not Lys-209 is required for IL-1β-induced Lys63-linked TAK1 polyubiquitination and IKK/NF-κB activation." Cell Signal **23**(4): 660-665.

Fan Y, Y. Y., Shi Y, Sun W, Xie M, Ge N, Mao R, Chang A, Xu G, Schneider MD, Zhang H, Fu S, Qin J, Yang J. (2010). "Lysine 63-linked polyubiquitination of TAK1 at lysine 158 is required for tumor necrosis factor alpha- and interleukin-1beta-induced IKK/NF-kappaB and JNK/AP-1 activation." J Biol Chem **285**(8): 5347-5360.

Fan YH, Y. Y., Mao RF, Tan XJ, Xu GF, Zhang H, Lu XB, Fu SB, Yang J. (2011). "USP4 targets TAK1 to downregulate TNFα-induced NF-κB activation." Cell death Differ **18**(10): 1547-1560.

Fitzgerald KA, M. S., Faia KL, Rowe DC, Latz E, Golenbock DT, Coyle AJ, Liao SM, Maniatis T. (2003). "IKKepsilon and TBK1 are essential components of the IRF3 signaling pathway." Nature Immunology **4**(5): 491-496.

Friedman CS, O. D. M., Legarda-Addison D, Ng A, Cárdenas WB, Yount JS, Moran TM, Basler CF, Komuro A, Horvath CM, Xavier R, Ting AT. (2008). "The tumour suppressor CYLD is a negative regulator of RIG-I-mediated antiviral response." EMBO **9**(9): 930-936.

Funakoshi-Tago M, K. N., Shimizu T, Hashiguchi Y, Tago K, Sonoda Y, Kasahara T. (2009). "TRAF6 negatively regulates TNFalpha-induced NF-kappaB activation." Cytokine **45**: 72-79.

Gack MU, K. A., Shin YC, Inn KS, Liang C, Cui S, Myong S, Ha T, Hopfner KP, Jung JU. (2008). "Roles of RIG-I N-terminal tandem CARD and splice variant in TRIM25-mediated antiviral signal transduction." PNAS **105**(43): 16743-16748.

Gao D, Y. Y., Wang RP, Zhou X, Diao FC, Li MD, Zhai ZH, Jiang ZF, Chen DY (2009). "REUL is a novel E3 ubiquitin ligase and stimulator of retinoic-acid-inducible gene-I." Plos One **4**(6).

Gardam S, S. F., Basten A, Mackay F, Brink R. (2008). "TRAF2 and TRAF3 signal adapters act cooperatively to control the maturation and survival signals delivered to B cells by the BAFF receptor." Immunity **28**(3): 391-401.

Gerlach B, C. S., Schmukle AC, Emmerich CH, Rieser E, Haas TL, Webb AI, Rickard JA, Anderton H, Wong WW, Nachbur U, Gangoda L, Warnken U, Purcell AW, Silke J, Walczak H. (2011). "Linear ubiquitination prevents inflammation and regulates immune signalling." Nature **471**: 591-598.

Goh ET, A. J., Cheung PC, Akira S, Toth R, Cohen P. (2012). "Identification of the protein kinases that activate the E3 ubiquitin ligase Pellino 1 in the innate immune system." Biochem J **441**(1): 339-346.

González-Navajas JM, L. J., Nguyen KP, Bhargava M, Corr MP, Varki N, Eckmann L, Hoffman HM, Lee J, Raz E. (2010). "Interleukin 1 receptor signaling regulates DUBA expression and facilitates Toll-like receptor 9-driven antiinflammatory cytokine production." J Exp Med **207**(13): 2799-2807.

Guicciardi ME, G. G. (2009). "Life and death by death receptors." FASEB J **23**(6): 1625-1637.

Haas TL, E. C., Gerlach B, Schmukle AC, Cordier SM, Rieser E, Feltham R, Vince J, Warnken U, Wenger T, Koschny R, Komander D, Silke J, Walczak H. (2009). "Recruitment of the linear ubiquitin chain assembly complex stabilizes the TNF-R1

signaling complex and is required for TNF-mediated gene induction." Molecular Cell **36**: 831-844.

Häcker H, R. V., Blagoev B, Kratchmarova I, Hsu LC, Wang GG, Kamps MP, Raz E, Wagner H, Häcker G, Mann M, Karin M. (2006). "Specificity in Toll-like receptor signalling through distinct effector functions of TRAF3 and TRAF6." Nature **439**(7073): 204-207.

Häcker H, T. P., Karin M. (2011). "Expanding TRAF function: TRAF3 as a tri-faced immune regulator." Nature Reviews Immunology **11**(7): 457-468.

Harhaj EW, D. V. (2011). "Deubiquitinases in the regulation of NF-κB signaling." Cell Research **21**: 22-39.

Harhaj EW, D. V. (2011). "Regulation of NF-κB by deubiquitinases." Immunol Rev **246**(1): 107-124.

Hass, T. L. e. a. (2009). "Recruitment of the linear ubiuitin chain assembly complex stabilizes the TNFR1 signalling complex and is required for TNF-mediated gene induction." Molecular Cell **36**: 831-844.

Heyninck K, D. V. D., Vanden Berghe W, Van Criekinge W, Contreras R, Fiers W, Haegeman G, Beyaert R. (1999). "The zinc finger protein A20 inhibits TNF-induced NF-kappaB-dependent gene expression by interfering with an RIP- or TRAF2-mediated transactivation signal and directly binds to a novel NF-kappaB-inhibiting protein ABIN." JOURNAL of cell biology **145**(7): 1471-1482.

Hiscott J, L. J., Lin R. (2006). "Recruitment of an interferon molecular signaling complex to the mitochondrial membrane: disruption by hepatitis C virus NS3-4A protease." Biochem Pharmacol **72**(11): 1477-1484.

Hoffmann JA, K. F., Janeway CA, Ezekowitz RA (1999). "Phylogenetic perspectives in innate immunity." Science **284**: 1313-1318.

Hornung V, E. J., Kim S, Brzózka K, Jung A, Kato H, Poeck H, Akira S, Conzelmann KK, Schlee M, Endres S, Hartmann G. (2006). "5'-Triphosphate RNA is the ligand for RIG-I." Science **314**: 994-997.

Hsu H, S. H., Pan MG, Goeddel DV (1996). "TRADD-TRAF2 and TRADD-FADD interactions define two distinct TNF receptor 1 signal transduction." Cell **84**(2): 299-308.

Hsu H, X. J., Goeddel DV. (1995). "The TNF receptor 1-associated protein TRADD signals cell death and NF-kappa B activation." Cell **81**(4): 495-504.

Huang OW, M. X., Yin J, Flinders J, Maurer T, Kayagaki N, Phung Q, Bosanac I, Arnott D, Dixit VM, Hymowitz SG, Starovasnik MA, Cochran AG. (2012). "Phosphorylation-dependent activity of the deubiquitinase DUBA." Nat Struct Mol Biol **19**(2): 171-175.

I., S. (2010). "The role of mitochondria in the mammalian antiviral defense system." Mitochondrion **10**: 316-320.

Ikeda F, D. Y., Skånland SS, Stieglitz B, Grabbe C, Franz-Wachtel M, van Wijk SJ, Goswami P, Nagy V, Terzic J, Tokunaga F, Androulidaki A, Nakagawa T, Pasparakis M, Iwai K, Sundberg JP, Schaefer L, Rittinger K, Macek B, Dikic I. (2011). "SHARPIN forms a linear ubiquitin ligase complex regulating NF-κB activity and apoptosis." Nature **471**: 637-643.

Inn KS, G. M., Tokunaga F, Shi M, Wong LY, Iwai K, Jung JU. (2011). "Linear ubiquitin assembly complex negatively regulates RIG-I- and TRIM25-mediated type I interferon induction." Immunity **41**(3): 354-365.

Iwasaki A, M. R. (2004). "Toll-like receptor control of the adaptive immune responses." Nature Immunology **5**: 987-995.

Jin W, C. M., Sun SC. (2012). "Peli: a family of signal-responsive E3 ubiquitin ligases mediating TLR signaling and T-cell tolerance." Cell Mol Immunol **9**(2): 113-122.

Jin X, J. H., Jung HS, Lee SJ, Lee JH, Lee JJ. (2010). "An atypical E3 ligase zinc finger protein 91 stabilizes and activates NF-kappaB-inducing kinase via Lys63-linked ubiquitination." Journal of Biological Chemistry **285**(40): 30539-30547.

Johnson, G. L., and Lapadat, R. (2002). "Mitogen-activated protein kinase pathways mediated by ERK, JNK, and p38 protein kinases." Science **298**: 1911-1912.

Jr., J. C. (1989). "Approaching the asymptote? Evolution and revolution in immunology." Cold Spring Harb Symp Quant Biol. **41**(1): 1-13.

Kang DC, G. R., Lin L, Randolph A, Valerie K, Pestka S, Fisher PB. (2004). "Expression analysis and genomic characterization of human melanoma differentiation associated gene-5, mda-5: a novel type I interferon-responsive apoptosis-inducing gene." Oncogene **23**(9): 1789-8000.

Kanneganti TD, L. M., Núñez G. (2007). "Intracellular NOD-like receptors in host defense and disease." Immunity **4**: 549-559.

Karin, M., and Galagher, E. (2009). "TNFR Signalling: Ubiquitn conjugated TRAFic signals control stop-and-go for MAPK signalling complexes." Immunological Reviews **228**: 225-240.

Karin M, B.-N. Y. (2000). "Phosphorylation meets ubiquitination: the control of NF-[kappa]B activity." Annu Rev Immunol **18**: 621-663.

Kato H, T. O., Mikamo-Satoh E, Hirai R, Kawai T, Matsushita K, Hiiragi A, Dermody TS, Fujita T, Akira S. (2008). "Length-dependent recognition of double-stranded ribonucleic acids by retinoic acid-inducible gene-I and melanoma differentiation-associated gene 5." J Exp Med **205**(7): 1601-1610.

Kawai T, A. S. (2009). "The roles of TLRs, RLRs and NLRs in pathogen recognition. Kawai T, Akira S." Int Immunol **21**(4): 317-337.

Kawai T, A. S. (2010). "The role of pattern-recognition receptors in innate immunity: update on Toll-like receptors." nature Immunology **11**(5): 373-384.

Kawai T, S. S., Ishii KJ, Coban C, Hemmi H, Yamamoto M, Terai K, Matsuda M, Inoue J, Uematsu S, Takeuchi O, Akira S. (2004). "Interferon-alpha induction through Toll-like receptors involves a direct interaction of IRF7 with MyD88 and TRAF6." Nature Immunology **5**: 1061-1068.

Kayagaki N, P. Q., Chan S, Chaudhari R, Quan C, O'Rourke KM, Eby M, Pietras E, Cheng G, Bazan JF, Zhang Z, Arnott D, Dixit VM. (2007). "DUBA: a deubiquitinase that regulates type I interferon production." Science **318**(5856): 1628-1632.

Kim JY, M. M., Kim DG, Lee JY, Bai L, Lin Y, Liu ZG, Kim YS. (2010). "TNFα induced noncanonical NF-κB activation is attenuated by RIP1 through stabilization of TRAF2." Journal of cell science **124**: 647-656.

Kirisako T, K. K., Murata S, Kato M, Fukumoto H, Kanie M, Sano S, Tokunaga F, Tanaka K, Iwai K. (2006). "A ubiquitin ligase complex assembles linear polyubiquitin chains." EMBO **25**(20): 4877-4887.

Kopp, E. M., R. Carothers. , J. Xiao. , C. Douglas, I., Janeway, C., Ghosh, S. (1999). "ECSIT is an evoluntionary conserved intermediate in the Toll/IL-1 signall transduction pathway." Genes and development **13**: 2059-2072.

Krikos A, L. C., Dixit VM (1992). "Transcriptional activation of the tumor necrosis factor alpha-inducible zinc finger protein, A20, is mediated by kappa B elements." Journal of Biological Chemistry **267**(25): 17971-17976.

Lee TH, S. J., Cusson N, Kelliher MA. (2004). "The kinase activity of Rip1 is not required for tumor necrosis factor-alpha-induced IkappaB kinase or p38 MAP kinase activation or for the ubiquitination of Rip1 by Traf2.
." Journal of Biological Chemistry **279**: 33185-33191.

Li S, Z. H., Mao AP, Zhong B, Li Y, Liu Y, Gao Y, Ran Y, Tien P, Shu HB. (2010). "Regulation of virus-triggered signaling by OTUB1- and OTUB2-mediated deubiquitination of TRAF3 and TRAF6." Journal of Biological Chemistry **285**(7): 4291-4297.

Liang J, S. Y., Lei T, Wang J, Qi D, Yang Q, Kolattukudy PE, Fu M. (2010). "MCP-induced protein 1 deubiquitinates TRAF proteins and negatively regulates JNK and NF-kappaB signaling." J Exp Med **207**(13): 2959-2973.

Lin R, Y. L., Nakhaei P, Sun Q, Sharif-Askari E, Julkunen I, Hiscott J. (2006). "Negative regulation of the retinoic acid-inducible gene I-induced antiviral state by the ubiquitin-editing protein A20." Journal of Biological Chemistry **281**: 2095-2103.

Lin SC, C. J., Lamothe B, Rajashankar K, Lu M, Lo YC, Lam AY, Darnay BG, Wu H. (2007). "Molecular basis for the unique deubiquitinating activity of the NF-kappaB inhibitor A20." J Mol Biol **376**(2): 526-540.

Lin Y, D. A., Rodriguez Y, Liu ZG (1999). "Cleavage of the death domain kinase RIP by caspase-8 prompts TNF-induced apoptosis." Genes and development **13**: 2514-2526.

Mahoney DJ, C. H., Mrad RL, Plenchette S, Simard C, Enwere E, Arora V, Mak TW, Lacasse EC, Waring J, Korneluk RG. (2008). "Both cIAP1 and cIAP2 regulate TNFalpha-mediated NF-kappaB activation." PNAS **105**(33): 11778-11783.

Malynn BA, M. A. (2010). "Ubiquitin makes its mark on Immune Regulation." Immunity **33**(6): 843-852.

Mao R, F. Y., Mou Y, Zhang H, Fu S, Yang J. (2011). "TAK1 lysine 158 is required for TGF-β-induced TRAF6-mediated Smad-independent IKK/NF-κB and JNK/AP-1 activation." Cell Signal **23**(1): 222-227.

Mashima R, S. K., Aki D, Minoda Y, Takaki H, Sanada T, Kobayashi T, Aburatani H, Yamanashi Y, Yoshimura A. (2005). "FLN29, a novel interferon- and LPS-inducible gene acting as a negative regulator of toll-like receptor signaling." Journal of Biological Chemistry **280**: 41289-41297.

Mauro C, P. F., Lavorgna A, Mellone S, Iannetti A, Acquaviva R, Formisano S, Vito P, Leonardi A. (2006). "ABIN-1 binds to NEMO/IKKgamma and co-operates with A20 in inhibiting NF-kappaB." Journal of Biological Chemistry **281**(27): 18482-18488.

Meylan E, B. K., Hofmann K, Blancheteau V, Martinon F, Kelliher M, Tschopp J. (2001). "RIP1 is an essential mediator of Toll-like receptor 3-induced NF-kappa B activation." Nature Immunology **5**: 503-507.

Morgan BP, M. K., Longhi MP, Harris CL, Gallimore AM. (2005). "Complement: central to innate immunity and bridging to adaptive responses." Immunology letters **97**(2): 171-179.

Moustakas A, H. C. (2003). "Ecsit-ement on the crossroads of Toll and BMP signal transduction." Genes and development **17**: 2855-2859.

Moynagh, P. N. (2005). "TLR signalling and activation of IRFs: revisiting old friends from the NF-kappaB pathway." Trends in Immunology **26**: 469-475.

Moynagh, P. N. (2005). "TLR Signalling and activation of IRFs: Revisiting old friends from the NFκB pathway." Trends in Immunology **26**(9): 469-476.

Moynagh, P. N. (2009). "The Pellino family: IRAK E3 ligases with emerging roles in innate immune signalling." Trends in Immunology **1**: 33-42.

Nakhaei P, M. T., Solis M, Sun Q, Zhao T, Yang L, Chuang TH, Ware CF, Lin R, Hiscott J. (2009). "The E3 ubiquitin ligase Triad3A negatively regulates the RIG-I/MAVS signaling pathway by targeting TRAF3 for degradation." PLoS pathogens **5**: 1000650.

Ninomiya-Tsuji J, K. K., Hiyama A, Inoue J, Cao Z, Matsumoto K. (1999). "The kinase TAK1 can activate the NIK-I kappaB as well as the MAP kinase cascade in the IL-1 signalling pathway." Nature **398**(6724): 252-256.

Nouws J, N. L., Houten SM, van den Brand M, Huynen M, Venselaar H, Hoefs S, Gloerich J, Kronick J, Hutchin T, Willems P, Rodenburg R, Wanders R, van den Heuvel L, Smeitink J, Vogel RO. (2010). "Acyl-CoA dehydrogenase 9 is required for the biogenesis of oxidative phosphorylation complex I." Cell metab **12**(3): 283-294.

O'Donnell, M. A., ., Ting, A.T. (2010). "RIP1 comes back to life as a cell death regulator in TNFR1 signalling." FEBS.

O'Donnell, M. A., Addison, D.L, Skountas, P., Yeh, C.H., Ting, AT. (2007). "Ubiquitination of RIP1 regulates an NFκB-Independent cell death switch in TNF signalling." Current Biology **17**: 418-424.

O'Donnell MA, H. H., Legarda D, Ting AT. (2012). "NEMO Inhibits Programmed Necrosis in an NFκB-Independent Manner by Restraining RIP1." PloS One **7**(7): 41238.

O'Donnell MA, P.-J. E., Oberst A, Ng A, Massoumi R, Xavier R, Green DR, Ting AT. (2012). "Caspase 8 inhibits programmed necrosis by processing CYLD." Nat Cell Biol **13**(12).

Oshiumi H, M. M., Hatakeyama S, Seya T. (2009). "Riplet/RNF135, a RING finger protein, ubiquitinates RIG-I to promote interferon-beta induction during the early phase of viral infection." Journal of Biological Chemistry **284**(2): 807-817.

Palm NW, M. R. (2009). "Pattern recognition receptors and control of adaptive immunity." Immunol Rev **227**(1): 221-233.

Parvatiyar K, B. G., Harhaj EW (2010). "TAX1BP1 and A20 inhibit antiviral signaling by targeting TBK1-IKKi kinases." Journal of Biological Chemistry **285**(2): 14999-50999.

Paz S, S. Q., Nakhaei P, Romieu-Mourez R, Goubau D, Julkunen I, Lin R, Hiscott J. (2006). "Induction of IRF-3 and IRF-7 phosphorylation following activation of the RIG-I pathway." Cell Mol Bio **52**: 17-28.

Pérez de Diego R, S.-S. V., Lorenzo L, Puel A, Plancoulaine S, Picard C, Herman M, Cardon A, Durandy A, Bustamante J, Vallabhapurapu S, Bravo J, Warnatz K, Chaix Y, Cascarrigny F, Lebon P, Rozenberg F, Karin M, Tardieu M, Al-Muhsen S, Jouanguy E, Zhang SY, Abel L, Casanova JL (2010). "Human TRAF3 adaptor molecule deficiency leads to impaired Toll-like receptor 3 response and susceptibility to herpes simplex encephalitis." Immunity **33**(3): 400-411.

Poeck H, B. M., Gross O, Finger K, Roth S, Rebsamen M, Hannesschläger N, Schlee M, Rothenfusser S, Barchet W, Kato H, Akira S, Inoue S, Endres S, Peschel C, Hartmann G, Hornung V, Ruland J. "Recognition of RNA virus by RIG-I results in activation of CARD9 and inflammasome signaling for interleukin 1 beta production." Nature Immunology **11**: 63-69.

Qu Y, M. S., Izrael-Tomasevic A, Newton K, Gilmour LL, Lamkanfi M, Louie S, Kayagaki N, Liu J, Kömüves L, Cupp JE, Arnott D, Monack D, Dixit VM. (2012). "Phosphorylation of NLRC4 is critical for inflammasome activation." Nature **1038**: 11429.

Rajput A, K. A., Bogdanov K, Yang SH, Kang TB, Kim JC, Du J, Wallach D. (2011). "RIG-I RNA helicase activation of IRF3 transcription factor is negatively regulated by caspase-8-mediated cleavage of the RIP1 protein." Immunity **34**: 340-351.

Rothe M, P. M., Henzel WJ, Ayres TM, Goeddel DV. (1995). "The TNFR2-TRAF signaling complex contains two novel proteins related to baculoviral inhibitor of apoptosis proteins." Cell **83**(7): 1243-1252.

Rothe M, W. S., Henzel WJ, Goeddel DV. (1994). "A novel family of putative signal transducers associated with the cytoplasmic domain of the 75 kDa tumor necrosis factor receptor." Cell **78**(4): 681-692.

S.C, S. (2012). "The noncanonical NF-κB pathway." Immunol Rev **246**(1): 125-140.

Saha SK, C. G. (2006). "TRAF3: a new regulator of type I interferons." Cell Cycle **5**(8): 804-807.

Satoh T, K. H., Kumagai Y, Yoneyama M, Sato S, Matsushita K, Tsujimura T, Fujita T, Akira S, Takeuchi O. (2010). "LGP2 is a positive regulator of RIG-I- and MDA5-mediated antiviral responses." PNAS **107**: 1512-1517.

SC., S. (2011). "Non-canonical NF-κB signaling pathway.
." Cell Research **21**(71-85).

Schneider M, Z. A., Roberts RA, Zhang L, Swanson KV, Wen H, Davis BK, Allen IC, Holl EK, Ye Z, Rahman AH, Conti BJ, Eitas TK, Koller BH, Ting JP. (2012). "The innate immune sensor NLRC3 attenuates Toll-like receptor signaling via modification of the signaling adaptor TRAF6 and transcription factor NF-κB." Nat Immunol **1038**.

Serhan CN, Y. R., Martinod K, Kasuga K, Pillai PS, Porter TF, Oh SF, Spite M (2008). "Rapid appearance of resolvin precursors in inflammatory exudates: novel mechanisms in resolution." Jounral of Immunology **181**(12): 8677-8687.

Shembade N, H. N., Liebl DJ, Harhaj EW. (2007). "Essential role for TAX1BP1 in the termination of TNF-alpha-, IL-1- and LPS-mediated NF-kappaB and JNK signaling." EMBO(26): 3910-3922.

Shembade N, H. N., Parvatiyar K, Copeland NG, Jenkins NA, Matesic LE, Harhaj EW. (2008). "The E3 ligase Itch negatively regulates inflammatory signaling pathways by controlling the function of the ubiquitin-editing enzyme A20." Nature Immunology **9**(3): 254-262.

Shembade N, M. A., Harhaj EW (2010). "Inhibition of NF-kappaB signaling by A20 through disruption of ubiquitin enzyme complexes." Science **327**: 1135-1139.

Shembade N, P. K., Harhaj NS, Harhaj EW. (2009). "The ubiquitin-editing enzyme A20 requires RNF11 to downregulate NF-kappaB signalling." EMBO(28): 513-522.

Siednienko J, G. T., Fitzgerald KA, Moynagh P, Miggin SM. (2011). "Absence of MyD88 results in enhanced TLR3-dependent phosphorylation of IRF3 and increased IFN-β and RANTES production.
." Journal of Immunology **186**(4): 2514-2522.

Siednienko J, H. A., Nagpal K, Golenbock DT, Miggin SM. (2011). "TLR3-mediated IFN-β gene induction is negatively regulated by the TLR adaptor MyD88 adaptor-like." Eur J Immunol **40**(11): 3150-3160.

Siednienko J, M. A., Yang S, Mitkiewicz M, Miggin SM, Moynagh PN. (2012). "Nuclear factor κB subunits RelB and cRel negatively regulate Toll-like receptor 3-mediated β-interferon production via induction of transcriptional repressor protein YY1." Journal of Biological Chemistry **286**(52): 44750-44763.

Smith H, L. X., Dai L, Goh ET, Chan AT, Xi J, Seh CC, Qureshi IA, Lescar J, Ruedl C, Gourlay R, Morton S, Hough J, McIver EG, Cohen P, Cheung PC. (2011). "The role of TBK1 and IKKε in the expression and activation of Pellino 1." Biochem J **434**(3): 537-548.

Sutterwala FS, O. Y., Flavell RA. (2007). "The inflammasome in pathogen recognition and inflammation." J Leukco. Biol **82**: 259-264.

Tang ED, W. C. (2010). "TRAF5 is a downstream target of MAVS in antiviral innate immune signaling." Plos One **5**(2).

Taylor C, J. C. (2005). "Ubiquitin protein modification and signal transduction: implications for inflammatory bowel diseases." Inflam Bow Dis **11**(12): 1097-1107.

Terzic J, M.-T. I., Ikeda F, Dikic I. (2007). "Ubiquitin signals in the NF-kappaB pathway." Biochem Soc Trans **35**(5): 942-945.

Thompson AJ, L. S. (2007). "Toll-like receptors, RIG-I-like RNA helicases and the antiviral innate immune response." Immunol Cell Biol. **85**(6): 435-445.

Travassos LH, G. S., Philpott DJ, Blanot D, Nahori MA, Werts C, Boneca IG. (2004). "Toll-like receptor 2-dependent bacterial sensing does not occur via peptidoglycan recognition." EMBO **5**: 1000-1006.

Tseng PH, M. A., Zhang W, Mino T, Vignali DA, Karin M. (2010). "Different modes of ubiquitination of the adaptor TRAF3 selectively activate the expression of type I interferons and proinflammatory cytokines." Nature Immunology **11**: 70-75.

Vallabhapurapu S, K. M. (2009). "Regulation and function of NF-kappaB transcription factors in the immune system." Annu Rev. Immunol **27**: 693-733.

Vallabhapurapu S, M. A., Zhang W, Tseng PH, Keats JJ, Wang H, Vignali DA, Bergsagel PL, Karin M. (2008). "Nonredundant and complementary functions of TRAF2 and TRAF3 in a ubiquitination cascade that activates NIK-dependent alternative NF-kappaB signaling." Nature Immunology **9**: 1364-1370.

Vandenabeele P, D. W., Van Herreweghe F, Vanden Berghe T. (2010). "The role of the kinases RIP1 and RIP3 in TNF-induced necrosis." Sci signal **3**(115).

Varfolomeev E, W. S., Dixit VM, Fairbrother WJ, Vucic D. (2008). "The inhibitor of apoptosis protein fusion c-IAP2.MALT1 stimulates NF-kappaB activation independently of TRAF1 AND TRAF2." Journal of Biological Chemistry **281**(39): 29022-29029.

Venkataraman T, V. M., Elsby R, Kakuta S, Caceres G, Saijo S, Iwakura Y, Barber GN. (2007). "Loss of DExD/H box RNA helicase LGP2 manifests disparate antiviral responses." Jounral of Immunology **178**: 6444-6455.

Viala J, C. C., Boneca IG, Cardona A, Girardin SE, Moran AP, Athman R, Mémet S, Huerre MR, Coyle AJ, DiStefano PS, Sansonetti PJ, Labigne A, Bertin J, Philpott DJ, Ferrero RL. (2004). "Nod1 responds to peptidoglycan delivered by the Helicobacter pylori cag pathogenicity island." Nature Immunology **5**: 1166-1174.

Vogel RO, J. R., van den Brand MA, Dieteren CE, Verkaart S, Koopman WJ, Willems PH, Pluk W, van den Heuvel LP, Smeitink JA, Nijtmans LG. (2007). "Cytosolic signaling protein Ecsit also localizes to mitochondria where it interacts with chaperone NDUFAF1 and functions in complex I assembly.
." Genes and development **21**(5): 615-624.

Vucic D, D. V., Wertz IE (2011). "Ubiquitylation in apoptosis: a post-translational modification at the edge of life and death." Nature Reviews **12**: 439-452.

Wang RP, Z. M., Li Y, Diao FC, Chen D, Zhai Z, Shu HB (2008). "Differential regulation of IKK alpha-mediated activation of IRF3/7 by NIK." Molecular Immunology **45**(7): 1926-1934.

Wang YY, R. Y., Shu HB. (2012). "Linear Ubiquitination of NEMO Brakes the Antiviral Response." Cell Host Microbe **12**(2): 129-131.

Wertz IE, D. V. (2010). "Regulation of death receptor signaling by the ubiquitin system." Cell death and differentiation **17**: 14-24.

Wertz IE, O. R. K., Zhou H, Eby M, Aravind L, Seshagiri S, Wu P, Wiesmann C, Baker R, Boone DL, Ma A, Koonin EV, Dixit VM. (2004). "De-ubiquitination and

ubiquitin ligase domains of A20 downregulate NF-kappaB signalling." Nature **430**: 694-699.

West, A. P., Brodsky, I.E., Rahner, C., Woo, D.K., Erdjument-Bromage, H., Tempst, P., Walsh, M.C., Choi, Y., Shadel, G.S., Ghosh, S. (2001). "TLR Signalling augments macrophage bactericidal activity through miochondrial ROS." Nature **472**: 476-482.

Wilson, N. S., Dixit, V., Ashkenazi, A. (2009). "Death receptor signal transducers: nodes of coordination in immune signalling networks." Nature Immunology **10**: 348-355.

Won M, P. K., Byun HS, Sohn KC, Kim YR, Jeon J, Hong JH, Park J, Seok JH, Kim JM, Yoon WH, Jang IS, Shen HM, Liu ZG, Hur GM. (2010). "Novel anti-apoptotic mechanism of A20 through targeting ASK1 to suppress TNF-induced JNK activation." Cell Death and Differentiation(17): 1830-1841.

Xia ZP, S. L., Chen X, Pineda G, Jiang X, Adhikari A, Zeng W, Chen ZJ. (2009). "Direct activation of protein kinases by unanchored polyubiquitin chains." Nature **461**(7261): 114-119.

Xiao, C. (2003). "ECSIT is required for BMP signalling and mesoderm formation during mouse embryogenesis
" Genes and development **17**: 2933-2949.

Xu G, T. X., Wang H, Sun W, Shi Y, Burlingame S, Gu X, Cao G, Zhang T, Qin J, Yang J. (2009). "Ubiquitin-specific peptidase 21 inhibits tumor necrosis factor alpha-induced nuclear factor kappaB activation via binding to and deubiquitinating receptor-interacting protein 1." Journal of Biological Chemistry **285**(2): 969-978.

Yamamoto M, O. T., Takeda K, Sato S, Sanjo H, Uematsu S, Saitoh T, Yamamoto N, Sakurai H, Ishii KJ, Yamaoka S, Kawai T, Matsuura Y, Takeuchi O, Akira S. and Source (2006). "Key function for the Ubc13 E2 ubiquitin-conjugating enzyme in immune receptor signaling." Nature Immunology **7**: 962-970.

Ye Y, R. M. (2009). "Building ubiquitin chains: E2 enzymes at work." Nat Rev Mol Cell Biol **10**(11): 755-764.

Yoneyama M, K. M., Matsumoto K, Imaizumi T, Miyagishi M, Taira K, Foy E, Loo YM, Gale M Jr, Akira S, Yonehara S, Kato A, Fujita T. (2005). "Shared and unique functions of the DExD/H-box helicases RIG-I, MDA5, and LGP2 in antiviral innate immunity." Jounral of Immunology **175**(5): 2851-2858.

Yount JS, M. T., López CB. and Source (2007). "Cytokine-independent upregulation of MDA5 in viral infection." J Virol **81**(13): 7316-7319.

Yu Y, H. G. (2011). "The ubiquitin E3 ligase RAUL negatively regulates type i interferon through ubiquitination of the transcription factors IRF7 and IRF3." Immunity **33**: 863-877.

Zarnegar B, Y. S., He JQ, Cheng G. (2008). "Control of canonical NF-kappaB activation through the NIK-IKK complex pathway." PNAS **105**(9): 3503-3508.

Zeng W, S. L., Jiang X, Chen X, Hou F, Adhikari A, Xu M, Chen ZJ. (2010). "Reconstitution of the RIG-I pathway reveals a signaling role of unanchored polyubiquitin chains in innate immunity." Cell **141**: 315-330.

Zhou L, M. Q., Shi H, Huo K. "NUMBL interacts with TRAF6 and promotes the degradation of TRAF6." biochemical and biophysical research communications **392**(3): 409-414.

Zhu S, P. W., Shi P, Gao H, Zhao F, Song X, Liu Y, Zhao L, Li X, Shi Y, Qian Y. (2010). "Modulation of experimental autoimmune encephalomyelitis through TRAF3-mediated suppression of interleukin 17 receptor signaling." J Exp Med **207**(12): 2647-2662.

Zotti T, U. A., Ferravante A, Vessichelli M, Scudiero I, Ceccarelli M, Vito P, Stilo R. (2011). "TRAF7 protein promotes Lys-29-linked polyubiquitination of IkappaB kinase (IKKgamma)/NF-kappaB essential modulator (NEMO) and p65/RelA protein and represses NF-kappaB activation." Journal of Biological Chemistry **286**(26): 22924-22933.